# *Design of reliable schedules and control strategies for improving bus system performance*

## Josep Mension i Camps

# PhD THESIS

# Design of reliable schedules and control strategies for improving bus system performance

Author:

**Josep Mension i Camps**

# Design of reliable schedules and control strategies for improving bus system performance

Author:

**Josep Mension i Camps**

Supervisors:

**PhD. Miquel Salicrú i Pagès**

**PhD. Miquel Àngel Estrada i Romeu**

This thesis is submitted in satisfaction of the requirements for the degree of

**Doctor of Philosophy in Civil Engineering**

**ETSECCPB**

**Universitat Politècnica de Catalunya - BARCELONA TECH**

Barcelona, July 2019

# Abstract

## Design of reliable schedules and control strategies for improving bus system performance

### Josep Mension i Camps
### Doctor of Philosophy in Civil Engineering

High-level service bus systems, even though in many different forms and local particularities, have been spread out around the globe over the last decades, driven by the administration and the transport authority, and in close cooperation with the operator agencies. Under the common denominator of a higher-level service, those bus systems succeeded quite a lot anywhere due to the best performance of their operational indicators, such as service regularity, commercial speed, and time-headway. Nevertheless, many actions should be undertaken and applied to be able to supply all those benefits.

Consistent with the above, this thesis defines several procedures enabling the design of reliable scheduled timetables and operating control strategies aimed at achieving an optimal operation. Also, more complicated route layouts, as in the case of transit corridors served by two routes, have been studied; and a specific methodology to evaluate the operational performance of the transfer areas has also been developed, as true cornerstones of those transfer-based bus networks.

The first theme of this thesis consists of setting up a methodology for drawing up efficient timetables, optimising recovery times at the bus terminals, fulfilling on-time departures, according to a predefined statistical percentage, and minimising resources in terms of vehicles and drivers, observing operating rules and constraints. In the example of route H12 from Barcelona's New Bus Network, travelling times could be adjusted and an increase by 40% of recovery time (from 5' to 7') could be implemented to be able to secure on-time departures.

After reviewing how service regularity is calculated, according to the leading worldwide agencies and transport authorities, a procedure to detect the bus bunching is determined as well as various strategies to control and mitigate its effect, making possible the adherence to the scheduled headway, and keeping the bus carrousel well-regulated. Up to 40% improvement has reached applying a strategy that combines bus speed dynamic control with traffic signal priority at the intersections.

The third issue is the operation of transit corridors served by two routes, a more complicated route scheme, advantageous to get a more efficient service -with optimal resource allocation- and to increase the service coverage. The objective is to keep the central section well-regulated and the studied headway adherence strategies are fundamental, although, as a general rule, an increase in resources is needed, which means in turn an increase of the agency costs.

The fourth subject of this thesis focuses on the transfer areas and provides a tool to assess the operational quality of their transfers. For a wide range of layouts, the operating quality of the entire node can be evaluated as well, considering the contributions of each one of their connections, weighted by ridership. This methodology is fully transferable to other modes of transport, such as the railways.

***Keywords:*** *Efficient networks; Optimisation, Timetable, Travel time; Recovery time; Service regularity, Headway adherence; Bus bunching; Signal priority; Operational Bus quality; Transfer; Transfer area; Quadratic approach.*

Dr Miquel Àngel Estrada

Associate Professor of Transportation
Department of Civil and
Environmental Engineering
UPC Barcelona TECH

Dr Miquel Salicrú

Full Professor of Statistics
Department of Genetics,
Microbiology and Statistics
University of Barcelona

# Resum

## Disseny de taules de temps fiables i estratègies de control per millorar el rendiment dels sistemes d'autobusos

Josep Mension i Camps
Doctor en Enginyeria Civil

Els sistemes d'autobusos d'altes prestacions, si bé amb diverses modalitats i particularitats locals, s'han estès per tot el món en les darreres dècades, impulsats per l'administració i els consorcis de transports, i amb el recolzament de les grans empreses operadores. Sota el denominador comú d'un alt nivell de servei, aquests sistemes d'autobusos han tingut força èxit arreu degut a les millors prestacions dels seus indicadors operacionals com són la regularitat, la velocitat comercial i l'interval de pas dels seus vehicles. No obstant això, per poder donar un bon servei, s'han de desenvolupar i aplicar nombroses accions de millora.

En línia amb tot l'anterior, aquesta tesi defineix un seguit de procediments per al disseny d'horaris fiables i d'estratègies de control operatiu que facin possible un adequat funcionament d'aquests tipus de serveis, també en esquemes de línies més complexos. A més, com que les àrees d'intercanvi esdevenen la pedra angular d'aquestes xarxes d'autobusos basades en les transferències, s'ha desenvolupat una metodologia especial per avaluar-ne el seu rendiment operatiu.
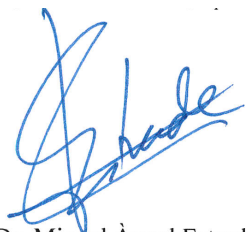
El primer tema estableix una metodologia per elaborar horaris eficients, optimitzar els temps de recuperació d'incidències (TRI) als terminals de línia, complir amb les sortides puntuals d'acord amb un percentatge estadístic preestablert i minimitzar els recursos en termes de número de vehicles i conductors, observant totes les reglamentacions operatives i restriccions existents. En l'exemple de la línia H12 de Barcelona, s'ha ajustat els temps de viatge i això ha permès un increment del 40% del TRI (de 5' a 7') per poder donar un millor servei i assegurar les sortides dels terminals.

Després de revisar la forma en què les principals agències de transport mundials i autoritats calculen la regularitat del serveis de bus, s'estableix un procediment per detectar el bus bunching (agrupació de busos), i diverses estratègies per controlar i mitigar el seu efecte, fent possible el compliment dels intervals de pas programats i mantenint el carrusel de vehicles adequadament regulat. Fins a un 40% de millora s'ha arribat a obtenir aplicant una de les estratègies que combina el control de la velocitat dels combois juntament amb la prioritat semafòrica a les interseccions.

El tercer tòpic estudia l'operació dels corredors de transport públic servits per dues línies, un esquema més complex, de molta utilitat per guanyar eficiència -amb una òptima col·locació dels recursos- i per incrementar la cobertura territorial. L'objectiu és mantenir la secció central regulada i, per aquest motiu, les estratègies d'adherència a l'interval són fonamentals, encara que, com a regla general, calgui un increment de recursos, que es tradueix en un increment del cost de l'operador.

El quart desenvolupament se centra en les àrees d'intercanvi i proporciona una eina per avaluar la qualitat operativa dels seus enllaços. També, per a un ampli espectre de casos, es pot determinar la qualitat operativa del node complet, tenint en compte les aportacions de cadascuna de les seves transferències, ponderades pel seu passatge. Aquesta metodologia és totalment transferible a altres modes de transport i pot ser d'aplicació també en el camp del serveis ferroviaris.

*Paraules clau: Xarxes eficients, Optimització, Taules de temps, Temps de viatge; Temps de recuperació d'incidències; Regularitat del servei, Adherència a l'interval de pas; Agrupació d'autobusos; Prioritat semafòrica; Qualitat operativa del servei de bus; Transferència; Àrea d'intercanvi; Aproximació quadràtica.*

Dr. Miquel Àngel Estrada

Professor Associat de Transports
Departament d'Enginyeria Civil
i Ambiental
UPC Barcelona TECH

Dr. Miquel Salicrú

Professor Titulat d'Estadística
Departament de Genètica,
Microbiologia i Estadística
Universitat de Barcelona

# Resumen

## Diseño de tablas de tiempo eficientes y estrategias de control para mejorar el rendimiento de los sistemas de autobuses

Josep Mension i Camps
Doctor en Ingeniería Civil

Los sistemas de autobuses de altas prestaciones, si bien con diversas modalidades y particularismos locales, se han extendido por todo el mundo en las últimas décadas, impulsados por la administración y los consorcios de transportes, y con la estrecha colaboración de las grandes empresas operadoras. Bajo el denominador común de un mayor nivel de servicio, estos sistemas de autobuses han tenido mucho éxito en todas partes debido a las prestaciones de sus indicadores operacionales como la regularidad, velocidad comercial e intervalo de paso. Sin embargo, para poder dar un buen servicio, deben desarrollarse y aplicarse numerosas acciones.

En línea con lo anterior, se define es esta tesis una serie de procedimientos para el diseño de horarios eficientes y estrategias de control operativo que posibiliten el adecuado funcionamiento de estos servicios, que pueden incluir esquemas de líneas más complejos. Además, como las áreas de intercambio se han convertido en la piedra angular de estas redes de autobuses, basadas en las transferencias, se ha desarrollado también una metodología especial para evaluar su rendimiento operativo.

El primer tema consiste en el establecimiento de un procedimiento para elaborar tablas de tiempos consistentes, optimizar los tiempos de recuperación de incidencias en los terminales de línea (TRI), cumplir puntualmente con las salidas según un porcentaje estadístico predefinido y minimizar los recursos en términos de vehículos y conductores, observando todas aquellas reglamentaciones operativas y restricciones existentes. En el ejemplo de la línea H12 de la Nueva Red de Bus de Barcelona, se ha llegado a un ajuste de los tiempos de viaje que han permitido un incremento de un 40% del TRI (de 5' a 7') para ajustar correctamente el servicio y asegurar las salidas de los terminales.

Después de revisar cómo calculan las principales agencias mundiales y autoridades de transporte la regularidad del servicio de bus, se establece un procedimiento para detectar el bus bunching (agrupamiento de autobuses), y se definen diversas estrategias para controlar y mitigar su efecto, posibilitando la adherencia al intervalo de paso programado y manteniendo el carrusel de la línea adecuadamente regulado. Hasta un 40% de mejora se ha llegado a obtener aplicando una de las estrategias que combina el control de la velocidad de los convoyes junto con la prioridad semafórica en las intersecciones.

El tercer tópico estudia la operación de corredores de transporte público servidos por dos líneas, un esquema de gran utilidad para ganar eficiencia -con optimización de los recursos- y para incrementar la cobertura territorial. El objetivo es mantener la sección central regulada y para ello las estrategias de adherencia al intervalo son fundamentales, aunque, como regla general, se requiera un incremento de recursos, cosa que se traduce en un incremento de los costes del operador de transporte.

El cuarto desarrollo se centra en las áreas de intercambio y proporciona una herramienta para evaluar la calidad operativa de sus enlaces, identificando y cuantificando cuantos factores penalizan. También, para un amplio espectro de casos, se puede determinar la calidad operativa del nodo en su totalidad, teniendo en cuenta las contribuciones de la totalidad de sus transferencias, ponderadas por su pasaje. Esta metodología es totalmente transferible a otros modos de transporte y puede aplicarse también en el campo ferroviario.

***Palabras clave:*** *Redes eficientes; Optimización; Tablas de tiempo; Tiempo de viaje; Tiempo de recuperación de incidencias; Regularidad del servicio, Adherencia al intervalo de paso; Agrupamiento de autobuses; Prioridad semafórica; Calidad operativa del servicio de bus; Transferencia; Área de intercambio; Aproximación cuadrática.*

Dr. Miquel Àngel Estrada

Profesor Asociado de Transportes
Departamento de Ingeniería Civil
y Ambiental
UPC Barcelona TECH

Dr. Miquel Salicrú

Profesor Titular de Estadística
Departamento de Genética,
Microbiología y Estadística
Universitat de Barcelona

# Publications derived from this thesis

**JCR Journals:**

— Estrada, M., Mension, J. Aymamí, J.M., Torres, L. (2016). Bus control strategies in corridors with signalized intersections, *Transportation Research Part C: Emerging Technologies*, 71, 500-520, ISSN 0968-090X. (2017 Impact Factor: 3.968, 5-year Impact Factor: 4.557) (Paper I)

Scientific papers currently under review:

— Estrada, M., Mension, J., Salicrú, M. (2018). Operation of transit corridors served by two routes. Physical design, synchronization and control strategies. Submitted to *Transportation Research – Part C, Emerging Technologies.* (2017 Impact Factor: 3.968, 5-year Impact Factor: 4.557) (Paper II)

— Salicrú, M., Mension, J., Estrada, M. (2019). Bus service quality at transfer areas. An assessment procedure based on temporal disutility. Submitted to *Transportation Science* (2017 Impact Factor: 3.338, 5-year Impact Factor: 4.581) (Paper III)

**Papers and presentations in other forums:**

— Mension, J. (2015). Betting High on a New Mobility Model Based on Rational, Smart, Sustainable, Efficient and Environmentally Friendly Bus System in Barcelona. Paper and presentation at the ETC, European Transport Conference. *Association for European Transport, AET*.
https://aetransport.org/public/downloads/x-lZd/4731-55e019d87b0cf.pdf

— Mension, J. Estrada, M. A. (2016). Headway Adherence. Detection and reduction of the Bus Bunching Effect. Paper and presentation at the ETC, European Transport Conference. *Association for European Transport, AET*.
https://aetransport.org/public/downloads/Bv7HG/4816-57cd5cc05c897.pdf

— Mension, J., Salicrú, M., Estrada, M. A. (2017). Performance Evaluation Procedure for Bus Interchange Areas. Paper and presentation at the ETC, European Transport Conference. *Association for European Transport, AET*.
https://aetransport.org/public/downloads/F8NXJ/5458-59cfdab5ab00a.pdf

— Mension, J., Pellot, M. (2018). Operation of a Fully Electric Bus Route. Case Study of Route H16, TMB-Barcelona. Paper and presentation at the ETC, European Transport Conference. *Association for European Transport, AET*.
https://aetransport.org/private/downloads/eNkzoq088pipDkhmPQ6boHTGTU8/Paper%20for%20ETC_2018_Pellot-Mension.pdf

— Mension, J. (2019). Prueba Piloto de TAD en el barrio de Torre Baró (Barcelona). Presentation at the "XVI Jornada Técnica: El transporte público como eje vertebrador de las nuevas formas de movilidad metropolitanas", Observatorio de la Movilidad Metropolitana.

— Mension, J., Pellot, M. (2019). Bus Demand Predictive Analysis on Barcelona Waterfront, Poster presentation at the UITP Global Public Transport Summit. Stockholm (Sweden), June 9-12, within the session: "The operation and maintenance cookbook for public transport"

— Estrada, M., Mension, J., Salicrú, M., Badia, H. (2019). Electric charging in battery bus systems. Submitted to *Transportation Research Part C: Emerging Technologies*. (2017 Impact Factor: 3.968, 5-year Impact Factor: 4.557)

# Congress, Conference, and Forum attendance and participation

— ETC, European Transport Conference. Frankfurt (Germany), September 28-30, 2015. Paper and presentation: "Betting High on a New Mobility Model Based on Rational, Smart, Sustainable, Efficient and Environmentally Friendly Bus System in Barcelona"

— UITP MENA Congress and Exhibition. Dubai (United Emirates), April 25-27, 2016, presentation: "Barcelona's New Bus Network"

— European Bus Forum. Manchester (United Kingdom), June 23, 2016. Presentation: "Introducing Barcelona's New Bus Network"

— ETC, European Transport Conference. Barcelona, October 5-7, 2016. Paper and presentation: "Headway Adherence. Detection and Reduction of the Bus Bunching Effect"

— ETC, European Transport Conference. Barcelona, October 4-6, 2017. Paper and presentation: "Performance Evaluation Procedure for Bus Interchange Areas", within the session: "Innovation in Barcelona"

— UITP Academic Meeting, 2018. Barcelona, May 14, 2018. Presentation: "Operation of a Fully Electric Bus Route. Case Study of Route H16"

— UITP Training Course on Network Design and Route Planning. Barcelona, October 1-3, 2018. Presentation: "Barcelona's New Bus Network"

— ETC, European Transport Conference. Dublin (Ireland), October 10-12, 2018. Paper and presentation: "Operation of a Fully Electric Bus Route. Case Study of Route H16", within the session: "Can buses achieve zero-emissions?"

— Observatorio de la Movilidad Metropolitana. Valencia, April 26, 2019. Presentation: "Prueba Piloto de Transporte a la Demanda en el Barrio de Torre Baró (Barcelona)", within the session: "Transporte a Demanda".

— UITP Global Public Transport Summit. Stockholm (Sweden), June 9-12, 2019. Presentation: Bus Demand Predictive Analysis on Barcelona Waterfront, within the session: "The operation and maintenance cookbook for public transport". Moderator of the workshop: E-buses and network design, within the session: "Tacking the challenges of operating fleets of e-buses"

# Declaration of contribution

The motivation of Paper I was from the joint discussion between Professor Miquel A. Estrada and Josep Mension, who were as well the main contributors in problem formulation, numerical analysis. Josep Mension carried out everything concerning numerical experiment design and result illustration and the other authors cooperated in finalising the idea, outcome interpretation and writing.

The motivation of Paper II was from the joint discussion between Professor Miquel A. Estrada and Josep Mension, who were as well the main contributors in problem formulation, modelling, computation and numerical analysis. Josep Mension carried out the part relating to numerical experiment design and result illustration, and Professor Miquel Salicrú cooperated in mathematical derivation and analysis of results.

The motivation of Paper III was from an idea of Josep Mension, who as well contributed in modelling, computation, numerical analysis, result illustration and writing. Professor Miquel Salicrú contributed to problem formulation, mathematical derivation and result interpretation. Professor Miquel A. Estrada helped greatly in collected data for references and findings interpretation.

# Glossary

| Topic | Variable | Description | Unit |
|---|---|---|---|
| Scheduled timetables | | | |
| | $Tp$ | Scheduled travel time | min |
| | $T_{ij}$ | Transit times on itinerary i, trip j | min |
| | $T..$ | Average actual travel time | min |
| | $(T..)_{TS}$ | Average actual travel time per time slot | min |
| | $RT$ | Recovery time | min |
| | $DBT$ | Driver's Break Time | min |
| | $T_T$ | Total time at the terminal | min |
| | $H$ | Headway | min |
| | $M_{st}$ | Maximum spectrum time | min |
| | $m_{st}$ | Minimum spectrum time | min |
| Headway adherence | | | |
| | $AWT$ | Actual Wait Time | min |
| | $SWT$ | Scheduled Wait Time | min |
| | $EWT$ | Excess Wait Time | min |
| | $C_{v.h}$ | The coefficient of variation of headways | - |
| | $J$ | Number of vehicles needed to maintain H | - |
| | $C_p$ | Traffic signal cycle time | sec |
| | $g_p$ | Green phase time | sec |
| | $r_P$ | Red phase time | sec |
| | $T_{r,s}$ | Running time | min |
| | $T_{p,s}$ | Time spent at the intersections | min |
| | $T_s$ | Time spent at stop s | min |
| | $\phi_s$ | Potential service disruption time | min |
| | $\theta_A$ | Recovery time at terminal A | min |
| | $\theta_B$ | Recovery time at terminal B | min |
| | $d_{j,p}$ | Delay caused by traffic signals | sec |
| | $t^a_{j,p}$ | Arrival time at intersection p | hh/mm/ss |
| | $t^d_{j,p}$ | Departure time at intersection p | hh/mm/ss |
| | $\Delta_p$ | Green offset about a general reference clock | sec |
| | $Y^t_{od}$ | O-D matrix | pax/day |

| | | |
|---|---|---|
| $q$ | Total Passenger Flow in one direction | pax/day |
| $y^t_{od}$ | Percentage of passengers travelling between stops (o,d) in time interval t | % |
| $a_j(s)$ | Alighting demand at stop s | pax/stop |
| $b_j(s)$ | Boarding demand at stop s | pax/stop |
| $F$ | Number of subsets of stationary periods in which the passenger flow distribution among stops is evaluated | num |
| $g_{jk}$ | This term is equal to 1 if the arrival of vehicle j at stop k is made in the time interval $t^*$ ($1 \leq t^* \leq F$) and 0 otherwise | 1 or 0 |
| $t_{oc}$ | Constant parameter time devoted to the door opening and closing operations of each vehicle | sec |
| $\gamma$ | Unit boarding time per passenger | sec/pax |
| $\eta$ | Unit alighting time per passenger | sec/pax |
| $v_j(s)$ | Cruising speed of bus j on section (s, s+1) | km/h |
| $A_j(s)$ | Total number of passengers alighting at stop s | pax/stop |
| $B_j(s)$ | Total number of passengers boarding at stop s | pax/stop |
| $D_j(s)$ | The total amount of passengers waiting at stop s that cannot get the bus j and must wait for the bus j+1 | pax/stop |
| $C$ | Capacity | pax/bus |
| $M_j(s)$ | Occupancy of the bus j during segment (s-1, s) | pax/bus |
| $\varepsilon_{j-1,j}(s)$ | Forward comparison to bus j | min |
| $\varepsilon_{j,j+1}(s)$ | Backward comparison to bus j+1 | min |
| $TT$ | In-vehicle travel time | pax·hour |
| $TW$ | Waiting time | pax·hour |
| $TPT$ | Total passenger travel time | pax·hour |
| $Z_O$ | Operating cost of the bus system | € |
| $Z_T$ | The total cost of the system | € |
| $C_v$ | The coefficient of variation of actual headway | - |

| Corridors served by two routes | | | |
|---|---|---|---|
| | $n^{iz}_s$ | Number of stops in direction z (i=1÷5) | num |
| | $s^{iz}_k$ | Distance between stop k and k+1, in direction z (k=1÷$n^{iz}_s$ -1) | m |
| | $l^z_i$ | Length of each route segment (i=1÷5) | m |
| | $I^{iz}$ | Set of intersections in direction z on each route segment (i=1÷5) | num |
| | $n^z_p$ | Total number of intersections on route segment i, in direction z | num |
| | $x(p^{iz}_j)$ | The total distance between the location of the j-th intersection to the initial section in direction z (j=1÷ $n^{iz}_p$) | m |

| | | |
|---|---|---|
| $g^{iz}_j$ | Green phase time of intersection j, route segment i, in direction z | sec |
| $\Delta^{iz}_j$ | Traffic light offset of intersection j, route segment i, in direction z | sec |
| $A^z_{ij}$ | Total number of alighting passengers in one hour in direction z of route segment i, whose destination is located along route segment j | pax/h |
| $B^z_{ij}$ | Total number of alighting passengers in one hour in direction z of route segment i, whose destination is located along route segment j | pax/h |
| $F^z_{a,ij}(k')$ | The cumulative distribution function of alighting passengers along with the segment i, in direction z ($1<k'\leq n^{iz}_s$) | pax/h |
| $F^z_{b,ij}(k')$ | The cumulative distribution function of boarding passengers along with the segment i, in direction z ($1<k'\leq n^{iz}_s$) | pax/h |
| $v_{max}$ | The maximum allowable speed of buses | km/h |
| $q^{iz}_{max}$ | Maximal passenger flow at the critical section of segment i, in direction z | pax/bus·h |
| $t^{iz}_0$ | Entrance time of bus to stop k=1 | hh/mm/ss |
| $t^{iz}_a(k)$ | Arrival time at stop k | hh/mm/ss |
| $d^{iz}_t(k)$ | Dwell time at stop k | sec |
| $t^{iz}_d(k)$ | Departure time from stop k | hh/mm/ss |
| $\Delta T^{iz}(t^{iz}_0)$ | Travel time needed to overcome the distance $l^z_i$ along route segment i, direction z, and perform the boarding and alighting operations at all stops ($k=1\div n^{iz}_s$) | min |
| $T_A$ | The round-trip travel time of a given vehicle of route A | min (hour) |
| $T_B$ | The round-trip travel time of a given vehicle of route B | min (hour) |
| $tt(s^{iz}_k)$ | The time required to overcome the stop spacing $s^{iz}_k$ between stops k and k+1 | min |
| $\tau_a$ | Unit alighting time | sec/pax |
| $\tau_b$ | Unit boarding time | sec/pax |
| $A^z_{T,i}(k)$ | Hourly transfer flow of passengers that alighted at stop k of route segment i, to get another bus route | pax/h |
| $B^z_{T,i}$ | Transfer flow of passengers that get on the bus at the initial stop of segment I from another route or segment | pax/h |
| $\Phi^z_A(k)$ | Boarding rate of passengers at stop k, segment i=2, direction z, that can only board on route A | % |
| $\Pi^z_A(k)$ | The alighting rate of passengers along segment i=2, in direction z, whose initial origin was located on a branched segment served by route A | % |
| $A^z_{T,A}(k)$ | Passengers travelling along central segment i=2 of route A that have previously boarded in a branched segment served by route A | pax/h |
| $t^{2z}_{0,A}$ | Arrival time at the first stop of segment i=2 in direction z of bus operating route A | hh/mm/ss |
| $t^{2z}_{0,B}$ | Arrival time at the first stop of segment i=2 in direction z of bus operating route B | hh/mm/ss |
| $m^z(k)$ | Mathematical operator $[x]^+$ and $[x]^-$ that provided the rounded value of term x to the upper and | - |

| | | |
|---|---|---|
| | lower integer | |
| $R^z_{2A}(k)$ | Onboard passengers between stops k, k+1 whose origin and destination are both located along the same central route segment (i=2) in direction z | pax/h·bus |
| $Q^z_{2A}(k)$ | Onboard passengers between stops k, k+1 whose origin and destination are not located along the same central route segment (i=2) in direction z | pax/h·bus |
| $\Lambda^z_A$ | Hourly rate of passengers that have boarded at a previous branched segment i≠2 and are still on board on central segment i=2 | pax/h |
| $w^{iz}_j(k)$ | Amount of time that the vehicle is stopped at intersection k | sec |
| $\tau$ | Additional time spent in the acceleration phase in comparison to one bus that would not perform the stop and would maintain a constant speed $v_{max}$; t= $v_{max}$/a | min |
| $k^{2z}_{a,B}(k)$ | The arrival time of that vehicle of route B that is running ahead of vehicle A | hh/mm/ss |
| $t^{iz}_{a,o}$ | Arrival time at intersection j(j=1÷$m^{iz}_{k+1}$) on route i direction z | hh/mm/ss |
| $W$ | User waiting time at stops | min |
| $IVTT$ | In-vehicle travel time | min |
| $W_T$ | Transfer time | min |
| $C_{v,h}$ | The coefficient of variation of the headway | - |
| $h^{z,z'}_{ij}$ | Difference between the next entrance time of the outbound route at the first stop of segment i in direction z | min |
| $m$ | An integer that must be specified to calculate the time difference between consecutive vehicle departures of the outbound route, about the inbound route arrival | - |
| $M_A$ | Fleet size on route A | num |
| $M_B$ | Fleet size on route B | num |
| $Z_A$ | Agency cost | €/pax |
| $Z_U$ | User cost | €/pax |
| $Z$ | Total cost | €/pax |
| $\theta_A(k)$ | Waiting time at stop A forced by the control strategy | sec |
| $\theta_B(k)$ | Waiting time at stop B forced by the control strategy | sec |
| $G$ | Duration of green phase at the traffic light | sec |
| $\Psi$ | Maximal percentage of the traffic light cycle, G/$C_p$<$\Psi$ | % |
| $\bar{x}_{p,p+1}$ | Mean distance between intersections | m |
| $C_{vx}, C_{vy}$ | The coefficient of variation in the service direction, x and y | - |
| $D_t$ | Percentage of pax flow boarding and alighting at the central segment | % |
| $S_A$ | Percentage of pax flow captured by route A | % |

| | | | |
|---|---|---|---|
| | $T_r$ | Percentage of pax flow transferring | % |
| Transfer areas | | | |
| | $C_p$ | Cycle time | sec |
| | $\mu_T$ | Transfer sequence mean | min |
| | $\sigma_T$ | Transfer sequence standard deviation | min |
| | $S$ | Operating satisfaction | % |
| | $(TQR)_s$ | Scheduled Transfer Quality Ratio | % |
| | $(IQR)_s$ | Scheduled Transfer Quality Ratio | % |
| | $(TQR)_a$ | Actual Transfer Quality Ratio | % |
| | $(IQR)_a$ | Actual Transfer Quality Ratio | % |
| | $\xi_i$ | Ridership flow of transfer i=1÷n | % |

# Acknowledgements

This thesis would not have been possible without the inspiration and support of several magnificent individuals. My heartfelt thanks and appreciation to all of them for being part of this journey and making this thesis possible.

I first wish to express my deepest gratitude to my supervisors, professors Miquel Àngel Estrada and Miquel Salicrú, for their continuous guidance and support, their excellent advice and expertise, and their kindness and commitment towards the completion of this thesis.

Likewise, I am thankful as well to my colleagues at TMB: Judith Reviejo, Juan Carlos Fernández, Juan Gordillo, Sergio Torres and Michael Pellot, for trusting me and helping me over these last four years. Their friendship and encouragement have given me more confidence and bravery for taking this work forward and eventually finishing it.

Finally, my deep and sincere gratitude to my family, always in my thoughts, for their unparalleled love, constant help, and unshakeable esteem.

I thank you all dearly!

# Content

# List of Figures

# List of Tables

Part I: GENERAL INTRODUCTION

<div align="right">

# Chapter I

# General introduction

</div>

Transit systems are a crucial element to promote sustainable mobility services in urban areas (European Commission, 2007). A competitive door-to-door travel time (including access, waiting and in-vehicle travel time) should be provided at a reasonable cost to capture demand from the car system (Iseki and Taylor, 2010). Therefore, the design of transit networks is aimed at identifying the proper balance between spatial design variables (stop spacing, route spacing) and temporary variables (time headways) that maximise the transit performance constrained by a given transit agency budget.

Over the last decades, multiple local authorities and big transport operators around the world pursued the optimisation of bus network design (Berlin, Brisbane, Stockholm, Barcelona, etc.). Due to the differential flexibility and economy of the bus operation against other modes of transport, decision makers envisaged a bus network reconfiguration to gain efficiency and provide a higher quality of service to the users, without adding much more resources to their systems.

This challenge has also been translated into the research with many contributions to the transit network design issue. Several analytical models highlighted the potentialities of the grid and hybrid bus networks, based on transfers (Estrada et al. 2011 and Daganzo 2010).

In a grid scheme, bus routes may run through perpendicular corridors in a specific given city at short (good) headways during a wide daily service span. In the outskirts, the hybrid design forces that each route may branch out in antennas, served at higher (worse) headways, but maintaining the same accessibility in the whole network. The system is quite well balanced in terms of supply and demand, with optimal use of resources, which leads to improving the efficiency and the quality of service. At each intersection between corridors, we assume that there is one stop at which users may transfer between perpendicular corridors, to provide service all around the city. This concept of bus grid/hybrid network is deployed when there is a grid street network, although similar contributions can be found when we have a ring-radial mesh of streets (Badia et al. 2014 and Chen et al. 2015).

The previous scheme proposes, therefore, the arrangement of corridors served by a minimum of two routes that, with different origins and destinations, run through a common section, at an excellent headway, to meet their ridership. On the peripheral branches, the lower boarding has the counterpart of a minor but enough supply, which results in the optimisation of resources that are placed where they are most in need. In any case, this provision requires a study to synchronize the services and to ensure the regularity of the common stretch, with headway adherence strategies to avoid the bunching effect, as it would make the quality of the service provided worse. There are several factors to consider for the feasibility of this scheme: demand, lengths of the common section and branches, the distance of stops, departure times for buses at the origins, distribution of ridership, etc., without in any case neglecting the cost. And, before the implementation of the described scheme, it is highly recommended to visualise its operation. In this sense, the models developed in this thesis allow the design and the adjustment of the parameters to guarantee correct operation, under certain boundary conditions. Should these conditions cannot be guaranteed, or should the design variables cannot be adjusted properly, we can consider the alternative of a trunk-feeder system, with transfers at both ends of the common section.

In Badia et al. (2016), the most convenient bus network configuration is analysed to minimise the total cost of the system among radial, hybrid, grid and door-to-door networks. The door-to-door network concept is based on multiple routes, each one connecting directly (without any transfer) the primary origin and destination demand points in the city. This work concluded that, for a broad domain of input cost parameters, the networks based on transfers (grid/hybrid) outperform the door-to-door networks (zero transfers) for low decentralised demand cities. It means that these transfer-based networks are more competitive from the user perspective even when users should spend an amount of time to transfer.

Preparation of route timetables is the key to success. Schedules must be adapted to the design configurations, the profile of the demand and the budget, with the maximum possible efficiency that guarantees the optimization of human and material resources. We must define a methodology that ensures: (a) on-time departures in a high statistic percentage, and (b) stability in travel times. All of this, at a reasonable cost.

Another key to success is the transition from the theoretical design schemes to the implantation of the service, defining and putting into operation headway adherence strategies to guarantee the regularity of the services. Two types of strategies have been studied by several authors: (a) a static strategy, based on the holding points available along the route (Xuan et al., 2009), (b) a dynamic strategy, based on the variation of bus speeds. In this work, a third (c) strategy, based on the change of speed is introduced, together with the signal synchronisation (Chen et al., 2012; Argote-Cabanero et al., 2015). The latter is the best and the one that can provide the best time savings, although it is also the one that most technology requires, and its deployment can be influenced by traffic conditions in the city.

Therefore, transfer areas play a crucial role in the performance of the new optimised bus networks. We would consider that a transfer area consists mainly of a group of stops placed as close as possible, served by multiple bus routes, with special signposting to assist and facilitate passenger flows among them, like what happens within the metropolitan railway network. The effects of transfer operations in the generalised cost of a single user can be summarised as a) the additional walking time needed overcome the distance between the inbound and outbound platforms in the transfer area and b) the incremental waiting time in the outbound platform for the departure of the outbound vehicle. Planners should foresee and

design bus transfer operations and transfers with the maximum comfort and the shortest time possible for the passengers. Several contributions addressed the effects of transfer operations in the generalized user cost (Deb and Chakroborty, 1998; Guihaire and Hao, 2008).

In Levinson et al. (2003) some insights about the proper design of physical elements and information devices of bus transfers were provided. Station locations and spacing strongly influence patronage. Several configurations may be considered depending on urban planning, volume applications, dedicated or grade-separated busways, etc. Site planning should separate premium bus, feeder bus, and private automobile traffic as much as possible, with the highest priority given to direct premium bus access. Site design should minimise walking distances and bus pedestrian conflicts for transferring passengers. Whenever possible, off-street transfer facilities should be provided, particularly when feeder bus bays are required. Adequate space for bus layover and short-term bus storage should be provided. It would also be very fruitful for transit agencies, a tool able to measure and control the scheduled and actual service quality, as well as their evolution over time.

In TRB (2013), Cascetta and Cartenì (2014), a set of objective performance indicators are presented to analyse the service at a stop, route and network perspective. Different levels of service are provided regarding the timely provision of the bus service (frequency, wait time, service span), reliability (coefficient of headway variations), service close to home, destination, crowding and fares, driver friendliness and safety/security. Unfortunately, there is not a compact methodology devoted to the measurement and levels of service in transfer areas, addressing the incremental waiting and walking time consumed by users.

The analysis of service quality has recently evolved to a user-oriented perspective (European Commission, 2007), where the customer expectations and satisfaction should be the pillar of the performance evaluation. In de Oña et al. (2016) there is a comprehensive review of the different techniques and available key performance indicators to monitor the perceived service quality. Dell' Olio et al. (2010) and dell'Olio et al. (2011a) conducted surveys at stops to analyse the perception of onboard users. They concluded that user satisfaction is strongly affected by the reliability of the service, the importance of minimising waiting times and the comfort during the journey. Focussed on transfer areas and intermodal networks, Iseki and Taylor (2010), dell'Olio et al. (2011b) and Hernandez et al. (2016) provides an

exhaustive analysis of the role of urban transfers in the customer service satisfaction. Attributes like the reliability of the system, the information provided, and safety and security conditions are critical aspects for users, rather than the physical characteristics of the station or the transfer layout. Nevertheless, the temporal coordination between transit services and the access time to stops have been identified to be crucial in a recent study of bus services in Bangkok (Cherry and Townsend, 2012).

To achieve that everything fits as it should and works perfectly, it is necessary to have a methodology that allows the provision of schedules that ensure an optimal bus operation. Thus, Travelling Times must be grouped according to time slots that secure stability; Recovery Times must be defined appropriately to allow trip variability mitigation and make possible on-time departures, with an operational cost that assures the feasibility of service. These schedules must be adapted to more complex route layouts, within the frame of optimised trunk networks, which can transport efficiently the highest demand from urban or metropolitan areas with growing needs for smart mobility. Transfer areas become the crucial points as they enable users to travel through the entire network. These areas need optimal design and monitoring tools to determine their performance and find out occasionally opportunity improvements that lead to better management of mobility at a global level. Finally, as service regularity is the KPI that ensures operational excellence, it is crucial to measure it properly defining and applying strategies for keeping it within the thresholds that ensure a high quality of service.

All these topics are detailed and studied along with the following chapters of this thesis, providing an innovative methodology and justifying each one necessary steps for its definition.

## 1.1 Objectives

The main objectives of this work have the common denominator of the service quality improvement that high-level service bus routes can offer to their users. And not only to achieve a certain threshold level in a predetermined horizon time but with the view to make proposals for continuous improvement that end up entailing a significant change in the user habits, favourably affecting the modal distribution of the trips made in a given urban area.

This research aims to provide tools to be able to design, measure, model, evaluate and improve all that part of the bus operation management that directly impacts on the service objectively. Thus, we will have a methodology to prepare timetables, measure regularity; design corridors operated by two routes and model their performance, evaluate the operation at the transfer areas and finally manage improvement opportunities with a clear likelihood of success.

It also wants to be innovative, analysing both traditional and new operational schemes, as a result of an evolution of the conventional ones; and designing disruptive, but possible improvement measures that can finally be applied through the several case studies, explained in Chapter 4.

It also aims to address the issues with a global vision as a whole, which offers the possibility of seeking operational improvements in the various fields of study, so that the possible feedback encourages the increase the actual performance.

Another important aspect is the scalability of the elements of analysis, which can be extrapolated to many areas and a multitude of management environments, always related to public transport.

Finally, the last, but not least, aspect to have considered is the cost; so that all the tools proposed are aimed at optimising the social value of the service provided, understood as the sum of the cost of the agency plus the cost of the user.

## 1.2    Contributions of this thesis

Within each of the four main fields of study, the main contributions of this thesis are aimed at the preparation of constructive and control strategies to offer, assess, and ensure an excellent bus service provision at a reasonable cost. Regarding timetables, the main contribution lies in the definition of a feasible statistic methodology, which ensures adherence to the committed headways, achieving high punctuality at departures from the terminals, and limited cost, using these three basic elements: travel times, recovery times and time slots.

Regarding service regularity and its fulfilment, apart from reviewing the most used formulation for calculating this indicator, a visual method that compares the scheduled and actual headways is proposed. It's valid in any environment and obtained without using any mathematical relation. Regarding the achievement of high regularity scores, beyond strategies based on slack times or even those that deal with the motion of buses, a more disruptive one is proposed that incorporate traffic light priority at the intersections and get higher adherence.

In the field of high capacity corridors, we propose the study of its operation with two routes that branch out at the ends to cover more territory and gain efficiency. The viability of this layout is evaluated, from a cinematic perspective, considering the synchrony in the common section and the optimisation of the total cost as a sum of the cost of the user plus the cost agency operating. All the above, taking into account various demand profiles, length of branches, space between stops and crossings, and several degrees of traffic light priority at the intersections.

Finally, because efficient networks may be achieved by the definition of high capacity transport corridors that interconnect each other at the transfer areas, we defined a methodology for evaluating the operational quality users have at their disposal. The innovation consists in doing all this based on the study of the time disutility that occur at a transfer area, considering a quadratic approach together with the common standards of the bus system schemes, although with a single study of each transfer area in particular to determine the values of the specific parameters.

## 1.3   Mapping

A relationship between the various topics studied in this thesis is proposed in this subsection. The first two topics establish the theoretical basis on which the bus route operation is supported. Nevertheless, these routes are often operating into a network and are interconnected with other routes of similar rank or hierarchy, either on the same corridor or through the transfer areas.

### 1.3.1 The linkage between the topics: schedules, headway adherence, corridors served by two routes and transfer area performance

Although the four issues of the study seem at first sight unconnected, they are strongly interlinked, and even a following continuity line can be established, which begins by the definition of optimised bus route timetables and schedules, followed by the calculation of the service regularity and the design of several headway adherence strategies. Finally, all these proposals can be tested on the operation of two different routes sharing a common section and can influence the performance of the transfer areas, as the methodology set forth on the previous chapter demonstrates.

Within the improved bus system framework, the most significant elements of the first part, the construction of timetables and schedules, are the following: vehicle hours, travel time, recovery time, time slot, distribution of driver shifts, work conditions, variability, normal distribution, AVL data, HASTUS IT Application, and the time-headway.

The most significant elements of the second part, headway adherence, are the following: metrics for calculating service regularity: Excess Wait Time, Standard Deviation, Service Regularity, Wait Assessment, Coefficient of Variation, Detection of Bus Bunching effect, Headway, Strategies for achieving headway adherence, TCQSM recommendations, Signal priority, and normal distribution.

The most relevant elements of the third part, corridors served by two routes, are the following: AVL data, traffic flow data, time-headway, headway adherence strategies, optimisation, and departure times from the several terminals at the branches.

The most relevant elements within the fourth part, transfer areas, are the following: transfer (connection between two routes), transfer area (layout), quadratic approach, transfer time sequence, time-headway, transfer ridership, TQR (Transfer Quality Ratio), IQR (transfer Quality Ratio), Taylor formula, ellipse, domain, and base change.

On the other hand, the existence of several elements that recurrently appear on the topics draws the attention: basic statistic (mean, standard deviation and variance); AVL data; normal distribution; time-headway; temporal sequences; scheduled and actual operation

schemes; etc. All of these common denominators allow us to explain the links between the issues, and what is true is that the best practices of the operation aim at defining efficient and reliable timetables, both for the users and for the agencies. Once the schedules have been run, it is necessary to evaluate the actual operation performance, measuring key indicators such as the service regularity and, if necessary, defining and applying strategies that make possible headway adherence at anytime and anywhere. On efficient route networks with high-level service routes, the transfer is virtually obligatory because former ubiquitous networks, made up by routes that directly link all origins to all destinations, are unaffordable due to their high operating costs. For this reason, it may also be necessary to analyse the transfer area performance because a good operation contributes enormously to the success of the overall bus system. To improve the efficiency of a high-level service route, or to gain territorial range, it could occasionally be recommended to define a branched route, with a common central section. In this instance, a detailed study presented in chapter 3.4 (which includes topics from 3.2 and 3.3) has been completed. Fig. 1, summarises all the above, with the most significant elements of every issue.

The possible improvement opportunities detected with the tools designed in this thesis should lead us to improve the operating service, as explained in the following section.
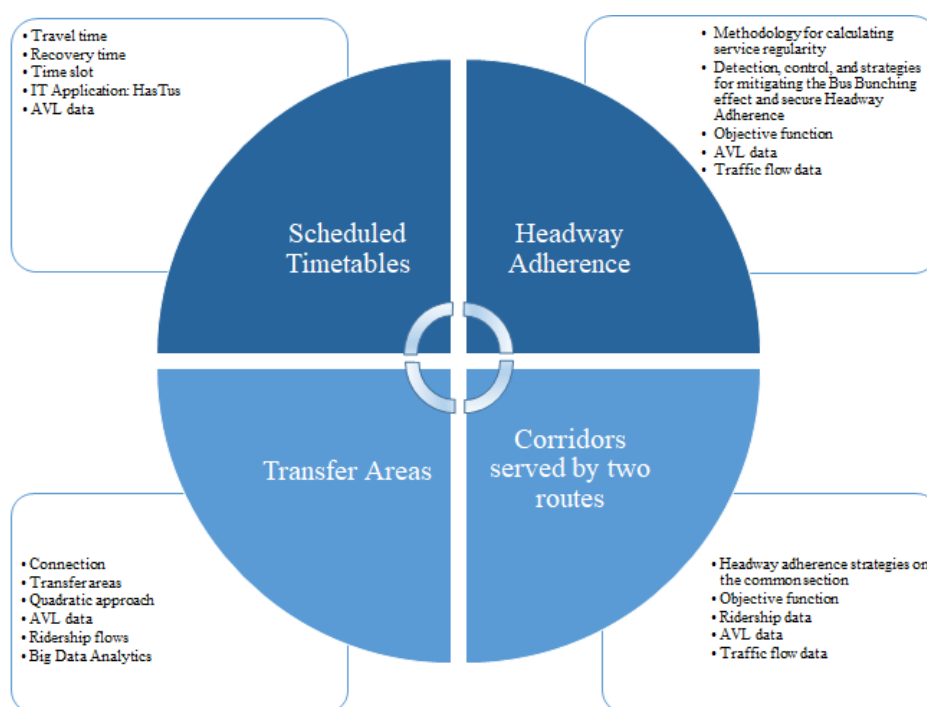


**Figure 1**: Areas of study covered by the thesis and their most significant elements

### 1.3.2 Operating action line

Fig. 2 outlines the various subjects of study, establishing a logical action line for optimal operational development and setting out occasional improvements. Starting with the preparation of the timetables, which lead to the construction of efficient schedules. Following by determining the regularity with which the service performs. To guarantee high values of the indicator, it is necessary to define and apply strategies that allow a strict headway adherence and secure a good service quality. The Bunching effect must be mitigated as much as possible because it negatively affects both the users and the agency. For that reason, based on the TCQSM recommendations, the coefficient of variation of the actual headway is calculated and compared with the TCQSM LoS (Level of Service) thresholds. We can even design part of our bus schemes so that two premium routes can serve a corridor. Once defined our network layout, schedules and headway adherence strategies, we can determine the performance route by route (1D problem) and as a full network level (2D problem), which includes branched routes and transfer areas.
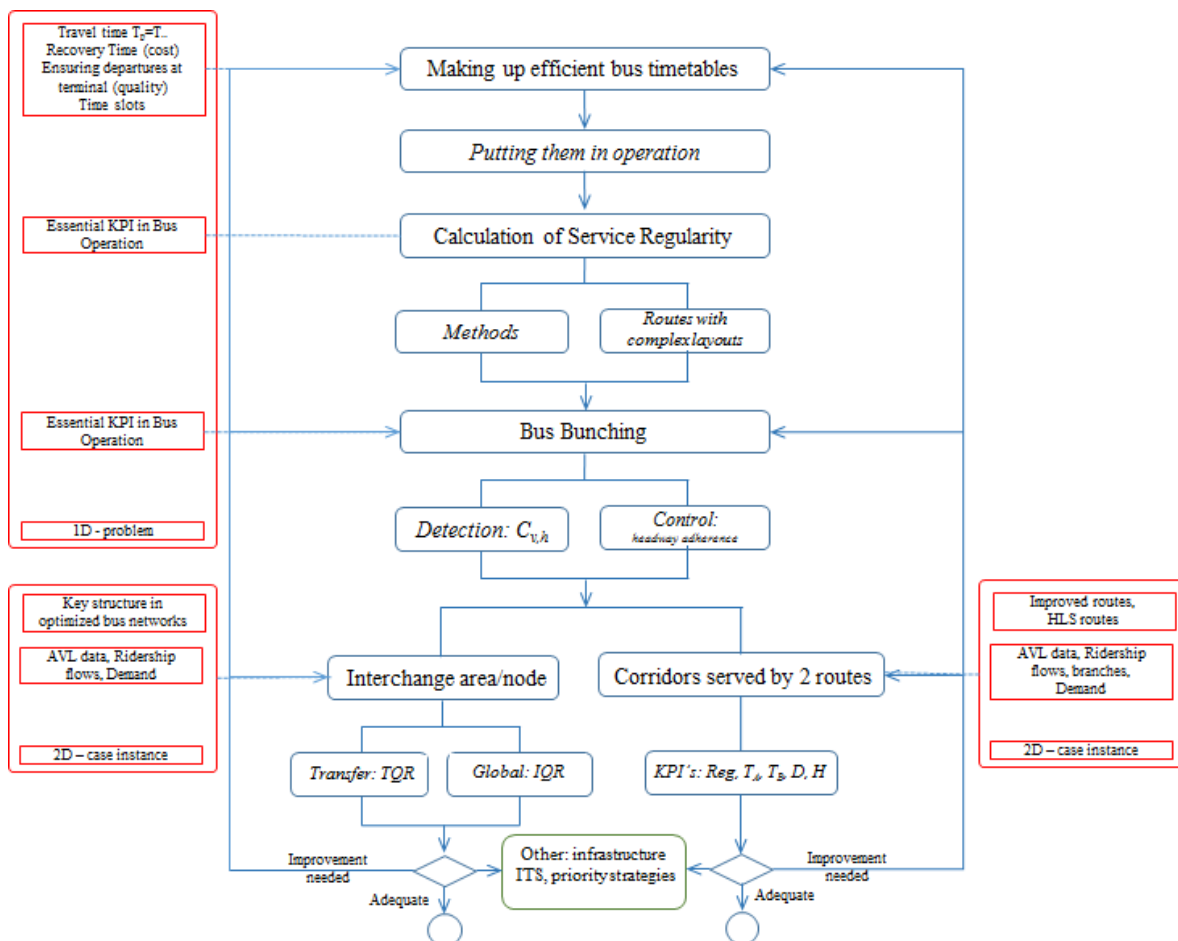


**Figure 2**: Schematic action workflow and line improving

In the event of poor operation, we should get back and define better schedules that better adapt to the journey variability, change the headway adherence strategies and apply stronger ones, or even improve the service regularity.

In the event of low operative performance at the transfer areas, it is necessary to check for the scheduled KPI's. If their values are appropriate, we must verify the punctuality or regularity of the intersected routes. In the event of poor punctuality or regularity, we have to deploy measures to improve them. However, should these KPI's are acceptable, we have to check the synchrony between the routes, or physical elements as the distance between the stops, and eventually introduce some changes on route schedules, when neither the scheduled services perform correctly. Fig. 3 displays all these improve options.
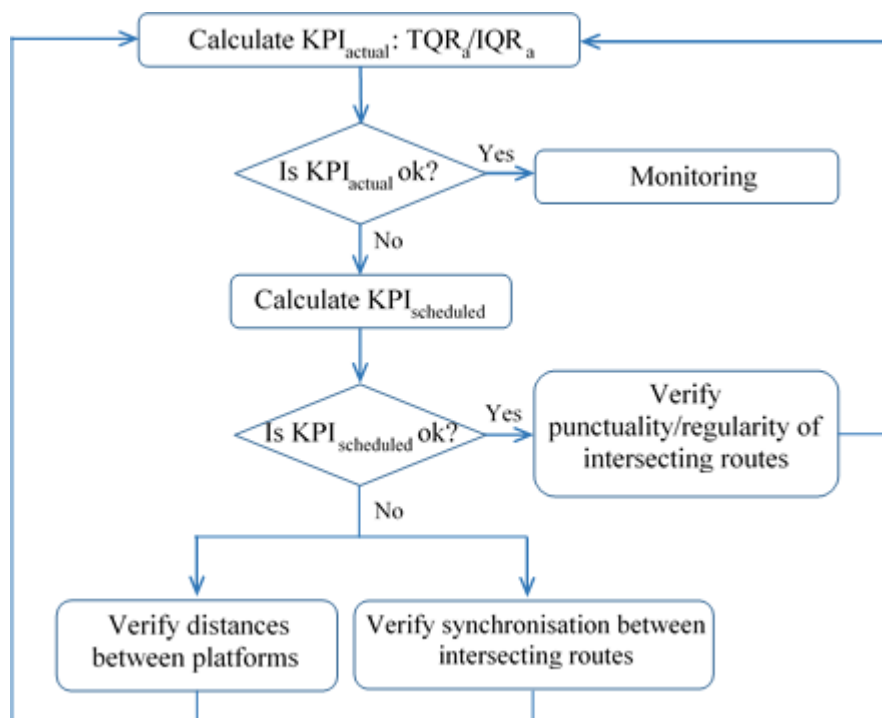


**Figure 3**: Schematic test for improving transfer area performance

## 1.4   Conclusions

These are the primary considerations and outcomes that it may be drawn on this chapter, General introduction:

— Concern about TP Agencies and Authorities to improve TP services, making them more attractive to users, at a reasonable price

— The common denominator of the study is the improvement of the bus service quality and the definition in an innovative way of several tools to elaborate, measure, design, model, evaluate and improve all that part of the management of the bus operations that impacts directly on the service provided. The social cost, understood as the sum of the cost of the user plus the cost of the agency, is also an element in every analysis

— The four topics of the study are strongly interlinked, and an action workflow and an improving line can be established: Preparing efficient bus timetables, putting them in operation, Calculating Service Regularity (essential KPI in bus operation); Methods (comparison between formulations, application on routes with complex layouts); Bus Bunching (crucial KPI in bus operation); Bus Bunching detection ($C_{v,h}$, Coefficient of variation of headways); Bus Bunching control (headway adherence); Application to routes with conventional layout and with complex design (corridor sharing two bus routes, 2D-approach); Transfer area (fundamental structure in optimised bus networks); Transfer area performance (2D-approach)

— Several elements recurrently appear on the topics as basic statistic: mean, standard deviation and variance; AVL data; normal distribution; time-headway; temporal sequences; scheduled and actual operation schemes; etc. All these common denominators allow us to explain the links between the issues

— The possible improvement opportunities detected with the tools proposed in this thesis should lead us to improve the operating service, both at a global level and particularised on each topic, as shown in Fig. 2 and 3.

# Part II: STATE OF THE ART

# Chapter II

# State of the art

This chapter introduces the four primary issues developed in this thesis: scheduled timetables, headway adherence, operating corridors served by two routes, and transfer areas, and the way these topics are being addressed in scientific research papers in recent years. Thus, we can have a general idea of the state of the art of every fundamental topic widely studied over the following chapters.

## 2.1 Research on Scheduled timetables

The preparation of schedules is a crucial task in the bus operation. It is necessary to adapt the pre-established offer to the variability of travel times, within the same time slot and throughout the entire daily service span and determining appropriate recovery times that secure the viability of the provided service at a reasonable cost. Other factors to consider are the scheduling for specific more complex layouts, the synchrony of the routes in the common corridors, as well as the consideration of demand as a factor that influences the variability of travel times. Several authors have published on the subject: Ceder et al. (2001), addresses the problem of generating a timetable for a given network of buses to maximise their synchronisation. Ceder (2001) states that bus timetables with even headways often require passengers to adjust to given timetables instead of adjusting the timetables to fluctuating

passenger demand. Michaelis and Schöbel (2009), analyses the classic planning process in public transportation. In a first step, the routes are designed; in a second step a timetable is calculated, and finally, the vehicle and crew schedules are planned. Ceder (2011) considers four necessary activities in the public transport (transit) operating planning process, usually performed in sequence: network design, timetable development, vehicle scheduling, and crew scheduling. This work addressed two activities: timetable development and vehicle-scheduling with different vehicles types. Salicrú et al. (2011), presents a new approach to generating run-time values that are based on analytical development and microsimulations and his work utilises previous research and the experience acquired by "Transports Metropolitans de Barcelona" (TMB) in operating bus routes based on timetables. Wu et al. (2016), argue about the definition of static bus timetables and justifies the re-planning of a bus network timetable. The existing timetable with even headways for the network is generated using route by route timetabling approach without considering the interactions between routes.

In terms of recovery times, some efforts are put into enhancing the robustness or delay-tolerance of pre-set schedules. Kramkowski et al. (2009) proposed a heuristic approach to redistribute the links (i.e. break times) of a given cost-optimal vehicle schedule, in which a first-in-first-out decomposition strategy is applied to even the links between consecutive trips. Their experimental results show that the delay-tolerance of given vehicle schedules can be enhanced. Later, Amberg et al. (2011) proposed two decomposition strategies of local decomposition and global decomposition for redistributing the links, in which the global decomposition utilizes the delay scenarios published in Huisman et al. (2004). The proposed method is applied to vehicle scheduling and integrated scheduling of vehicle and crew and the resulting Y. Shen et al. (2016) schedules show higher tolerance to delay without increasing the costs of given pre-set schedules. However, the degree of improvement on the delay-tolerance (or robustness) of a schedule is considerably limited by given original schedules. To compile a robust vehicle schedule from scratch, Naumann et al. (2011) proposed a stochastic programming approach, aiming to minimise the expected cost consisting of planned expenditures and disruption costs caused by delays.

All these proposals deal with important topics and use diverse heuristic algorithms, maximizing the number of simultaneous bus arrivals at the connection nodes, improving the

correspondence of vehicle departure times with passenger demand while minimizing resources, reordering the classic sequence of the planning steps, timetable development and vehicle-scheduling with different vehicles types, and re-planning timetables to bring in the interactions between routes at the nodes. To enhance the robustness of the vehicle schedule for premium bus routes, operated in a (short-very good) headway basis, the methodology proposed in section 3.2 is aimed at preparing efficient timetables, optimising recovery times, fulfilling departures from terminals (quality), and minimising resources (cost). It proposes a close partnership between planning and the day-to-day operation, minimising times and costs.

## 2.2    Research on Service Regularity and headway adherence

Service regularity is a crucial indicator in the bus operation. All transit agencies measure it, using various methods, all of which have advantages and disadvantages, as explained in section 3.3. In addition, in order to improve the value of this indicator and the customer travel experience, several strategies of headway adherence are proposed. Some of them, introduced by several researchers (holding point and dynamic speed strategies) and others of our own making, based on bus speed control combined with a traffic signal priority in some cases to minimise the reduction of the vehicle speed wasted at holding points.

### 2.2.1    Calculating service regularity

Regarding service regularity calculation on high-performance routes, in Trompet et al. (2012) various options for a suitable key performance indicator that comparably illustrates differences in performance between urban bus operators are presented. The International Bus Benchmarking Group, facilitated by Imperial College London, collected the data used for this study and relates to twelve media to large sized urban bus operators from different countries. Apart from this, the method for measuring the bunching effect can be found on the TCQSM, Transit Capacity and Quality of Service Manual, 3rd Edition (Chapter 5/Quality of Service Methods, page 5-30 to 5-31).

### 2.2.2    Headway adherence

The reliability of transit modes is an important issue to ensure their competitiveness against the extended use of private cars in major cities. However, in overall surface transit services with the partial right of way, route travel times are highly dependent on transit demand and traffic states. There are several reasons in these systems that cause service disruptions such as

illegal freight loading/unloading operations; taxi stops, use of bus lanes by slow vehicles (bikes, street sweepers) or car merging operations due to the right turns. These facts, combined with transit demand fluctuations at stops, make it challenging to maintain time-headway adherence and control the transit system performance. In bus routes with high demand, when a single bus is delayed from its schedule, the number of waiting passengers will increase at the following stops, resulting in a higher vehicle delay. This local disruption propagates to the whole fleet producing vehicle bunching, irregular vehicle arrivals at stops, unstable time-headways and more top user waiting times.

Some research has been done to describe the dynamic performance of the bus system operations. Newell and Potts (1964) and Osuna and Newell (1972) were the first contributions that described the unstable performance of a cyclic bus fleet operation. In order to tackle the bus bunching problem, several control strategies are available. Traditionally, the bus pairing has been mitigated allocating slack times in bus schedules at determined stops (holding points) along the route (Barnett, 1974; Turnquist, 1981; Rossetti and Turitto, 1998). Slack times should compensate for the delays of those buses experiencing random disruptions so that the schedule adherence would be still satisfied. Nevertheless, the obligation that all buses must remain a common slack time in a holding point represents a reduction of commercial speed. Indeed, it causes a significant inefficiency in the system's productivity. Moreover, this control strategy for maintaining the schedule of a single bus does not take into account the real performance of the others. Therefore, some studies propose dynamic control strategies to monitor the response of the whole fleet to random disruptions in a short time horizon (Eberlein et al., 2001; Dessouky et al., 2003; Adamski and Turnau, 1998). These contributions determine the location of a holding point and a specific amount of slack time for each bus, based on suboptimal procedures and the dynamic bus performance data. Real-time information is supposed to be available, as Automated Vehicle Location (AVL) and Automatic Passenger Counter (APC) systems will be equipped in the vehicles. In Yu and Yang (2007) an improved holding-point optimization procedure is presented based on genetic algorithms to minimize total passenger costs. Other contributions develop optimization models based on holding points and stop skipping strategy, where the performance of the bus system is predicted over a rolling horizon. This prediction is made considering that all variables are deterministic and known in advance (Delgado et al., 2012) or even stochastic (Sáez et al., 2012; Cortés et al., 2010). Fonzone et al. (2015) proposed bus overtaking at stops

to accommodate better the waiting passengers in buses that didn't reach its vehicle capacity constraint.

Although the previous contributions are generally based on short term predictions of the system behaviour, other approaches propose adaptive strategies to the real performance of buses. They actuate over the system variables in the interstation segments of a single bus route. Based on control theory principles, Daganzo (2009) defines an adaptive variable cruising speed patterns for public vehicles. This control strategy may be conceived as dynamic holding times in a segment of the route: if a fast vehicle is catching up the vehicle ahead, the speed of the former vehicle is linearly reduced with regard to the difference between the target and the actual headway. The results provided by this method outperform the former static holding point strategies in terms of system productivity and regularity. Nevertheless, this procedure does not respond properly when headway adherence is significantly poor. Daganzo and Pilachowski (2011) improved the determination of the cruising speed pattern when the time-headway variance is significant. In Xuan et al. (2011), a family of dynamic holding strategies are presented to improve both user and operating costs. This method improves the efficiency of existing control strategies since it minimizes the required slack times by 40% compared to conventional schedule-based methods. In Bartholdi and Eisenstein (2012), a method based on Markov-chains is presented where headways are dynamically self-equalized to natural value. In addition to that, Argote-Cabanero et al. (2015) extend a dynamic control method for several interacting bus routes. The proposed method consists of a combination of dynamic holding and driver guidance that shows the proper cruising speed of buses along the route based on real-time data.

As is stated in Muñoz et al. (2013), previous contributions based on control theory assume that buses have an infinite capacity to accommodate all the passengers waiting at stops. However, the scalable reduction of bus speeds in high transit demand corridors may lead to a problem of vehicle capacity. Experience shows that some users cannot get on overcrowded buses arriving at the stop and need to wait for the following transit vehicles. Indeed, both holding point and dynamic speed strategies are aimed to guarantee time-headway adherence at the expense of losing commercial speed (in the whole fleet or passenger travel time) and increasing operating costs. Nevertheless, few contributions assessed the cost in which transit agencies will incur to deal with bus bunching. Indeed, transit agencies would take advantage

of dynamic transit signal priority measures to minimize the reduction of the vehicle speed due to the time spent at holding points. In TRB (2013) there is an extended analysis of different techniques of transit vehicle actuated strategies that design off-line and on-line synchronization of traffic signals. The connection of buses to the transit control centre (TCC) and the deployment of a coordinated Transit System Priority (TSP) system may significantly reduce the bus delay by 55–75% about static transit priority systems (Hu et al., 2015).

To our knowledge, there are no contributions analysing how traffic signal priority may help the system to maintain a good regularity. Therefore, this paper proposes an adaptive dynamic bus control strategy, based on active signal priority for buses. Taking into account real-time headway information and traffic signal variables, we propose an adaptive transit speed pattern combined with a signal offset modification at specific intersections, to avoid the bus bunching effect. The adaptive transit speed pattern has been adapted from the contributions of Daganzo (2009) and Daganzo and Pilachowski (2011). All stops are conceived as checkpoints where the time-headway adherence control is estimated using AVL technologies. When the time-headway of one bus (concerning the bus ahead) is larger than a targeted value, the green phase of downstream traffic lights may be extended (constrained to a maximum value) to allow the bus to pass through the signal without stopping. At the same time, the speed of buses showing smaller time-headways about the target value with the vehicle ahead will be reduced. However, in this paper, this speed reduction is lower than presented in Daganzo and Pilachowski (2011). This strategy outperforms comparatively user costs and the coefficient of headway variation about existing control procedures. Besides, it also improves the operating costs, since no additional vehicles are required in comparison to slack time strategies. Moreover, the modelling approach alleviates some of the drawbacks of the former contributions as stated in Muñoz et al. (2013): the occupancy of the vehicles is considered when activating the control criteria. However, it requires that APC systems should be deployed in vehicles to put in practice these control strategies.

Although the largest bus transit agencies in developed countries have already deployed expensive AVL systems, in recent years, affordable technology has arisen to trace each bus in the line. Last developments use simple, smartphones equipped in each bus with a single ad-hoc application to implement coordinated dynamic speed control strategy in a bus corridor. On the other hand, the development of Radio Frequency Identification Devices (RFID) of

large range, allows the communication between vehicles with the infrastructure. This cheap technology is currently able to recognise a specific bus at upstream sections of traffic light intersections and activate some modifications of signal settings (TSP). The integration of the former technologies would make it possible for any kind of transit agency all over the world to deal with the schedule adherence problem. Moreover, the time-headway adherence problem will be a crucial issue for those bus agencies that are willing to deploy full electric vehicles in routes to mitigate the local emissions and Green House Gases (GHG). In fact, the European Union is fostering electromobility services in cities using several research projects (ZeEUS and Eliptic). Different bus technologies and charging infrastructure solutions will be analysed in demonstration sites. Based on the experience gained by the authors in these projects, it can be stated that there is not any fully-electric bus of 18 m of length in the market (or even an articulated bus prototype) able to provide continuous service (15–16 h per day) with an initial charge at the bus garage (September 2015). All of them need on-route charging operations at charging stations located along the route. The slack time reserved at specific holding stops should be sufficient to perform these charging operations under perfect time-headway adherence conditions. Nevertheless, if the bus arrivals at these points are irregular, vehicles cannot be charged at full capacity, unless some queues of vehicles at the charging stations appear (causing more disturbances and schedule variance) or

redundant charging stations (more servers) are deployed.

## 2.3   Research on Transit corridors served by two routes

The efficiency of urban transit networks is highly influenced by the spatial configuration of the different transit routes over the city. Other tactical and operating decisions in the transit planning problem are based on the network design, previously defined in the logical sequence of planning steps (Desaulniers and Hickman, 2007; Ceder, 2007). The transit route layout, together with the frequency setting, present a trade-off between the performance experienced by users (accessibility, temporal coverage and speed) and the operating costs (mileage, resources) incurred by transit agencies (Ibarra –Rojas et al., 2015). Therefore, urban decision makers are required to find the equilibrium point between route performance and cost, considering economic, social and political constraints.

The most suitable fixed transit route structure for users and transit agencies has been widely analysed in the literature under the forms of total cost minimisation problems. Continuous

approximation and parsimonious models were developed to estimate both, user and agency costs, in idealised route pattern designs. The best element of each network concept could be chosen by continuous optimisation. Perfect grid networks (Holroyd, 1967) and radial or hub and spoke route schemes (Newell, 1979; Byrne, 1975) were assessed. The radial designs benefit transit agencies with low infrastructure investment, while grid structures provide competitive door-to-door travel time for users (Nourbakhsh and Ouyang, 2012). Recently, hybrid configurations, combining a mesh of routes in the city centre and branching lines in the city periphery (Daganzo, 2010 and Estrada et al., 2011), were developed to merge the potentialities of both networks in the same design concept. In all these idealised network concepts, the demand is assumed to be uniformly distributed on the area of service, and any trip in the city can be made transferring at the intersection between corridors. These designs, complementary to the street network, shape the physical distribution of trips over the city. Recently, Badia et al. (2016) compared the performance of the previous models based on transfer, with the corresponding level of service provided by ubiquitous designs. The latter schemes connect the most demanded trip origin and destination zones by a direct route, without transfers. They concluded that the transfer-based hybrid design generally outperforms the total cost of the transit service, especially when demand is consolidated in the city centre. Other discrete-based optimisation models (Ceder and Wilson, 1986; Baaj and Mahmassani, 1990 and 1995, Zhao, 2006) propose direct-based transit routes that optimise an objective function, given an origin-destination matrix. As a difference from demand-shaped layouts based on hybrid networks, in that case, the demand distribution over the region configures the deployment of the transit infrastructure, creating bus network layouts that result in neither readable nor comprehensive bus design.

In either demand-shaped designs or demand–based layouts, a single transit corridor may be served by multiple lines. Generally, these lines run along with a common sketch of the corridor, and at special points, they branch out to provide service to peripheral regions of the city. Doing this, the accessibility in the whole area of the city is guaranteed, although the waiting time in the branched parts of the corridor is worsened in the economic balance between user and agency cost.

Nevertheless, the flow of vehicles belonging to multiple lines along the same corridor increases the operation's complexity and contributes to the transit vehicle bunching

phenomena, firstly described by Newell and Potts (1964). The demand at stops, and consequently, the stop boarding time in the central corridor depends on the real-time headway between serial buses. In transit corridors with high passenger flows, especially operated by buses, the natural motion of vehicles causes irregular vehicle arrivals at stops, so that any potential exogenous disturbance is propagated to the whole route. Therefore, these multiple routes should be jointly planned. Control strategies are required to maintain constant headways among buses and alleviate the unstable motion of buses.

A lot of research regarding control strategies in bus systems have been developed. Some researchers proposed the introduction of slack times into bus schedules at holding points to control the system regularity (Barnett, 1974; Turnquist and Blume, 1980; Rossetti and Turitto, 1998). Holding times allow recovering the target bus headway when vehicles are delayed, at the expenses of increasing the target roundtrip travel time. However, schedule-based holding points are significantly inefficient since each bus is controlled without any input of the rest of the vehicles. To tackle this problem, a dynamic slack introduction is proposed in several works, predicting the evolution of the system in a rolling horizon (Eberlein et al., 2001, Delgado et al., 2009; Liu et al., 2013). This control strategy was also combined along the route with the possibility of skipping some stops (Delgado et al., 2012, Sáez et al., 2012; Cortés et al., 2010) and vehicle overtaking (Fonzone et al., 2015) to recover the desired time-headway. Muñoz et al. (2013), pointed out the capacity problems arisen by holding point strategies due to the scalable reduction of bus speeds.

Other contributions propose adaptive strategies to the actual performance that do not consider system predictions. Daganzo (2009), presented a new control principle, based on variable cruising speeds, to improve the regularity of transit systems. This procedure, similar to the holding point strategy, reduces the cruising speed of buses based on the current headway with the vehicle ahead.

However, the first analysis of the bus bunching effect and joint operation of multiple routes in the same corridor is addressed in Hernández et al. (2015). A control system based on dynamic holding points at stops proposed by Delgado et al. (2012) is implemented, comparing the transit system performance under two scenarios: i) all routes are jointly managed by a central operator that considers the multiple routes as a whole system and, ii)

each route is operated independently to maximize its profit. The objective function to be minimised is the total travel time of passengers. The join control strategy demonstrated to reduce the waiting time of passengers by 55% in comparison to the independent operation of lines. Later, Schmöcker et al. (2016) extend the former Newell and Potts (1964) propagation model to the motion of buses along corridors operated by two lines when overtaking is allowed. Under this situation, a new passenger queue distribution for buses is presented. The overtaking operation always produces a positive effect on the system performance in terms of the total waiting time of passengers and the time-headway variance metrics. Finally, Argote-Cabanero et al. (2015) extended the adaptive control strategy proposed in Daganzo (2009) to complex transit systems, made up for many lines operating along the same corridor. The slack time at each stop for a given bus is based on the current deviation of the vehicle under study and previous vehicles (belonging to different lines) from the target headway. These deviations are multiplied by a dimensionless parameter responsible for propagating the bunching effect, which accounts for the expected increase in the dwell time due to boarding when the headway is increased by the one-time unit.

Unfortunately, all these contributions for multiple services assume that the unstable motion of buses is caused by the exogenous disruption. Their modelling approaches do not consider those key route design aspects that may generate irregular arrivals of buses in a corridor with multiple bus services, such as traffic lights, demand distribution and lengths of the branched routes. Besides, a small fraction of these works addressed the impacts of control strategies on the operating cost incurred by transit agencies, apart from the common effect on the user side.

This paper addresses the bus corridor design problem served by two branched lines. Two versions of an optimisation model are presented, aimed at minimising the total cost incurred by both transit agency and users, or minimising the headway variation among buses. The effects of the length uniformity of the branched segments, the fraction of demand captured by the branched segments about the central sketch, and traffic lights settings on the efficiency and regularity of the bus corridor are analysed. The analysis considers a base case scenario when the bus motion is not controlled, and overtaking is allowed. Results obtained under other scenarios for control strategies based on holding points, speed modification and traffic light priority measures are also provided. The objective of this work, as Schmöcker et al. (2016) suggested as further research, is to provide network design recommendations and the

implementation of the best control strategy to alleviate the lack of regularity in a corridor with multiple lines at the minimum operating cost. To the best of our knowledge, this is the first time that the effect of traffic light settings and the operating cost variation caused by the deployment of control strategies are considered in corridors operated by bus branched lines. In Section 3.4.1, the formulation for the bus corridor design problem with two bus services is presented, with the associated constraints, significant assumptions and boundary conditions. A bus motion model is then developed, with analytical formulations to estimate the time spent in segments between stops, dwell time at stops and delays intersections due to traffic lights. The model considers a uniform acceleration parameter in the kinematic equations, outperforming previous simplified models (Estrada et al. 2016) that supposed immediate speed profile changes at stops or intersections. In Section 3.4.2, the analysis of the different metrics measuring the effects in stakeholders as well as the optimisation models is presented. Section 3.4.3 gathers the optimisation problem and the formulas needed to consider the control strategies in the bus modelling approach. Later, the numerical results of the optimisation process in a set of problem instances are introduced in Section 3.3.4. Finally, in Section 3.3.5 several physical network design, control strategies recommendations and general conclusions are drawn.

## 2.4 Research on Transfer areas

The transfer areas allow connections between the routes that intersect on them and facilitate the movement of public transport users. In the service quality assessment, transfers deserve a specific analysis due to the opposite effects that they generate on temporal cost and perceptions. Local authorities and transit agencies have configured transit networks with transfers to supply hierarchical services in large areas. In several cities, the urban sprawl phenomena created ubiquitous transit networks, made up of multiple routes, to provide competitive door-to-door services between zones with high demanded trips (Thompson 1977). In those systems, the final design was a summation of multiple unconnected routes. They did not work as a unique system and, moreover, the operational cost was extremely high. To overcome these limitations, transfer-based transit network configurations are proposed to improve route connectivity, legibility, simplicity and travel times. An extensive list of contributions justifies the implementation of transfer-based networks, from the system connectivity.

Turnquist and Bowman (1980) examined how the transit network structure affects the number of transfers. Holroyd (1967) analysed the performance and advantages of grid-shaped transit networks with transfers. Orthogonal transit corridors can reduce the number of bus routes in a given area while maintaining the service performance within the service standard thresholds. Other alternatives propose hybrid bus networks (Estrada et al. 2011 and Daganzo 2010) that only present a grid scheme in the city centre. In the outskirts, the hybrid design forces each line to branch out in antennas, served at higher headways but maintaining the same accessibility in the whole network. This concept of bus grid/network is deployed when there is an orthogonal mesh of streets, although similar contributions can be found when we have a ring-radial mesh of streets (Badia et al. 2014 and Chen et al. 2015). In all studies, a more affordable network scheme with fewer routes can be achieved at the expenses of introducing passenger transfer operations at transfer areas. However, transfer operations at transfer areas are the cornerstone of the system, that constraint the service performance and the user's satisfaction (Nielsen et al., 2005 and Nielsen et al., 2006).

Transfers are necessary to provide connectivity among transit services and constitute dense multimodal networks with adequate spatial coverage. Mishra et al. (2012) developed connectivity indicators to represent the potential ability of a transit system in a multimodal transport network. Nevertheless, this network effect is achieved at the expenses of increasing the disutility at facilities and introducing inconveniences and psychological factors associated with the trip disruption (Hadas and Ranjitkar, 2012). Apart from the incremental walking and waiting times costs components in the generalised cost of passengers, the simple fact of transferring among vehicles penalises the passenger transfer experience (Guo and Wilson, 2011, Ortúzar and Willumsen, 2011). Many researchers estimated the transfer penalty within the door-to-door travel chain of users, relative to the perception of the transit in-vehicle time). The results were obtained applying discrete choice models to transit available data or preference surveys (Horowitz and Zlosel, 1981, Lui et al., 1997, Guo and Wilson 2004, Iseki and Tailor, 2009, Yoo 2015, Curie 2005, Gong et al., 2018, Garcia-Martinez, 2018). Unfortunately, there is not any universal community-accepted transfer penalty value. In all studies, the transfer penalty shows a significant variation, depending on different factors and the transportation modes involved.

Therefore, transfers should be designed to burden the temporal cost and inconveniences for passengers. Chowdhury and Ceder (2013) stated that the main attributes of a planned transfer are network connectivity or integration, integrated schedules or timed-transfer, the integrated physical connection of transfers, information integration, and fare and ticketing integration. This classification specifies for the transfer, the general list of attributes and dimensions proposed by Parasuraman et al. (1988) to evaluate the perceived quality of any system. Chowdhury and Ceder (2016) complete the analysis of the physiological factors that affect the travel behaviour of users.

The importance of each attribute, its metrics of analysis and improvement strategies have been analysed independently in each factor dimension. The role of transfers in the network connection has been examined through spatial analysis and performance indicators. A set of connectivity indicators based on disutility functions or user temporal cost are presented in Hadas and Ceder (2010) and Hadas and Ranjitkar (2012). These contributions also show a typological transfer classification based on the physical connection. Concerning the integration of schedules, there are several contributions of optimisation techniques to minimise waiting times at transfer facilities (Deb and Chakroborty, 1998; Guihaire and Hao, 2008; Knoppers and Muller, 1995, and Bookbinder and Désilets, 1992). These contributions coordinate the planned transit vehicle arrivals, based on lofty physical layouts. Unfortunately, they seldom consider temporal deviations from the scheduled timetable and the vehicle bunching phenomena caused by disturbances along the transit route. A bright and straightforward information system is required to reduce the user reluctance to make transfers, especially for unfamiliar or occasional passengers with the interchange (Dziekan, 2008, and Dziekan and Kottenhoff, 2007). Finally, the integrated fare structure is crucial to reduce the generalised cost of the trip and increase the ridership of multimodal systems. This ridership increment has been revealed to be higher than 15% in several studies (Sharaby and Shiftan, 2012; Chowdhury et al. 2015).

Other user-oriented studies have accurately calculated the derived importance and weights of transfer elements in the perception of whole transfer disutility. Dell'Olio et al. (2011) analysed the relative importance of information, fare and available services in multimodal areas on passenger behaviour, utilising discrete choice models. Chowdhury et al. (2014) incorporate the effect of shelters and other variables that affect the generalised user cost

(frequency and travel time). Navarrete and Ortúzar (2013) examined the relative valuation of the different time components of trips affected by one or more transfers in Santiago de Chile. The analysis revealed that the time component that presents the highest penalty was the transfer waiting time. Surprisingly, the transfer walking time was one of the lowest disutility components. In Hernández and Monzón (2016), thirty-seven observed variables were analysed, using principal-component techniques to identify uncorrelated quality factors that affected user satisfaction. These factors were grouped into the perspective that considers the interchange or transfer area as a transportation node (information, transfer conditions, safety and security and emergency conditions) or as a place (design, environment, services and facilities or comfort). Based on this study, the general importance of each variable was obtained in Hernández et al. (2016) for an underground interchange facility in Madrid (Spain), where security and emergency dimensions prevailed over the others. The temporal coordination between transit services was the first critical operational element, representing a normalised weight of 45% about available information (the more important attribute, 100%). However, the walking distance between modes was less negatively perceived by users, with a weight of 25.8%. Similarly, Schakenbos et al. (2016) highlighted that schedule synchronisation was a crucial issue to reduce the transfer disutility, and transfer agencies should undergo measures to improve it.

Most studies pointed out that the transfer experience mainly depends on a subset of strategic elements, which can be categorised as facility-related (transfer as a place) or a transportation-related attribute. However, while the former attributes (comfort, amenities) may be evaluated quite homogeneously in the same temporal period, the valuation of characteristics related to the generalised travel time (walking and waiting) may present a vast domain of variation in a short period. Generally, the target transfer-connection time is different even for two consecutive vehicle connections (arrival-departure). Only when integrated services present the same target headway, the waiting time at transfer can be kept constant in serial connections. In addition to this, transit vehicles, especially in bus systems, usually present irregular arrivals at stops, which causes a variation between actual and target schedule. Hence, the lack of headway adherence or schedule fulfilment at transfers adds more heterogeneity in the transit performance. A similar justification can be done with variable walking times affected by pedestrian traffic lights (on-street), elevators (off-street facility) and the available gates or platforms where transit vehicles can be assigned. As a result, transit

operators need to assess the quality of their temporal synchronisation and connection distances among services from real-time data (GPS and AVL at transfer areas), capturing the performance of all possible movements over time and space. Considering the relative importance of each temporal component provided by users, an aggregated quality metric may be utilised to monitor the provision of the service and prioritise improving measures in a short temporal horizon. Also, some authors have highlighted the importance of considering the walking and waiting time at the reception route variances (Ceder, 2007; Ceder et al., 2009). These variances have been related to the need to provide more travel time to get the destination on time (compensate for uncertainty due to time) and psychological factors that also affect satisfaction.

However, this thesis is aimed at developing a methodology to evaluate the quality of operation in transfers, based on the measurement of generalised temporal cost. The paper examines the relative importance of walking and waiting time of users in the overall assessment of transfer temporal disutility, based on the combination of objective operational data and perceptions, as Eboli and Mazzulla (2011), and Nathanail (2008) do. This approach is consistent with the cause-effect logic established in strategic planning models and, in particular, in the Balanced Scorecard (Kaplan and Norton, 1996, Bhuiyan and Baghel, 2005). Recognizing the cause-effect logic between the client/user perspective (satisfaction) and the internal processes perspective (quality of service) the focus is on obtaining a weighting of operational indicators (planning, execution, reliability, comfort, information, cost, etc.) that allows estimating the satisfaction perceived by the user (Parasuraman et al. 1988, 1991, Barabino et al. 2012). In this context, the weights of the components will be balanced considering the relative importance expressed by users using customer surveys. A quality transfer area operational metric is presented based on its physical configuration, the synchronisation of timetables and the time headway adherence of transit services. The attributes related to the comfort, safety and security, amenities and the facility itself are not considered. In Section 3.5.1, the second-order functional approach (quadratic) for user satisfaction is justified, and the parameters of the model are calibrated based on three criteria: 1) customer satisfaction survey; 2) consensus of experts; and 3) incomplete consensus of experts and regularity conditions. In Section 4.5.1, the methodology has been applied to the Barcelona bus network. Mainly, the planned quality and the quality performed at the transfer area of "Eixample Dret" (routes H10 and V17) have been evaluated, as well as the disutility associated to generalised transfer time components. Main results are discussed in 4.5.2.

# Part III: ANALYSIS

.

<div style="text-align: right;">

# Chapter III

# Analysis

</div>

This chapter presents the theoretical part of the work, explaining in detail the procedures and models proposed, as well as those elements of computer support for calculating and solving the mathematical problems posed.

For the scheduled timetable topic, statistics have been used as a mathematical tool, and the reference application has been HASTUS. For the development of the strategies aimed at headway adherence, Excel and Aimsun (IT simulation application) have been used. For the development of the operation model of corridors served by two lines, Visual Basic and Excel have been used. Finally, for the development of the operational satisfaction assessment at a transfer area, the computer IT applications used were Visual Basic, Excel, and MatLab.

## 3.1    Methodological approach

The methodology consists first in a problem approach, then its theoretical development is carried out, along with the corresponding justification, and the required calculation (establishment of the formulation, optimisation of the model once the values of the variables are defined, resolution of a nonlinear system of equations, etc.) In chapter 4 "Case Studies",

there are several examples of the application of the theoretical part, all of which respond to the scheme of Fig. 4.
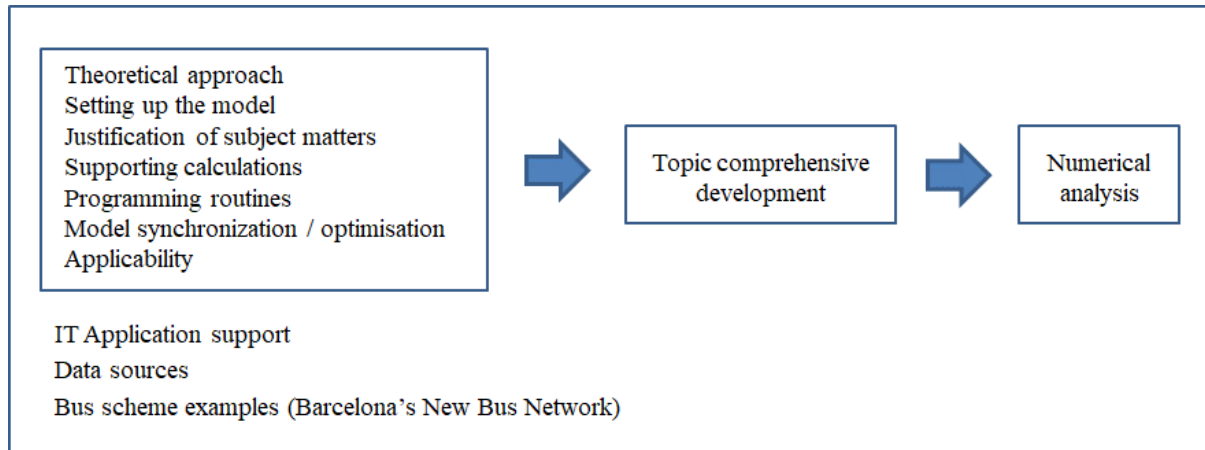


**Figure 4**. Methodology generic diagram

Fig. 5 to 8 detail the simplified schemes of the methodological process of the four main topics analysed in this thesis.
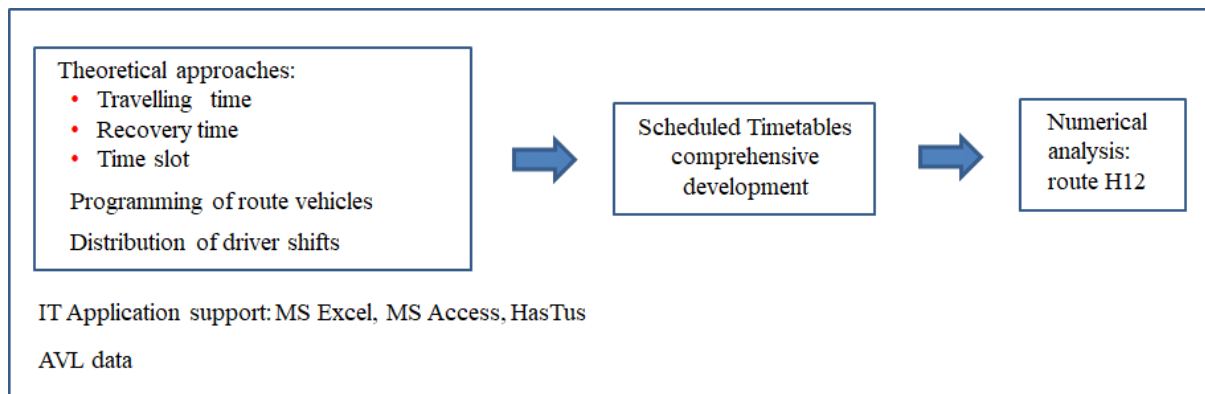


**Figure 5**. Headway adherence methodology generic diagram
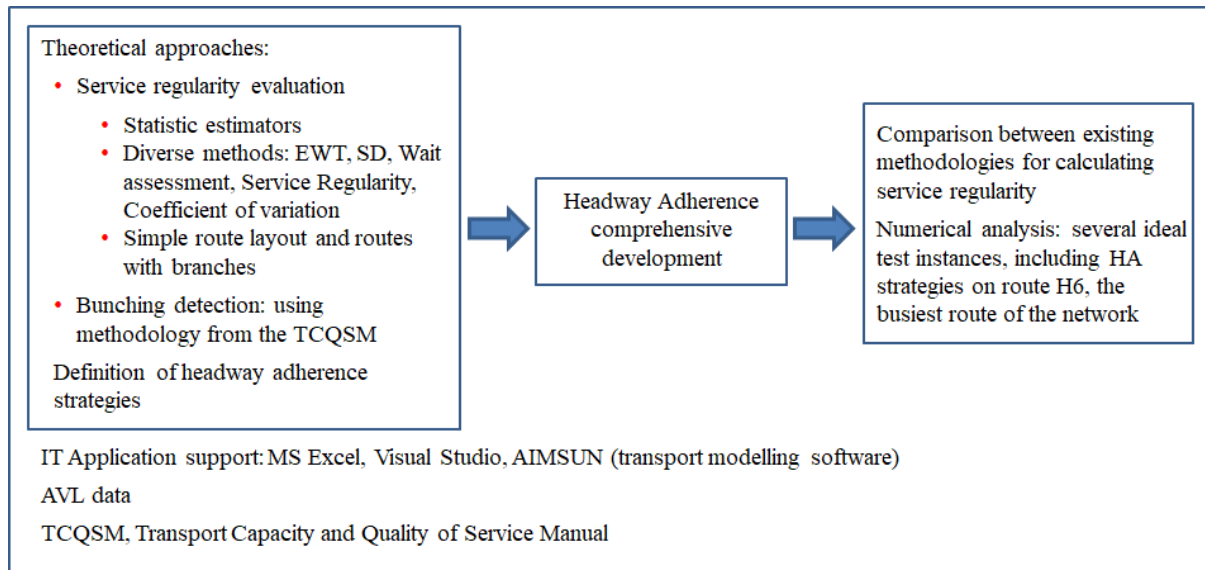
**Figure 6**. Headway adherence methodology generic diagram
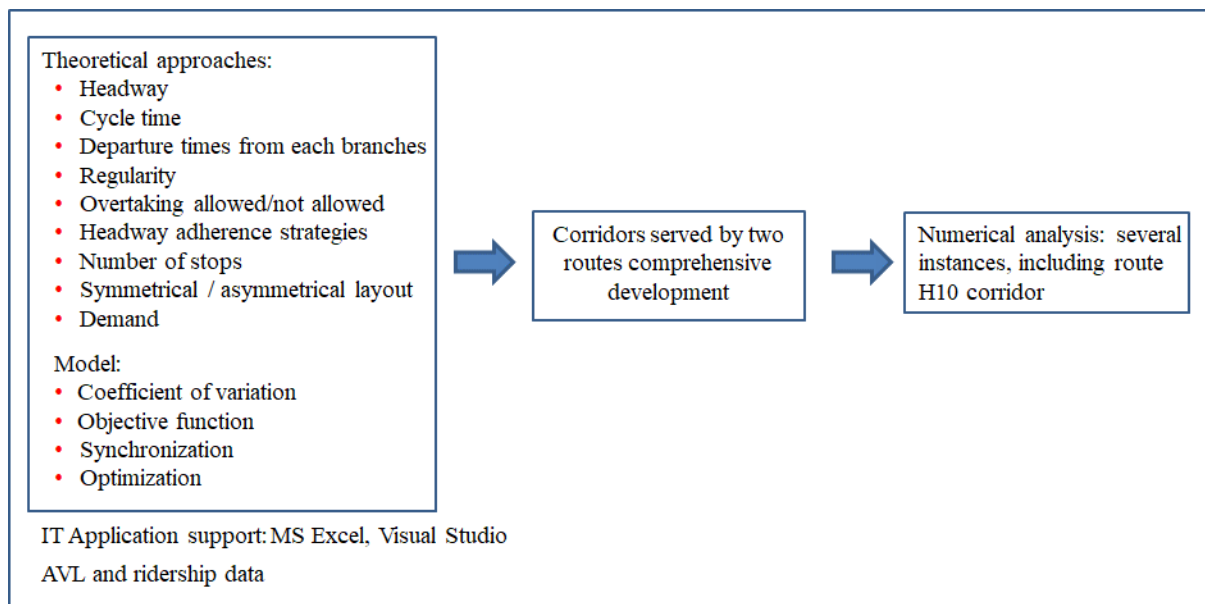


**Figure 7**. Corridors served by two routes methodology generic diagram
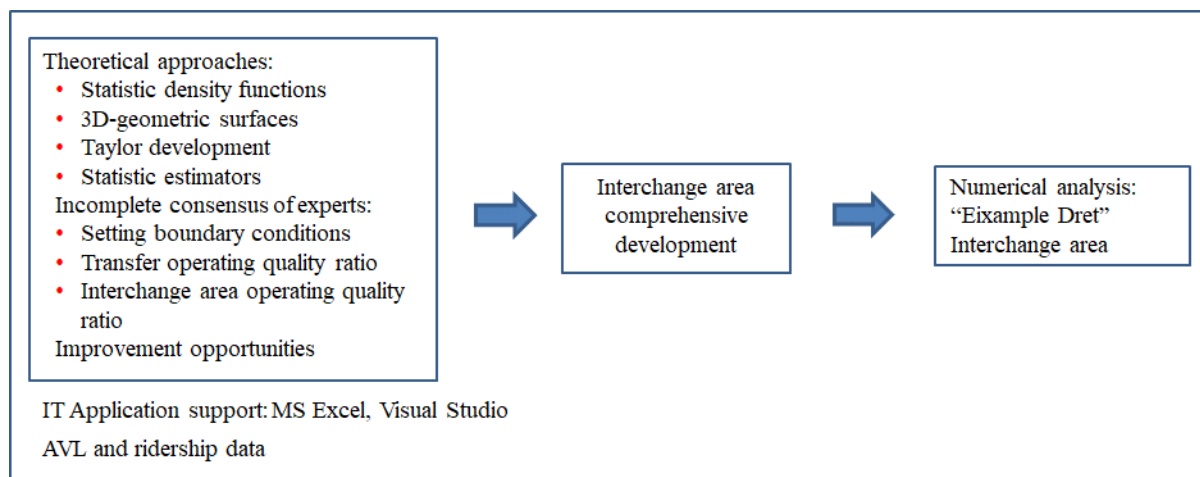
**Figure 8**. Transfer area methodology generic diagram

## 3.2 Scheduled timetables

This chapter defines a methodology for constructing efficiently scheduled timetables on premium bus routes, operated on a time-headway basis; and, as an example, it also includes the procedure applicable to the case study of route H12 from Barcelona's New Bus Network.

A bus route schedule is made of two differentiated parts: the programming of route vehicles and the distribution of driver shifts and applies to a specific type of day (working day, Saturday or bank holiday) and at one annual period (winter, summer, Easter, Christmas, etc.).

To prepare the programming of route vehicles, the following data is needed:
— Route code and description
— Type of bus and depot in charge of providing the service (in medium-sized or large agencies with several operation centres)
— Route layout (outbound and inbound)
— Route terminals and intermediate checkpoints
— Mileage between successive checkpoints
— Timetables (travel times and recovery times)
— Minimum waiting times and at the route terminals
— Supply: number of vehicles per time slot

To prepare the distribution of driver shifts, the following data is needed:
— Work conditions
    — Minimum and maximum shift length
    — Number and length of breaks
    — Maximum shift span
    — Any other kind of restriction or constraint
— Shift change points

This chapter will focus on the elaboration of the bus route timetables, a fundamental element of the first part of the preparation of a schedule, defining a methodology that allows for its optimisation, which will result in obtaining a more efficient timetable.

There are several IT tools to support scheduling (HASTUS, Trapeze, etc.). One of the most commonly used by many worldwide agencies is HASTUS, developed by the Canadian company, Giro.

The proposed methodology is based on the optimisation of the recovery times, i.e. time that buses remain stopped at the terminals, the fulfilment of departures from terminals (quality), and the resource minimisation (cost), using the support of HASTUS. Main advantages are the usage of real travel times; that is, the defined travel times are based on the actual travel times, recorded by the AVL system. The recovery time is calculated based on the variability of the actual trips, recorded by the AVL system, and guarantees departures at terminals by 97.5%. A more precise operational information is provided to the customer. Both the information about the bus status (ahead or behind schedule) supplied to the driver and the operator, as well as the predictive information received by the customer about next bus arrivals, is better because the defined travel time is consistent with its necessary value. There is greater stability concerning headway adherence: the unification of time slots avoids the disparity time-headways throughout the day. Finally, an increase in regularity is achieved due to the minimisation of deviations between scheduled and actual travel times. Also, applying this method, the homogenization of criteria for making up schedules is guaranteed: a common rule is applied, regardless of the person who executes the data extraction and the construction of the timetables.

For the application of the procedure, the working day winter period timetable for route H12, a premium route from Barcelona's New Bus Network, will be made up and explained in detail. This route has a length of 24.5 km, a provision of 21 vehicles, and it's an entirely rectilinear route, with the two direction trips through the same axis, Gran Via de les Corts Catalanes, in Barcelona, and Granvia Av., in l'Hospitalet de Llobregat.

### 3.2.1 Service Planning: drawing up timetables

The objective is to establish the criteria for the construction of timetables (time slots, the time between trips and total trip time) and estimate the RT (recovery time) on high-level service bus routes. The method is oriented to maximise the headway adherence and to minimise the need for resources, providing the necessary recovery time for any incidences at the terminals. When lower than the actual transit times are scheduled, buses can't fulfil their service and,

consequently, regulatory measures (which are extraordinary in general) become normal. On the contrary, higher than the actual transit times penalise the operating service costs.

The study will be based on three significant issues: Travel Time, Recovery Time and Time Slot. Determinant aspects will be:

1.- Systematic deviations concerning the scheduled travel time affect the operating service costs.

2.- The heterogeneity (variability) existing in each Time Slot requires a specific Recovery Time (cost) to secure departures at the terminals (quality).
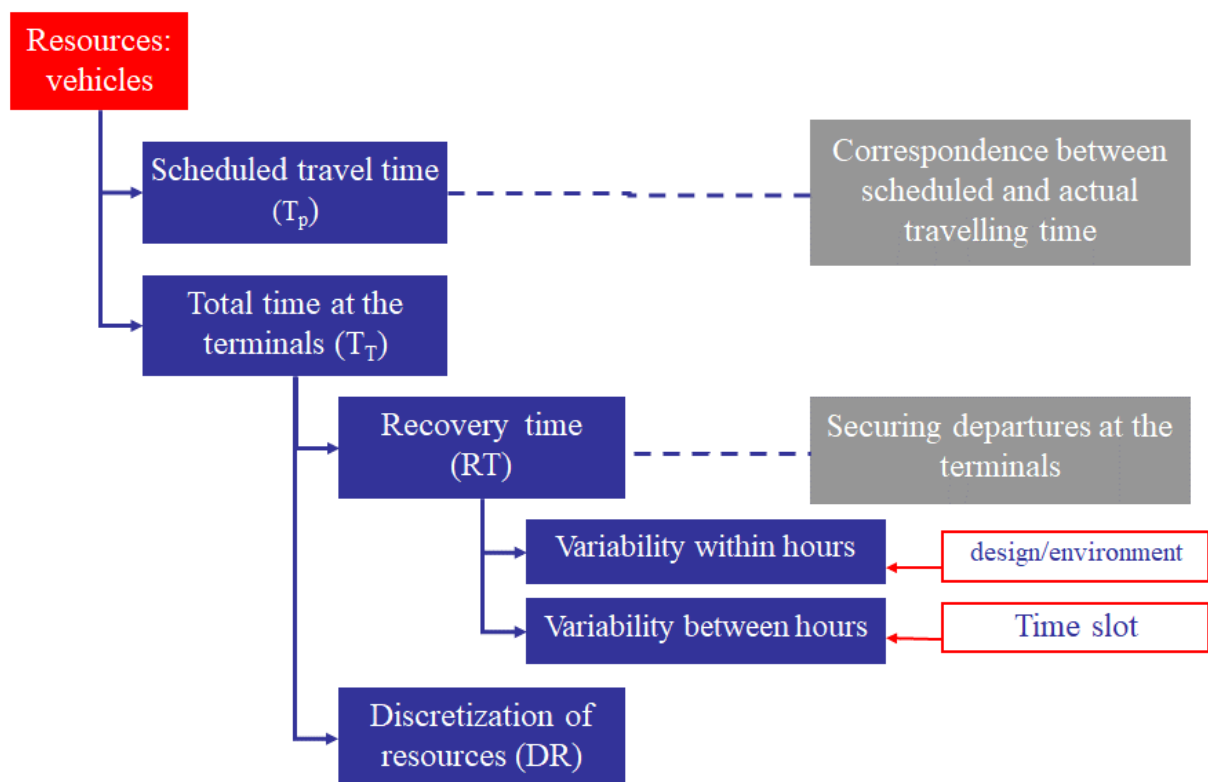


**Figure 9**. Summary diagram

### 3.2.1.1  Scheduled travel time, $T_p$

The aim is achieving the maximum concordance between actual travel times ($T_{ij}$: transit time on itinerary i, trip j) and scheduled travel time ($T_p$) when s trips ($TR_1$, $TR_2$, …, $TR_s$) are

considered in any time slot. It can be demonstrated that the maximum concordance is reached when the scheduled travel time ($T_p$) fits with the average actual travel time in each time slot $(T..)_{TS}$, e.g., $T_p = T..$

$$min_{T_P}\left\{\sum_{i=1}^{p}\sum_{j=1}^{n}|T_{ij} - T_P|\right\} = min_{T_P}\left\{\sum_{i=1}^{p}\sum_{j=1}^{n}(T_{ij} - T_P)^2\right\}$$

$$= min_{T_P}\left\{\sum_{i=1}^{p}\sum_{j=1}^{n}(T_{ij} - T_{..})^2 + \sum_{i=1}^{p}\sum_{j=1}^{n}(T_{..} - T_p)^2 + 2\cdot\sum_{i=1}^{p}\sum_{j=1}^{n}(T_{ij} - T_{..})(T_{..} - T_p)\right\} = (*)$$

$$2\cdot\sum_{i=1}^{p}\sum_{j=1}^{n}(T_{ij} - T_{..})(T_{..} - T_p) = 2\cdot\left\{\sum_{i=1}^{p}(T_{..} - T_p)\right\}\left\{\sum_{j=1}^{n}T_{ij} - \sum_{j=1}^{n}T_{..}\right\} = (**)$$

$$(**) = 2\cdot\left\{\sum_{i=1}^{p}(T_{..} - T_p)\right\}\cdot\left\{\sum_{j=1}^{n}T_{ij} - \frac{1}{n}\left(\sum_{j=1}^{n}T_{ij}\right)\cdot n\right\} = 0$$

$$(*) = min_{T_P}\left\{n\cdot p\cdot\sigma_{ST}^2 + n\cdot p\cdot(T_{..} - T_p)^2 + 0\right\} = min_{T_P}\left\{n\cdot p\cdot(T_{..} - T_p)^2\right\}$$

but, $n\cdot p\cdot(T_{..} - T_p)^2 \geq 0 \Rightarrow$ we'll get the min when: $n\cdot p\cdot(T_{..} - T_p)^2 = 0 \Rightarrow$

$$T_P = T_{..} \tag{1}$$

Where:

$T_p$: is the scheduled travel time

$T_{ij}$: is the actual travel time in the j-trip (j=1, ..., n) into the i-hour (i=1, ..., p)

$T..$: is the average travel time within the time slot.

### 3.2.1.2 Recovery Time

The total time a bus stays at the terminal makes possible (a) to ensure the break time (layover time) of the driver and (b) to provide an on-time departure for the next trip (headway adherence). Accepting that actual travel times are adjusted to a normal distribution, the total time at the terminal ($T_T$) for any time slot that ensures the available resources (vehicles) for a 97.5% on-time departure is given by the expression:

$$(T_T)_{TS} = \max\{DBT, RT_{TS}\} = \max\left\{DBT, 1.96\cdot\left(\frac{\sum_{i=1}^{p}\sum_{j=1}^{n}(T_{ij} - T_{..})^2}{np}\right)^{1/2}\right\} \tag{2}$$

Where:

DBT: Driver's Break Time, fixed by law or company agreement

$RT_{TS}$: Recovery Time
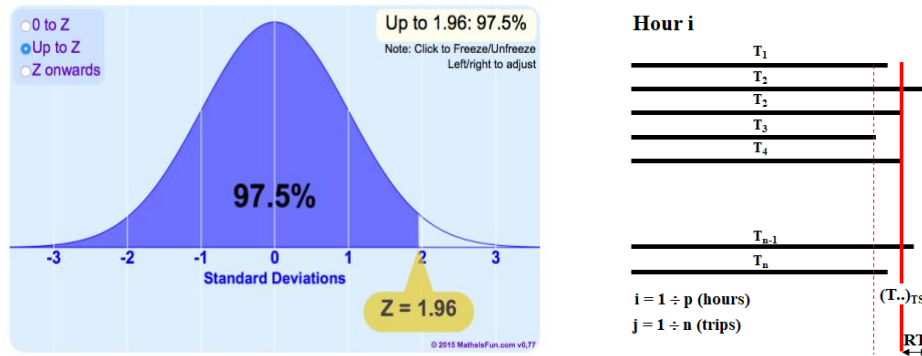
**Figure 10**. a) Corresponding value to a probability of 97.5% in a Normal distribution. b) Calculation of RT from T..

The variability can explain heterogeneity in travel times for a specific time slot within hours (primarily attributable to the route layout design) and variability between hours (fundamentally due to the environmental conditions and time slot definition). The quantitative translation of this conceptual statement requires considering the breakdown of the sum of squares into grouped data structures. In this respect, for the accumulated transit times within a p hour time slot, the algebraic relation:

$$\sum_{i=1}^{p}\sum_{j=1}^{n}\left(T_{ij}-T_{..}\right)^2 = \sum_{i=1}^{p}\sum_{j=1}^{n}\left((T_{ij}-T_{i.}) + (T_{i.} - T_{..})\right)^2 = \sum_{i=1}^{p}\sum_{j=1}^{n}\left(T_{ij}-T_{i.}\right)^2 + \sum_{i=1}^{p}\sum_{j=1}^{n}(T_{i.}-T_{..})^2$$

$$+2\sum_{i=1}^{p}\sum_{j=1}^{n}(T_{ij}-T_{i.})\cdot(T_{i.}-T_{..}) = \sum_{i=1}^{p}\sum_{j=1}^{n}\left(T_{ij}-T_{i.}\right)^2 + \sum_{i=1}^{p}n(T_{i.}-T_{..})^2 + 2\sum_{i=1}^{p}\left[(T_{i.}-T_{..})\sum_{j=1}^{n}(T_{ij}-T_{i.})\right]$$

$$= \sum_{i=1}^{p}\sum_{j=1}^{n}\left(T_{ij}-T_{i.}\right)^2 + \sum_{i=1}^{p}n(T_{i.}-T_{..})^2 + 2\sum_{i=1}^{p}(T_{i.}-T_{..})\cdot(nT_{i.}-nT_{i.})$$

$$= \sum_{i=1}^{p}\sum_{j=1}^{n}\left(T_{ij}-T_{i.}\right)^2 + \sum_{i=1}^{p}n(T_{i.}-T_{..})^2$$

$$\underbrace{\frac{\sum_{i=1}^{p}\sum_{j=1}^{n}\left(T_{ij}-T_{..}\right)^2}{np}}_{s^2_{TS}} = \underbrace{\frac{\sum_{i=1}^{p}\sum_{j=1}^{n}\left(T_{ij}-T_{i.}\right)^2/n}{p}}_{s^2_{WH}} + \underbrace{\frac{\sum_{i=1}^{p}(T_{i.}-T_{..})^2}{p}}_{s^2_{BH}}$$

$$RT_{TS} = 1.96\left(\frac{\sum_{i=1}^{p}\sum_{j=1}^{n}\left(T_{ij}-T_{..}\right)^2}{np}\right)^{1/2} = 1.96(s^2_{BH} + s^2_{WH})^{1/2} \qquad (3)$$

being:

$s_{BH}$: is the variability between hours

$s_{WH}$: is the variability within hours

reveals that the transit times variability corresponding to the trips within a certain time slot can be broken down into the sum of two components: the variability between hours $s_{BH}^2$ and the variability within hours $s_{WH}^2$.

### 3.2.1.3 Time slots

The objective is to construct time slots combining homogeneity and spread over a wide range. The criterion ±1 minute makes it possible to cover a wide range and minimises the travel time divergences related to the variability within hours since travel times differ at most in 2 minutes (Table 1). A minimum of 1-hour time slot is typically used. Exceptionally, 30-minute have been considered for periods in which the activity of the city has a high variability (early in the morning and in the evening on a working day, student drop-off and pick-up times, during rush hours in commercial or recreational areas, etc.).

**Table 1**. Calculation of $s_{BH}$ max considering all possible cases, using the criterion ±1minute

| Case | Average times | Standard deviation, $s_{BH}$ |
|:---:|:---:|:---:|
| 1 | T-1, T, T+1 | $\left(\dfrac{1^2 + 0^2 + 1^2}{2}\right)^{1/2} = 1$ |
| 2 | T-1, T-1, T+1 | $\left(\dfrac{0.66^2 + 0.66^2 + 1.33^2}{2}\right)^{1/2} = 1.15$ |
| 3 | T-1, T+1, T+1 | $\left(\dfrac{1.33^2 + 0.66^2 + 0.66^2}{2}\right)^{1/2} = 1.15$ |

This way $s^2_{BH}=1.15^2=1.32$ min.

### 3.2.1.4 Probabilistic headway

The probabilistic headway is achieved according to the travel times and the number of resources (buses) of a particular route, this way:

$$H_{TS}(p) = \frac{((\bar{T} + RT)_o + (\bar{T} + RT)_i)_{TS}}{Nv_{TS}} \quad (4)$$

being:

$H_{TS}$: is the possibilistic headway within the time slot, TS

$\bar{T}$: is the average travel time within the time slot, TS

$RT$: is the recovery time within the time slot, TS

$Nv$: is the available number of vehicles within the time slot, TS

o: outbound, i: inbound

### 3.2.1.5  Data filtering

The need to have reliable information leads to remove all those transit times corresponding to atypical situations (non-regular service incidences and errors associated with information systems). In this respect, the proposal is applying the same criteria described in Salicrú et al., (2011). The aberrant transit time records between two consecutive stops have been eliminated (differences in transit times between stops, greater or equal than a fixed constant), as well as the atypical records in transit times between two consecutive stops and in accumulated transit times until arriving at each route stop (differences in transit times that are out of the median confidence interval).

### 3.2.2  Methodology

The semiautomated construction of schedules forces to carry out the following tasks: a) obtaining and exporting historical transit times through stops and checkpoints; b) filtering and debugging data; c) setting up homogeneous time slots; d) obtaining transit times between checkpoints and total travel times; e) setting up recovery times; and f) determining the time headway (compatible with available resources). The objectives of all these components are displayed schematically in Table 2, and more detailed specifications come right after.

**Table 2**. Methodology components and their objectives

| Component | Objective |
|---|---|
| *Obtaining and exporting historical data* | To know the historical references about transit times at the stops (checkpoints) |
| *Filtering and debugging of atypical data* | To have reliable information about transit times at the stops (checkpoints) |

| | |
|---|---|
| *Transit times between stops and checkpoints* | To maximise the concordance between actual transit times and scheduled ones (estimated with historical data) |
| *Building homogeneous time slots* | To stabilise the transit times in programming the trips |
| *Setting up recovery times within times slots* | To secure departures at the origin (according to a pre-set trip percentage) |
| *Determining the possibilist time headway* | To establish (predict) the minimum time headway, compatible with the available resources |

On headway basis routes, and mainly, for high-performance routes, optimisation is achieved under the following conditions:

— ***Obtaining and exporting historical data*** to have the historical data corresponding to the travel times and transit times between consecutive stops/checkpoints. This historical information will be used as a reference when planning (repository: HASTUS).

— ***Filtering and debugging atypical data*** to eliminate those transit times corresponding to atypical or abnormal situations. This process is supported by the application of confidence intervals for the mean (IT application: HASTUS).

— ***Travel times between stops (consecutive and full trip)***. The aim is to fit the scheduled travel times to the actual ones. The maximum concordance is achieved when the scheduled travel time fits the actual average transit times within a time slot (IT application: HASTUS).

— ***Building homogeneous time slots***. Some research must be done to determine a criterion that, with the minimum cost, ensures stability in the programmed transit times. In the city of Barcelona, the criterion ± 1 minute, works correctly. Thus, the time slot groups consecutive hours in which the average transit times differ by at the most 2 minutes (Non-automated procedure).

— ***Recovery time (RT) within time slots***. To guarantee 97.5% of the departures at the terminal, the RT is evaluated according to Eq. (3), having considered the variability of the trips within the time slot, the variability of the trips between hours and the variability of the journeys within each hour (Non-automated procedure).

— ***Possibilist time headway***. The possibilist time headway is obtained according to the travel times and the number of available vehicles. According to Eq. (4), the average transit time within the slot time (outbound and inbound trips), the recovery time of incidences within the time slot (outbound and inbound trips) and the available number of vehicles within the time slot (Non-automated procedure).

Fig. 11 shows in detail the activity flow that make up the construction process of timetables: obtaining information (IT application: HASTUS), treatment of data (Worksheet environment: Excel) and construction of the schedule by individual journeys (IT application: HASTUS).
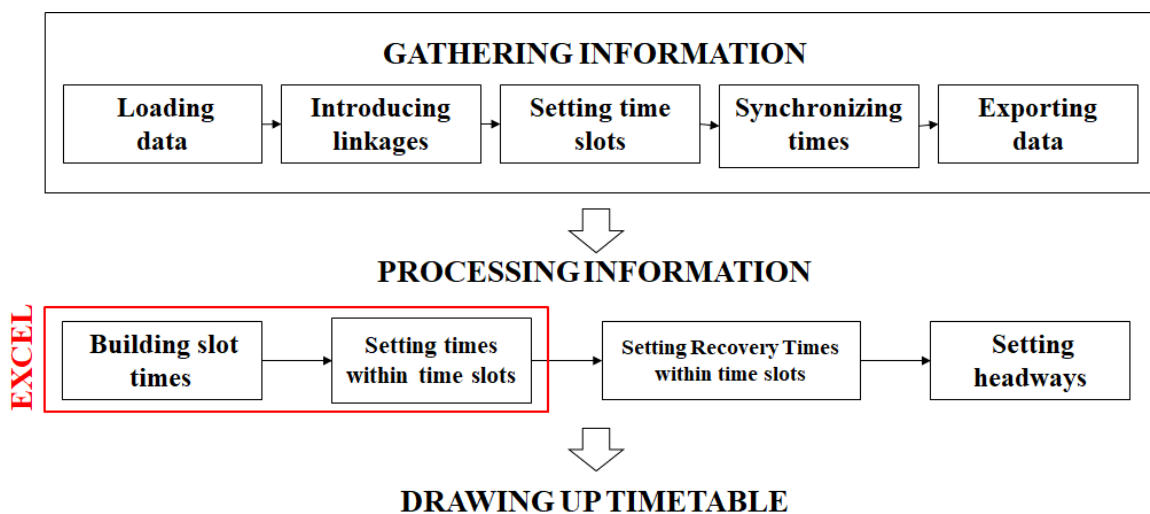
**Figure 11**. Workflow for drawing up timetables

## 3.3 Headway adherence

This chapter review the existing methodologies for calculating service regularity on a bus route. Putting aside the specific peculiarities and small differences that can be introduced, it can be said that there are five generalised metrics to calculate the regularity: The Excess Wait Time, the Standard Deviation, the Wait Assessment (absolute regularity band), the Service Regularity (proportional regularity band), and the Coefficient of Variation. Also, there is also a general calculation procedure for regularity on routes with special layouts, considering its different branches or antennas.

Following the procedure included in the Transport Capacity and Quality of Service Manual, TCQSM[1], the bus bunching calculation methodology is also explained, as the headway adherence of buses, using the values of the Coefficient of variation of the headway, tabulated according to various thresholds indicating the corresponding levels of service achieved by the bus carousel.

It also proposes a new dynamic bus control strategy aimed at reducing the adverse effects of time-headway variations on route performance, based on real-time bus tracking data at stops. On high-demand routes, any delay of a single vehicle ends up causing an unstable motion of buses and producing the bus bunching phenomena. This strategy controls the cruising speed of buses and considers the extension of the green phase of traffic lights at intersections when a bus is significantly delayed. The performance of this strategy will be compared to the current static operation technique based on the provision of unproductive slack times at holding points. An operational model is presented to estimate the operational effects of each controlling strategy, considering the vehicle capacity constraint. Controlling strategies are assessed in terms of passenger total travel and waiting time, as well the coefficient of variation of time-headways.

Moreover, the number of vehicles needed to provide the service is estimated in comparison to the holding point strategy. The effects of controlling strategies are tested in an idealised bus

---

[1] The TCQSM is a handbook to assess the public transport quality; edited by the Transportation Research Board of the National Academies, it has already become a worldwide reference tool in the transport field.

route under different operational settings and the bus route of the highest demand in Barcelona by simulation. The results show that the proposed dynamic controlling strategy reduces passenger travel time by 21-37% as well as the coefficient of variation of headway by 78-83% regarding the uncontrolled case, providing a bus performance like the expected when time disturbance is not presented.

### 3.3.1  Methods for calculating service regularity on bus routes

There are several methods for estimating bus service regularity. The definition and characteristics of the most common procedures are explained below, giving their main strengths and weaknesses and several examples.

#### 3.3.1.1  EWT, Excess Wait Time

The Excess Wait time (EWT) methodology, used by London Buses, is a measure of perceived regularity, measuring the average additional waiting time passengers experience as compared to the waiting time they expect. The lower the EWT, the more likely it is that passengers will not wait more than scheduled and perceive the service as regular.

$$AWT = \frac{\sum_{i=1}^{n} AH_i^2}{2 \cdot \sum_{i=1}^{n} AH_i}; \ SWT = \frac{\sum_{i=1}^{n} SH_i^2}{2 \cdot \sum_{i=1}^{n} SH_i}$$

$$EWT = AWT - SWT \tag{5}$$

being:

$AH$: actual headway

$SH$: schedued headway

$EWT$: Excess wait time

$AWT$: actual wait time

$SWT$: scheduled wait time

For example, a 10 min headway route has an SWT of 5 minutes (e.g. half the headway). The EWT methodology assumes uniform arrival of passengers. An EWT of 1-minute means that customers are likely to wait 6 min instead of the expected 5 min.

The EWT is not designed to be used with irregular scheduled headways, which could even lead to a negative EWT score. However, the EWT is the only method tested that is indeed incorporating the experience of all passengers, as its output is a result of all data in the dataset.

### 3.3.1.2 Standard deviation

We calculate the standard deviation of the difference between scheduled and actual headways.

$$\sigma = \left( \frac{1}{N} \cdot \sum_{1}^{N} (AH_i - SH_i)^2 \right)^{1/2} \tag{6}$$

being:

$$AH: actual\ headway;\ SH: schedued\ headway$$

This indicator does not normalise for differences in scheduled headways. It's expressed in minutes. For example, a standard deviation of 2 minutes means that approximately 68% of actual headways are within ±2 minutes from the scheduled headway. A pre-requisite to use this indicator is that the data is normally distributed. A sufficiently large data sample is therefore necessary.
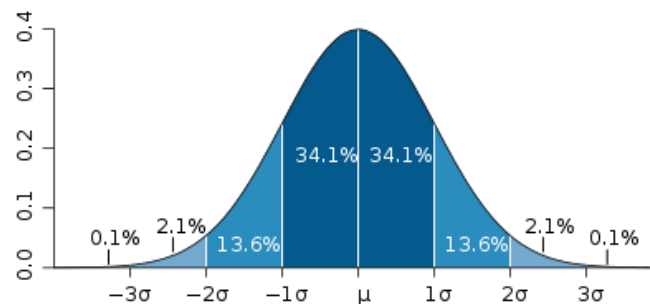


**Figure 12**. Standard deviation graph

### 3.3.1.3 Wait assessment and Service regularity

These regularity KPI's are the percentages of headways that deviate no more than a specified amount, the regular threshold, from the scheduled interval. The 'regular threshold' can be a percentage of the scheduled headway (Service regularity) or an absolute number of minutes (Wait assessment). These indicators, likely due to their simplicity, are currently most used by bus operators; however, the regular thresholds are often defined differently.

— **Regularity within the absolute band**. The percentage of actual headway is within ±2 minutes of scheduled headway. The higher the percentage, the more regular the service is.

— **Regularity within the proportional band** (20% of scheduled headway). The percentage of actual headway within ±20% of scheduled headway. The higher the percentage, the more regular the service. The width of the proportional band may vary if the scheduled headway is not constant.

Unlike EWT and the standard deviation, these methods are therefore subjective, e.g. the chosen regular threshold can determine which of the bus operators performs best; However, the output of these indicators, e.g. the percentage of service, which is regular, is the easiest to communicate.

Although these indicators represent the proportion of regular services perceived by customers, they do not provide information on the level of irregularity that the other customers have experienced; an observation is either regular or irregular. In other words, a headway that is 1 minute longer than the regularity threshold is treated in the same way as a headway that is 10 minutes longer than allowed. Both EWT and the standard deviation indicators do take all data into account in their calculations.

Some agencies that use this Wait Assessment are Brussels (STIB-MIVB), Milan (ATM), New York City (NYCT), Paris (RATP), Singapore (SMRT), and Vancouver (CMBC). Lisbon (Carris) uses Service Regularity.

### 3.3.1.4 The coefficient of variation of headways

The coefficient of variation of headways, $C_{v.h}$ is defined as the standard deviation of headways (representing the range of actual headways), divided by the average (mean) headway.

$$C_{v,h} = \frac{s(h_A)}{\overline{h_A}} \tag{7}$$

being:

$C_{v.h}$:    *Coefficient of variation*
$s$:    *Standard deviation*

$h_A:$    *Actual headway*

$\bar{h}_A:$    *Average actual headway*

This KPI is not immediately or intuitively understandable for senior management or non-expert external stakeholders, and bus agencies rarely use it, but it's quite important a lot when measuring headway adherence and it will be studied in more detail in 3.4. The lower the coefficient is, the better adherence to the headway is achieved.

### 3.3.1.5   The graphics distribution of time-headway (Visual headway)

A visual methodology based on the time-headways distribution corresponding to the whole service span is proposed to determine service regularity. All scheduled and actual daily time headways are grouped in 1-minute slots.

Fig. 13 shows an example of Barcelona's New Bus Network premium routes. The scheduled headways are distributed mostly in a band ranging from 6 to 8 minutes. Nevertheless, the actual operation is distributed over a much broader band, spread out in practically the entire spectrum from 0 to 15 minutes. This route would straightforward require applying any of the headway adherence strategies explained in section 3.3.6.

**Actual and scheduled headways < 15'**
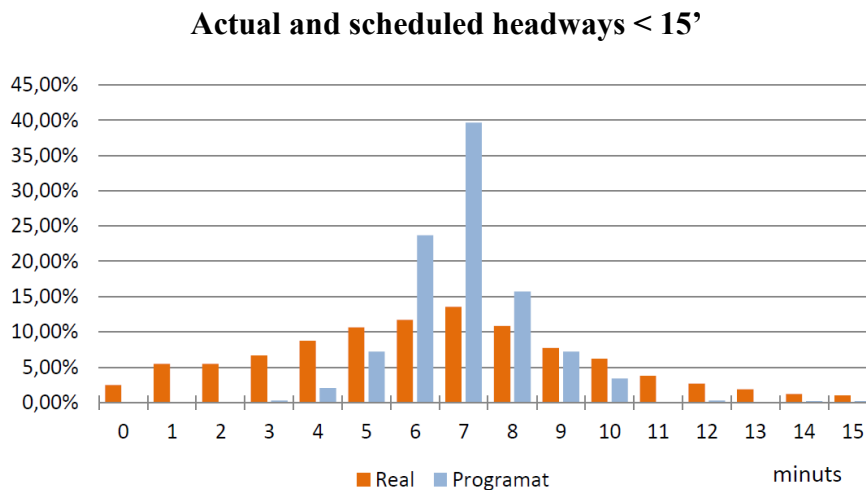


**Figure 13**. Actual and scheduled time-headway (<15 minutes) during the whole day service

### 3.3.1.6   Comparison between the six methods

Table 3 gives a comparison of several methodologies to calculate bus service regularity, described above:

**Table 3**. Comparison of service regularity metrics

|  | EWT | SD | WA | SR | $C_{v,h}$ | VH |
|---|---|---|---|---|---|---|
| **Communication** | Easy | Complex | Easy | Easy | Complex | Easy |
| **Subjective / objective** | Objective | Objective | Subjective | Subjective | Objective | Objective |
| **Customer oriented** | Yes | Partially | No | No | No | Yes |
| **Long headways** | Penalises | Penalises | No penalises | No penalises | No penalises | No penalises |
| **Condition requirements** | Not to be used with irregular scheduled headways | Normal distribution | Headways at least longer than regularity threshold | Similarly, scheduled headways | Normal distribution | N/A |
| **Other** | Assumes uniform arrival of passengers | A sufficiently large data is necessary | usually: ± 2 minutes of scheduled headway | usually: ± 20 % of scheduled headway | Similarly, scheduled headways | Valid in any condition |

EWT: Excess Wait Time, SD Standard Deviation, WA: Wait Assessment, SR Service Regularity, $C_{v,h}$ Coefficient of Variation, and VH, Visual Headway

### 3.3.2 Calculating service regularity on routes with special layouts

Calculating bus service regularity on routes with several antennas at the ends, using the above formulation.
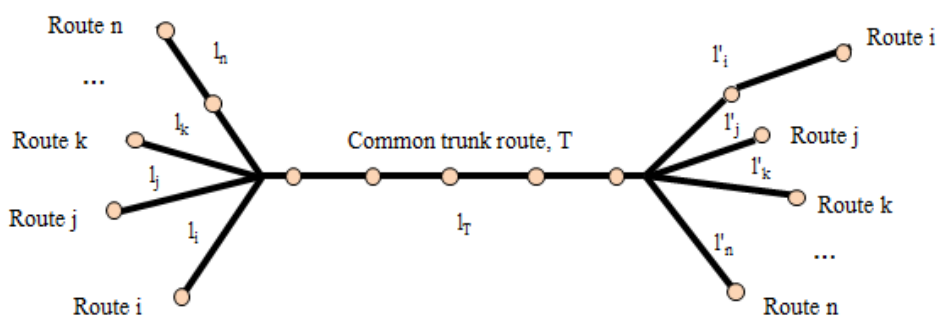


**Figure 14**. The route with several antennas.

A methodology for calculating service regularity based on the number and length and demand of the antennas is proposed.

Two restrictions will also be applied: the number of antennas will be limited to 3, and only those cases with the same range of headways will be considered.

The formula for calculating the regularity of the set, based on the partial regularities of the various sections, (common trunk and antennas), depending on their lengths, would be as follows:

$$Reg_{br} = \frac{Reg_T L_T + \sum_{I=1}^{n} Reg_i l_i + \sum_{I=1}^{n} Reg'_i l'_i}{L_{total}} \tag{8a}$$

being:

$Reg_{br}$: *Regularity overall branched route*
$Reg_T$: *Regularity on common trunk*
$L_T$: *length common trunk*
$Reg_i$: *Regularity corresponding to left branch i. i=1÷n*
$l_i$: *length corresponding to left branch i. i=1÷n*
$Reg'_i$: *Regularity corresponding to right branch i. i=1÷n*
$l'_i$: *length corresponding to right branch i. i=1÷n*
$L_{total}$: *Total length*

Introducing the demand for each section, a second proposal to calculate the regularity of the system would be:

$$Reg_{br} = \frac{Reg_T L_T D_T + \sum_{I=1}^{n} Reg_i l_i d_i + \sum_{I=1}^{n} Reg'_i l'_i d'_i}{L_{total} D_{total}} \tag{8b}$$

being:

$Reg_{br}$: *Regularity overall branched route*
$Reg_T$: *Regularity on common trunk*
$L_T$: *length common trunk*
$D_T$: *Average daily Demand corresponding to common trunk*
$Reg_i$: *Regularity corresponding to left branch i. i=1÷n*
$l_i$: *length corresponding to left branch i. i=1÷n*
$d_i$: *Average daily Demand corresponding to left branch i. i=1÷n*
$Reg'_i$: *Regularity corresponding to right branch i. i=1÷n*
$l'_i$: *length corresponding to right branch i. i=1÷n*
$d'_i$: *Average daily Demand corresponding to right branch i. i=1÷n*
$L_{total}$: *Total length*
$D_{total}$: *Total average daily demand*

For the calculation of the service regularity of each section, any of the five previous procedures can be used. Nevertheless, the methodology, once chosen, must be the same everywhere.

### 3.3.3 Detection, control and mitigation of the Bus Bunching effect

When transit vehicles operate at headways of 10 minutes or less, vehicle bunching can occur. This way, two or more vehicles on the same route arrive together or in close succession, followed by a long gap between them.

The bunching effect can be measured in terms of headway adherence, the regularity of transit vehicle arrivals with respect to the scheduled headway, and it is calculated as the coefficient of variation of headways, $C_{v.h}$: the standard deviation of headways (representing the range of actual headways), divided by the average (mean) headway. Eq. (7).

The headway variations are calculated as the actual headway between consecutive transits and the scheduled headway. The coefficient of variation is a non-dimensional and non-negative KPI. The usage of the coefficient of variation for estimating service regularity (quality offered to customers) is statistically consistent. Additionally, the use of the coefficient of variation has a physical meaning, because it simulates the overrun of the users in terms of waiting time at the tops due to the irregularity of service.

For that matter, the average waiting time of the users at a bus stop, $\overline{w}$, may be estimated as shown in Eq. (9), TCQSM, (TRB, 2009):

$$\overline{w} = \frac{1}{2} \cdot \overline{h} \cdot (1 + C_{v,h}^2) \qquad (9)$$

So, the user average waiting time at the stops increases in a quadratic way with the coefficient of variation of the bus headway. It can be concluded that service regularity affects the user's costs and the KPI that reflects all the above is the coefficient of variation.

The second part of the parenthesis of Eq. (9) estimates the waiting time increase of the users regarding an ideal situation where the system is working perfectly, with full regularity. In that case, the value of the coefficient of variation would be 0 and the average waiting time would be just half the transit headways and service regularity will be evaluated according to a level of service A. However, when the coefficient of variation exceeds the reference value of 0.5, the simultaneous arrival of buses to the stops will occur. In that case, the level of service will be E or even F, if $C_{v,h} > 0.75$.

The Transit Capacity and Quality of Service Manual, $3^{rd}$ edition, chapter 5/Quality of Service Methods, proposes a service regularity assessment while setting the various level of service based on the coefficient of variation of the headway (shown in Table 4).

According to the TCQSM, the coefficient of variation of headways can also be related to the probability, P that a given transit vehicle's headway, $h_i$ will be off-headway by more than one-half the scheduled headway h. Twice the area measures this probability to the right of Z on one tail of a Normal distribution curve, where Z, in this case, is 0.5 divided by $C_{v,h}$. See Appendix C.2.

**Table 4**. Levels of service according to service regularity of a bus route. Source: TCQSM, Transit Capacity and Quality of Service Manual

| LoS | $C_{vh}$ | $P(abs[h_i - h] > 0,5 \cdot h)$ | Passenger and Operator Perspective |
|:---:|:---:|:---:|---|
| A | 0,00 – 0,21 | ≤2% | Service provided like clockwork |
| B | 0,22 – 0,30 | ≤10% | Vehicles slightly off headway |
| C | 0,31 – 0,39 | ≤20% | Vehicles often off headway |
| D | 0,40 – 0,52 | ≤33% | Irregular headway, with some bunching |
| E | 0,53 – 0,74 | ≤50% | Frequent bunching |
| F | ≥0,75 | >50% | Most vehicles bunched |

Note: it applies to average scheduled headway of 10 minutes or less

### 3.3.4 Strategies for headway adherence and total user travel time improvement in Bus systems

#### 3.3.4.1 Background

Transit agencies have promoted the creation of expensive ICT systems to track the fleet, calculate the bus regularity and perform control strategies to maintain the desirable headway. This way, several control strategies have been proposed to tackle the bus bunching effect. These strategies modify the natural motion of buses to keep the vehicle temporal spacings constant. Traditionally, the bus bunching is addressed deploying recovery times at holding points in the bus route (Barnett, 1974; Turnquist, 1981; and Rossetti and Turitto, 1998). Nevertheless, this recovery time increases the round-trip time of buses and therefore, increases the fleet size allocated to this bus route. Other studies propose dynamic strategies that hold vehicles at stops a variable amount of time to alleviate the propagation of random

disruptions in a short time horizon (Eberlein et al. 2001; Dessouky et al. 2003; Adamski and Turnau, 1998). Other contributions determine control theory approaches to modify the kinematic variables of each vehicle depending on the exact location of other vehicles in the route. Daganzo (2009) defines an adaptive variable cruising speed for bus routes with good frequencies. If a vehicle is running close to the vehicle ahead, the former vehicle is slowed down. The modification of speed is proportional to the difference between the target and the actual headway. Nevertheless, control strategies generally achieve good regularity at the expenses of high operating costs. In fact, all control strategies maintain the time-headway regularity allocating slacks or slowing the motion of buses along the route.

Apart from the well-known static allocation of slack times at holding points, other dynamic control strategies are considered over the following subsections. These new and innovative adaptive control strategies to tackle the bus bunching effect require the real-time headway monitoring of bus departures at stops and a robust methodology to measure the headway variation. These dynamic strategies are based on both the modification of speed profiles of buses and the deployment of dynamic traffic light priority for delayed buses. Therefore, delayed buses are speed up since the green time is extended when they arrive at signalized intersections. This strategy may help bus agencies minimizing the operating cost of control protocols.

### 3.3.4.2   Modelling framework

A dynamic bus following a model like that introduced in Daganzo (2009) is presented for describing the physics of bus behaviour and their trajectories. This method may be adaptive to the actual performance of the bus system. It can reproduce strategies controlling the headway variation and oscillatory effects. We consider a straight bus route of length 2L as it is depicted in Fig. 15. Buses run along the route in two directions (from A to B and from B to A). The route presents 2N bus stops, where the distance between stop s and s+1 is denoted by ls. Let J be the total number of buses operating the route in the two directions. Each bus is labelled by j=1, …, J and is supposed to travel the roundtrip, stopping at each stop s, s=1, …, 2N. It is considered that bus $j=j^*+1$ is in the rear of bus $j^*$ ($j^*$=1, ..., J-1). Since buses may operate the route several cycles, the stops are labelled by s=1+(k2N), 2+(k2N), ..., 2N+(k2N), where k ($0 \leq k < \infty$) is an integer number that denotes the completed number of round trips made by the bus in the line. Stops s=1+(k2N) and s=N+1+(k2N) denote the starting points for

each route direction trip. Thus, stop pairs (s=1+k2N; s=2N+k2N) and (s=N+k2N; s=N+1+k2N) represent the same physical point (terminals or headers) but refers to bus stops belonging to different directions of service.

We also assume that buses run along a corridor equipped with a set of I signalised intersections controlled by the Traffic Control Centre. Each intersection p=1, 2, ..., I is characterised by the traffic signal cycle time ($C_p$) and the green offset regarding a general reference clock $\Delta_p$ ($0 \leq \Delta_p < C_p$). For the sake of simplicity, we consider that the signal cycle time consists of a green phase time ($g_p$) followed by the red phase time ($r_p$).

Eq. (10) defines the number of vehicles needed (J) in the route to maintain the targeted bus headway H as a function of the bus travel time in a roundtrip. It is estimated as the sum of four-time components for each route segment between stop s and s+1: running time, ($T_{r,s}$), time spent at intersections ($T_{p,s}$), time spent at stop s ($T_s$) and the slack time introduced in schedule at stop s in order to compensate potential service disruptions ($\phi_s$). The fourth term allows us the assessment of "static holding point strategies" to tackle bus bunching. In addition to that, it is supposed that at terminals A and B (s=N+k2N and s=2N+k2N) layover times $\theta_A$ and $\theta_B$ are allocated to let drivers rest an amount of time before continuing the service. This extra time is defined by a mandatory labour rule for each agency and it is independent of the slack time devoted at holding points. The mathematical operator $[x]^+$ denotes the upper integer of the term x.
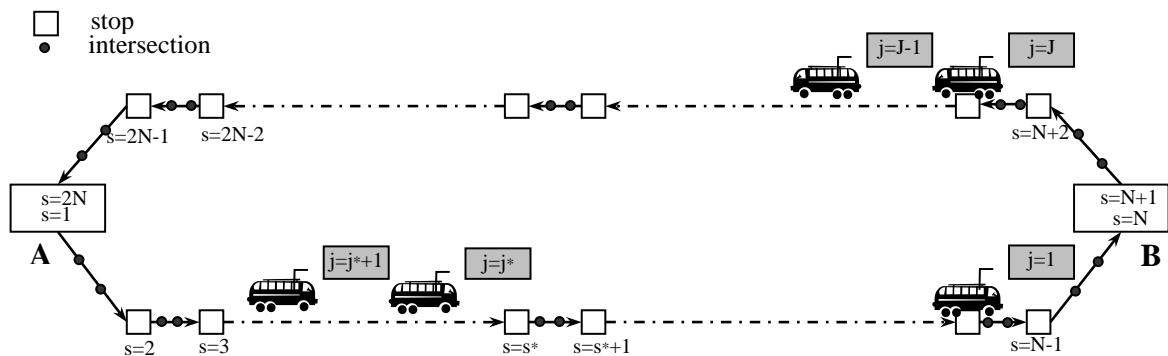


**Figure 15**. Schematic illustration of the bus route

$$J = \left[ \frac{\sum_{s=1}^{2N} [T_{r,s} + T_{p,s} + T_s + \phi_s] + \theta_A + \theta_B}{H} \right]^+ \tag{10}$$

The travel time of bus j between stops s and s+1 ($T_j(s)$) can be calculated by Eq. (11), where $v_j(s)$ is the cruising speed of bus j in this section. If the time headway is perfectly regular, the bus cruising speed is supposed to be the maximal, $v_b$. We will see later that one of the strategies to tackle bus bunching will consist of the modification of the speed of bus j.

$$T_j(s) = T_{r,s} + T_{p,s} = \frac{l_s}{v_j(s)} + \sum_{p=1}^{l_s} d_{p,s} \qquad (11)$$

The first term of Eq. (11) captures the running time of bus j in the segment between stops (s; s +1). The second term represents the delay caused by traffic signals on the bus performance. We suppose that the section between stops (s; s+1) encompasses a total amount of $I_s$ intersections ($I_s < |I|$). The variable $d_{j,p}$ is the time that bus j waits at each intersection $p \in I_s$ in the route section between stops (s, s+1). If bus j arrives at intersection p when the green phase is active, the variable $d_{j,p}$ will be equal to 0. In other situations, the bus trajectory needs to be modified.

The second term of Eq. (11) represents the effect of traffic signals on bus performance. We suppose that the section between stops (s; s+1) encompasses a total amount of $I_s$ intersections ($I_s < |I|$). The variable $d_{j,p}$ is the time that bus j waits at each intersection $p \in I_s$ in the route section between stops (s,s+1). If bus j arrives at intersection p when the green phase is active, the variable $d_{j,p}$ will be equal to 0. In other cases, the bus trajectory needs to be modified.

Eq. (12) allows the evaluation of the arrival time at intersection p, $t_{j,p}^a$, based on the departure time at the previous intersection or stop ($t_{j,p-1}^a$) and the location of intersections (p-1, p), as it is depicted in Fig. 16. It is supposed that the length $x_p$ between the location of intersection p regarding the first stop is known. Eq. (13) establishes the number of signal cycles of $C_p$ time ($n_{j,p}^*$) that have been completed before the arrival of bus j at intersection p, where $[x]^-$ denotes the mathematical operator estimating the lower integer of x. From this value, it is possible to determine the departure time at intersection p as well as the total signal delay time by Eqs. (14) and (15) respectively. The first case of Eq. (14) determines that bus j arrives at intersection p when the green phase is activated; consequently, there is no vehicle delay. Otherwise, the second case represents that the traffic signal is red when this bus arrives at this intersection. Therefore, its departure must be postponed to the green phase of the next signal

cycle $C_p$. Finally, the delay at intersection p is assessed in Eq. (15) as the difference between the departure and arrival time of bus j at this intersection. The time spent in accelerating/deaccelerating the vehicles up to/from the cruising speed due to a stop or a traffic light is neglected.

$$t_{j,p}^a = t_{j,p-1}^a + \left[\frac{x_p - x_{p-1}}{v_j(s)}\right] \qquad p = 2, \dots, I_s \tag{12}$$

$$n_{j,p}^* = \left[\frac{t_{j,p}^a - \Delta_p}{C_p}\right]^- \tag{13}$$

$$t_{j,p}^d = \begin{cases} t_{j,p}^a & \text{if } t_{j,p}^a \leq (C_p n_{j,p}^* + \Delta_p + g_P) \\ C_p(n_{j,p}^* + 1) + \Delta_p & \text{in other cases} \end{cases} \tag{14}$$

$$d_{j,p} = t_{j,p}^d - t_{j,p}^a \tag{15}$$

The estimation of the arrival time of bus j to the first intersection of the section (s; s+1), i.e. p=1, is made by Eq. (12) replacing $t_{j,p-1}^d$ by the departure time of the last stop s ($t_j^d(s)$ and $x_{p-1}$ by the coordinate of stop s($x_s$).

Furthermore, the time that each bus j spent at each stop s is evaluated as a function of the number of boarding and alighting passengers. We assume that $Y_{od}^t$ is the O-D matrix which defines the passenger flow at time interval t that boards at stop o and alights at stop d (o=1, …, N-1; d=o+1, ..., N in direction A-B; o=N, …, 2N-1; d=o+1, ..., 2N for direction B-A). The total passenger flow in one direction of service can be calculated as $q = \sum_{0=1}^{2N-1} \sum_{d>o}^{2N} Y_{od}^t$. Therefore, the percentage of passengers travelling between stops (o, d) in time interval t is evaluated by $y_{od}^t = (1/q) Y_{od}^t$. In Section 3.3.6.3, the performance of the bus route will be assessed, keeping the percentage of the passenger flow distribution constant between stops ($y_{od}^t$), and scaling the total passenger demand q in the route.

The time interval t may have different time lengths, from minutes to several hours. It depends on how the information has been obtained from the real world (onboard O-D survey, boarding alighting counters). Although actual implementations usually have estimations for

the passenger O-D matrix, aggregated in hours or even for the whole day, the variation of $Y_{od}^t$ over short domains of time intervals implies a significant disturbance of the dwell time at stops and consequently of the headway adherence. Hence, the number of passengers alighting ($a_j(s)$) and boarding ($b_j(s)$) at stop s (s=1, ..., N-1) for each bus j when the headway adherence is perfect, may be estimated using Equation (16a) and (16b). The term ($H_q$) captures the total number of passengers that have got on bus j in the whole direction of service (A-B). We sum the passenger flow percentages from all potential origins (k=1, ..., s-1) to the stop s, when the alighting passengers of bus j at stop s is addressed in Equation (16a). The boarding passengers are addressed in a similar way, adding the flow percentage from stop s to all potential downstream destinations (k=s+1, ..., N). The term $g_{jk}$ is equal to 1 if the arrival of vehicle j at stop k is made in the time interval $t^*$ ($1 \le t^* \le F$) and 0 otherwise. The parameter F is the number of subsets of stationary time periods in which the passenger flow distribution among stops is evaluated. To be consistent, the boarding and alighting demand values at starting and ending stops of a route must defined ($a_1 = a_{N+1} = b_N = b_{2N} = 0$). The calculation in direction B-A can be done easily adapting Equations (16) to the corresponding passenger flows and demand patterns. If we do not find empirical data to estimate boarding and alighting passengers, Equations (16a) and (16b) may be substituted by stochastic functions according to the assumption of probabilistic distributions of these variables.
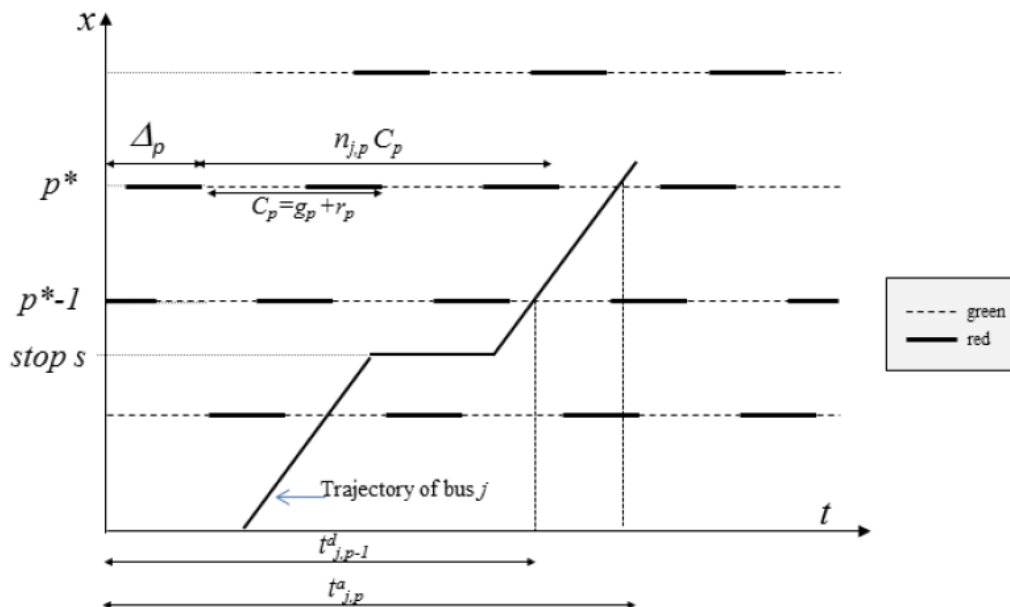


**Figure 16**. Schematic representation of the trajectory of bus j

$$a_j(s) = H \sum_{k=1}^{s-1} \sum_{t=1}^{F} q y_{ks}^t g_{jk} \quad \text{in direction } A - B \tag{16a}$$

$$b_j(s) = H \sum_{k=s+1}^{N} \sum_{t=1}^{F} q y_{ks}^t g_{jk} \quad \text{in direction } A - B \tag{16b}$$

Thus, the time spent by each bus at stop s when the system is regular ($T_s$) can be calculated by Eq. (17). The parameter $t_{oc}$ is a constant time devoted to the door opening and closing operations of each vehicle and parameters $\gamma$, $\eta$ are respectively the unit boarding and alighting time per passenger. Eq. (17) states that the boarding and alighting operations are performed independently by differentiated doors.

$$T_s = t_{oc} + \max_s [\gamma b_s; \eta a_s] \tag{17}$$

Once the bus travel time has been estimated for each phase of the route roundtrip (links, intersections, stops and holding points) in a regular state, the bus motion model is described by Eqs. (18)–(20). The variables $t_j^d(s\text{-}1)$, $t_j^a(s)$ refer to the departure time of bus j from a stop (s-1) and its arrival time at stop s respectively. The variable $t_j^d(s\text{-}1)$ is estimated through Eq. (18) as a function of the arrival time of the bus of study j at the previous stop (s-1) and the corresponding dwell time at this stop s-1. The variables $B_j(s\text{-}1)$ and $A_j(s\text{-}1)$ determine the total number of boarding passengers and alighting passengers at a stop (s-1) respectively. When the system is totally regular (perfect time-headway adherence), we assume that $B_j(s\text{-}1) = b_j(s\text{-}1)$ and $A_j(s\text{-}1) = a_j(s\text{-}1)$ respectively.

However, the calculation of arrival times at stops needs to identify three different cases of study. When the stop under analysis is not one of the first stops of the two route directions (terminals), arrivals are estimated regarding the travel time from the previous stop and the potential delays at intersections (first case of Eq. (19)). Nevertheless, when we analyse the variable $t_j^a(s)$ at the terminals (s=1+2kN or s=N+1+2kN), we should consider the layover and slack times. If the arrival of bus j and its passenger alighting process at the ending stop is made without a relevant delay, this bus j may start running in the opposite direction trip, satisfying a perfect correspondence to the target headway. It means that buses should depart at each H units of time. Therefore, we add kJ times the headway H to the arrival time at this stop of each bus j in the first-round cycle, where the time disturbance is still not present in the system. This situation is represented in the third case of Eq. (19). Finally, if that bus has a

significant arrival delay at the last stop of one direction, there wouldn't be enough slack time in the terminal to compensate this irregularity. Therefore, bus j would not start from the first stop at the target time headway H (second case of Eq. (19)) so that the disturbances would still be propagating in the opposite direction trip. In that case, the vehicle starts the service in the opposite direction just after being held the mandatory layover time ($\theta_{min}$) at this terminal.

The model only needs the insertion time of each vehicle j (j=1, …, J) in the system to characterise its trajectory along the route correctly. This information can be defined by Equation (20).

$$t_j^d(s-1) = t_j^a(s-1) + t_{oc} + \max_s \left( \gamma B_j(s-1); \eta B_j(s-1) \right) \tag{18}$$

$$t_j^a(s) = \begin{cases} t_j^d(s-1) + \dfrac{L}{v_j(s-1)} + \sum_p t_p^r & \text{if } s \neq 1 + (2kN) \text{ and } s \neq N+1+(2kN) \\ t_j^d(s-1) + \theta_{min} & \text{if } t_j^d(s-1) + \theta_{min} > t_j^a(s) + H \text{ and } s = 1+(2kN); N+1+(2kN) \\ t_j^d(s-2kN) + kJH & \text{if } t_j^d(s-1) + \theta_{min} \leq t_j^a(s) + H \text{ and } s = 1+(2kN); N+1+(2kN) \end{cases} \tag{19}$$

$$t_j^a(1) = (j-1)H \qquad j = 1, \dots, J \tag{20}$$

### 3.3.4.2.1  Modelling the unstable motion of buses

The analysis of bus system performance under service disruptions is conducted by the insertion of an extra time $U_j(s)$ in the arrival time of specific bus j to stop s (Eq. (19)). The exogenous variable $U_j(s)$ represents the potential delay that bus j may experience during the trip between stops (s-1; s). It would cause the headway variation among the whole fleet. Moreover, the model considers the traffic signal settings along the corridor. When the time-headway of the bus route is not multiple of the signal cycle time ($H/C_p$ is not an integer number), buses will find a different sequence of green–red phases at intersections. This is an additional source of instability in bus performance. The proposed dynamic model will analyse the performance of the system and passenger's behaviour because of this alteration $U_j(s)$, considering the current signal settings in the route.

In this state of service irregularity, the assumption regarding the estimation of terms $B_j(s-1) = b_j(s-1)$ and $A_j(s-1) = a_j(s-1)$ is not valid. The number of boarding passengers of vehicle j at a stop (s-1) will directly depend on the real headway with the bus operating ahead. As we track

the arrival and departure time of all vehicles at the overall bus stops, the evaluation of terms $B_j(s-1)$ and $A_j(s-1)$ can be easily done by Eqs. (21) and (22). The term $t_j^a(s-1) - t_{j-1}^a(s-1)$ represents the current time-headway between buses (j, j-1). On one hand, the boarding passengers on bus j at stop s will depend on the waiting passengers at this stop, term $D_{j-1}(s-1)$ in Eq. (21). The model here also improves the existing contributions in bus bunching because it considers the vehicle capacity constraint. This constraint is addressed in the following Eqs. (23) and (24). Therefore, the total number of passengers that cannot get on the previous bus (j-1), $D_{j-1}(s-1)$, also contributes to the number of boarding passengers on bus j at stop s-1, calculated in Eq. (1). The summation of Eq. (21) represents the number of trips carried out, in the same direction of service, between stop (s-1) and all potential downstream destinations (m, m > s-1). Therefore, parameter $k^*$ denotes the number of roundtrips completed from the initial time of study. Parameter β refers to the route direction in the roundtrip where bus j is running (β = 0 for direction A-B and β = 1 for direction B-A).

On the other hand, the number of alighting passengers at stop s-1, $A_j(s-1)$, does not depend on the headway between buses but, on the current onboard passengers of bus j alighting at this stop. In Eq. (22) we assume that the amount of the onboard passengers getting off the bus at stop s is proportional to the ratio of the hourly passenger flow to stop destination s divided by the total demand of the static hourly O-D matrix.

$$B_j(s-1) = \left( t_j^a(s-1) - t_{j-1}^a(s-1) \right) \cdot \sum_{m>s-1}^{(2+2k^*-\beta)N} qy_{s-1,m}^t + D_{j-1}(s-1) \qquad s > 1 \qquad (21)$$

$$\text{where } k^* \mid 1 + 2k^*N \leq s \leq 2N + 2k^*N; \ k^* \in \mathbb{N}$$

$$\beta = \begin{cases} 1 & \text{if } 1 + 2k^*N \leq s \leq 2N + 2k^*N \\ 0 & \text{otherwise} \end{cases}$$

$$B_j(s-1) = \sum_{m=1+p}^{s-2} B_j(m) \frac{y_{m,s-1}}{\sum_{r=m}^{1+p+N} y_{m,r}} \qquad s > 1 \qquad (22)$$

$$\text{where} \quad p = 2k^*N + (1-\beta)N$$

The occupancy $M_j(s)$ of the bus j during the segment between stops s-1 and s can be evaluated by Eq. (23) considering the vehicle capacity, C. For formulation consistency, we state that $M_j(0)=0$. Eq. (24) evaluates the total amount $D_j(s)$ of passengers waiting at stop s

that cannot get on the bus j (if they exist) and may board on the following bus j+1. It is supposed that the definition of the targeted headway H (input of this model) is appropriately defined to accommodate the passenger demand in the static system with buses of capacity C.

$$M_j(s) = \min\{C; M_j(s-1) + B_j(s) - A_j(s) + D_{j-1}(s)\} \tag{23}$$

$$D_j(s) = \max\{0; M_j(s-1) + B_j(s) - A_j(s) - C\} \tag{24}$$

All strategies aimed at controlling fixed bus intervals are based on the real-time headway monitoring of bus departures from stops. Eq. (25) evaluates the actual time headway between two consecutive buses $(\Delta t_j^d(s))$ considering the departure time from stop s. Therefore, it is necessary that each time any bus j is going to depart from one stop s, the variable $\Delta t_j^d(s)$ is updated. It should be noted in Eq. (25) that the real-time evaluation of current headway of bus j is made regarding the bus j-1 ahead, at stop s (forward comparison). This information should be used to calculate the adherence regarding the targeted headway H (see Eq. (26a)).

The headway analysis of bus j regarding bus j + 1 (backwards) is infeasible because bus j + 1 has not arrived yet at stop s. Hence, the backward comparison of headway with the following bus (Eq. (26b)) will be made considering the difference of departure time of bus j and j + 1 at the last stop s$^*$ visited by bus j + 1 $(\Delta t_{j+1}^d(s^*))$ up to this moment.

$$\Delta t_j^d(s) = t_j^d(s) - t_{j-1}^d(s) \quad \forall s \tag{25}$$

$$\text{forward comparison to bus j} - 1 \quad \varepsilon_{j-1,j}(s) = \Delta t_j^d(s) - H \tag{26a}$$

$$\text{backward comparison to bus j} + 1 \quad \varepsilon_{j,j+1}(s^*) = \Delta t_j^d(s^*) - H \tag{26b}$$

### 3.3.4.2.2 Control strategies

The model developed in section 3.3.6.2.1 only considers the usual practice of bus agencies, consisting of the allocation of slack time at the holding points (terminals) to tackle the lack of regularity. However, as it is reported in Daganzo (2009), this solution presents several problems. The controlling strategy is not adaptive since slack times are not dependent on the

deviation of targeted time headways. These slacks represent an unproductive allocation of time in the cycle time of buses when the performance of the system is regular.

Therefore, this paper analyses two complementary fleet management strategies to alleviate the bus bunching problem that may overcome the limitations of the previous operation. On the one hand, one strategy will be based on "dynamic holding points", so that the cruising speed of buses will be varied depending on the time-headway between buses. This strategy is quite similar to the presented in Daganzo (2009). On the other hand, the second strategy will encompass the previous variable bus speed pattern combined with an additional signal priority for buses.

### 3.3.4.2.2.1 Strategy S1

This strategy obliges drivers to adapt the cruising speed of their bus when the headway adherence is irregular. Considering the deviations between real and targeted time-headway for a bus j at stop s, the motion law that modifies the speed of the bus is defined by Eq. (27) when the vehicle capacity constraint of vehicles ahead and at the rear is not achieved. Therefore, this formulation is only valid when $M_{j+1}(s^*) < \varphi C$ and $M_{j-1}(s') < \varphi C$, where $\varphi \cong 1$ and s' is the last visited stop of the vehicle (j-1) in the route.

$$v_j(s) = \begin{cases} \dfrac{L}{L/v_j(s-1)+f_f(\varepsilon_{j,j+1}-\varepsilon_{j-1,j})} & \text{if } \varepsilon_{j,j+1} > \varepsilon_{j-1,j};\ \varepsilon_{j,j+1} > 0 \\[2mm] \min\left\{v_b;\ \dfrac{L}{L/v_j(s-1)+f_b(\varepsilon_{j,j+1}-\varepsilon_{j-1,j})}\right\} & \text{if } \varepsilon_{j-1,j} > \varepsilon_{j,j+1};\ \varepsilon_{j-1,j} > 0 \text{ and } L/v_j(s-1)+f_b(\varepsilon_{j,j+1}-\varepsilon_{j-1,j}) > 0 \\[2mm] v_b & \text{otherwise} \end{cases} \tag{27}$$

$$v_j(s) = v_b \qquad \text{if } M_{j-1}(s') \geq \varphi C \text{ or } M_{j+1}(s^*) \geq \varphi C \tag{28}$$

The first case of Equation (18) reduces the actual cruising speed when: i) bus j is getting further away from bus j+1 than the desired headway H (i.e. $\varepsilon_{j,j+1}(s^*) > 0$); and ii) this time spacing is greater than the corresponding value with the vehicle ahead at stop s. It is desirable that this bus j will operate the stretch up to the next station at a cruising speed below the maximal value to re-establish the desired time headway. The parameter $f_f$ is a speed adjusting factor ($f_f > 0$). Therefore, the speed reduction of vehicle j is proportional to the difference between the total headway deviation and the vehicle at the rear and ahead ($\varepsilon_{j,j+1} - \varepsilon_{j-1,j}$).

On the other hand, the second case of Equation (27) increases the current cruising speed when: i) bus j presents a higher headway with bus j-1 than the target value H in stop s (i.e. $\varepsilon_{j-1,j}(s) > 0$); and ii) this headway is higher than the corresponding with the vehicle at rear at stop s*. The reason is that bus j will find more passengers at stops than the expected (increase in dwell time). These additional passengers would be supposed to get on bus j+1 if bus regularity would be perfect. If no control measures are implemented, one may assume that this tendency will be amplified until bus j+1 reaches bus j (bus pairing phenomena). To tackle this problem, it is recommended that bus j will run at a higher speed than the previous segment $v_j(s) > v_j(s-1)$. As defined in Equation (27), the speed modifications are proportional to the difference of the time headway adherence between buses (j, j+1) and buses (j-1, j). Note that this difference ($\varepsilon_{j, j+1} - \varepsilon_{j-1, j}$) has a negative value in the second case of Equation (27), where $f_b$ ($f_b > 0$) is the speed adjusting factor in this situation. If we set a value of the speed adjusting parameter $f_b$ that produces $L/(v_j(s-1)) + f_b \cdot (\varepsilon_{j, j+1} - \varepsilon_{j-1, j}) \leq 0$; the corresponding cruising speed will present a negative value too. That possibility is constrained in the second case of Equation (27) since the system will require a higher cruising speed and de facto we will use $v_j(s) = v_b$ in these situations.

As it is pointed out in Daganzo (2009), the dimensionless speed adjusting parameters $f_f$ and $f_b$ represents the marginal increase in expected bus delay caused by a unit increase in headway. It may be considered as the expected number of passenger arrivals at one stop during the average marginal delay induced by one boarding move. Therefore, $f_f$ is also conceived as a speed factor to re-establish the desired headway between two serial buses. If $f_f = 1$, the current headway will be close to the targeted headway in the next stop, but it will produce a significant reduction of bus speeds. Otherwise, if $f_f \rightarrow 0$, it will maintain the modified speed close to $v_b$ and it will take a high number of stops to overcome the deviation from desired headway. Similar statements can be provided for the adjusting parameter $f_b$. However, when the occupancy of the bus ahead or at the rear of bus j is equal or slightly lesser than the vehicle capacity, it is preferable that bus j runs at the maximal speed as it is defined in Equation (28). The reason for this statement is justified as the vehicle ahead or at the rear will also present a passenger load like the vehicle capacity. It will experience shorter dwell times at stops since boarding operations are not made. Therefore, it will run at a maximal speed $v_b$ (it will follow the 3rd case of Equation (27)).

This strategy improves previous protocols aimed at maintaining regular time headways in two major aspects. Firstly, the speed reduction of Equation (27) is only activated for irregular arrival periods so that the production of the rest of the service is made at maximal speed. Secondly, the modification of bus speeds is adaptive to the range of deviation of time headways, overcoming the fixed holding points of the common practice of bus agencies. However, the speed reduction of those buses delayed keeping regular headways may suppose a reduction of the average commercial speed of the bus route. All strategies in this field present a trade-off between speed (travel time) and regularity objectives. Therefore, the presented strategy of this section should be complemented with several operational actions aimed at increasing the speed of those delayed buses. Hence, bus agencies may tackle the regularity problems without affecting the average commercial speed of the line or maintaining idle times in the service.

### 3.3.4.2.2.2 Strategy S2

This new strategy radically increases the commercial speed of the delayed vehicles, providing activated traffic light priority at intersections. It also encompasses the modification of speed proportional to $\varepsilon_{j,\ j+1} - \varepsilon_{j-1,\ j}$ (reduction or increase) proposed in strategy S1 through the Equations (27) and (28). Here, the time headway adherence can also be tackled by the elimination of several vehicles stops at signalised intersections, due to a time extension of the green phase. This measure is the only strategy that increases the commercial speed of buses in the route. The variable G, expressed in units of time, represents a little extra green time introduced in every intersection (if necessary) to avoid the stop of a delayed vehicle at a traffic light section. If the arrival time of delayed bus j at intersection p is estimated during an interval G after the end of the green phase, the TCC can keep the green phase a total amount of g+G seconds. Since the traffic light cycle time is significantly lower than the time headway ($C_p$ <H), the TCC may revert and even truncate the available green time in the following cycle (g-G). The reason is to guarantee the evacuation rate of the intersection and alleviate traffic or pedestrian's queues. Therefore, high values of G are not considered (G $\leq$ $0.4C_p$).

The activation of the green extension is only permitted when bus j presents time headways regarding the vehicle ahead (advanced) higher than the target headway and the actual

headway with the vehicle at the rear. It is equivalent to the situation when cruising speed in Strategy S1 is evaluated through the second case of Equation (27). Under those circumstances, the bus travel time in the segment (s; s+1) maybe even reduced due to soft modifications of red phase at the intersections located along the segment. To do so, it is necessary to verify the state of the traffic light phases when delayed buses arrive at intersections to activate the green extension strategy. The first case of Equation (20) determines the departure time of vehicle j from intersection p when the green extension is activated. It replaces Equation (14) to describe the vehicle motion law under the implementation of this regularity controlling strategy. The right condition of the first case of Equation (29) represents that vehicle j arrives within a green phase of g+G length considering the initial offset $\Delta_p$. When this constraint is not accomplished, the vehicle must wait until the red phase in the traffic light is finished (second case of Eq. (29).

$$t_{j,p}^d = \begin{cases} t_{j,p}^a & \text{if } t_{j,p}^a < \left( \left( C_p n_{jp}^* \right) + \Delta_p + \left( g_p + G \right) \right) \\ C_p \left( n_{jp}^* + 1 \right) + \Delta_p & \text{in other cases} \end{cases} \tag{29}$$

### 3.3.4.3 Evaluations

The bus motion law and the controlling strategies explained in the last section have been programmed into a simulation tool. Some performance indicators have been defined to measure the time headway adherence, the travel time of passengers and the operating cost to provide the service under each controlling strategy. Moreover, three set of bus problems have been generated to assess the system performance when a control strategy is activated to overcome headway variation. The first set is based on an idealised bus route of 40 stops evenly distributed. Three key parameters will be modified: the capacity of vehicles, the bus disturbance and the passenger demand. The second set of problems embraces different traffic signal settings and the number of intersections along the corridor. Eventually, the third problem represents a real route of Barcelona's high-performance bus network. All the information concerning bus stops, traffic light management and traffic behaviour has been collected from campaigns or provided by both the bus agency and city council.

### 3.3.4.3.1  Performance indicators definition

Four metrics are proposed to assess the quality of the solutions associated with each control strategy. One of the objectives of the operating manager is to provide fast service to minimise the time spent in the system by the passengers. It is evaluated using the first indicator, the total passenger travel time (Eq. (32)) which includes the in-vehicle travel time (Eq. (30)) and waiting time (Eq. (31)) of all passengers in the system (excluding access and egress time).

$$TT = \sum_{j=1}^{J} \sum_{s=2N+1}^{(m^*+\alpha_j)(2N)} \left( t_j^a(s+1) - t_j^a(s) \right) M_j(s)$$

$$+ \max\left( \gamma B_j(s);\ \delta A_j(s) \right)\left( M_j(s) - A_j(s) \right) \tag{30}$$

$$TW = \sum_{j=1}^{J} \sum_{s=2N+1}^{(m^*+\alpha_j)(2N)} \left( \frac{q}{2}\left(t_j^a(s) - t_{j-1}^a(s)\right)^2 \sum_{r>s}^{(2+2k^*-\beta)N} y_{sr} + D_j(s)\left(t_j^a(s) - t_{j-1}^a(s)\right) \right) \tag{31}$$

$$TPT = TT + 2.2TW \quad (\text{in pax} - \text{hours}) \tag{32}$$

The estimation of total travel time through Eqs. (30)–(32) will be made during a temporary period of analysis that has been defined as a predefined number of vehicles departures D from stop s = 2N + 1. It refers to the initial stop in direction A-B but once each vehicle has completed one round trip to warm up the system. If the analysis had been done for a given period (2 h for example), the number of onboard passengers would have been lower for highly unstable bus routes, where several vehicles would have moved in platoons. Therefore, the first indicator would have presented lower user cost in those situations than in perfect regularity lines, which is incorrect. Let $m^*$ be the number of completed round trips by all fleet ($m^*/ = [D/J]^+$) when D vehicle departures would be considered to evaluate TT and TW variables. The first ($D - m^*J$)th vehicles will have run an additional round trip. Parameter $a_j$ is equal to 1 if bus $j \leq (D - m^*)$ and 0 otherwise to account for this extra round trip. In Eq. (32), the first term within brackets captures the waiting time of passengers that have arrived at stop s after the boarding process of bus $j - 1$. As we consider a constant arrival rate of passengers at stop, it is calculated as one half of the current time spacing between buses ($j;\ j - 1$) multiplied by the number of passengers arrived within this interval. The latter is addressed as the product of the passenger flow in one direction (q), the flow percentage between stop s and all potential destinations stops $r(y_{sr})$ and the lapse of time between the arrival of bus j and j − 1. The second term considers the passengers arrived at stop s before the arrival of the bus (j − 1) that could not get on this bus (or even previous buses) due to the capacity constraint. The

total amount of passengers under this situation ($D_j(s)$) must wait for the period between the arrival of consecutive buses (j, j −1). $D_j(s)$ is updated at each stop s for each bus j considering the boarding capacity of the predecessor buses. In Eq. (32), the total passenger waiting time is multiplied by a factor of 2.2 to magnify the higher perception of waiting time by users related to in-vehicle travel time. This value is consistent with the factors proposed in TRB (2013) and Hill (2003), which range from 2.1 to 2.8 times the amount of in-vehicle time.

The second indicator is the operating cost of the bus system in the period under analysis ($Z_0$), defined in Eq. (33). It is estimated as the product of the total vehicle hours in service by the unit temporal cost of one vehicle ($c_t$, in terms of €/veh-h). The hours in service by the whole fleet are estimated as the difference between the arrival times at the end of the route in the $(m^* + \alpha_j)^{th}$ and first roundtrip.

$$Z_0 = c_t \sum_{j=1}^{J} \left[ t_j^a \left( (m^* + \alpha_j) 2N \right) - t_j^a (2N + 1) \right] \quad \text{(in Euros)} \tag{33}$$

The third indicator proposed is the total cost of the system ($Z_T$), including the operating cost and the temporal cost incurred by passengers. As control strategies present a trade-off between reducing bus headways variations and increasing operating cost, this metric will capture which strategy is more cost-efficient regarding the others. Eq. (34) defines how this variable is evaluated based on the former indicators and the passenger value of time, $\mu$ (€/pax-h).

$$Z_T = Z_0 + \mu \cdot TPT \quad \text{(in Euros)} \tag{34}$$

The last metric is the coefficient of headway variation. It is defined as the sum of the change in time between the arrival of one bus and the arrival of the next bus at a stop, divided by the average time headway in the period of analysis. It is necessary to point out that the overall headway alterations in our model take place when the first bus is currently serving the second cycle. The first cycle is only used to introduce the whole vehicles uniformly in the route, in other words, to warm up the simulation. By this reason, the time headways between buses in the first cycle are not taken into account. In TRB (2013), Eq. (35) is proposed to evaluate the average headway variation overall stops,

$$c_v = \frac{S}{\bar{h}} \geq 0 \tag{35}$$

where cv is the coefficient of headway variation, S the standard deviation of all headways observed in all potential stops during the complete tracking of D departures from the stop s = 2N + 1 (first round cycle is excluded as we suppose that the system is under a perfect time-headway adherence) and $\bar{h}$ the average headway. In TRB (2013), the level of service (LoS) concerning time-headway adherence is ranged considering the following domains: A($c_v \leq$ 0.21), B($0.21 < c_v \leq 0.3$), C ($0.3 < c_v \leq 0.39$), D($0.39 < c_v \leq 0.52$), E($0.52 < c_v \leq 0.74$) and ($c_v \geq 0.75$).

## 3.4 Transit corridors served by two routes

To improve the efficiency of bus systems in the field of study of this thesis, the provision of a system consisting of two routes that share a common section is many times highly recommended. In this way, in the peripheral urban areas, the lowest (worse) headway is adapted to the lower existing demand. Through the central corridor, with higher demand, the patronage is well-served by the two routes running together along on it. In this sense, the value of the various indicators that take part plays a determining role at the same time as to find out the viability of these schemes.

A study on the operation of transit corridors served by two routes is presented in this chapter. This study aims at estimating the effect of the physical design of the corridor in branches, the demand distribution and the traffic lights on the total cost of the system as well as its regularity. A kinematic model to estimate the natural motion of buses of different routes along the corridor has been carried out. An optimisation procedure is presented to determine the optimal headway and the relative synchronisation of routes that would minimise the total cost incurred by transit agencies and users or the headways variations in the common route segment. The performance of bus control strategies based on a combination of holding points and green extensions at traffic signals is addressed in generic test instances and the H10 corridor of Barcelona's new bus network.

### 3.4.1 Notation and modelling framework

Let us assume that there is a ground transit corridor in a given city. This corridor presents a central segment between points PC1 and PC2 (Fig. 17). At the two edges PC1 and PC2, the corridor branches out into two segments, to provide wider accessibility in the peripheral region up to the ending points P1, P3, P4 and P5. Therefore, four independent branches are identified, referred by $1 = \overline{P_1 - PC_1}$, $3 = \overline{PC_2 - P_3}$, $4 = \overline{P_4 - PC_1}$ and $5 = \overline{PC_2 - P_5}$, in addition to the central corridor segment (referred by $2 = \overline{PC_1 - PC_2}$). We assume that two transit routes will provide service along the corridor: Transit route A runs along corridor segments 1,2 and 3 and route B provides service along segments 4,2,5.
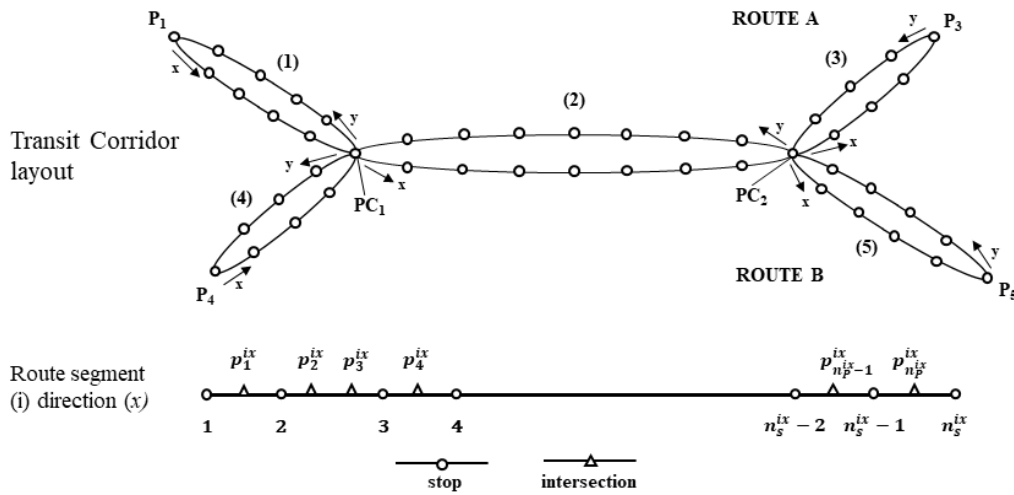
**Figure 17**. Scheme of the transit system composed by a branched corridor with two routes (route A and B).

Each route segment $i=1,..5$ is operated in two directions of service: direction $x$ (to the East in Fig. 17) and $y$ (to the West). From this point on, we will use the superscript $z$ to represent the two available directions of service, $z=x$ or $z=y$. Each route segment $i$ presents $n_s^{iz}$ stops ($i=1, \dots, 5$) in direction $z$. In each route segment, the distance between stop $k$ and $k+1$ is labelled by $s_k^{iz}$ $\left(s_k^{iz} \geq 0\right)$ in direction $z$ ($k=1, \dots, n_s^{iz}-1$). Note that stop $k=1$ is equivalent to the starting point of the route segment and stops $k=n_s^{iz}$ to the ending point (points $P_1$, $P_3$, $P_4$, $P_5$, $PC_1$ and $PC_2$). Therefore, the length of each route segment $i$ in direction $z$ is computed by $l_i^z = \sum_{k=1}^{n_s^{iz}-1} s_k^{iz}$.

In each route segment $i=1,..,5$, we suppose that there is a set $I^{iz} = \left\{ p_1^{iz}, \dots, p_{n_p}^{iz} \right\}$ of intersections in the direction $z$. The parameter $n_p^z$ captures the total number of intersections on route segment $i$ in direction $z$; while $x(p_j^{iz})$ denotes the distance between the location of the $j$-$th$ intersection to the initial section of the segment in direction $z$ $\left(j=1, \dots, n_p^{iz}\right)$.

We assume that all intersections of the problem present the same traffic signal cycle time $C_p$. However, each intersection $j$ in direction $z$ is defined by its green phase time $g_j^{iz}$ and traffic light offset $\Delta_j^{iz}$, where superscripts refer to the route segment $i$ and the direction of service $z$. Therefore, one route segment will consist of a sequence of stops and intersections.

The total number of boarding passengers in one hour in direction $z$ of route segment $i$, whose destination is located along route segment $j$ ($i$, $j$=1,..,5) is defined by $B_{ij}^z$ . Hence, the number of cumulative boarding passengers per hour from stop 1 to stop $k$' ($1 < k' \leq n_s^{iz}$) in direction $z$ of segment $i$ that goes to route segment $j$ can be calculated by $B_{ij}^z(k')=B_{ij}^z F_{b,ij}^z(k')$. Indeed, the variable $0 \leq F_{b,ij}^z(k') \leq 1$ is the cumulative distribution function of boarding passengers along the segment $i$ in direction z.

Similarly, the term $A_{ij}^z$ captures the total number of alighting passengers per hour in direction $z$ of route segment $j$, whose origin is located along route segment $i$ ($i,j$=1,..,5). In this case, the number of cumulative alighting passengers from stop 1 to stop $k$' ($1 \leq k' \leq n_s^{iz}$) in direction $z$ of route segment $j$ is estimated by $A_{ij}^z(k')=A_{ij}^z F_{a,ij}^z(k')$, where $F_{a,ij}^z(k')$ is the cumulative distribution function of alighting passengers from stop $k$=1 to stop $k$'. AVL devices can deterministically calculate these cumulative distributions of boarding and alighting passengers, measuring the real distribution of origins or destinations along the route. They can be also represented by probabilistic assumptions.

Along with this Section, we present an analytical model to reproduce the bus motion in a transit system with two branched lines, as described below. This model will be able to estimate arrival and departure times of buses along the route segments and, eventually, several bus route metrics required to assess user performance and operational cost. To represent possible transit demand states, the definition of the previous variables must satisfy some properties. Equation (36) states that the boarding passenger rate in between segments $i$ and $j$ on both directions of service ($x$ and $y$) must equal the alighting rate between the same route segments. Eq. (37) states the same conservation condition when the boarding and alighting operations are made in the same route segment $i$ in direction $z$. Finally, Equation (38) obliges that the cumulative number of boarding counts of passengers whose origin and destination are in the same route segment must be higher or equal to the corresponding number of alighting counts, at a given stop $k$.

$$B_{ij}^x + B_{ij}^y = A_{ij}^x + A_{ij}^y \ \forall i,j \ i \neq j \tag{36}$$

$$B_{ii}^z = A_{ii}^z \quad \forall i, \quad z = \{x,y\} \tag{37}$$

$$B_{ii}^z(k) \geq A_{ii}^z(k) \ \ k=1,..,n_s^{iz} \tag{38}$$

### 3.4.1.1 Operational assumptions

The operation of transit services in the two branching routes are supposed to fulfil the following operational hypotheses:

i.   For the sake of generality, we assume that buses operate both transit routes A and B, where the dwell time at stops is profoundly affected by the number of boarding and alighting passengers at each stop.

ii.  Both routes, A and B, are operated at the same time headway $H$, $H_A = H_B = H$. Therefore, the mean time headway in the central segment $i=2$, assuming perfect time-headway adherence, is $H/2$; while in the branching segments the headway is equal to $H$.

iii. Time headway $H$ is multiple numbers of the traffic light cycle, $H = nC_p$, $n \in \mathbb{N}$. Hence, the travel times of consecutive transit vehicles belonging to the same route on each segment are identical.

iv.  We suppose that each passenger needs $\tau_b$ units of time to get on the bus, and $\tau_a$ units of time to alight. Although the operational time to proceed these operations may vary among passengers, we will use these deterministic parameters as mean values. Boarding and alighting operations have different vehicle doors assigned. Therefore, since these operations can be done independently, the dwell time can be calculated as the maximal time spent at each operation.

v.   Bus travel times and demand are characterised by deterministic functions that do not consider random effects.

vi.  The capacity of all vehicles operating on both routes A and B, referred by C, is homogeneous.

vii. All transfer operations between routes A and B are supposed to be made at the last available transfer stop along the inbound route. Therefore, users are assumed to travel the longest distance in the first route of their path. Example: users travelling from route segment 1 to segment 5 will transfer at PC-2 although they could do it at any stop of route segment 2.

viii. In the general version of the analysis, overtaking between buses is allowed. Vehicles of route B can overtake vehicles of route A (and vice versa) in the central segment.

ix.  Vehicles modify the instantaneous speed vi at a constant acceleration rate *a* (positive or negative). The maximal allowable instantaneous speed is $v_{max}$ ($v_i < v_{max}$).

### 3.4.1.2 Maximal operating headway to verify capacity constraint

The headway $H$ at which both routes A and B are operated is constrained by the assumptions ii) and iii). However, since vehicles are assumed to present a finite capacity $C$, we need to estimate the maximally expected passenger occupancy and verify that it does not exceed the parameter $C$. In Equation (39) this constraint is presented, where the occupancy (left hand) is computed as the product of the operating headway $H_i$ on segment $i=1,..,5$ and the maximal passenger flow $q_{max}^{iz}$ at the critical section of segment $i$ in direction $z$. The determination of this constraint for each potential combination of route segments and directions is presented in Appendix D1.

$$H_i q_{max}^{iz} \leq C \quad i = 1, \dots, 5, \quad z = \{x, y\} \tag{39}$$

The operational headway in all branched segments is equal to $H$. However, in the central segment, the passenger whose origin and destination are located on the same central segment $i=2$ may board at the first arriving vehicle between route A and B. Therefore, the contribution of these passengers to the vehicle occupancy will be calculated considering a real headway of $H/2$, assuming a perfect spacing between consecutive buses of route A and B.

### 3.4.1.3 Arrival and departure time compatibility between segments

Let $t_0^{iz}$ be the entrance time of one bus to stop $k=1$, $t_a^{iz}(k)$ be the arrival time at stop $k$ and $dt^{iz}(k)$ be the dwell time at stop $k$ of the bus route segment $i=1,..,5$ in the direction $z$ ($z=x$ or $y$). The entrance time $t_0^{iz}$ at the first stop of route segments $i=1$ and $i=4$ in direction $x$ should be defined by the bus agency to maintain proper time headway adherence along the central segment. Indeed, the entrance times $t_0^{1x}, t_0^{4x}$ will be considered as decision variables in the model and vary in the following domain $0 < t_0^{1x} < H$, and $0 < t_0^{4x} < H$. In other segments and directions, these entrance times should be defined in accordance to the exit times of the vehicle at the last stop of the previous segment of the route, ensuring travel time compatibility between segments.

Therefore, the travel time needed to overcome the distance $l_i^z$ along route segment $i$, direction $z$, and perform the boarding and alighting operations at all stops ($k=1$ to $k=n_s^{iz}$) is defined by the variable $\Delta T^{iz}(t_0^{iz})$. This travel time of segment $i$ in direction $z$ can be

computed by Equation (40), as the difference between the exit time and entrance time in segment $i$. The exit time is computed by the arrival time at the last stop of segment $i$, $t_a^{iz}(k = n_s^{iz})$, plus the dwell time at the last stop to perform passenger alighting operations, $dt^{iz}(k = n_s^{iz})$.

$$\Delta T^{iz}(t_0^{iz}) = t_a^{iz}(k = n_s^{iz}) + dt^{iz}(k = n_s^{iz}) - t_0^{iz} \tag{40}$$

It should be noted that the travel time of route segment $i$ in direction z, $\Delta T^{iz}$, depends on the traffic light setting along the segment and, consequently, on the entrance time at the first stop $t_0^{iz}$. However, if the demand rates $B_{ij}^z, A_{ij}^z$ and time headway $H$ are kept constant, the total travel time in the route segment $i$ is equal for all entrance times spaced by $C_p$, $\Delta T^{iz}(t_0^{iz}) = \Delta T^{iz}(t_0^{iz} + qC_p)$, where $C_p$ is the cycle time of traffic lights and $q$ is any integer number. This statement is also valid for route segment $i$=2. In route segment $i$=2, one vehicle of route A is followed by a vehicle of route B. If the entrance time of these consecutive buses are equally spaced, the real time headway $h_{AB}$ along tram $i$=2 is $h_{AB}$=H/2. Therefore, both lines capture the same number of boarding passengers. However, if the entrance time of these buses is not synchronised (for example $h_{AB} > H/2$ and $h_{BA} < H/2$), or boarding passengers are not evenly distributed between routes, the resulting trajectories of these buses will not be parallel. In that situation, the bus of one route will catch up the bus ahead of the other route in some point of segment $i$=2, if we consider enough distance. Despite this fact, the trajectories of all vehicles belonging to the same route (A or B) will be parallel lines, that means that the round-trip travel time of all vehicles operating route A or B will be the same. The variables $t_0^{iz}$, except for $t_0^{1x}, t_0^{4x}$, are defined imposing compatibility of travel times between route segments (1x→2x→3x→ 3y→2y→1x in route A and  4x→2x→5x→5y→2y→4y in route B).  In Appendix 2, the estimation of these variables is provided.

Therefore, the round-trip travel time of a given vehicle of route A ($T_A$) is calculated in Equation (41), assuming that the entrance time in segment $i$=1 was $t_0^{1x}$. The subscript A in the variables $t_{0,A}^{2y}$ $t_{0,A}^{2y}$ specifies the entrance time of route A in the route segment operated by two routes.  The corresponding roundtrip travel time for a vehicle operating route B is defined by Equation (42).

$$T_A = \Delta T^{1x}(t_0^{1x}) + \Delta T_A^{2x}(t_0^{2x}) + \Delta T^{3x}(t_0^{3x}) + \Delta T^{3y}(t_0^{3y}) + \Delta T_A^{2y}(t_{0,A}^{2y}) + \Delta T^{1y}(t_0^{1y}) \tag{41}$$

$$T_B = \Delta T^{4x}(t_0^{4x}) + + \Delta T_B^{2x}(t_0^{2x}) + + \Delta T^{5x}(t_0^{5x}) + \Delta T^{5y}(t_0^{5y}) + \Delta T_B^{2y}(t_{0,B}^{2y}) + \Delta T^{4y}(t_0^{4y}) \quad (42)$$

### 3.4.1.4 Travel time between consecutive stops k, k+1

The calculation of travel times $\Delta T^{iz}$ for all route segments $i=1,...,5$ in both directions $z=x,y$ is proceeded consecutively, calculating the travel time between stops along each segment, starting from the first stop (where we have already defined $t_0^{iz}$) and ending at the last stop $k = n_s^{iz}$ of the route segment. In this subsection, we provide the general formulation for estimating the bus travel time between two consecutive stops $k$, $k+1$ ($k < n_s^{iz}$) in a given route segment $i$ ($i=1$ to $5$).

The arrival time at the next stop $k+1$, $t_a^{iz}(k+1)$, in the route segment $i$, direction $z$ ($z=x$ or $y$) depends on the arrival time at the previous stop $k$, the dwell time $d_t^{iz}(k)$ at the previous stop $k$ and the time needed to overcome the distance between stops $k$, $k+1$. The sum of the terms $t_a^{iz}(k) + d_t^{iz}(k)$ captures the departure time from stop $k$, denoted by $t_d^{iz}(k)$. The time required to overcome the stop spacing $s_k^{iz}$ between stops $k$, $k+1$ is denoted by $tt(s_k^{iz})$ and it is affected by the delays caused by traffic lights. Hence, the arrival time $t_a^{iz}(k+1)$ at the next stop $k+1$ can be computed by Equation (43),

$$t_a^{iz}(k+1) = \{t_a^{iz}(k) + d_t^{iz}(k)\} + \{tt(s_k^{iz})\} \quad k = 1, ..., n_s^{iz} - 1 \quad (43)$$

The definition of the term $t_a^{iz}(k)$ is known from the analysis in the previous iteration at stop $k$-1 or by setting the initial condition when $k=1$ ($t_0^{iz}$). In the following sections, the estimation of the two bracketed terms of Equation (43) is presented independently.

#### 3.4.1.4.1 Departure time from stop k

The estimation of the departure time from any stop of the transit system should be specified when we are analysing either branched route segments (a1) or the central segment (a2):

**Case a1.** The departure time $t_d^{iz}(k)$ from stop $k$ at any branched segment $i$ ($i=1,3,4,5$), will be the sum of the arrival time $t_a^{iz}(k)$ and the dwell time at this stop $k$, $d_t^{iz}(k)$ as Equation (44) states. For any intermediate stop $k$ ($1<k\leq n_s^{iz}$) in the segment $i$, the dwell time is calculated as the maximal value between the number of boarding passengers and alighting passengers, times the corresponding unit boarding $\tau_b$ or alighting time $\tau_a$ per passenger respectively

(assumption iv). The term $A_{T,i}^z(k)$ accounts the hourly transfer flow of passengers that alighted at stop $k$ of route segment $i$, to get on another bus route. Taken into account assumption vii), this term is only different than 0 when $k=n_s^{iz}$. Therefore, the terms with positive values are $A_{T,1}^x(k = n_s^{1x}) = B_{1,4}^x = A_{1,4}^y$; $A_{T,4}^x(k = n_s^{4x}) = B_{4,1}^x = A_{4,1}^y$; $A_{T,3}^y(k = n_s^{3y}) = B_{3,5}^y = A_{3,5}^x$ and $A_{T,5}^y(k = n_s^{5y}) = B_{5,3}^y = A_{5,3}^x$.

$$t_d^{iz}(k) = \begin{cases} t_a^{iz}(k) + \max\left\{\sum_{j=1}^{5} \Delta B_{ij}^z(k) \cdot H \cdot \tau_b; \sum_{j=1}^{5}\left(\Delta A_{ji}^z(k) + A_{T,i}^z(k)\right) \cdot H \cdot \tau_a\right\} & k > 1 \\ t_0^{iz} + \sum_{j=1}^{5}\left(B_{ij}^z(1) + B_{T,i}^z\right) \cdot H \cdot \tau_b & k = 1 \end{cases} \tag{44}$$

where:   $\Delta B_{ij}^z(k) = B_{ij}^z(k) - B_{ij}^z(k-1)$ and $\Delta A_{ji}^z(k) = A_{ji}^z(k) - A_{ji}^z(k-1)$

Finally, the term $B_{T,i}^z$ corresponds to the transfer flow of passengers that get on the bus at the initial stop of segment $i$ from another route and segment. Similarly to the term $A_{T,i}^z(k)$, the term $B_{T,i}^z$ is only different than 0 in the following combinations of route segments and directions: $B_{T,4}^y = B_{1,4}^x + B_{3,4}^y$; $B_{T,1}^y = B_{4,1}^x + B_{5,1}^y$; $B_{T,5}^x = B_{3,5}^y + B_{1,5}^x$, and $B_{T,3}^x = B_{5,3}^y + B_{4,3}^x$.

**Case a2.** The dwell times of routes A and B at stops distributed along segment $i=2$ must be calculated simultaneously from stop $k=1$ to $k=n_s^{2z}$, since dwell times of both routes depend on the relative time headway between buses of route A and B. Let $t_{d_A}^{2z}(k)$ and $d_{t_A}^{2z}(k)$ be the departure time and the dwell time of vehicle A from/at stop $k$ $(k = 1, ..., n_s^{2z})$ respectively. The corresponding variables for a vehicle of route B are $t_{d_B}^{2z}(k)$ and $d_{t_B}^{2z}(k)$.

$$t_{d_A}^{2z}(k) = \begin{cases} t_{a_A}^{2z}(k) + \max\{\beta_A; \alpha_A\} & k > 1 \\ t_{0,A}^{2z} + \Phi_A^z(k) \cdot H \cdot \tau_o + B_{22}^z(k) \cdot \tau_o \cdot \left(t_{a,A}^{2z}(k) - \kappa_{a,B}^{2z}(k)\right) & k = 1 \end{cases} \tag{45}$$

where: $\beta_A = \left(\Phi_A^z(k) - \Phi_A^z(k-1)\right) \cdot H \cdot \tau_o + \left(B_{22}^z(k) - B_{22}^z(k-1)\right) \cdot \tau_o \cdot \left(t_{a,A}^{2z}(k) - \kappa_{a,B}^{2z}(k)\right)$

and $\alpha_A = \left(\pi_A^z(k) - \pi_A^z(k-1)\right) \cdot H \cdot \tau_d + R_{2A}^z(k) \frac{A_{22}^z(k)}{B_{22}^z(k)} \cdot \tau_d + A_{T,A}^z(k) \cdot H \cdot \tau_d$

Equation (45) provides the estimation of the departure time from stop $k$ for bus route A, considering the boarding and alighting operations at this stop (dwell time) and the arrival

time. The term $\Phi_A^x(k)$ represents the boarding rate of passengers at stop $k$, segment $i=2$, direction $z$, that can only board on route A. The passenger destination is located on a branched segment (ahead), only served by this route A, different from the central segment. This term is $\Phi_A^x(k) = B_{23}^x(k)$ for direction $x$ and $\Phi_A^y(k) = B_{21}^y(k)$ for direction $y$. Similarly, the term $\pi_A^z(k)$ represents the alighting rate of passengers along segment $i=2$ in direction $z$ whose initial origin was located on a branched segment served by route A. This term is $\pi_A^x(k) = A_{12}^x(k)$ for direction $x$ and $\pi_A^y(k) = A_{32}^y(k)$ for direction $y$. Finally, the term $A_{T,A}^z(k)$ accounts for those passengers travelling along central segment $i=2$ of route A that have previously boarded in a branched segment served by route A. These passengers are alighting at the last stop of central segment $i=2$. Then, they will transfer to vehicles of route B in order to arrive at a branched segment only served by route B. Taking into account the assumption vii), this term is equal to 0 except for $k=n_s^{2x}$ in direction $x$ where $A_{T,A}^x(n_s^{2x}) = B_{15}^x = A_{15}^x$ ; and $k=n_s^{2y}$ in direction $y$ where $A_{T,A}^y(n_s^{2y}) = B_{34}^y = A_{34}^y$.

The estimation of the relative time headway between buses in Equation (45) deserves mention. Let $t_{0,A}^{2z}$ $t_{0,B}^{2z}$ be the arrival time at the first stop of segment $i=2$ in direction $z$ of the bus operating route A and B respectively. Depending on the length, demand rates and traffic lights in the branched segments, the entrance time of these buses at the segment $i=2$ may be spaced more than the target headway $H$ ($t_{0,A}^{2z} - t_{0,B}^{2z} > H$ or $t_{0,B}^{2z} - t_{0,A}^{2z} > H$). This situation means that these buses are not running the central segment consecutively. This situation can also occur at any stop along central segment if overtaking is allowed between vehicles belonging to different routes. To solve this issue, we calculate the arrival time $\kappa_{a,B*}^{2z,}(k)$ at stop $k$ of that bus B running ahead bus A. This term $\kappa_{a,B*}^{2z,}(k)$ is calculated summing or subtracting $m^z(k)$ times the headway $H$ to the bus A under analysis.

If the arrival times at stop $k$ of vehicles belonging to route A and B satisfy $t_{a,B}^{2z,}(k) < t_{a,A}^{2z,}(k)$, Equation (4.6a) calculates the arrival time $\kappa_{a,B}^{2z}(k)$ of that vehicle of route B that is running ahead of vehicle A. The estimation of the new arrival time $\kappa_{a,B}^{2z}(k)$ of the vehicle B when $t_{a,B}^{2z}(k) > t_{a,A}^{2z}(k)$ is provided in Equation (46b). Therefore, the number of potential passengers boarding on bus A at stop $k$ will be proportional to $\left( t_{a,A}^{2z}(k) - \kappa_{a,B}^{2z}(k) \right)$. Equations (46) are valid even for the first stop of segment $i=2$ when $t_{a,A}^{2z}(k) = t_{0,A}^{2z}$ and $t_{a,B}^{2z}(k) = t_{0,B}^{2z}$. The

mathematical operators $[x]^+$ and $[x]^-$ provide the rounded value of term $x$ to the upper and lower integer, respectively.

$$\kappa_{a,B}^{2z}(k) = t_{a,B}^{2z}(k) + m^z(k)H \quad \text{if} \quad t_{a,B}^{2z}(k) < t_{a,A}^{2z}(k) \tag{46a}$$
$$\text{where } m^z(k) = \left[ \frac{t_{a,A}^{2z}(k) - t_{a,B}^{2z}(k)}{H} \right]^-$$

$$\kappa_{a,B}^{2z}(k) = t_{a,B}^{2z}(k) - m^z(k)H \quad \text{if} \quad t_{a,B}^{2z}(k) > t_{a,A}^{2z}(k) \tag{46b}$$
$$\text{where } m^z(k) = \left[ \frac{t_{a,B}^{2z}(k) - t_{a,A}^{2z}(k)}{H} \right]^+$$

Finally, the term $R_{2A}^z(k)$ in Equation (47) represents the onboard passengers between stops $k$, $k+1$ whose origin and destination are both located along the same central route segment ($i=2$) in direction z. Oppositely, $Q_{2A}^z(k)$ represents the onboard passengers between stops $k,k+1$ whose origin or destination are not located along the route segment $i=2$ in direction z. The sum of both terms' accounts for the real occupancy of the vehicle $O_{2A}^z(k) = R_{2A}^z(k) + Q_{2A}^z(k)$. The term $Q_{2A}^z(k)$ does not depend on the entrance time of buses of route A and B at the first stop. Unfortunately, this statement is not true for term $R_{2A}^z(k)$. The hourly boarding rate $B_{22}^z(k')$ of those passengers with origin and destination at segment $i=2$ is split into route A and B, proportionally to the relative headway of one vehicle with regard to the vehicle ahead. Hence, the equivalent number of these passengers that will alight at a further stop $k$ ($k>k'$) should be calculated considering the real occupancy of vehicles of route A, i.e. $R_{2A}^z(k)$. Therefore, the number of passengers alighting at stop $k$ that previously boarded along segment $i=2$ in Equation (45) is calculated by the product between $R_{2A}^z(k)$ and the quotient $\frac{A_{22}^z(k)}{B_{22}^z(k)}$. Note that this quotient is equal to 1 at the last stop $k=n_s^{2z}$. The estimation of $R_{2A}^z(k)$ and $Q_{2A}^z(k)$ are provided through Equations (47) and (48) respectively.

$$R_{2A}^z(k) = \begin{cases} R_{2A}^z(k-1) + \left( t_{a,A}^{2z}(k) - \kappa_{a,B}^{2z}(k) \right) \Delta B_{22}^z(k) - R_{2A}^z(k-1) \dfrac{A_{22}^z(k)}{B_{22}^z(k)} & k > 1 \\[2mm] \left( t_{a,A}^{2z}(1) - \kappa_{a,B}^{2z}(1) \right) \left( B_{22}^z(1) \right) & k = 1 \end{cases} \tag{47}$$

$$Q_{2A}^z(k) = \begin{cases} Q_{2A}^z(k-1) + \left( \Delta\Phi_A^z(k) - \Delta\pi_A^z(k) \right) \cdot H & k > 1 \\[2mm] H \cdot \Lambda_A^z + H \left[ \displaystyle\sum_{j=1}^{5} \left( B_{2j}^z(1) \right) \right] & k = 1 \end{cases} \tag{48}$$

where: $\Delta B_{22}^z(k) = B_{22}^z(k) - B_{22}^z(k-1)$; $\Delta\Phi_A^z(k) = \Phi_A^z(k) - \Phi_A^z(k-1)$; and $\Delta\pi_A^z(k) = \pi_A^z(k) - \pi_A^z(k-1)$

The definition of $Q_{2A}^z(1)$ in Equation (48) needs the boundary condition at stop $k$=1 to verify the passenger flow conservation. The term $\Lambda_A^z$ is the hourly rate of passengers that have boarded at a previous branched segment $i{\neq}2$ and are still onboard at the first stop on central segment $i$=2. The corresponding boundary condition for this term in direction $x$ and $y$ is $\Lambda_A^x(1) = B_{12}^x + B_{13}^x + B_{15}^x$ and $\Lambda_A^y(1) = B_{32}^y + B_{31}^y + B_{34}^y$, respectively.

Equation (13) defines the departure time of the bus of route B from stop $k$. The term $\Phi_B^z(k)$ is equal to $\Phi_B^x(k) = B_{25}^x(k)$ for direction $x$ and $\Phi_B^y(k) = B_{24}^y(k)$ for direction $y$. In addition, the term $\pi_B^z(k)$ is equal to $\pi_B^x(k) = A_{42}^x(k)$ for direction $x$ and $\pi_B^y(k) = A_{52}^y(k)$ for direction $y$. Similarly, the term $A_{T,B}^z(k)$ accounts for those passengers that are alighting at the last stop of segment $i$=2, to transfer to vehicles of route A. These passengers have previously boarded in a branched segment and are travelling along the central segment. Taking into account the assumption vii), this term is equal to 0 except for $k=n_s^{2x}$ $(A_{T,B}^x(n_s^{2x}) = B_{15}^x = A_{15}^x)$ in direction $x$ and $k =n_s^{2y}$ $(A_{T,A}^y(n_s^{2y}) = B_{34}^y = A_{34}^y)$. In that case, the real time headway of the bus B with the bus A ahead is estimated by $[\kappa_{a,B}^{2z}(k) + H - t_{a,A}^{2z}(k)]$, where $\kappa_{a,B}^{2z}(k)$ is provided by Equations (46a and b). In fact, $\kappa_{a,B}^{2z}(k) + H$ is the arrival time at stop $k$ of the vehicle B that is running rear to the bus of route A.

$$t_{d_B}^{2z}(k) = \begin{cases} t_{a_A}^{2z}(k) + \max\{\beta_B; \alpha_B\} & k > 1 \\ t_{0,B}^{2z} + \Phi_B^z(k) \cdot H \cdot \tau_o + B_{22}^z(k) \cdot \tau_o \cdot \left(\kappa_{a,B}^{2z}(k) + H - t_{a,A}^{2z}(k)\right) & k = 1 \end{cases} \quad (49)$$

where: $\beta_B = \left(\Phi_B^z(k) - \Phi_B^z(k-1)\right) \cdot H \cdot \tau_o + \left(B_{22}^z(k) - B_{22}^z(k-1)\right) \cdot \tau_o \cdot \left(\kappa_{a,B}^{2z}(k) + H - t_{a,A}^{2z}(k)\right)$

and $\alpha_B = \left(\pi_B^z(k) - \pi_B^z(k-1)\right) \cdot H \cdot \tau_d + R_{2B}^z(k)\frac{A_{22}^z(k)}{B_{22}^z(k)} \cdot \tau_d$

$$R_{2B}^z(k) = \begin{cases} R_{2B}^z(k-1) + \Delta B_{22}^z(k) \cdot \left(\kappa_{a,B}^{2z}(k) + H - t_{a,A}^{2z}(k)\right) - R_{2B}^z(k-1)\frac{A_{22}^z(k)}{B_{22}^z(k)} & k > 1 \\ \left(\kappa_{a,B}^{2z}(k) + H - t_{a,A}^{2z}(k)\right)\left(B_{22}^z(1)\right) & k = 1 \end{cases} \quad (50)$$

$$Q_{2B}^z(k) = \begin{cases} Q_{2B}^z(k-1) + \left(\Delta\Phi_B^z(k) - \Delta\pi_B^z(k)\right) \cdot H & k > 1 \\ H \cdot \Lambda_B^z + H \left[\sum_{j=1}^{5}\left(B_{2j}^z(1)\right)\right] & k = 1 \end{cases}$$

(51)

where $\Delta\Phi_B^z(k) = \Phi_B^z(k) - \Phi_B^z(k-1)$; $\Delta B_{22}^z(k) = B_{22}^z(k) - B_{22}^z(k-1)$ and $\Delta\pi_B^z(k) = \pi_B^z(k) - \pi_B^z(k-1)$

Like the analysis of route, A, Equation (50) and (51) define the corresponding occupancy terms $R_{2B}^z(k)$ and $Q_{2B}^z(k)$ to the vehicles of route B. In order to fulfill the passenger conservation condition, the initial passenger flow of route B at the initial stop must be $\Lambda_B^x(1) = B_{42}^x + B_{45}^x + B_{43}^x$ and $\Lambda_B^y(1) = B_{52}^y + B_{54}^y + B_{51}^y$, in direction $x$ and $y$ respectively.

The previous Equations (45) and (51) allow the estimation of the departure time of buses of route A and B from stop $k$, once all boarding and alighting passenger operations have been finished.

### 3.4.1.4.2 Estimation of travel time between consecutive stops (k, k+1)

We assume that there are $m_k^{iz}$ intersections in the sketch between stops ($k$, $k$+1) in segment $i$ and direction $z$. The travel time to overcome the distance $s_k^{iz}$ between the aforementioned stops ($k$, $k$+1) in this route segment is $tt^{iz}(k)$. The term $tt_0^{iz}(k)$ denotes the travel time to overcome the distance between stop $k$ and the first intersection $j$=1; $tt_j^{iz}(k)$ the travel time to overcome the distance between intersections $j$,$j$+1; $tt_{m_k^{iz}}^{iz}(k)$ the travel time to cover the distance between intersection $m_k^{iz}$ and stop $k$+1, and finally, $t_j^{iz}(k)$ the traffic delay caused by the complete detention of vehicle at intersection $j$ ($j = 1, ..., m_k^{iz}$). Therefore, the estimation of the travel time between consecutive stops $k$, $k$+1 can be assessed by Equation (52).

$$tt^{iz}(k) = tt_0^{iz}(k) + \sum_{j=1}^{m_k^{iz}-1} tt_j^{iz}(k) + tt_{m_k^{iz}}^{iz}(k) + \sum_{j=1}^{m_k^{iz}} w_j^{iz}(k)$$

(52)

The estimation of the first three components of Equation (52) is further analysed in Appendix 3. Equation (53) defines the required time to overcome the distance between stop $k$ and intersection $p$, considering that the assumption ix) is valid and that the vehicle departs from

stop $k$ at speed $v_i=0$, where $\Delta z = x(p_j^{iz}) - \sum_{j=1}^k s_j^{iz}$ is the distance between stop $k$ and

intersection $j$, and $\tau = \frac{v_{max}}{a}$ is the additional time spent in the acceleration phase in

comparison to one bus that would not perform the stop and would maintain a constant speed

$v_{max}$. The estimation of the travel time between intersection $j$ and $j+1$, $tt_j^{iz}(k)$ ($j=1,..,m_k^{iz} - $

1) is provided in Equation (54) for different cinematic conditions, where $v_{dep}$ ($0 \leq v_{dep} \leq v_{max}$) is

the instantaneous speed when the bus departs from intersection $j$.

$$tt_0^{iz}(k) = \begin{cases} \dfrac{\Delta z}{v_{max}} + \dfrac{\tau}{2} & if \ \Delta z > \dfrac{1}{2}a\tau^2 \\ \sqrt{2 \cdot \Delta z/a} & otherwise \end{cases} \tag{53}$$

$$tt_j^{iz}(k) = \begin{cases} \dfrac{\Delta z}{v_{max}} + \dfrac{(\Delta v)^2}{2av_{max}} & if \quad \dfrac{v_{dep}\Delta v}{a} + \dfrac{1}{2}\dfrac{(\Delta v)^2}{a} < \Delta z \\ \dfrac{-v_{dep} + \sqrt{2 \cdot \Delta z \cdot a + v_{dep}^2}}{a} & otherwise \end{cases} \tag{54}$$

Where $\Delta v = v_{max} - v_{dep}$

Finally, Equation (55) states the travel time between the last intersection $j=m_k^{iz}$ to the next

stop $k+1$.

$$tt_{m_k^{iz}}^{iz}(k) = \begin{cases} \dfrac{\Delta z}{v_{max}} + \dfrac{v_{max} - v_{dep}\left(1 - \frac{v_{dep}}{2v_{max}}\right)}{a} & if \quad d_1 < \Delta z \\[3mm] \dfrac{2\sqrt{a\Delta z + \frac{(v_{dep})^2}{2}} - v_{dep}}{a} & if \quad d_1 > \Delta z > d_2 \\[3mm] \dfrac{\sqrt{2a\Delta z}}{a} - \dfrac{(v_{max} - \sqrt{2a\Delta z})^2}{2av_{max}} & if \ \Delta z < d_2; v_{dep} = v_{max}; t_{cruise} > \dfrac{v_{max} - \sqrt{2a\Delta z}}{a} \\[3mm] \dfrac{\sqrt{2(v_{max}^2 + 2a\Delta z + 2v_{max}at_{cruise})} - v_{max}}{a} - t_{cruise} & if \ \Delta z < d_2; v_{dep} = v_{max}; t_{cruise} < t_1 \\[3mm] \dfrac{\left(\sqrt{2(v_{dep}^2 + 2a\Delta z)} - v_{dep}\right)}{a} & if \ \Delta z < d_2; v_{dep} < v_{max} \end{cases} \tag{55}$$

Where: $d_1 = \dfrac{(v_{max})^2}{a} + \dfrac{(v_{dep})^2}{2a}$; $d_2 = \dfrac{1}{2}a\left(\dfrac{v_{dep}}{a}\right)^2$; $t_1 = \dfrac{v_{max} - \sqrt{2a\Delta z}}{a}$

The previous estimations of travel times allow decision makers to calculate the arrival time of

the bus at intersections in an increasing order along direction $x$ or $y$. This arrival time requires

to check if the traffic light at intersections will be in green or red phase. In the latter

condition, we may expect a delay of a bus. Therefore, the arrival time $t_{a,p}^{iz}$ at intersection $j$

($j=1,\ldots, m_{k+1}^{iz}$) in route $i$ in direction $z$ is estimated by Equation (56), where the departure time from the last stop $k$ , $t_d^{iz}(k)$, and from the ($j$-1) previous intersections are known.

$$t_{a,j}^{iz} = t_d^{iz}(k) + tt_0^{iz}(k) + \sum_{h=1}^{j-1} w_h^{iz}(k) + \sum_{h=1}^{j-1} tt_h^{iz}(k) \tag{56}$$

To fulfil the reference code of all intersections in the tram, $j^* = j + \sum_{h=1}^{k} m_h^{iz}$. Let $n_j^{iz} = \left\lceil \frac{t_{a,j}^{iz} - \Delta_{j*}^{iz}}{C_p} \right\rceil^{-}$ be the number of traffic light cycles that have been completed from $t$=0 at this intersection $j^*$ when the bus under study arrives. The term $\Delta_{j*}^{iz}$ is the global traffic light offset of this intersection. Therefore, the delay at intersection $j$ is estimated by Equation (57), considering the amount of time that the vehicle is completely stopped at an intersection. The time lost in the acceleration and braking phase is considered in the travel time component evaluated in Equation (54). Finally, the term $\Delta g$ is the green extension parameter to be defined when the control strategy S3 is activated (see Section 3.4.3). For the base case implementation of the bus motion modeling, this parameter is set $\Delta g = 0$ seconds.

$$w_j^{iz}(k) = \begin{cases} 0 & \text{if} \quad t_{a,p}^{iz} \leq C_p n_j^{iz} + \Delta_{j*}^{iz} + g_{p_{p}^{iz}}^{iz} + \Delta g \\ \left(C_p(n_j^{iz} + 1) + \Delta_j^{iz} - t_{a,j}^{iz}\right) & \text{otherwise} \end{cases} \tag{57}$$

### 3.4.2   Optimisation

The key performance indicators to analyse the proper operational design of the corridor, as well as the effects on the user side, are presented in this section. Compact estimations for the operating cost incurred by the transit agency and the temporal costs experienced by users are provided, based on the modelling framework presented in Section 3.4.1. An optimisation procedure of the vehicle synchronisation and headway is developed, aimed at minimising both, the total cost of the system and the vehicle regularity.

#### 3.4.2.1   User performance

The effects of the bus performance on the user's side will be mainly evaluated by the total travel time of users and the coefficient of variation of headways. The former metric is the sum of the time spent by users in the waiting (*W*), in-vehicle (*IVTT*) and transferring (*W*T) components of all user trips. The latter, denoted by $c_{vH}$, is a commonly used metric to assess

the quality of the service, in terms of reliability and time-headway adherence. These metrics are consistent to Estrada et al. (2016).

On the one hand, the in-vehicle travel time $IVTT_i$ and the waiting time $W_i$ in route segment $i$ ($i$=1, 2, 3,4, 5) are estimated by Equations (58) and (59) respectively. The waiting time of the passengers that make one transfer is evaluated in Equation (60). In this equation, the unique terms $B_{ij}^z$ different than 0 are the ones that compose the variable $B_{T,i}^z$ of Equation (44). The term $h_{ij}^{z,z'}$ is the difference between the next entrance time of the outbound route at the first stop of route segment $j$ in direction $z$ and the arrival time of the inbound route at the last stop of segment $i$ in direction z. When $z$ and $z'$ are different, the inbound and outbound routes are operating branched lines and this time difference is calculated by $h_{ij}^{z,z'} = \left(t_0^{jz'} \pm mH\right) - t_a^{iz}\left(n_S^{iz}\right)$. The term $m$ is an integer variable that must be specified to calculate the time difference between consecutive vehicle departures of the outbound route with regard to the inbound route arrival. When $z$ and $z'$ denote the same direction of service ($x$ or $y$), it represents the situation in which the inbound route segment at the transfer point is $i$=2 (route A or B). In that case, the difference between outbound departure and inbound arrival is assessed by $h_{ij}^{z,z} = \left(t_0^{jz} \pm mH\right) - t_{a,A}^{2z}(n_S^{2z})$ or $h_{ij}^{z,z} = \left(t_0^{jz} \pm mH\right) - t_{a,B}^{2z}(n_S^{2z})$.

$$IVTT_i = \begin{cases} \displaystyle\sum_{z\in\{x,y\}}\left(\sum_{k=1}^{n_S^{2z}-1} O_{2A}^z(k)\cdot\left(t_{a,A}^{2z}(k+1)-t_{a,A}^{2z}(k)\right) + \sum_{k=1}^{n_S^{2z}-1} O_{2B}^z(k)\cdot\left(t_{a,B}^{2z}(k+1)-t_{a,B}^{2z}(k)\right)\right) & i=2 \\ \displaystyle\sum_{z\in\{x,y\}}\left(\sum_{k=1}^{n_S^{iz}-1}\left\{O_i^z(k)\cdot\left(t_a^{iz}(k+1)-t_a^{iz}(k)\right)\right\}\right) & i=1,3,4,5 \end{cases}$$

(58)

Where: $O_{2A}^z(k) = Q_{2A}^z(k) + R_{2A}^z(k)$; $O_{2B}^z(k) = Q_{2B}^z(k) + R_{2B}^z(k)$

$$W_i = \begin{cases} \sum_{z\in\{x,y\}}\left\{\sum_{k=1}^{n_S^{2z}}\left(\Delta\Phi_B^z(k)+\Delta\Phi_A^z(k)\right)\cdot\frac{H^2}{2} + \Delta B_{22}^z(k)\cdot\left(\frac{\left(t_{a,A}^{2z}(k)-\kappa_{a,B}^{2z}(k)\right)^2}{2}+\frac{\left(\kappa_{a,B}^{2z}(k)+H-t_{a,A}^{2z}(k)\right)^2}{2}\right)\right\} & i=2 \\ \sum_{j=1}^5 \frac{H^2}{2}\cdot B_{ij}^z & i=1,3,4,5 \end{cases}$$

(59)

Where $\Delta\Phi_A^z(k) = \Phi_A^z(k) - \Phi_A^z(k-1)$; $\Delta\Phi_B^z(k) = \Phi_B^z(k) - \Phi_B^z(k-1)$; $\Delta B_{22}^z(k) = B_{22}^z(k) - B_{22}^z(k-1)$

$$W_T = \sum_{\substack{i=1\\i\neq2}}^{5}\sum_{\substack{j=1\\j\neq2}}^{5} H\left\{B_{ij}^z\cdot h_{ij}^{z,z'}\right\}$$

(60)

On the other hand, the coefficient of variation of headways is only calculated for segment $i=2$ by $c_{vh} = \frac{s_H^2}{H/2}$, where $s_H^2$ is the variance of the time headway deviation between consecutive buses from $H/2$ in all stops along segment $i=2$.

### 3.4.2.2   Agency metrics

The operating cost incurred by the bus operator will depend on the fleet size and the distance run by the whole fleet in the period of analysis ($V$). The estimation of the fleet size in route A and B (denoted by $M_A$ and $M_B$ respectively) can be obtained through Equation (61), considering the roundtrip travel times $T_A$ and $T_B$ provided by Equations (41) and (42). The mathematical operator $[x]^+$ provides the rounded value of $x$ to the upper integer.

$$M_A = \left[\frac{T_A}{H}\right]^+ \qquad M_B = \left[\frac{T_B}{H}\right]^+ \tag{61}$$

On the other hand, the distance run in one hour of service by the vehicles of each bus route (V_A and V_B respectively) can be estimated by Equation (62), as the total length of each route divided by the target headway.

$$V_A = \frac{l_1^x + l_2^x + l_3^x + l_3^y + l_2^y + l_1^y}{H} \quad ; \quad V_B = \frac{l_4^x + l_2^x + l_5^x + l_5^y + l_2^y + l_4^y}{H} \tag{62}$$

### 3.4.2.3   Optimisation procedure

The problem optimisation aimed at minimising the user and agency costs is presented in Equation (63). This problem is referred to as Problem P1. User costs $Z_U$ are computed as the product of waiting and in-vehicle travel times of all passengers by the value of the time parameter $\mu_N(\text{€/pax} - h)$. This parameter accounts for the monetary value of one hour spent by an average user in the system. The agency cost component $Z_A$ considers the number of resources and distance travelled by the whole fleet multiplied by the unit temporal and unit distance cost parameters, $c_t$ (€/veh-h) and $c_d$ (€/veh-km).

$$(\text{P1}) \min_{H, t_0^{1x}, t_0^{4x}} Z = Z_A + Z_N = (M_A + M_B)c_t + (V_A + V_B)c_d + \mu_N\left\{W_T + \sum_{i=1}^{5}(W_i + IVTT_i)\right\} \tag{63}$$

$$H \geq nC_p; \ 0 \leq t_0^{1x} \leq H; 0 \leq t_0^{4x} \leq H, \ \ \text{n integer} \tag{64}$$

$$HR_{2B}^z(k) + Q_{2B}^z(k) \leq C \ ; R_{2A}^z(k) + Q_{2A}^z(k) \leq C \ \ \ \forall k \tag{65}$$

Equation (64) states the non-negative nature of the decision variables of the problem: time-headway ($H$) and the entrance time of buses at the beginning of segments $i$=1 and $i$=4 in direction $x$ (variables $t_0^{1x}$ and $t_0^{4x}$). This problem must verify the capacity constraint presented in Equation (39). However, the previous constraint for route segment $i$=2 was calculated considering a perfect time headway of buses of routes A and B. Hence, if entrance times $t_0^{1x}$ and $t_0^{4x}$ are not properly synchronised to ensure constant headways in the central segment, the capacity constraint should be reformulated in Equation (65) for this route segment $i$=2.

Nevertheless, the optimal set of $H^*, (t_0^{1x})^*, (t_0^{4x})^*$ minimizing the objective function of P1 may cause a poor regularity in the central segment. In fact, this situation may occur when the transfer time component $W_T$ of the objective function is quite important due to the significant demand between branched segments. Hence, we propose a second optimisation problem labeled P2, aimed at minimizing the coefficient of variation of headways in the central route segment. This problem P2 is defined in Equation (66), considering the same constraints (28)-(29) stated in Problem P1. However, the optimisation process is only addressed at obtaining the best synchronisation of vehicle entrances of route A and B (variables $t_0^{1x}, t_0^{4x}$). Therefore, the time headway in the P2 problem is not considered as a decision variable and we use the optimal time headway $H^*$ obtained in problem P1.

$$\text{(P2)} \qquad \min_{t_0^{1x}, t_0^{4x}} \ c_{vh} = \frac{s_H^2}{H^*/2} \tag{66}$$

The optimisation procedure followed was based on the enumeration of the objective function Z ($H'$, $t_0^{1x'}, t_0^{4x'}$) or $c_{vh}(t_0^{1x'}, t_0^{4x'})$ for different variable intervals in the domain of the decision variables. Due to the assumptions ii) and iii) regarding the time headway variable, the objective function Z will be just evaluated for multiples values of the traffic light cycle $C_p$, $H'$=$n·C_p$, *n integer*. The maximal value of this integer number *n* is the one that fulfills the Equation (39). For other decision variables, we define a temporal pace of $\Delta$=1 second. The

entrance times of vehicles in segment $i$=1 (route A) and segment $i$=4 (route B) are then calculated respectively as $t_0^{1x'} = k_1 \cdot \Delta$ and $t_0^{4x'} = k_2 \cdot \Delta$; $k_1, k_2$ integers. Although these variables may range between $[0,H]$, we have only analysed the subdomains $t_0^{1x'} \in [0, C_p]$ and $t_0^{4x'} \in [t_0^{1x'}, H]$. These subdomains already contain the same solutions that we would obtain in the complementary subdomains excluded from the analysis.

### 3.4.3 Control strategies

As it is explained in section 3.4.1, there are different sources of instability in the proper definition of the problem that will cause a low level of service in segment i=2, in terms of regularity. To tackle this problem, we consider three potential bus control strategies to alleviate the lack of time headway adherence, in addition to the "do nothing" strategy defined as Strategy S0. They are enumerated in the following lines.

**Strategy S0**. This strategy resembles the assumptions listed in Section 3.5.1 where there is no key constraint to the bus motion nature. It considers that buses do not have any holding points along the route and overtaking between buses is allowed. Buses maintain the maximal cruising speed whatever the bus spacing about vehicle ahead will be. The formulation developed up to this point reflects this strategy.

**Strategy S0-NO**. This strategy considers that buses of different routes cannot overtake each other in the route segment i=2. We refer to buses A and B as the buses under study operating route A and B respectively. The overtaking of bus A by a bus B would take place when the departure time of the bus B, running theoretically rear to the bus A, will be lower than the corresponding to the vehicle of route A (ahead). Therefore, the departure time of bus B provided by Equation (49) must be replaced by the corresponding value given by Equation (67a), where the motion of the former bus B has been modified to depart later than bus A. Equation (67b) shows the same constraint in the case that bus A would overtake bus B. In both formulas, a delay ξ is imposed to the bus that would overtake the other one to maintain the order. This delay should be equal to the dwell time of the bus ahead at that stop k.

$$t_{d,B}^{2z}(k) = \begin{cases} t_{d,B}^{2z}(k) & \text{if } t_{d,A}^{2z}(k) < \kappa_{a,B}^{2z}(k) + H + d_{t_B}^{2z}(k) \\ t_{d,A}^{2z}(k) + d_{t_A}^{2z}(k) - nH + \xi & \text{otherwise} \end{cases} \quad (67a)$$

$$t_{d,,A}^{2z}(k) = \begin{cases} t_{d,A}^{2z}(k) & \text{if } t_{d,A}^{2z}(k) > \kappa_{a,B}^{2z}(k) + d_{t_B}^{2z}(k) \\ t_{a,B}^{2z}(k) + d_{t_B}^{2z}(k) - nH + \xi & \text{otherwise} \end{cases} \tag{67b}$$

being:

$$n = \begin{cases} \left[ \left( t_{a,A}^{2z}(k) - t_{a,B}^{2z}(k) \right) / H \right]^{-} & \text{if} \quad t_{a,B}^{2z,}(k) < t_{a,A}^{2z,}(k) \\ -\left[ \left( t_{a,B}^{2z}(k) - t_{a,A}^{2z}(k) \right) / H \right]^{+} & \text{if} \quad t_{a,B}^{2z}(k) > t_{a,A}^{2z}(k) \end{cases}$$

**Strategy S1.** We consider the provision of slacks at holding points (stops) in the central route segment $i$=2. This strategy is aimed at maintaining a constant headway of $H/2$ at the expenses of enlarging bus travel times along the central segment $i$=2. We assume that the maximal slack (i.e. available synchronisation time at a stop) is $\theta_{\max}$. Therefore, we inserted into the schedule the amount of $\theta_{\max}$ units of time at each stop of the route segment $i$=2. The modelling formulation modification to represent this strategy is presented in the following lines. Consider that the arrival time of vehicle of route A at stop $k$ in the central segment is $t_{a,A}^{2z}(k)$. As it is explained in section 2.4.1, the vehicle of route B, running ahead of the vehicle A under analysis, would have arrived at a time $\kappa_{a,B}^{2z}(k)$. Hence, the real time headway of vehicle A with regard to the vehicle at the rear of the route B is $\kappa_{a,B}^{2z}(k) + H - t_{a,A}^{2z}(k)$. The corresponding headway of vehicle B with regard to the vehicle of route A at the rear is $t_{a,A}^{2z}(k) - \kappa_{a,B}^{2z}(k)$. The control strategy forces vehicles of route A and B to wait $\theta_A(k)$ and $\theta_B(k)$ respectively at the stop $k$ when the previous real headways are higher than the target $H/2$ value. The determination of these slacks are estimated by Equations (68a) and (68b) depending on the difference between real and target headways. The first condition of formula (68a) does not force vehicle A to be held when the headway with regard to the vehicle at rear is lower than the target headway $H/2$. This situation means that vehicle B is catching up the vehicle A so that any additional delay of vehicle A will contribute to worsen the regularity. However, in the second and third conditions of Equation (68a), since the real headway between vehicles is higher than $H/2$, the provision of slacks will alleviate the lack of regularity. In the second condition, the maximal slack time is not sufficient to correct the real time headway to the desired $H/2$. In that case, the bus of route A will be held the maximal slack $\theta_{\max}$. On the contrary, in the third condition, the bus A needs lower holding time than the maximal slack to eliminate the deviation between real and target time headway in this section. Similar explanation could be made in Equation (68b) for the holding time of bus B running at rear of bus A under study.

$$\theta_A(k) = \begin{cases} 0 & if \left( \kappa_{a,B}^{2z}(k) + H - t_{a,A}^{2z}(k) \right) \leq \dfrac{H}{2} \\ \theta_{max} & if \left( \kappa_{a,B}^{2z}(k) + H - t_{a,A}^{2z}(k) \right) > \dfrac{H}{2} \ and \ \left( \kappa_{a,B}^{2z}(k) + \dfrac{H}{2} - t_{a,A}^{2z}(k) \right) > \theta_{max} \\ \left( t_{a,A}^{2z}(k) - \kappa_{a,B}^{2z}(k) - \dfrac{H}{2} \right) & if \left( \kappa_{a,B}^{2z}(k) + H - t_{a,A}^{2z}(k) \right) > \dfrac{H}{2} \ and \ \left( \kappa_{a,B}^{2z}(k) + \dfrac{H}{2} - t_{a,A}^{2z}(k) \right) \leq \theta_{max} \end{cases} \tag{68a}$$

$$\theta_B(k) = \begin{cases} 0 & if \left( t_{a,A}^{2z}(k) - \kappa_{a,B}^{2z}(k) \right) \leq \dfrac{H}{2} \\ \theta_{max} & if \left( t_{a,A}^{2z}(k) - \kappa_{a,B}^{2z}(k) \right) > \dfrac{H}{2} \ and \ \left( t_{a,A}^{2z}(k) - \kappa_{a,B}^{2z}(k) - \dfrac{H}{2} \right) > \theta_{max} \\ \left( t_{a,A}^{2z}(k) - \kappa_{a,B}^{2z}(k) - \dfrac{H}{2} \right) & if \left( t_{a,A}^{2z}(k) - \kappa_{a,B}^{2z}(k) \right) > \dfrac{H}{2} \ and \ \left( t_{a,A}^{2z}(k) - \kappa_{a,B}^{2z}(k) - \dfrac{H}{2} \right) \leq \theta_{max} \end{cases} \tag{68b}$$

Finally, these slacks must be added into the formulation of vehicle departures times from stop $k$. Therefore, the new departure times of route A and B vehicles from stop $k$ with this Strategy S2, denoted by $\left[ t_{d_A}^{2z}(k) \right]_{S2}$ and $\left[ t_{d_B}^{2z}(k) \right]_{S2}$ respectively, are calculated in Equations (69). The terms $t_{d_A}^{2z}(k)$ and $t_{d_B}^{2z}(k)$ are calculated through Equations (45) and (49). The calculation procedure should be also made in an increasing order of stops, so that both $\left[ t_{d_A}^{2z}(k) \right]_{S2}$ and $\left[ t_{d_B}^{2z}(k) \right]_{S2}$ should be an input of Equation (43) to calculate the arrival time at the next stop $(k+1)$.

$$\left[ t_{d_A}^{2z}(k) \right]_{S2} = \theta_A(k) + t_{d_A}^{2z}(k) \qquad \left[ t_{d_B}^{2z}(k) \right]_{S2} = \theta_B(k) + t_{d_B}^{2z}(k) \tag{69}$$

**Strategy S2.** This strategy extends the duration of the green phase at traffic lights to avoid delayed buses to stop at intersections. Therefore, we assume that the trajectories of vehicles are monitored to activate traffic light priority to buses in real time. Let $G$ be the extension time of the green phase allowed by traffic conditions. This green extension should be defined by a maximal percentage $\psi$ of the total traffic light cycle, $\dfrac{G}{C_p} < \psi$. However, this green extension time is only provided to those buses that present real time headway with the vehicle at the rear, lower than the desired value $H/2$. Therefore, the extension parameter $\Delta g$ of Equation (57) is replaced by $\Delta g_A$ for vehicles of route A and by $\Delta g_B$ for vehicles of route B, given in Equation (70).

$$\Delta g_A = \begin{cases} G & if \left(\kappa_{a,B}^{2z}(k) + H - t_{a,A}^{2z}(k)\right) \leq \dfrac{H}{2} \\ 0 & if \left(\kappa_{a,B}^{2z}(k) + H - t_{a,A}^{2z}(k)\right) > \dfrac{H}{2} \end{cases} \qquad \Delta g_B = \begin{cases} G & if \left(t_{a,A}^{2z}(k) - \kappa_{a,B}^{2z}(k)\right) \leq \dfrac{H}{2} \\ 0 & if \left(t_{a,A}^{2z}(k) - \kappa_{a,B}^{2z}(k)\right) > \dfrac{H}{2} \end{cases} \qquad (70)$$
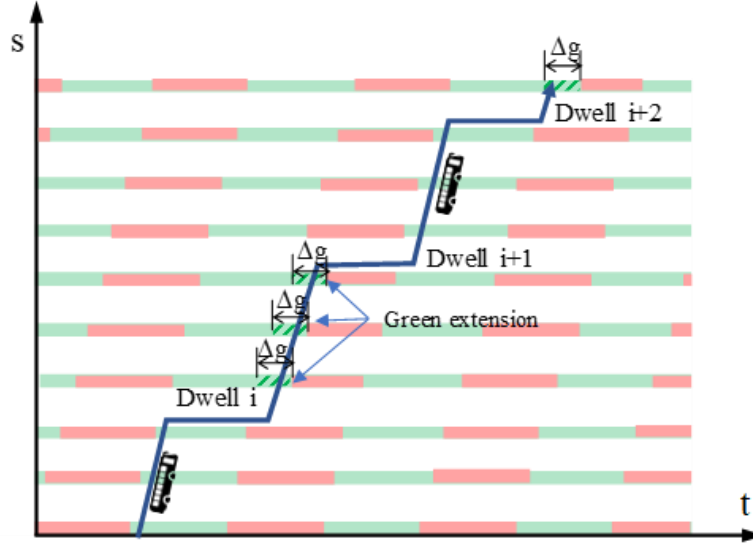


**Figure 18**. Scheme of green time extension in a time-space diagram.

**Strategy S3.** This strategy is a combination of Strategy S1 and S2. It extends the duration of the green phase at traffic lights (G>0) and introduces some slack at each stop ($\theta_{max}$>0). As suggested in Estrada et al. (2016), this was the most effective control strategy for minimising the total cost of the system, in corridors operated by a single line with exogenous bus disruptions.

## 3.5 Transfer areas

This chapter aims to develop a methodology to evaluate the performance of the bus operation at the transfer areas on a statistical-based approach. Although this methodology is based on objective estimations of the service provided, the most important design and operation-based factors that affect the quality perception of the users are addressed: reliability of the service and access between stops. Here, two levels of study are proposed: the transfer between inbound and outbound routes and the whole transfer area. Two quality measurement ratios are proposed to analyse the supplied quality considering this spatial differentiation: the TQR, Quality Transfer Ratio and the global IQR, Transfer Quality Ratio for the entire area. These ratios will be calculated both for scheduled and actual service, providing a level of service gradation based on the expected variance of the operating variables. The values corresponding to the real and planned performance can be compared and the evolution over time can be assessed as well. These ratios measure the expected additional walking time and waiting time as well as the variability of these variables.

To define these ratios, various mathematical and statistical approaches have been used as well as data from several devices currently involved in the bus operation: AVL, Automated Vehicle Location, passenger counting systems, ticketing systems validation, among others and even direct observations. For data treatment, we used MSExcel, an ad-hoc property application developed with ©Visual Studio, and several routines with MatLab.

Finally, a real example is proposed: the transfer area of "Eixample Dret" in Barcelona, intersected by two high levels of service routes: H10 and V17, part of the Barcelona's new premium routes. In Badia et al. (2016), a hybrid network based on transfers was justified to be the most cost-efficient one for Barcelona. The scientific analysis presented there is consistent with the new bus network design project started by the bus operator and city council in 2012. The methodology can be applied to railroad transfer areas, mixed systems with premium bus routes and train or tramway lines, and it also works with conventional bus route systems.
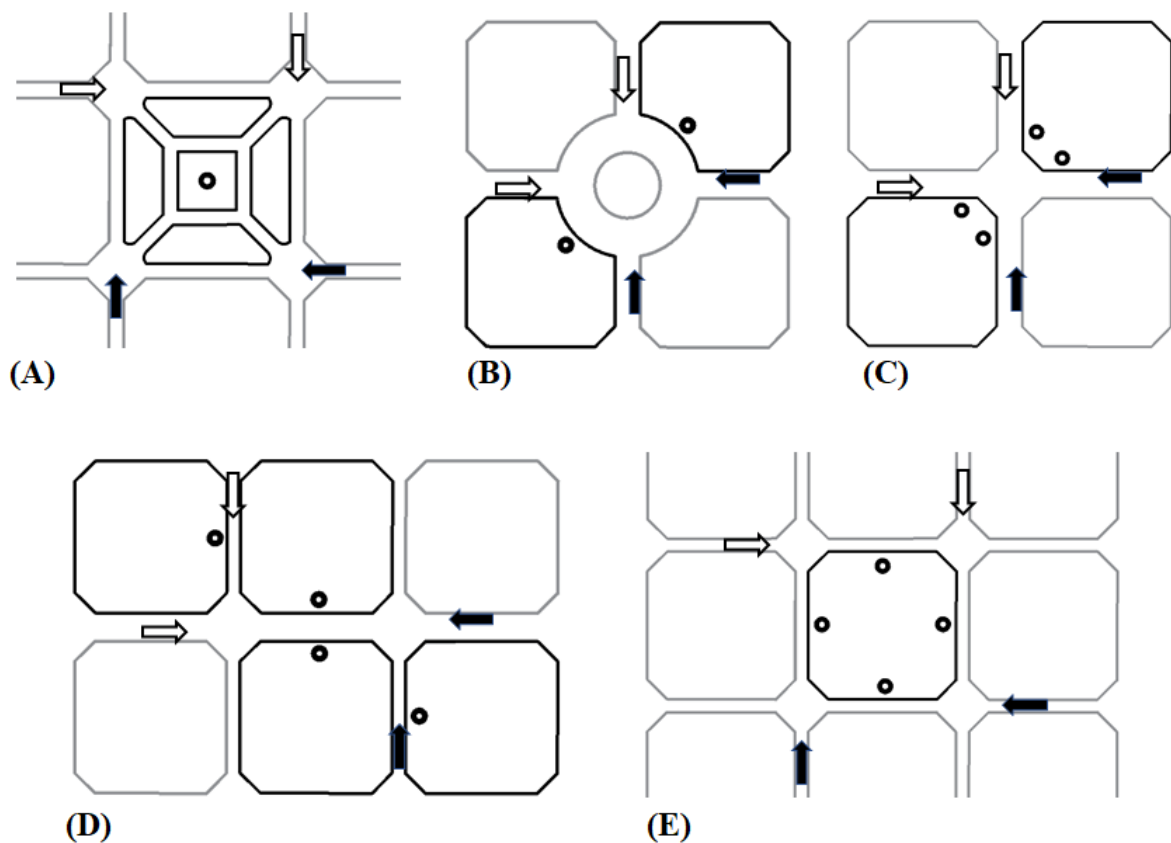
**Figure 19**. Various types of transfer areas: (A) ideal, (B) circular, (C) close to the junction, (D) when one of the streets have two directions, and (E) in a block.

### 3.5.1 Customer satisfaction and service quality

The user's level of satisfaction in a transfer area is the result of integrating the quality perception of multiple attributes regarding planning, service adherence, reliability/uncertainty, passenger information, safety and cleanliness (Parasuraman et al. 1988, 1991, Barabino et al. 2012). We assume that customer satisfaction is related to the average time spent to complete the transfer ($\mu_T$: walking travel time between stops and waiting time at the reception route stop) and the standard deviation of the transfer walking and waiting times ($\sigma_T$). These two variables may describe the temporal disutility of the transfer, affected by the operational planning, service adherence and reliability components. Formally, the satisfaction can be characterised by a regular function (two times differentiable with second derivative continuous), $S(\mu_T, \sigma_T): R^2 \rightarrow R$, which is strictly decreasing in the two coordinates $\mu_T$ and $\sigma_T$ ($\mu_T > 0$ and $\sigma_T > 0$), and has a maximum value of 100 at the point with minimum transferring time and maximum reliability ($\mu_T, \sigma_T$) = (0, 0).

### 3.5.1.1 Functional approach

In this context, the quality of a transfer and the operational component of the customer's satisfaction can be considered as synonyms or linearly related terms. Therefore, without prejudice to the generality, the *transfer quality ratio* can be defined by TQR($\mu_T$, $\sigma_T$)=S($\mu_T$, $\sigma_T$) (quality=satisfaction). Although the expression of the satisfaction function S($\mu_T$, $\sigma_T$) may be unknown, the second order Taylor development of function S($\mu_T$, $\sigma_T$) at point ($\mu_T$, $\sigma_T$) = (0, 0) has the following approach:

$$TQR(\mu_T, \sigma_T) = S(\mu_T, \sigma_T) \cong S(0,0) + \frac{\partial S}{\partial \mu_T}\bigg|_0 (\mu_T - 0) + \frac{\partial S}{\partial \sigma_T}\bigg|_0 (\sigma_T - 0)$$

$$+ \frac{1}{2}\left[ \frac{\partial^2 S}{\partial \mu_T^2}\bigg|_0 (\mu_T - 0)^2 + \frac{\partial^2 S}{\partial \sigma_T^2}\bigg|_0 (\sigma_T - 0)^2 + 2\frac{\partial^2 S}{\partial \mu_T \partial \sigma_T}\bigg|_0 (\mu_T - 0)(\sigma_T - 0) \right]$$

$$= S(0,0) + a_{11}\mu_T{}^2 + a_{22}\sigma_T{}^2 + 2a_{12}\mu_T\sigma_T$$

Where $S(0,0) = 100$, $\partial S/\partial \mu_T|_0 = \partial S/\partial \sigma_T|_0 = 0$ (to get a maximum at the point $(\mu_T, \sigma_T) = (0,0)$), $a_{11} = \frac{1}{2}\partial^2 S/\partial \mu_T^2|_0$, $a_{22} = \frac{1}{2}\partial^2 S/\partial \sigma_T^2|_0$, and $a_{12} = \frac{1}{2}\partial^2 S/\partial \mu_T \partial \sigma_T|_0$

Therefore, the quality of a transfer can be evaluated using the following quadratic expression:

$$TQR(\mu_T, \sigma_T) = 100 + a_{11}\mu_T{}^2 + a_{22}\sigma_T{}^2 + 2a_{12}\mu_T\sigma_T \tag{71}$$

being $a_{11}, a_{22}$ and $a_{12}$ three constants to be determined.

**Remark 1**. In integrated transport networks, one transfer area may present multiple potential transfer movement among stops and loading areas. The partial quality assessment of a single transfer movement must be placed in the context of the whole transfer area. Hence, it is appropriate to consider weighting factors $\xi_i$ based on the relative passenger flow in each movement *i* (*i*=1, ..,n, where *n* is the total number of transfers movements considered within the transfer area), to define the *quality at the transfer area* (IQR) as follows:

$$IQR = \frac{\sum_{i=1}^n \xi_i TQR_i}{\sum_{i=1}^n \xi_i} \tag{72}$$

**Remark 2.** From the customer's point of view, the perception of satisfaction is not proportional to the time spent at the transfer area. For example, if 1 minute penalizes the satisfaction by 1% (TQR (1, 0) = 99 %), it is not reasonable to assume that 10 minutes penalize by 10% (TQR (10, 0) = 90%). Consequently, the simplification provided by the first order (linear) Taylor's approach is not a valid method to characterise the quality of a transfer. In contrast, the customer's perception can be properly modelled by a second-order approach

(quadratic) since the modelled quality losses can grow at a higher rate than the measured transfer temporal components do.

**Remark 3.** For a pre-set quality$(TQR(\mu_T, \sigma_T) = TQR_0)$, the values that meet the equation,

$$TQR_0 = 100 + a_{11}\mu_T{}^2 + a_{22}\sigma_T{}^2 + 2a_{12}\mu_T\sigma_T \tag{73}$$

define an oblique ellipse, centred at the point (0, 0). This geometric interpretation is based on:

   a.  The conic section that defines (2.1), can be written in a matrix form, such as,

$$(1, \mu_T, \sigma_T) \cdot \begin{pmatrix} 100 - TQR_0 & 0 & 0 \\ 0 & a_{11} & a_{12} \\ 0 & a_{12} & a_{22} \end{pmatrix} \cdot \begin{pmatrix} 1 \\ \mu_T \\ \sigma_T \end{pmatrix} = 0$$

   b.  $a_{11} < 0$, $a_{22} < 0$, $a_{12} < 0$ and $|Hes| = det\begin{pmatrix} a_{11} & a_{12} \\ a_{12} & a_{22} \end{pmatrix} > 0$, since the maximum value of $TQR(\mu_T, \sigma_T)$ is reached at point $(\mu_T, \sigma_T) = (0, 0)$

   c.  Invariants meet the conditions: $I_1 = |A| = (100 - S_0) \cdot |Hes| \neq 0$, $I_2 = |Hes| \neq 0$ and sg $I_3$ = sg $(a_{11} + a_{22}) \neq$ sg $I_1$ (Spain, B., 2007)

**Remark 4.** Linear and quadratic models define conic sections that conform to planes (hyperplanes), ellipses (ellipsoids) and parabolas (paraboloids). This approach is justified with the following arguments: 1) when varying the curvature, these approximations allow a lot of flexibility and, consequently, provide good adjustments when the characterized functions are monotonous in their arguments (increasing or decreasing); 2) approximations of three, four or higher orders define regions that may have two or more extremes (maximum and minimum) and, therefore, the adjustment of the monotone indexes in their arguments is limited to monotonous subregions that lie between two extremes; and 3) the parameters of the model remarkably grow with the approach order and, consequently, the collinearity increases, and more regularity conditions are required.

### 3.5.1.2  Calibration of parameters $a_{11}$, $a_{22}$ and $a_{12}$

The functional approach defined in Eq. (3.5.1.1) defines a model that relates the quality of service (TQR) with the time spent at the transfer and its uncertainty. The estimation of the unknown parameters $(a_{11}, a_{22}, a_{12})$ is done considering the information provided through customer satisfaction surveys (see, as an example, de Oña and de Oña 2014) or specialist panels. The data collected in these information campaigns is the basis for the definition of the boundary conditions.

### 3.5.1.2.1 Customer's Satisfaction Survey

Let us assume that a customer satisfaction survey has been carried out to N customers. Each customer $i=1,.., N$ may be asked about his/her transfer satisfaction ($TQR_i$), i.e. the perception of the temporal disutility that he or she has experienced. We also assume that we may know from which vehicles and loading areas the passenger $i$ has transferred. Therefore, the transit agency may calculate the average time spent to perform this transfer movement and its potential uncertainty, $(\mu_i, \sigma_i)$, from the available information systems. Finally, the relational model defined in (3.5.1.1) provides the estimated quality index $(\widehat{TQR})$ based on the variables $(\mu_i, \sigma_i)$ evaluated for each user (see Table 5) and the given coefficients $(a_{11}, a_{22}, a_{12})$. Once the boundary conditions are established, so as not to penalise the customer, in general we have $(\mu_T, \sigma_T) = (0, 0)$. Therefore, the coefficients $(a_{11}, a_{22}, a_{12})$ may be calibrated minimising the quadratic error between the perceived and the estimated quality, $E(a_{11}, a_{22}, a_{12})$, Where N is the survey sample size,

$$E\left(a_{11}, a_{12}, a_{22}\right) = \sum_{i=1}^{N}\left(TQR_i - \widehat{TQR_i}\right)^2 = \sum_{i=1}^{N}\left(TQR_i - (100 + a_{11}\mu_i^2 + a_{22}\sigma_i^2 + 2a_{12}\mu_i\sigma_i)\right)^2$$

The coefficients $\left(a_{11}, a_{12}, a_{22}\right)$ should meet the following system of equations, resulting from setting to zero the partial derivatives $(\partial E/\partial a_{11} = 0, \ \partial E/\partial a_{22} = 0, \ \partial E/\partial a_{12} = 0)$:

$$\left. \begin{array}{l} a_{11}\sum_{i=1}^{N}\mu_i^4 + a_{22}\sum_{i=1}^{N}\mu_i^2\sigma_i^2 + 2a_{12}\sum_{i=1}^{N}\mu_i^3\sigma_i = \sum_{i=1}^{N}(TQR_i - 100)\mu_i^2 \\[2mm] a_{11}\sum_{i=1}^{N}\mu_i^2\sigma_i^2 + a_{22}\sum_{i=1}^{N}\sigma_i^4 + 2a_{12}\sum_{i=1}^{N}\mu_i\sigma_i^3 = \sum_{i=1}^{N}(TQR_i - 100)\sigma_i^2 \\[2mm] a_{11}\sum_{i=1}^{N}\mu_i^3\sigma_i + a_{22}\sum_{i=1}^{N}\mu_i\sigma_i^3 + 2a_{12}\sum_{i=1}^{N}\mu_i^2\sigma_i^2 = \sum_{i=1}^{N}(TQR_i - 100)\mu_i\sigma_i \end{array} \right\}$$  (73)

**Table 5**. Perceived quality $(TQR)$ and estimated quality $\widehat{(TQR)}$. Parameters $(\mu_i, \sigma_i)$ are the mean and the standard deviation of the time sequence spent at the transfer under study by customer $i$ ($i=1,.., $ N)

| $TQR$ | $\mu_T$ | $\sigma_T$ | $\widehat{TQR} = 100 + a_{11}\mu_T{}^2 + a_{22}\sigma_T{}^2 + 2a_{12}\mu_T\sigma_T$ |
|---|---|---|---|
| $TQR_1$ | $\mu_1$ | $\sigma_1$ | $\widehat{TQR}_1 = 100 + a_{11}\mu_1{}^2 + a_{22}\sigma_1{}^2 + 2a_{12}\mu_1\sigma_1$ |
| $TQR_2$ | $\mu_2$ | $\sigma_2$ | $\widehat{TQR}_2 = 100 + a_{11}\mu_2{}^2 + a_{22}\sigma_2{}^2 + 2a_{12}\mu_2\sigma_2$ |
| $\vdots$ | $\vdots$ | $\vdots$ | $\vdots$ |
| $TQR_N$ | $\mu_N$ | $\sigma_N$ | $\widehat{TQR}_N = 100 + a_{11}\mu_N{}^2 + a_{22}\sigma_N{}^2 + 2a_{12}\mu_n\sigma_N$ |

### 3.5.1.2.2  The consensus of experts

The quality of a transfer from the temporal disutility perspective has been linked to the user's walking time (or the distance between the loading areas of crossing routes), the user's waiting time, the synchronisation between the schedules of both routes (adjustment of the departures to the arrivals) and the service regularity of the routes (headway adherence). Once the components that determine the quality of a transfer are identified, the loss of satisfaction can be related to physical limitations of the loading areas, to the service planning inefficiencies or the actual operation provided.

At ideal transfer areas, user walking time and its uncertainty can be considered zero. Nevertheless, in many surface modes of transport, the reality is entirely different. Thus, surface transfers are usually placed in existing built-up areas, and as a result, displacements are strongly constrained by traditional urban planning. Accepting those limitations from the urban planning, the satisfaction penalty must be minimum when walking times and uncertainty are reasonable $(\mu_0, \sigma_0)$ (efficient design, conditioned by urban architecture).

The time synchronisation between the intersecting routes is desirable, but not always possible. If headways of the two routes are not multiple to each other, a pseudo-random effect on the departure/arrival time differences can occur. With neither time synchronisation nor regularity on the intersecting routes, the waiting time adjusts to a uniform distribution ($\mathcal{U}(0, H)$, being $H$ the headway of the receiving route). As a result, the average waiting time and uncertainty are estimated to be $\left(H/2, (H^2/12)^{1/2}\right)$, when both routes are not synchronised. On the other hand, the regularity of the affected routes is not imputable to the transfer layout, but it can significantly impact on the quality perception. When vehicles arrive irregularly at stops and, the well-known bus bunching effect occurs, the waiting times adjust to a uniform distribution ($\mathcal{U}(0, 2H)$) and consequently, the average waiting time and uncertainty can be estimated by $(2H/2, ((2H)^2/12)^{1/2}) = (H, (H^2/3)^{1/2})$.

Hence, the quality attributable to the optimal scenario (ideal physical transfer, with excellent synchronisation and regularity) is unquestionable $TQR(\mu_T, \sigma_T) = TQR(0,0) = 100$. On the contrary, the panel of experts must reach a consensus regarding the total penalty caused by

the progressive loss of the quadratic function components. Particularly, the scenarios proposed to discuss and approve are the following:

— The experimental situation I: constructing an efficient transfer, constrained by urban planning, with proper synchrony between routes and regularity. The walking time and its standard deviation is $(\mu_0, \sigma_0)$ and the waiting time and its standard deviation is (0, 0). In this case, TQR has been set in $TQR_0 = TQR(\mu_0, \sigma_0)$

— The experimental situation II: constructing an efficient transfer, constrained by urban planning, with reasonable regularity, but without any synchrony. The walking time and its standard deviation is $(\mu_0, \sigma_0)$ and the waiting time adjusts to an uniform distribution $\mathcal{U}(0, H)$. In this case, $(\mu_T, \sigma_T) = (\mu_1, \sigma_1) = \left(\mu_0 + H/2, (\sigma_0{}^2 + H^2/12)^{1/2}\right)$ and TQR has been set in $TQR_1 = TQR(\mu_1, \sigma_1)$

— The experimental situation III: constructing an efficient transfer, constrained by urban planning, without any synchrony, any regularity and high bunching effect. The walking time and its standard deviation is $(\mu_0, \sigma_0)$ and the waiting time adjusts to an uniform distribution $\mathcal{U}(0, 2H)$. In this case, $(\mu_T, \sigma_T) = (\mu_2, \sigma_2) = \left(\mu_0 + H, (\sigma_0{}^2 + H^2/3)^{1/2}\right)$ and TQR has been set in $TQR_2 = TQR(\mu_2, \sigma_2)$

Once the boundary conditions are set, the parameters $a_{11}, a_{22}, a_{12}$ are the solutions of the following System of linear equations:

$$\left.\begin{array}{l} TQR_0 = 100 + a_{11}\mu_0{}^2 + a_{22}\sigma_0{}^2 + 2a_{12}\mu_0\sigma_0 \\ TQR_1 = 100 + a_{11}\mu_1{}^2 + a_{22}\sigma_1{}^2 + 2a_{12}\mu_1\sigma_1 \\ TQR_2 = 100 + a_{11}\mu_2{}^2 + a_{22}\sigma_2{}^2 + 2a_{12}\mu_2\sigma_2 \end{array}\right\} \tag{74}$$

**Remark 5.** The customer perceptions or conditions agreed upon by experts may be inconsistent. In other words, the system of equations (73) or (74) can provide non-decreasing solutions in $\mu_T$ or $\sigma_T$. ($a_{11} \geq 0$, $a_{22} \geq 0$, or $a_{12} \geq 0$) or the maximum value is not reached at the point $(\mu_T, \sigma_T) = (0, 0)$. In those cases, the following optimisation problem needs to be solved:

a. The customer perception,

$$\min_{\{a_{11},\, a_{22},\, a_{12}\}} \sum_{i=1}^{N} \left( TQR_i - (100 + a_{11}\mu_i{}^2 + a_{22}\sigma_i{}^2 + 2a_{12}\mu_i\sigma_i) \right)^2$$

conditioned on: $a_{11} < 0, a_{22} < 0, a_{12} < 0$ and $a_{11}a_{22} - a_{12}^2 > 0$

b. The consensus of experts,

$$\min_{\{a_{11},\, a_{22},\, a_{12}\}} \sum_{i=0}^{2} \left( TQR_i - (100 + a_{11}\mu_i{}^2 + a_{22}\sigma_i{}^2 + 2a_{12}\mu_i\sigma_i) \right)^2$$

conditioned on: $a_{11} < 0, a_{22} < 0, a_{12} < 0$ and $a_{11}a_{22} - a_{12}^2 > 0$

The previous non-linear quadratic optimisation problems can be written in a more general form as follows:

$$\min_{\{a_{11},\, a_{22},\, a_{12}\}} \left\| M\vec{a} - \vec{b} \right\|$$

subject to: $a_{11} < 0, a_{22} < 0, a_{12} < 0$ and $a_{11}a_{22} - a_{12}^2 > 0$

where: $\vec{a} = (a_{11}, a_{22}, a_{12})^t$, $\vec{b} = (b_1, \dots, b_n)^t$, $b_i = TQR_i - 100$, $M = (m_{ij})$ and $(m_{i1}, m_{i2}, m_{i3}) = (\mu_i{}^2, \sigma_i{}^2, 2\mu_i\sigma_i)$. This type of problem can be solved using numerical methods implemented in standard programs (MatLab: optimisation toolbox, "fmincon" function; R: packages "nloptr" and "Alabama", among others).

**Remark 6.** When the system of equations (2.5) is incompatible, the solution obtained by numerical methods provides the best fit to the proposed model. In this case, it is interesting to evaluate the discrepancies,

$$TQR_i - (100 + a_{11}\mu_i{}^2 + a_{22}\sigma_i{}^2 + 2a_{12}\mu_i\sigma_i) \quad i{=}1,2,3$$

When these discrepancies are substantial, we must identify the root causes that bring about the inconsistencies and rethink the experimental conditions or the consensual values of $TQR_0$, $TQR_1$ and $TQR_2$. On the other hand, the coefficient of correlation and the mean squared error provide a measure of agreement between the operative component of the perceived satisfaction (user/survey) and the estimated operational satisfaction with the model.

### 3.5.1.2.3 The incomplete consensus of experts and regularity conditions

The consensus of experts, however desirable, is not always possible. Regarding the physical attributes of the transfer movement performed by the passenger, walking can be understood in different ways: 1) a short, pleasant and inevitable walk (in warm weather environments);

or 2) an avoidable movement (in colder climates) to be minimized with resources and policies promoting collective transport. On the other hand, synchronisation is only possible when route headways are equal or multiple of each other. In many other cases, the pseudo-randomness effect occurs. In this context, arguments from the point of view of both the passenger and the transit agency may also be considered to justify the lack of synchronisation and its effect on satisfaction: 1) the customer understands that generally the route headways are defined according to demand, and consequently it is not possible to completely harmonise all route headways, or 2) by adding resources, it is possible to totally or partially align the headways and consequently to improve the performance.

For these reasons, an alternative calibration procedure based on the consensus has been considered with a single boundary condition and two further regularity conditions. The boundary condition is the most unfavourable (TQR($\mu_2$, $\sigma_2$)=100-TQR$_2$): 1) efficient physical transfer but constrained by the urban environment; 2) without synchronisation, and 3) without regularity. Regarding regularity conditions, two geometric criteria for the ellipse that define the quality ratio TQR$_2$ (Remark 3) have been considered: 1) the semi-axes of the ellipse that define the TQR$_2$ must be homothetic (proportional) to the admissible maximum ($\mu$, $\sigma$) values (b/a=$\sigma_2$/$\mu_2$); and 2) the rotation angle of the ellipse must guarantee the formulation quadratic component. The condition b/a=$\sigma_2$/$\mu_2$ is justified by the pseudo-linearity between $\mu_T$ and $\sigma_T$, when the quality of service worsens, and because the direction defined by points (0, 0) and (a, b) provides the mean square gradient $(((a^2 + b^2)/2)^{1/2})$ in the quality levels (minimum=b: direction (0, $\sigma_T$) and maximum=a: direction ($\mu_T$, 0)). On the other hand, the rotation angle $\theta_{max}$/2 minimises the mean square error in the admissible range [$\theta_{max}$, 0]. In particular, T = $\theta_{max}$/2 is the solution to the optimisation problem: $min_T\ E(\theta - T)^2$, subject to $\theta \approx U$ [$\theta_{max}$, 0]. The technical justification for the regularity conditions have been included in the Appendixes E.I, E.II, E.III (proportionality of the maximum permissible semi-axes and values) and E.IV. In this context, the parameters a$_{11}$, a$_{12}$ and a$_{22}$ that define the Eq. (71) must satisfy the following system of non-linear equations:

$$\left.\begin{array}{l} a_{11}\mu_2{}^2 + a_{22}\sigma_2{}^2 + 2a_{12}\mu_2\sigma_2 + (100 - TQR_2) = 0 \\[2mm] \dfrac{a_{11} + a_{22} + [(a_{11} - a_{22})^2 + 4a_{12}{}^2]^{1/2}}{2(a_{11}a_{22} - a_{12}{}^2)^{1/2}} + \dfrac{\sigma_2}{\mu_2} = 0 \\[2mm] a_{11}(0.426\sigma_2) - a_{22}(0.426\sigma_2) + a_{12}(2\mu_2) = 0 \end{array}\right\} \qquad (75)$$

This system of equations can be solved using numerical methods implemented in standard programs (MatLab: function "fsolve"; r: multiroot function in rootsolve package, "nleqslv" package and "BBsolve" in BB package, among others).

However, the system of equations (75) admits an explicit solution when the following constraints are satisfied: $a_{11} < 0, a_{22} < 0, a_{12} < 0, a_{11}a_{22} - a_{12}^2 > 0$ and $a_{11} > a_{22}$ ($\mu_{max} > \sigma_{max}$). First and third equations of (75) enable to express $a_{11}$ and $a_{22}$ as linear functions of $a_{12}$: $a_{11} = -\alpha - (\beta + \gamma)a_{12}$ and $a_{22} = -\alpha - \beta a_{12}$. Replacing them into the second equation, the system is reduced to,

$$\frac{-2\alpha - (2\beta + \gamma)a_{12} + [(\gamma^2 + 4)a_{12}^2]^{1/2}}{2(\alpha^2 + (2\alpha\beta + \alpha\gamma)a_{12} + (\beta(\beta + \gamma) - 1)a_{12}^2)^{1/2}} + \frac{\sigma_2}{\mu_2} = 0$$

being,

$$\alpha = \frac{100 - TQR_2}{\mu_2^2 + \sigma_2^2}, \quad \beta = \frac{2}{\mu_2^2 + \sigma_2^2}\left(\mu_2\sigma_2 - \frac{\mu_2^3}{0.426\sigma_2}\right), \quad \gamma = \frac{2\mu_2}{0.426\sigma_2}$$

Considering that $a_{12} < 0$ and after some algebra, the system of equations (75) can be turned into a second-degree equation, with an immediate solution:

$$c_1 a_{12}^2 + c_2 a_{12} + c_3 = 0$$

where:

$$c_1 = 4(\beta(\beta + \gamma) - 1)\sigma_2^2 - \left(2\beta + \gamma + (\gamma^2 + 4)^{1/2}\right)^2 \mu_2^2$$
$$c_2 = 4(2\alpha\beta + \alpha\gamma)\sigma_2^2 - 4\alpha\left(2\beta + \gamma + (\gamma^2 + 4)^{1/2}\right)\mu_2^2$$
$$c_3 = 4\alpha^2(\sigma_2^2 - \mu_2^2)$$

The development of these expressions can be found in Appendix E.V.

**Remark 7**. To facilitate the resolution of this second-degree equation, a worksheet has been designed (Appendix V). Also, the coefficient of correlation and the mean squared error

provide a measure of agreement between the operational component of perceived satisfaction (user/survey) and the estimated operational satisfaction with the model.

**Remark 8.** Following a scheme parallel to that described to get the system of equations (2.6), it is possible to define another boundary condition or other regularity conditions. In new scenarios, the system of equations can be solved using numerical methods implemented in standard programs (MatLab: function "fsolve", R: multiroot function in rootsolve package, "nleqslv" package and "BBsolve" in BB package, among others).

# Part IV: CASE STUDIES AND NUMERICAL

# ANALYSIS

# Chapter IV

# Case studies and numerical analysis

This chapter deals with a series of case studies applying the theoretical developments of the previous chapter. Most of these are from Barcelona's New Bus Network, a new bus layout model, implemented in the city of Barcelona and part of its metropolitan area between 2012 and 2018. The following section contains a summary of this model, and in Annex A.1.2 a much more detailed description is shown.

## 4.1  Barcelona's new Bus network

The city of Barcelona has only 100 km$^2$ and a population of 1.6 million inhabitants, which leads to a density of nearly 16,000 inhabitants/km$^2$. However, its urban area extends far beyond the administrative city limits forming a larger urban territory known as the Barcelona's Metropolitan Area, with a population of over 3.3 million inhabitants.

Long straight streets characterise the central part of the city, a perfect grid pattern crossed by 20-metre-wide ways, and square blocks with chamfered corners. This was a futuristic and innovative design created by Ildefons Cerdà in the 19$^{th}$ century.

A single transit agency provides the local bus service in Barcelona. With a fleet of more than 1,000 buses, the local bus service transported over 200 million passengers in 2018. The bus network has been evolving into a hybrid model over the last six years (2012-2018), in which, an orthogonal premium route network and a conventional complementary network with lesser hierarchy coexist. The high-performance grid network offers user-friendliness, high frequency, lower total travel time and accessibility as the private vehicle, although it also includes transfers between premium and conventional routes. With an organised and progressive implementation of the project, the conventional network has been eliminating redundant routes and has focused attention on priority axes, in peripheral areas and in meeting primary neighbourhood needs.

Premium routes are arranged on an orthogonal grid scheme, which has been proved as the most efficient in urban environments. Horizontal routes, vertical routes and diagonal routes have been designed and implemented, which improved connectivity among other modes of transport and premium routes themselves and ensures accessibility for all users.

This new scheme is not only functional but also more "readable" and is structured similarly to the metro. This way, the network becomes easily understandable and the great majority of destinations are reached with a single transfer, simplifying the use of the bus network and avoiding the current need to know each line individually.

Other features are their excellent frequencies; from 7:00 am to 9:00 pm, buses run at rush hour headway (5' to 8' headway on working days, depending on the route). This way, users have to wait very short for the bus at the stops, which contributes to increasing customer satisfaction ratios

The orthogonal network also promotes intermodality, strategically placing the stops to facilitate the connection between the lines and with other public transport means (tram, metro, bicycle hire, etc..).

The first routes were launched in October 2012. The network has been implemented gradually over the next six years, at a rate of 4-5 routes per year, to reach the 28 routes

finally. Each time premium routes were implemented, some changes were done on the conventional routes, while local routes barely experienced any modification.

More precisely, the high-performance network consists of a set of 28 horizontal (8), vertical (17) and diagonal (3) bus routes and more than 100 transfer areas. The total demand of these routes is 470,000 pax/working day over an aggregate bus network demand of 775,000 pax/working day, that is 60% of the overall bus network. The horizontal routes are the longest and more crowded. They connect the two corners of the city from the NE to the SW. Their demand is very high; in particular, route H10 transports every working day more than 20.000 pax, using high capacity vehicles. Vertical routes are shorter and have less transport capacity. They link the coastline of the city with the Collserola mountainside, running in a sea-mountain direction. In particular, route V17 transport every day up to 12.000 pax, using standard buses. Figure 20 shows the schematic layout of the premium routes and the transfer areas at the intersection of the routes.



**Figure 20**. map of the 28 premium bus routes (8H in blue, 17V in green and 3D in purple) of Barcelona's Bus Network.

— Horizontal: H2, H4, H6, H8, H10, H12, H14, and H16

— Vertical: V1, V3, V5, V7, V9, V11, V13, V15, V17, V19, V21, V23, V25, V27, V29, V31, and V33

— Diagonal: D20, D40, and D50

## 4.2 Scheduled timetables: H12 corridor

### 4.2.1 Identifying the route and its checkpoints

Route H12 is one of the premium routes from Barcelona's New Bus Network. Main KPI's of this route are shown in Table 6.

**Table 6**. Route H12 main KPI's.

| KPI | Value |
|---|---|
| Length (km) | 22.5 |
| Num. of vehicles (articulated and bi-articulated buses) | 21 (18, 3) |
| Headway (min) | 6.5 |
| Ridership (pax/day) | 28,000 |
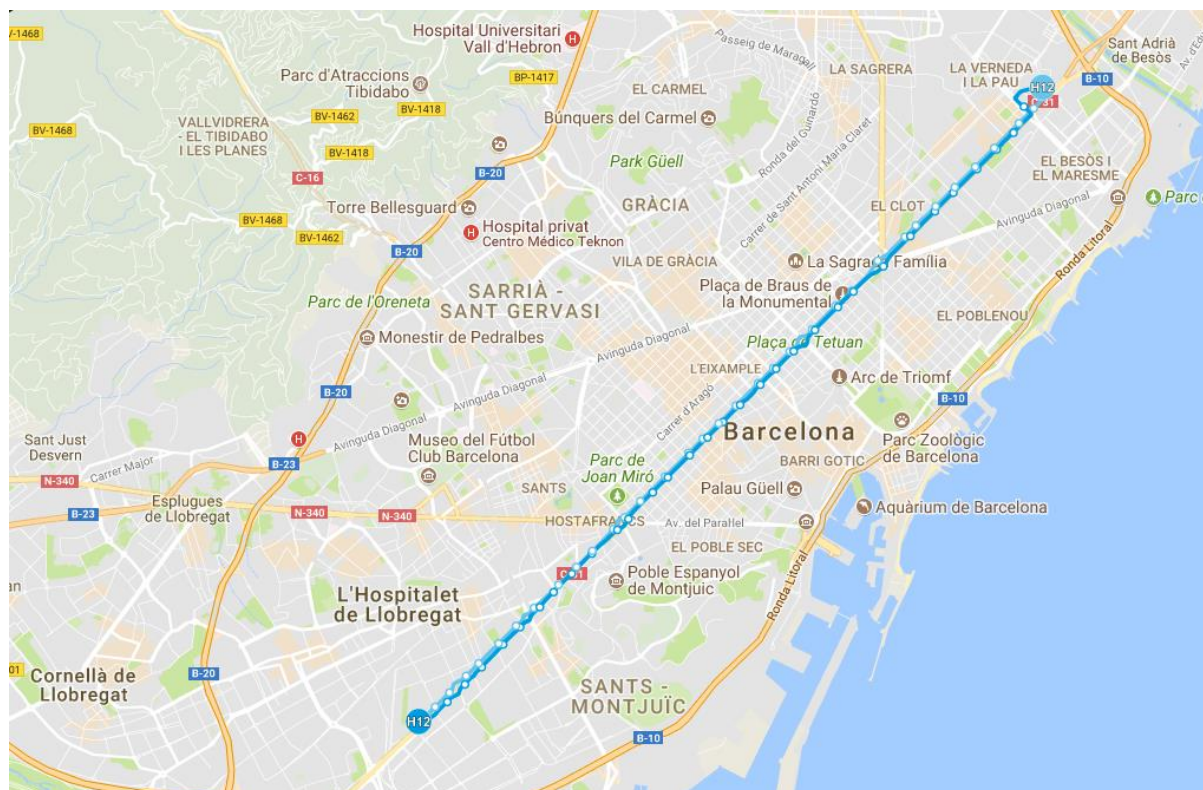


**Figure 21**. Route H12 layout, Gornal – Besos/Verneda.

---

| TMB | **LÍNIA: Gornal / Besòs Verneda** | **212** |
|---|---|---|
| Transports Metropolitans de Barcelona | | Horari: AF16 |
| ÀREA OPERATIVA D'AUTOBUSOS | **COTXERA: Zona Franca BUS** | Versió: FH24 |
| DISSENY D'OFERTA | | Vigència: __/__/__ |

Outbound:

**NOMENCLÀTOR:** Punt 1 : 3225 - Av. Granvia/Av. Carmen Am    Punt 2 : 2363 - Gran Via C.Catalanes/Pl.    Punt 3 : 3247 - Pl. Espanya/Gran Via C.Ca

Punt 4 : 1075 - Pl. Universitat/Gran Via    Punt 5 : 914 - Gran Via C.Catalanes/Mar    Punt 6 : 385 - Gran Via C.Catalanes/Bil

Punt 7 : 572 - Concilio Trento(Grup "La

Inbound:

**NOMENCLÀTOR:** Punt 1 : 572 - Concilio Trento(Grup "La    Punt 2 : 383 - Gran Via C.Catalanes/Esp    Punt 3 : 247 - Gran Via C.Catalanes/Cas

Punt 4 : 1081 - Gran Via C.Catalanes/Pg.    Punt 5 : 7 - Gran Via C.Catalanes/A    Punt 6 : 3236 - Gran Via C.Catalanes/Espa

Punt 7 : 3023 - Gran Via C.Catalanes/Radi    Punt 8 : 3225 - Av. Granvia/Av. Carmen Am

**Figure 22**. Route H12 Control nodes (outbound and inbound).

## 4.2.2    Previous developments with HASTUS

The previous works with HASTUS consist of loading data, inserting links, obtaining average travel times, syncronising times and exporting to a worksheet. All these procedures are detailed in Appendix B.1.

## 4.2.3    Building the time slots

Time slots are built to achieve stability regarding scheduled travel times. This initial stability is achieved by increasing the variability (higher cost), but it is necessary not to be forced to make a big amount of manual adjustments, which also end up increasing the average travel time. For Barcelona's high-performance bus routes, it has been established the criterion ± 1 minute (minimum possibilist). Thus, the time slot groups consecutive hours in which the average travel times differ by at the most 2 minutes.

Step 1. Identifying the central strip susceptible to grouping. For route H12-Outbound, the homogeneity in the total travel time (spectrum) is observed in the period between 9:00 and 18:59. The travel time between 8:00 and 8:59 has a discontinuity of 3 minutes with the next hour and the travel time between 7:00 pm and 7:59 pm presents a discontinuity of three minutes with the previous hour. Following the same criteria, for route H12-Inbound, the homogeneity in travel time (spectrum) is observed in the period between 9:00 and 19:59.

Step 2. Establishing the minimum number of groupings in the central zone. The minimum number of clusters required in the central zone is obtained by rounding up to the above integer number.

$$\frac{M_{st} - m_{st} + 1}{3}$$

Being:

$M_{st}$: maximum spectrum time

$m_{st}$: minimum spectrum time

For route H12-Outbound, the period between 9:00 and 18:59 requires at least 3-time slots:

$$Round\ up\left(\frac{M_{st} - m_{st} + 1}{3}\right) = Rup\left(\frac{60 - 54 + 1}{3}\right) = 3$$

For route H12-Inbound, the period between 9:00 and 19:59 requires at least two-time slots:

$$Round\ up\left(\frac{M_{st} - m_{st} + 1}{3}\right) = Rup\left(\frac{55 - 52 + 1}{3}\right) = 2$$

Step 3. Establishing the groupings in the central zone. From among the possible gatherings fulfilling the criterion ± 1 minute,

**Table 7**. Route H12 – Outbound, possible Time slots.

| **RH12-outbound** | 9:00 9:59 | 10:00 10:59 | 11:00 11:59 | 12:00 12:59 | 13:00 13:59 | 14:00 14:59 | 15:00 15:59 | 16:00 16:59 | 17:00 17:59 | 18:00 18:59 |
|---|---|---|---|---|---|---|---|---|---|---|
| Option 1 | 54-55-56 | | | 57-57-57-57-58-59 | | | | | | 60 |
| Option 2 | 54-55-56 | | | 57-57-57-57-58 | | | | | 59-60 | |
| Option 3 | 54-55-56 | | | 57-57-57-57 | | | | 58-59-60 | | |
| Option 4 | 54-55 | | 56-57-57-57-57-58 | | | | | | 59-60 | |
| Option 5 | 54-55- | | 56-57-57-57-57 | | | | | 58-59-60 | | |
| Option 6 | 54 | 55-56-57-57-57-57 | | | | | | 58-59-60 | | |

the one with the greatest homogeneity in the spectrum and the greatest compatibility in the links is chosen. Options 1 and 6 are inferior to the others: heterogeneity is poorly distributed (the distribution is very asymmetric), while the other options are all plausible. In all cases, the differences in the intermediate links are at the most two minutes. The choice of option 4 is since the greatest heterogeneity is distributed over the greater time slot (6 hours) and the time

distribution is very symmetric (centre 57, in four hours, and complement in extremes, 56 and 58).

**Table 8**. Route H12 – Outbound, grouping Time slots.

| Hour | | Links | | | | | | | Spectrum | |
| Start | End | 3225-2363 | 2363-3247 | 3247-1075 | 1075-914 | 914-385 | 385-572 | SUMA | 3225-572 | s |
|---|---|---|---|---|---|---|---|---|---|---|
| 6:00 | 6:59 | 7 | 8 | 5 | 7 | 8 | 8 | **43** | 46 | 4,0 |
| 7:00 | 7:59 | 9 | 10 | 7 | 8 | 9 | 9 | **52** | 52 | 2,6 |
| 8:00 | 8:59 | 10 | 11 | 7 | 9 | 9 | 10 | **56** | 57 | 2,9 |
| 9:00 | 9:59 | **9** | **11** | 7 | 9 | 9 | 9 | **54** | 54 | 2,6 |
| 10:00 | 10:59 | **10** | **10** | 7 | 9 | 9 | 9 | **54** | 55 | 3,2 |
| 11:00 | 11:59 | **10** | **10** | **7** | **9** | 9 | 10 | **55** | 56 | 3,2 |
| 12:00 | 12:59 | 10 | 10 | 7 | **10** | 9 | 10 | **56** | 57 | 3,3 |
| 13:00 | 13:59 | 10 | 10 | 8 | 10 | 9 | 10 | **57** | 57 | 2,9 |
| 14:00 | 14:59 | 10 | 10 | 8 | 10 | 9 | 10 | **57** | 57 | 3,4 |
| 15:00 | 15:59 | **11** | 10 | 7 | 9 | 9 | 10 | **56** | 57 | 2,9 |
| 16:00 | 16:59 | 10 | **11** | **8** | 9 | 9 | 10 | **57** | 58 | 3,1 |
| 17:00 | 17:59 | 11 | 10 | 8 | **9** | 9 | 11 | **58** | 59 | 2,7 |
| 18:00 | 18:59 | 11 | 10 | 8 | **10** | 9 | 11 | **59** | 60 | 3,3 |
| 19:00 | 19:59 | 11 | 10 | 8 | 10 | 9 | 11 | **59** | 57 | 3,0 |
| 20:00 | 20:59 | 10 | 9 | 8 | 9 | 9 | 10 | **55** | 53 | 3,0 |
| 21:00 | 21:59 | 9 | 9 | 7 | 8 | 8 | 8 | **49** | 48 | 3,1 |
| 22:00 | 22:59 | 9 | 7 | 6 | 7 | 7 | 8 | **44** | 43 | 2,8 |

Route H12-Inbound

With the same criteria, the application to the route H12-Inbound is included in Table 9 (there is no single solution, several are also possible).

**Table 9**. Route H12 – Inbound, grouping Time slots.

| Hour | | Links | | | | | | | | Spectrum | |
| Start | End | 572-383 | 383-247 | 247-1081 | 1081-707 | 707-3236 | 3236-3023 | 3023-3225 | SUMA | 572-3225 | s |
|---|---|---|---|---|---|---|---|---|---|---|---|
| 6:00 | 6:59 | 6 | 6 | 9 | 3 | 7 | 6 | 6 | **43** | 45 | 3,5 |
| 7:00 | 7:59 | 9 | 7 | 9 | 3 | 7 | 9 | 7 | **51** | 56 | 5,0 |
| 8:00 | 8:59 | 10 | 9 | 10 | 3 | 8 | 11 | 8 | **59** | 58 | 3,1 |
| 9:00 | 9:59 | **8** | **8** | **10** | 3 | 8 | **10** | 7 | **54** | 54 | 2,9 |
| 10:00 | 10:59 | **7** | **7** | **11** | 3 | 8 | **9** | 7 | **52** | 54 | 2,7 |
| 11:00 | 11:59 | 7 | 7 | 10 | 3 | **8** | **9** | 7 | **51** | 53 | 3,0 |
| 12:00 | 12:59 | 7 | 7 | 10 | 3 | **9** | 9 | 7 | **52** | 53 | 2,8 |
| 13:00 | 13:59 | 7 | 7 | 10 | 3 | 9 | **10** | 7 | **53** | 53 | 2,5 |

| 14:00 | 14:59 | 7 | 7 | 10 | 3 | 8 | 9 | **8** | **52** | 52 | 2,8 |
| 15:00 | 15:59 | 7 | 7 | 10 | 3 | 8 | 9 | 8 | **52** | 53 | 3,0 |
| 16:00 | 16:59 | **7** | 7 | **10** | 3 | 9 | **9** | 8 | **53** | 54 | 2,7 |
| 17:00 | 17:59 | 7 | 7 | 11 | 3 | 9 | **10** | 8 | **55** | 55 | 2,8 |
| 18:00 | 18:59 | **8** | 7 | **11** | 3 | 9 | 9 | 8 | **55** | 55 | 2,7 |
| 19:00 | 19:59 | 7 | 7 | 10 | 4 | 9 | 9 | 8 | **54** | 53 | 3,0 |
| 20:00 | 20:59 | 7 | 6 | 9 | 3 | 9 | 8 | 7 | **49** | 49 | 2,4 |
| 21:00 | 21:59 | 6 | 6 | 9 | 3 | 7 | 8 | 7 | **46** | 45 | 2,6 |
| 22:00 | 22:59 | 6 | 6 | 8 | 3 | 7 | 7 | 6 | **43** | 43 | 3,2 |

In this case, the possible groupings with criterion ± 1 minute (with two and three groupings) are shown in Table 10. Option 3 is inferior to the others, which all plausible with the spectrum grouping (they meet the criterion and, in all cases, the differences between the intermediate links are two minutes at the most), but they do not comply with the criterion with the sum of the sub-sections. Option 4 is the best choice because the heterogeneity is well distributed in the spectrum, the criterion is also met for the amount of the sub-sections, the number of central bands is quite reasonable, and the time slot structure is very similar to that obtained oppositely. This similarity in time structure for both directions favours the optimisation of resources.

**Table 10**. Route H12 – Inbound, possible Time slots

| **H12- Inbound** | 9:00 9:59 | 10:00 10:59 | 11:00 11:59 | 12:00 12:59 | 13:00 13:59 | 14:00 14:59 | 15:00 15:59 | 16:00 16:59 | 17:00 17:59 | 18:00 18:59 |
|---|---|---|---|---|---|---|---|---|---|---|
| Option 1 | 54-54-53-53-53-52-53-54 | | | | | | | | 55-55 | |
| Option 2 | 54-54-53-53-53-52-53 | | | | | | | 54-55-55 | | |
| Option 3 | 54-54-53-53-53-52 | | | | | | 53-54-55-55 | | | |
| Option 4 | 54-54 | | 53-53-53-52-53 | | | | | 54-55-55 | | |

Step 4. Treatment of periods of deceleration and acceleration. The periods corresponding to the acceleration and deceleration sometimes require specific treatment. The abrupt change in the average travel times has been partly reflected in the schedule (Remark 1), and the coincidence with vehicle arrivals and departures can be used to keep the headway. On route H12, the deceleration effect in travel times has been clearly shown in the time slot 7:00-7:59 (s =5.0 and the difference in the average travel time with the previous hour 56-45=11). In the

other 1-hour time slots corresponding to the deceleration and acceleration periods, the standard deviation and the difference in the average journey times are moderate. Using the uniform approximation, the standard deviation collected in the scheduled timetable has been estimated approximately in difference/3.5 (superscripts in Table 11).

**Table 11**. Route H12 – Special treatment in the morning and the evening

| Hour | | H12 Outbound | | | H12 Inbound | | |
|---|---|---|---|---|---|---|---|
| Start | End | 3225-572 | Difference | s | 572-3225 | Difference | s |
| 6:00 | 6:59 | 46 | - | 4,0 | 45 | | 3,5 |
| 7:00 | 7:59 | 52 | $6^{(1.7)}$ | 2,6 | 56 | $\mathbf{11^{(3.1)}}$ | **5,0** |
| 8:00 | 8:59 | 57 | $5^{(1.4)}$ | 2,9 | 58 | 2 | 3,1 |
| 19:00 | 19:59 | 57 | - | 3,0 | 53 | - | 3,0 |
| 20:00 | 20:59 | 53 | $4^{(1.1)}$ | 3,0 | 49 | $4^{(1.1)}$ | 2,4 |
| 21:00 | 21:59 | 48 | $5^{(1.4)}$ | 3,1 | 45 | $4^{(1.1)}$ | 2,6 |
| 22:00 | 22:59 | 43 | $5^{(1.4)}$ | 2,8 | 43 | $2^{(0.6)}$ | 3,2 |

To reduce the deceleration effect in the variability of the average journey times in the 7: 00-7: 59-time slot (inbound), the time slot has been subdivided into two intervals of 30 minutes.

**Table 12**. Route H12 – Inbound, a subdivision of 1-hour Time slots in 2-half an hour Time slots

| Hour | | Links | | | | | | | Spectrum | |
|---|---|---|---|---|---|---|---|---|---|---|
| Start | End | 572-383 | 383-247 | 247-1081 | 1081-7 | 07-3236 | 3236-3023 | 3023-3225 | 572-3225 | s |
| 7:00 | 7:29 | 7 | 7 | 9 | 3 | 7 | 8 | 7 | 51 | 3,2 |
| 7:30 | 7:59 | 10 | 8 | 9 | 3 | 7 | 9 | 7 | 58 | 3,3 |

The subdivision at intervals of 30 minutes has not been extended to the other 1-hour time slots since the standard deviation corresponding to the hour is acceptable (compatible with the rest of the day standard deviations). Nevertheless, the subdivision (at the discretion of the programmer) would also have been correct.

**Remark 1**. The reduction of the standard deviation s = 5 with time slot subdivisions into 30-minute intervals has not been immediate on route H12. With the initial data, the descriptive analysis has provided: average = 53, s = 5.0, for 7:00-7:29; and average = 58.3, s = 3.3, for 7: 30-7:59. The little or lack reduction of variability in the sub time slot 7:00-7:29 (s = 5) has raised suspicions regarding the reliability of the information.

The detailed travel analysis (standard deviation at departure time and travel time) has revealed irregularities on the trip 040 and, to a lesser extent, on the trip 124.

**Table 13**. Route H12 – trip irregularities

| Viaje | 4 | 22 | **40** | 57 | 73 | 91 | **124** | 278 | 296 |
|---|---|---|---|---|---|---|---|---|---|
| $s_{departure}$ | 0,74 | 0,69 | **5,90** | 0,59 | 0,94 | 1,28 | **3,33** | 0,11 | 0,49 |
| $s_{trip}$ | 3,11 | 3,19 | **5,94** | 1,87 | 3,51 | 2,92 | **3,52** | 1,58 | 1,49 |

The list of transit times has shown that a part of the journeys 040 (approximately half of them) have their departure much earlier than the scheduled time. They are false departures, which increase the travel time and cause fictitious variability. Considering these trips corresponding to the interval 7:00-7:29 as not valid, we obtained: average = 51.5 and s = 3.2. The division into two sub time slots is necessary in this case, even having eliminated the false departures. Without these trips, the variability in the time slot 7:00-7:59 would have been evaluated in 4.6.

**Remark 2.** From 6:00-6:59 to 7:00-7:29 and from 7:00-7:29 to 7:30-7:59, the difference in average travel time is approximately 6 minutes. In the deceleration period, the absorption of this time (to ensure headway adherence) can be achieved with the synchronised entry of vehicles (in node 3225, one at approximately 7:00 and another at approximately 7:30).

### 4.2.4 Average travel times and RT within the TS (worksheet)

The maximum concordance between the actual and scheduled transit times is achieved when the scheduled travel time is adjusted to the actual average transit time in the time slot. Manually, the averages of the journey times (links and complete trip) are shown in Table 14. The RT has been evaluated approximately with the expression:

$$RT \cong 1.96(\bar{s}_{WH}^2 + 1.15^2)^{1/2}$$

**Table 14**. Route H12 – Outbound

| Hour | | Links | | | | | | Spectrum | | RT |
|---|---|---|---|---|---|---|---|---|---|---|
| Start | End | 3225-2363 | 2363-3247 | 3247-1075 | 1075-914 | 914-385 | 385-572 | 3225-572 | s | 1.96·s |

| Start | End | 572 383 | 383 247 | 247 1081 | 1081 07 | 07 3236 | 3236 3023 | Spectrum | s | RT |
|---|---|---|---|---|---|---|---|---|---|---|
| 6:00 | 6:59 | 7 | 8 | 5 | 7 | 8 | 8 | 46 | 4,0 | $6^{(8.1)}$ |
| 7:00 | 7:59 | 9 | 10 | 7 | 8 | 9 | 9 | 52 | 2,6 | $6^{(5.6)}$ |
| 8:00 | 8:59 | 10 | 11 | 7 | 9 | 9 | 10 | 57 | 2,9 | $6^{(6.1)}$ |
| 9:00 | 10:59 | $\mathbf{9}^{(9.5)}$ | $\mathbf{11}^{(10.5)}$ | 7 | 9 | 9 | 9 | $\mathbf{55}^{(54.5)}$ | 2,9 | $6^{(6.1)}$ |
| 11:00 | 16:59 | $\mathbf{10}^{(10.17)}$ | $\mathbf{10}^{(10.17)}$ | $8^{(7.5)}$ | $\mathbf{9}^{(9.5)}$ | 9 | 10 | **57** | 3,2 | $\mathbf{6}$ o $7^{(6.5)}$ |
| 17:00 | 18:59 | 11 | 10 | 8 | $10^{(9.5)}$ | 9 | 11 | **60** | 3,0 | 6 o $\mathbf{7}^{(6.3)}$ |
| 19:00 | 19:59 | 10 | 10 | 8 | 10 | 9 | 11 | 57 | 3,0 | 6 o $\mathbf{7}^{(6.3)}$ |
| 20:00 | 20:59 | 10 | 9 | 8 | 9 | 9 | 10 | 53 | 3,0 | 6 o $\mathbf{7}^{(6.3)}$ |
| 21:00 | 21:59 | 9 | 9 | 7 | 8 | 9 | 8 | 48 | 3,1 | $\mathbf{6}$ o $7^{(6.5)}$ |
| 22:00 | 22:59 | 9 | 7 | 6 | 8 | 9 | 8 | 43 | 2,8 | $6^{(5.9)}$ |

\* The values in parentheses in superscript correspond to the mean of the time slot. Roundup has been applied to the sum of remainders, and by default, it is first adjusted and then expanded.

**Remark 3**. The number of trips corresponding to the time slot 6:00-6:59 is very low, and consequently, the reliability in the estimation of s is reduced. The experience in previous schedules has shown that the variability in this time slot is like the rest of the earlier and final hours. For this reason, a recovery time of 6 minutes has been attributed.

**Remark 4**. The RT of the 11:00-16:59 range can be 6 or 7 depending on the roundup (both values are acceptable). If the information of the links did not have rounded up or roundups were by the excess (more time), we would choose RT = 6. The round-trip time has been evaluated more than 0.19:

$$1- 0.17 - 0.17 - 0.17 - 0.3 = 0.19$$

and the RT in the opposite direction also (5.8 and 5.9 have been rounded to 6). To avoid overstressing schedule, the upper rounding has been applied to the next band 17:00-18:59 with RT = 7.

**Table 15**. Route H12 – Inbound

| Hour | | Links | | | | | | | Spectrum | | RT |
|---|---|---|---|---|---|---|---|---|---|---|---|
| Start | End | 572 383 | 383 247 | 247 1081 | 1081 07 | 07 3236 | 3236 3023 | 3023 3225 | 572 3225 | s | |
| 6:00 | 6:59 | 6 | 6 | 9 | 3 | 7 | 6 | 6 | 45 | 3,5 | $7^{(7.2)}$ |

| | | | | | | | | | | |
|---|---|---|---|---|---|---|---|---|---|---|
| 7:00 | 7:29 | 7 | 7 | 9 | 3 | 7 | 8 | 7 | 51 | 3,2 | **6** o 7$^{(6.1)}$ |
| 7:30 | 7:59 | 10 | 8 | 9 | 3 | 7 | 9 | 7 | 58 | 3,3 | **6** o 7$^{(6.3)}$ |
| 8:00 | 8:59 | 10 | 9 | 10 | 3 | 8 | 11 | 8 | 58 | 3,1 | 6 o 7$^{(6.5)}$ |
| 9:00 | 10:59 | **7**$^{(7.5)}$ | **8**$^{(7.5)}$ | **10**$^{(10.5)}$ | 3 | 8 | **10**$^{(9.5)}$ | 7 | 54 | 2,8 | 6$^{(5.9)}$ |
| 11:00 | 15:59 | 7 | 7 | 10 | 3 | **8**$^{(8.4)}$ | **10**$^{(9.2)}$ | 7 | 53$^{(52.8)}$ | 2,8 | 6$^{(5.9)}$ |
| 16:00 | 18:59 | **7**$^{(7.3)}$ | 7 | **11**$^{(10.7)}$ | 3 | 9 | **9**$^{(9.3)}$ | 8 | 55$^{(54.7)}$ | 2,7 | 6$^{(5.8)}$ |
| 19:00 | 19:59 | 7 | 7 | 10 | 4 | 9 | 9 | 8 | 53 | 3,0 | **6** o 7$^{(6.3)}$ |
| 20:00 | 20:59 | 7 | 6 | 9 | 3 | 9 | 8 | 7 | 49 | 2,4 | 5 o **6**$^{(5.2)}$ |
| 21:00 | 21:59 | 6 | 6 | 9 | 3 | 7 | 8 | 7 | 45 | 2,6 | 6$^{(5.6)}$ |
| 22:00 | 22:59 | 6 | 6 | 8 | 3 | 7 | 7 | 6 | 43 | 3,2 | 7$^{(6.7)}$ |

**Remark 5**. The TRI in the range 19:00-21:59 has been rounded up considering the round-trip times. The range 19:00-20:59 has been rounded upwards in the Outbound direction and has been rounded downwards in the Inbound direction. The range 21:00-21:59 has been rounded downwards in the Outbound direction and rounded upwards in the Inbound direction. These manual adjustments must be compatible with progressive vehicle removal.

### 4.2.5   The average time and standard deviations within time slots

Once created the links and generated the time slots with time amplitude, HASTUS allows for subdividing the slots and getting a more adjusted estimation of the average transit times and the standard deviation per time slot. The details of this subsection are explained in Appendix B.2

### 4.2.6   Building the scheduled timetable

By entering the timetable (partial times of the links in the defined time slots) and the corresponding RT, HASTUS constructs the schedule of the journeys (Fig. 23). Next, all those constraints regarding the timetable (working conditions, shift change points, etc.) should be inserted. The final aspect of the schedule is shown in Fig. 24.
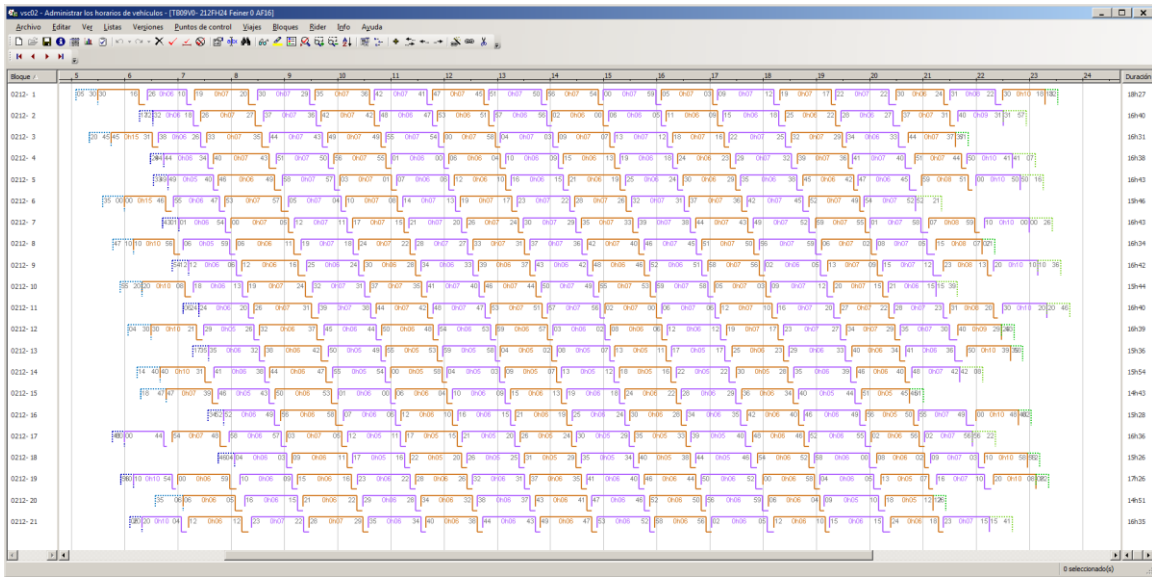
**Figure 23**. HASTUS 2009.Vehicle schedule corresponding to route H12. Source: TMB

Each horizontal line represents a bus, and the segments of different colours on each line represent the successive trips of that bus during the whole daily service.
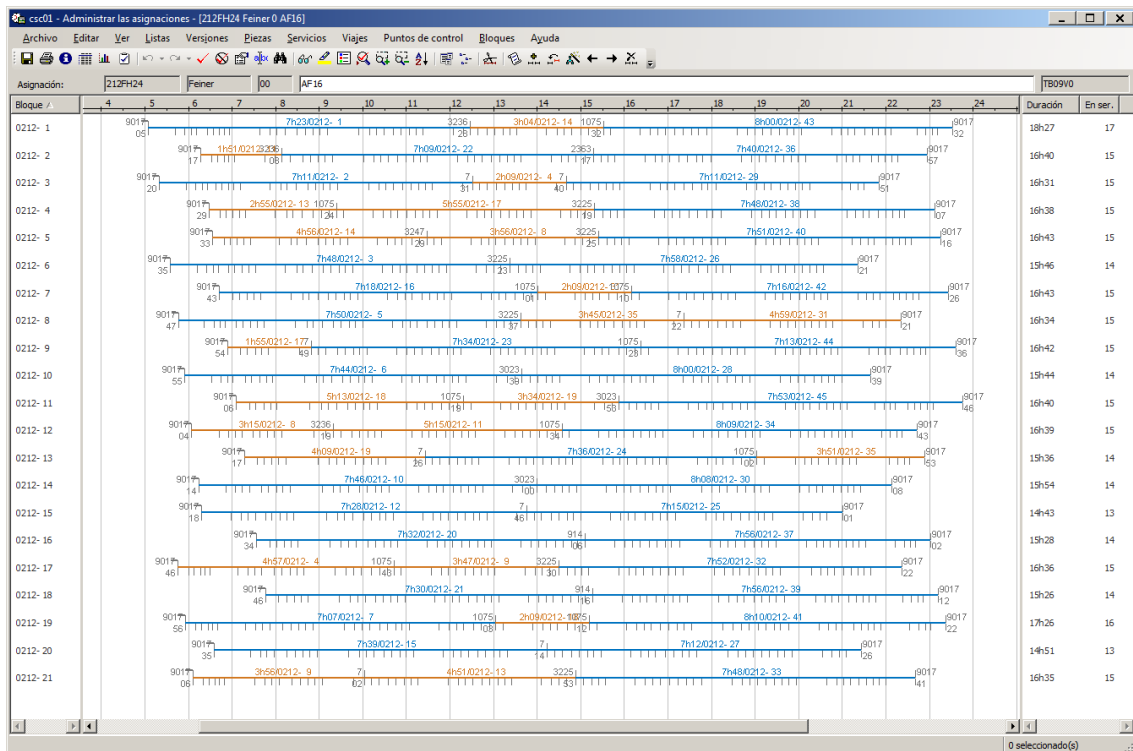


**Figure 24**. HASTUS 2009. Shift schedule corresponding to route H12. Source: TMB

126

Each horizontal line represents a bus, and the segments of different colours represent the driving services on that bus during the whole daily service span. Blue segments represent full services and orange segments, partial services.



**Figure 25**. Shift schedule corresponding to route H12. Source: TMB

127

Outbound, direction Besòs Verneda:

— Former RT: 5 min

— New RT: 7 min (+40%)

Inbound, direction Gornal:

— Former RT: 5 min

— New RT: 7 min (+40%)

### 4.2.7   Final considerations and conclusions

These are the primary considerations and conclusions that it may be drawn on this topic, Scheduled Timetables:

— A good Schedule must offer an excellent service to the users, optimise the available resources, comply with the driver's working conditions, and it is essential to maintain service costs at an acceptable level both for the operator and the system

— Drawing up a bus route schedule is not simple and requires historical data, computer support, an appropriate methodology for obtaining timetables, as well as programmer's expertise for the completion

— The schedule consists basically of two parts: vehicle scheduling and driving services. Vehicle scheduling represents the succession of scheduled trips throughout the day. The driving services are made up of workpieces that cover all those service hours defined in the vehicle scheduling and are always consistent with the conditions and regulations coming from the Union Agreement and the Operations Committees

— The methodology for calculating optimal timetables is based on three elements: travel time, recovery time at route terminals, and time slots. HASTUS, developed by the Canadian company, Giro, has been the IT support since it allows the usage of historical data and makes processing all that information easy

— The problems that must be faced in the construction of timetables are the heterogeneity (variability) that exists over the route service span, which requires a specific recovery

time to secure bus departures from the terminals. The systematic deviations from the programmed times significantly affect the cost of the service

— It has been proved that, within each time slot, the scheduled travel time agrees with the average actual travel times

— Regarding the Recovery Time, it can be calculated by linking it to a statistical threshold of achievement. In this way, to ensure 97.5% of the departures at the terminals and, within a time slot, Recovery Time can be calculated, assuming that the data follow a Normal distribution, such as the square root of the sum of variability of the travel times within the various hours of the time slot, and the variability of the travel times between the hours, multiplied by 1.96, factor associated with the probability of 97.5%

— Regarding the time slots, with the idea of combining a maximum homogeneity with a maximum extension, the ± 1 criterion fits very well and minimises the deviation within the time slots

— Once these parameters are determined and the time slots are built, the appropriate supply can be sized from the headway, or set up this according to the available resources

— This methodology has been applied to determining the timetables and the complete schedule of route H12, Gornal-Besos/Verneda, one of the Barcelona's New Bus Network premium routes. In this case study, travelling times could be adjusted and an increase by 40% of recovery time (from 5' to 7') could be implemented to be able to secure on-time departures. The support IT tool has been HASTUS

## 4.3    Headway adherence

### 4.3.1    Numerical analysis

Formulations (36)-(69) were implemented to a set of problem instances to see how the selected metrics that control the performance of the branched transit routes are influenced by different transit features, vehicle entrance synchronisation and control strategies. The model was coded in Visual Basic programming language, compatible with the input files developed in Microsoft Excel.

### 4.3.2    Problem generation

The first set of problems analysed is composed of three test instances that differ in the key parameters, playing a significant role in headway control techniques. These parameters are the passenger flow (q = 1000 or 1400 pax/h in each direction), a similar vehicle capacity (C = 75 or unlimited) and the total amount of time disturbance that any occasional event may cause in a specific bus (2 or 4 min). A list of values for other common parameters in the first set of problems is summarised in Table 16. Problem Set 2 is aimed at analysing the behaviour of the control strategies for different traffic signal settings.

The estimation of the boarding and alighting passenger flow at each bus stop for each direction is made considering a stationary passenger flow matrix between stops (o, d) during the whole analysis, $Y_{od}$, where o = 1, … , N–1; d = o + 1, …, N in direction A-B; o = N, …, 2N–1 ; d = o + 1, …, 2N for direction B-A. This matrix is estimated by the product of the former passenger flow in the line (q) and the percentage of passenger flow matrix $y_{od}$ between stops. The latter is considered to be constant in the Problem Set 1 and it is evaluated from Tables 17 and 18. It is supposed that the O-D distribution of trips is equal in both route directions (A-B, B-A). The door opening and closing time $t_{oc}$ is neglected in this set of problems.

For simplicity, we assume that stops are evenly distributed along the route in Problem Set 1 and 2. These problems are constituted by 40 stops (N = 20 in each direction) uniformly distributed every 300 m along the route. In Problem Set 1, the intersections are located every l = 150 m while in Problem Set 2 the intersection spacing is l = {100; 210; 300} meters. It is

assumed that the first intersection (i = 1) is xo = l/2 m away from the stop s = 1 (origin of coordinates). The signal offsets of the overall intersections are calculated to avoid the stop of private vehicles along the corridor, i.e. a ''green wave'' is guaranteed for cars. If the average car speed is vc (m/s), it is possible to infer the initial time of green phase $t_{g,i}$ at the intersection I by Eq. (76):

$$t_{g,i} = \frac{x_0 + l(i-1)}{v_c} \qquad i = 2, ..., I \tag{76}$$

In the Problem Set 1 and 2, it is supposed that the deviation Uj(s) from the time-headway takes place at vehicle j = 2 at stop s = 42 ($U_2(42) \geq 0$; otherwise Uj(s) = 0). The stop location has been chosen for two reasons: to allow all vehicles to complete one round trip in the bus route (to warm up the system); its occurrence is far away enough from a holding point (located at stop s = 60) so that the deviation will propagate up-stream and down-stream during a large part of one direction of the service.

The implementation of strategy S0 considers two different slack time settings of $\varphi_s$ = 3 and 6 min at each holding point of the route. The holding points are located at the ending stop of each route direction (terminals or headers) where it is supposed that no passengers are on board the vehicles. This fact means that a different number of resources will be needed to operate the service depending on the value of slack time ($\varphi_s$) provided in the route, as it is determined in Eq. (10). We enumerated the total system cost and the coefficient of headway variation for different combinations of values of $f_f$, $f_r$.

The values considered for both parameters were $f(n) = 0.0001 \cdot \{2^{mod(n,2)} \cdot 0.5 \cdot 10^{[n/2]^-}\}$ for n = 1, ..., 9. The mathematical operator mod(x, y) defines the remainder after x is divided by y; whereas $[x]^-$ rounds x to the lower nearest integer number of x. We found out that the pair of parameter values that minimised the total cost and headway variations in the implementation of Strategy S1 in Problem 1.1 were $f_f$ = 0.01, $f_r$ = 0.05. Therefore, the evaluation of strategy S1 and S2 is made in the whole problems considering $f_f$ = 0.01, $f_r$ = 0.05 and a vehicle capacity threshold of u = 0.95 in Eq. (28). Finally, the results obtained with the previous strategies are compared with the corresponding of strategy S2, in which the green phase extension is chosen to be G = 5, 10 and 20 sec. Moreover, the results provided by

the implementation of strategy S1 and S2 together with a slack time $\varphi_s = 3$ min at the headers (holding point) are also assessed.

**Table 16**. Input parameters in the modelling of Problem set 1, 2, and Problem 3

| Concept | Value | | | | |
|---|---|---|---|---|---|
| | | Problem Set 1 | | Problem Set 2 | Problem 3 |
| Maximal cruising speed, $v_b$ (m/s) | | 10 | | 10 | 13.88 |
| Number of bus stops in the round trip (2N) | | 40 | | 40 | 39 |
| Boarding time per passenger, $\gamma$ (s) | | 3 | | 3 | 3.7 |
| Alighting time per passenger, $\delta$ (s) | | 2 | | 2 | 2.1 |
| Targeted time headway, $H$ (s) | | 300 | | 300 | 300 |
| Stop when disturbance takes place | | 2(42)[a] | | 2(42)[a] | -- |
| Vehicle affected by time disturbance | | #3 | | #3 | -- |
| Intersection spacing, $l$ (m) | | 150 | | 100-300 | |
| Traffic light cycle time, $C_p$ (s) | | 100 | | 90 | Var. |
| Green phase time, $g$ (s) | | 50 | | 22.5-67.5 | Var. |
| Green extension in strategy S2, $G$ (s) | | 5-20 | | 5-20 | 5-20 |
| Door opening and closing time, $t_{oc}$ (s) | | 0 | | 0 | 2 |
| Layover time, $\theta_A, \theta_B$ (s) | | 180 | | 180 | 180 |
| | Problem | Problem | Problem | | |
| Vehicle capacity, $C$ (pax/veh) | unlimited | 75 | 75 | 75 | 134 |
| Hourly Passenger flow in direction A-B and | 1000 | 1000 | 1400 | 1400 | 1400 |
| Time disturbance, $U$ (s) | 120 | 120 | 240 | 240 | -- |

[a]The term in brackets denotes that disturbance takes place once vehicle has completed one round trip (40 stops) before visiting stop 2

**Table 17**. Matrix $y_{od}$ (percentage of passenger trips among stops).

| O/D | 1 | 2 | 3 | 4 | 5 | 6 | 7 | 8 | 9 | 10 | 11 | 12 | 13 | 14 | 15 | 16 | 17 | 18 | 19 | 20 |
|---|---|---|---|---|---|---|---|---|---|---|---|---|---|---|---|---|---|---|---|---|
| 1 | | 0.094 | 0.283 | 0.283 | 0.283 | 0.283 | 0.283 | 0.283 | 0.283 | 0.283 | 0.283 | 0.189 | 0.189 | 0.189 | 0.189 | 0.189 | 0.189 | 0.189 | 0.094 | 0.094 |
| 2 | | | 0.094 | 0.283 | 0.283 | 0.283 | 0.283 | 0.472 | 0.472 | 0.472 | 0.472 | 0.378 | 0.378 | 0.378 | 0.378 | 0.189 | 0.189 | 0.189 | 0.189 | 0.094 |
| 3 | | | | 0.094 | 0.283 | 0.472 | 0.472 | 0.472 | 0.850 | 0.850 | 0.850 | 0.850 | 0.661 | 0.661 | 0.378 | 0.283 | 0.283 | 0.189 | 0.189 | 0.189 |
| 4 | | | | | 0.094 | 0.283 | 0.472 | 0.661 | 0.661 | 0.944 | 0.944 | 0.944 | 0.661 | 0.661 | 0.661 | 0.472 | 0.472 | 0.472 | 0.472 | 0.472 |
| 5 | | | | | | 0.094 | 0.378 | 0.661 | 0.661 | 0.661 | 1.133 | 1.133 | 1.133 | 0.850 | 0.850 | 0.661 | 0.661 | 0.567 | 0.567 | 0.567 |
| 6 | | | | | | | 0.094 | 0.189 | 0.472 | 0.472 | 0.850 | 0.850 | 0.850 | 0.850 | 0.850 | 0.567 | 0.472 | 0.567 | 0.567 | |
| 7 | | | | | | | | 0.094 | 0.378 | 0.378 | 0.378 | 0.850 | 0.850 | 0.850 | 0.850 | 0.850 | 0.755 | 0.755 | 0.755 | 0.378 |
| 8 | | | | | | | | | 0.094 | 0.472 | 0.755 | 0.755 | 0.755 | 0.755 | 0.850 | 0.850 | 0.567 | 0.472 | 0.567 | 0.567 |
| 9 | | | | | | | | | | 0.094 | 0.567 | 0.567 | 0.850 | 0.850 | 0.850 | 0.850 | 0.661 | 0.661 | 0.472 | 0.472 |
| 10 | | | | | | | | | | | 0.094 | 0.378 | 1.133 | 1.133 | 1.133 | 0.755 | 0.755 | 0.661 | 0.378 | |
| 11 | | | | | | | | | | | | 0.094 | 0.472 | 0.661 | 0.755 | 0.755 | 0.850 | 0.944 | 1.039 | 0.944 |
| 12 | | | | | | | | | | | | | 0.094 | 0.378 | 0.755 | 0.755 | 0.850 | 0.755 | 0.755 | 0.378 |
| 13 | | | | | | | | | | | | | | 0.094 | 0.472 | 0.661 | 0.661 | 0.850 | 0.850 | 0.472 |
| 14 | | | | | | | | | | | | | | | 0.094 | 0.755 | 0.755 | 0.850 | 0.850 | 0.567 |
| 15 | | | | | | | | | | | | | | | | 0.094 | 0.378 | 0.567 | 0.567 | 0.850 |
| 16 | | | | | | | | | | | | | | | | | 0.094 | 0.283 | 0.283 | 0.283 |
| 17 | | | | | | | | | | | | | | | | | | 0.094 | 0.094 | 0.189 |
| 18 | | | | | | | | | | | | | | | | | | | 0.094 | 0.189 |
| 19 | | | | | | | | | | | | | | | | | | | | 0.094 |
| 20 | | | | | | | | | | | | | | | | | | | | |

**Table 18**. Percentage of boarding and alighting passengers

Origin/Destination distribution

(Bar chart — y-axis: Percentage of trips, from 0,000 to 0,070; x-axis: Bus stop, 1–20; legend: boarding, alighting, occupancy)
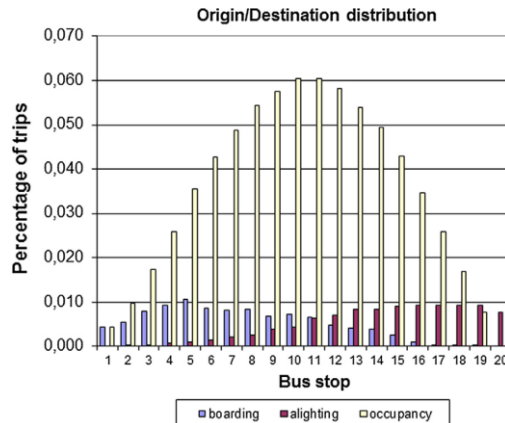
The results provided by each controlling strategy (S0, S1 and S2) in Problem Set 1 and 2 can be compared to a Baseline case in which no alteration is considered (U = 0). This case represents a perfect time-headway adherence among buses and regular bus arrivals at stops so that no controlling strategy is needed. In addition to that, we also assessed the performance of the route under the time disturbance when no controlling strategy is implemented, and the system is uncontrolled (Uncontrolled case). In the modelling framework, this case is equivalent to the implementation of strategy S0 when /s = 0 min.

The other test instance considered (Problem 3 in Table 16) is the route with the highest demand for Barcelona local bus network (route H6). This straight-shaped route connects several university campuses and new business areas to residential districts, running along quite congested streets and avenues (Fig. 25). The line presents a target time headway of H = 5 min and total passenger flow of q = 1,400 pax/h in the period of study. The line has a mandatory layover time of 3 min and an additional slack time of several minutes to tackle bus bunching (/s = 1, 3 and 6 min), with 22 buses operating the roundtrip service. The capacity of these buses is 134 pax/veh. The line is 19.3 km long with 39 bus stops.

Moreover, in this example, the unit boarding and alighting time are respectively c = 3.7 sec/pax and g = 2.1 sec/pax; while the opening and closing door time is $t_{oc}$ = 2 sec. The maximal speed in the bus lane is considered to be v = 50 km/h. These data were determined to take into account average values from the real operation of this line reported by TMB (major bus operator of Barcelona). The details of the traffic light settings are summarised in Appendix C.3.

The simulation of this instance has been developed through the software Aimsun, which includes a microscopic simulator of traffic and transit systems. This software allows us to analyse the performance of bus route under the influence of other traffic (private cars) and taking into account the real synchronisation of traffic lights along the corridor. The information about (car) traffic flows in the streets and the traffic lights parameters is provided by the Barcelona City Council-Mobility Department. Moreover, the activation of strategy S1 and S2 is only considered when $\varepsilon_{j-1,j}(s)$ > E (E ≥ 0). It means that the modification of bus speeds and traffic lights offsets is only activated if the time headway deviation is greater than a target threshold E. The potential values considered are E (sec) = {0; 15; 30}.

### 4.3.2.1 Results and discussion

The results obtained by the former control strategies are compared independently for each problem set. Problem Set 1 encompasses several idealistic instances where the target bus headway was a multiple of the traffic signal cycle time ($H/C_p$ is an integer value). It means that for the baseline case where no exogenous disturbance is considered ($U_j(s) = 0 \; \forall \; j, s$), all vehicles present the same roundtrip time and, consequently, the coefficient of headway variation will be $c_v = 0$.
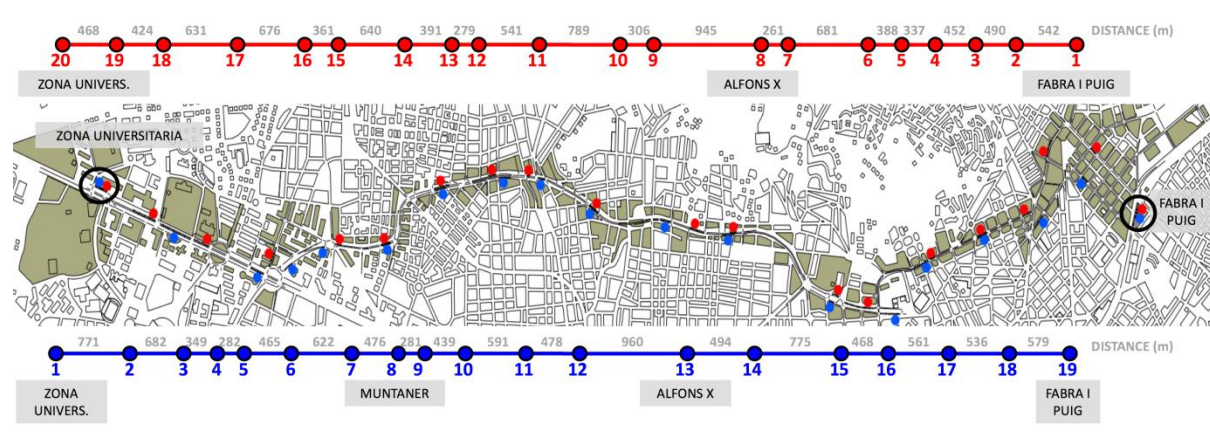


**Figure 26**. The layout of the bus route H6 operated by TMB

Problem Set 2 is aimed at carrying out a sensitivity analysis about the effect of traffic signal setting on the performance of each strategy, especially for Strategy S2. In these instances, we force that $H/C_p$ will not be an integer value. Vehicles will find different sequences of green–red phases at intersections even in the baseline case; therefore $c_v > 0$. Finally, the third problem represents a real instance of a high-performance bus route in Barcelona, where each intersection presents a different signal setting from the others.

#### 4.3.2.1.1 The unstable motion created by exogenous disturbances (Problem set 1)

The results provided in Problem 1.1 with the implementation of each controlling strategy are summarised in Fig. 27. The numerical analysis encompasses the whole round trips of D = 27 vehicles departed from the original stop of the route. In an idealized system with no disturbances (baseline case), the indicator values are TPT = 910 h, $Z_O$ = 11,844 €, $Z_T$ = 25,499 € and $c_v = 0$. The line segment between stops (11, 12) presents the critical passenger load, $O_{max}$ = 50.44 pax/veh. When we introduce a time disturbance U = 2 min, the Uncontrolled case provides an enormous total user travel time, total cost as well as a high value of the coefficient of headway variation associated to bunching effect. In this case, as we

suppose that vehicles have unlimited capacity, any bus suffering a delay will be able to serve all waiting passengers in the following route stops. Hence, the commercial speed of this bus drops due to increasing dwell times at stops. It will be considered as a movable bottleneck since overtaking is not allowed. At the end of the simulation, buses move in platoons of 5 vehicles. Therefore, the total travel time of the users is constrained by the commercial speed of that bus. The disturbance propagates along the route with no control. The variable TPT is 187 times greater than the corresponding value for the situation in which no disturbance occurs (baseline case). As some slack time is introduced, the user costs, agency cost and regularity are partially improved. Although a slack time $/s = 3$ is provided at each header in strategy S0 (greater than the disturbance $U = 2$ min), the system still presents a high total travel time, operating and total cost (TPT = 30,678 h, $Z_O$ = 85,567 Euros and $Z_T$ = 495,256 €). The total cost is 19.4 times greater than the baseline case. Only when the slack time is $\varphi_s$ = 6 min, the user and agency costs are comparable with the results of the baseline case. The time headway adherence is significant since the value $c_v = 0.17$ corresponds to a level of service A according to TRB (2013). The control of system regularity with strategy S0 $\varphi_s$ = 6 min is made at expenses of deploying 3 additional buses (compared to the baseline, $J = 9$ vehicles). However, the total cost of the system is only 1.12 times greater than the baseline. This fact reflects the non-scalable and adapting nature of this strategy. While the slack time of $\varphi_s = 3$ min was not enough to prevent the propagation of bus disturbances, strategy S0 with $\varphi_s = 6$ min can maintain a proper level of service and total cost compared to the baseline case. Bus operation controllers do not know in advance the potential propagation; hence the slack time definition will be made blindly.

Strategy S1 can significantly reduce the total user travel time by 82% compared to the Uncontrolled case (S0, $\varphi_s = 0$). Strategy S1 mitigates the increasing dwell times of a delayed bus by reducing the cruising speed of the vehicle ahead and at the rear to maintain the targeted headway. It reduces the number of vehicles moving in bunches, but the performance of the line can be still considered negative. The total cost of the system is still 5.8 times greater than the baseline case. The combination of strategy S1 with the provision of minimal holding times (S1, $\varphi_s = 3$ min) outperforms the results given by Strategy S0 with $\varphi_s = 3$ min. Therefore, the provision of slack times can improve the behaviour of Strategy S1. However, the coefficient of headway variation ($c_v = 0.79$) is still unacceptable. Finally, the

implementation of strategy S2 improves the metrics of the service performance and costs (TPT, ZO, ZT and $c_v$) provided by strategy S1 without slack times. Generally, all indicators can be enhanced as the green extension time (G) is increased. It is noticeable that when the green extension time is set to G = 20 sec, the cost-oriented indicators are even less than the corresponding value for the baseline scenario (TPT = 901.8 h, ZO = 11,745 €, ZT = 25,254 €). However, the metric time headway adherence is now cv = 0.17, the same value obtained by strategy S0 when $\varphi_s$ = 6 min. Strategy S2 maintains constant the number of vehicles that run the service (J = 9 veh) whereas a slack time of $\phi_s$ = 6 min increases the fleet size to J = 12 veh. For these reasons, we can state that strategy S2 can guarantee the same level of service as static holding points (strategy S0) without increasing the operating costs.
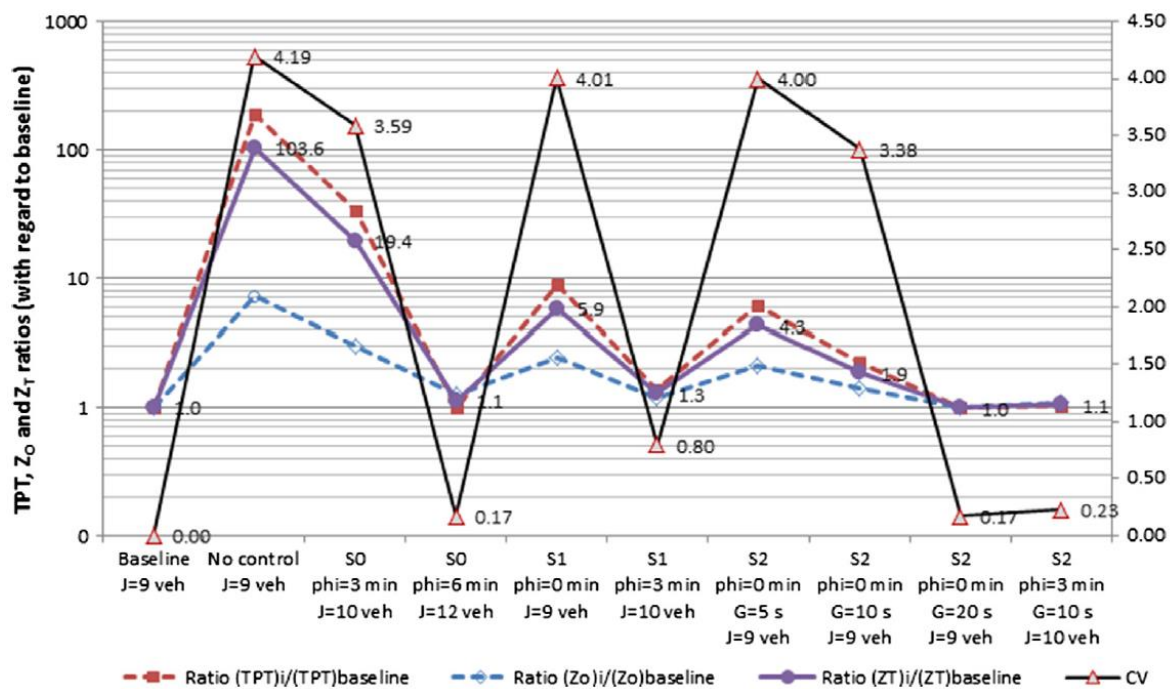


**Figure 27**. Total passenger travel time and coefficient of headway variation for each controlling strategy in Problem 1.1.

The analysis of the results in Problem 1.2 highlights the importance of the vehicle capacity in the headway control strategies. Fig. 28 summarises the main results considering the full round trip of D = 27 departed vehicles. As it is the same bus route, the baseline scenario presents the same results as Problem 1.1. The metrics for the uncontrolled case (TPT = 1562 h, $Z_O$ = 13,170 €, $Z_T$ = 36,599 €, $c_v$ = 1.10) are significantly lesser than those obtained in Problem 1.1 (TPT = 170,341 h, $Z_O$ = 85,567 €, ZT = 2,640,687 €, $c_v$ = 4.19). For this problem, the uncontrolled case presents values of TPT, Zo and $Z_T$ that are, respectively, 1.7,

1.11 and 1.43 times greater than the metrics obtained in the baseline case. As delayed buses arrive at stops, the number of waiting passengers is steadily growing, but the boarding passenger operation is constrained. Therefore, when the capacity constraint is active, the dwell time of this vehicle drops significantly as it only allows passengers to alight. The unserved passengers at stops will wait for the next bus that will arrive with a shorter headway. Therefore, the activation of capacity constraint mitigates and stabilises the headway variations without any controlling strategy. As a result, the commercial speed of the vehicle that suffers the disturbance is quite higher than the same vehicle in Problem 1.1.

The provision of a slack time of $\varphi_s = 3$ min (strategy S0) to control the headways provides good results to compensate for the time disturbance U3(42) = 2 min. The total cost is now 1.08 times the corresponding cost in the baseline case. The extension of slack time to $\varphi_s = 6$ min improves the user travel time in comparison to strategy S0 $\varphi_s = 3$ min and reduces the headway variation up to cv = 0.16. However, the operating cost is increased due to the provision of 2 additional vehicles. Now, the strategy S0 with short slack times ($\varphi_s = 3$ min) is more efficient than larger slacks ($\varphi_s = 6$ min), in terms of the total cost. The total passenger time savings with the implementation of strategy S1 are not as crucial as in Problem 1.1 since the capacity constraint also helps to stabilise the performance (15% of improvement about the uncontrolled case). This fact is consistent with the statement in Muñoz et al. (2013) where it is said that the adaptive controlling speed proposed by Daganzo does not work in routes with high demand and where the capacity constraint is not considered. The total cost of this strategy is 1.27 times the baseline case, even higher than the corresponding figures of strategy S0.

Additionally, the time headway adherence is not acceptable since it is graded as LoS E ($c_v$ = 0.72). If we add a slack time of /s = 3 min, strategy S1 outperforms strategy S0, especially in the time headway adherence analysis whose metric is reduced to $c_v$ = 0.22. Finally, the implementation of strategy S2 can compensate the passenger time lost due to disturbance and the natural motion of buses with travel time savings at the traffic lights. If the green extension time is minimal (G 6 10 sec), the cost metrics are slightly higher than the baseline case. Nevertheless, this strategy outperforms the metrics provided by strategy S1. However, as this green extension is determined to be G > 10 sec, the results are comparable to those of

Strategy S0 with slack times. If this traffic light controlling parameter is set to G = 20 sec, it produces the minimal total cost ($Z_T$ = 25,275 €). However, the coefficient of headway variation is slightly higher than the corresponding to strategy S0 $\varphi_s$ = 6 min, due to the discrete time-saving at traffic lights. It is also remarkable that the hybrid controlling strategy (S2 with slack time /s = 3 min) gives good results (variable $Z_T$ is only 1.007 times greater than the baseline and $c_v$ = 0.17) without imposing massive dynamic changes in traffic light management. The idea is to allocate a minimal slack time at headers (estimated as a function of an expected or recurrent disturbance value in the route) and mitigate more significant disturbances performing strategy S2 (variable cruising speed pattern and green traffic lights extension).

Problem 1.3 is aimed at stressing the performance of the previous bus route with higher demand flow (q = 1400 pax/h in both directions) and time disturbance (U = 4 min). Fig. 29 plots the results when the round trip of D = 30 vehicle departures have been completed. The performance in the baseline case where no disturbance is considered is summarised by TPT = 1,547 h, $Z_O$ = 14,701 €, ZT = 37,912 €, $c_v$ = 0 and J = 10 veh. The highest vehicle passenger load in the route $O_{max}$ = 70.56 pax/veh is detected between stops 11 and 12, and almost equals the vehicle capacity (C = 75 pax/veh). When the disturbance of U = 4 min occurs, when no controlling strategy is activated, the TPT, ZO and ZT are increased respectively by 60%, 7% and 40% about the baseline case. The time headway adherence reaches cv = 0.96. Strategy S0 can stabilise the system. When slack times are $\varphi_s$ = 6 min at terminals, the results in terms of total cost are quite similar to the baseline case (ZT is increased by 9.3%) and the level of service of time headway adherence ($c_v$ = 0.18) is stated as LoS A. In this problem, strategy S1 without slacks is not effective since the metrics are comparable to the corresponding values of the uncontrolled case. It is noticeable that only by reducing the speed of vehicles in systems with high demand, low vehicle capacity and short headways; we cannot maintain a good performance of the route. On the contrary, strategy S2 outperforms the results of the previous controlling strategies. The total cost of the system (ZT metric) is increased by 3.9% (G = 5 sec), 1.8% (G = 10 sec) and -0.3% (G = 20 sec) compared to the baseline case. In these situations, the performance in terms of time headway adherence can be considered as LoS B. In this problem, the implementation of strategy S2 with G = 10 sec and slack times $\varphi_s$ = 3 min even improves the total travel time regarding the baseline case and cv

= 0.15 (LoS A). However, the total cost is slightly greater than the baseline case and strategy S2 with G = 10 sec due to the inclusion of an additional vehicle.
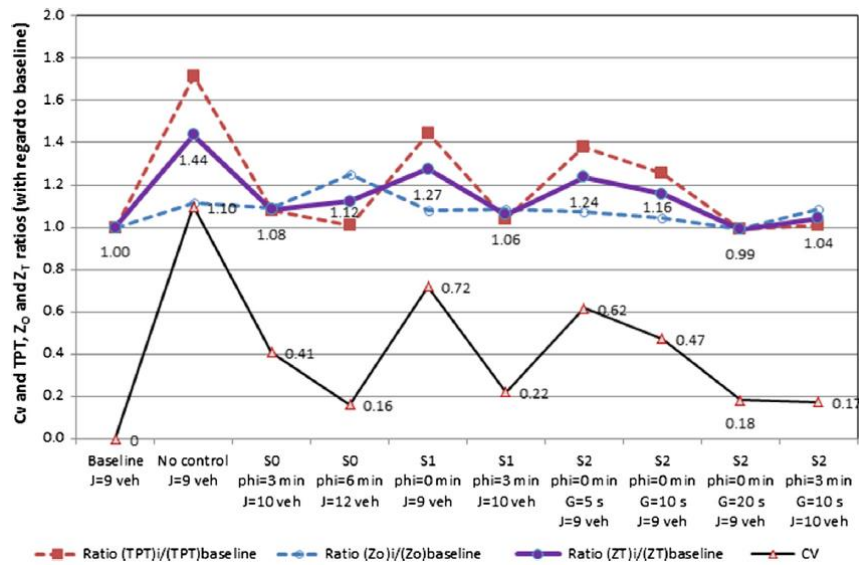


**Figure 28**. Total passenger travel time and coefficient of headway variation for each controlling strategy in Problem 1.2.
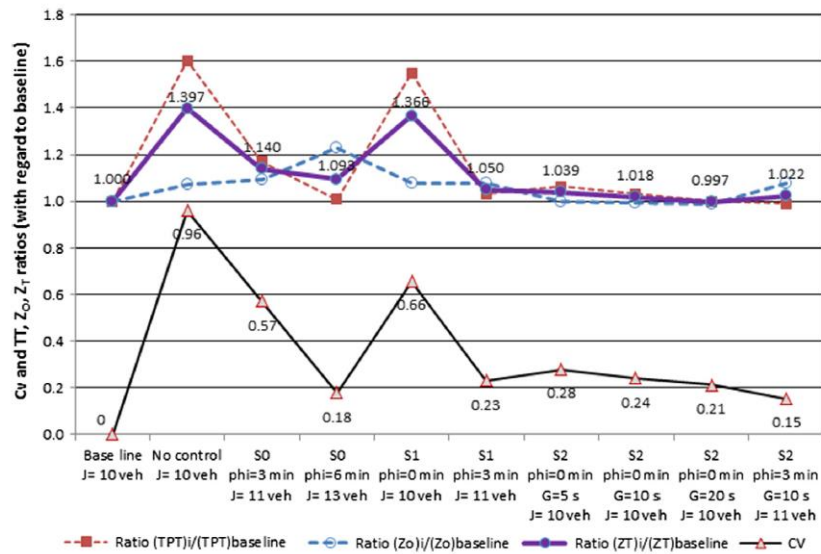


**Figure 29**. Total passenger travel time and coefficient of headway variation for each controlling strategy in Problem 1.3.

### 4.3.2.1.2 The unstable motion created by traffic lights and exogenous disturbances (Problem Set 2)

A sensitivity analysis of the performance of each control strategy has been done in Problem Set 2 about the traffic light settings. We considered three different intersection spacing along

the route: l = {100; 210; 300} m. Moreover, we have also generated problems with different green time at signalled intersections, ranging among g = {22.5; 45; 67.5} sec.

In this case, the traffic light cycle length has been considered to be $C_p$ = 90 sec. Since the time headway (H = 5 min) is not multiple of the cycle time of traffic lights, buses arrive at intersections at different times of the red-green signal sequence. This fact may worsen the bus headway adherence, even when no exogenous disturbance is generated (baseline scenario). The results are summarised in Fig. 31 considering the departure of 27 consecutive buses from bus stop s = 1. All instances with equal green time (g) are presented together. The relative increment of all performance indicators (TPT, ZO, ZT, cv) is roughly equal in those instances with the same green time allocation. The spacing between intersections seldom affects the behaviour of the control strategies for a given traffic light setting. The variations of all indicators are lower than 5%, except for Strategy S1, where these differences are up to 10%.

Therefore, the differential behaviour of control strategies is only identified for instances with different green time settings. When the green time is equal to g = 67.5 sec (g/Cp = 0.75), the bus delays at intersections generate by themselves low headway variations. In this situation (baseline scenario), the level of service can be stated as LoS B (cv = 0.28). The generation of a time disturbance of U = 4 min to vehicle j = 3 (Uncontrolled scenario) makes the system more unstable, increasing the variation of headways up to cv = 0.72 (LoS D). Strategy S0 significantly reduces the travel time of users regarding no control scenario, at expenses of increasing operating costs, deploying more vehicles.

Strategy S1 with no slacks is not effective, since the total cost of the system (agency and users) is 1.15 times greater than the baseline scenario. Vehicles often arrive at an intersection when the green phase is active (g/Cp = 0.75), so that the efficiency of strategy S2 is still limited. This strategy cannot improve the values of all performance indicators in the baseline scenario. The best control criteria are strategy S2 with the slack of /s = 3 min, characterised by cv = 0.24 and a total cost of 1.019 times greater than the baseline scenario. It is remarkable that Strategy S0 with /s = 3 min presents similar results as the former one.

The analysis of the bus performance when g = 45 sec (g/Cp = 0.5) is substantially different. In the baseline case, the stoppings of vehicles at intersections significantly increase the bus bunching phenomena, presenting cv = 0.75. It can be stated as LoS F. Therefore, the creation

of an exogenous service disruption U = 4 min in the Uncontrolled scenario worsens the total cost by 6.5% and seldom increases the bus bunching effect (cv = 0.82).

In strategy S0, a slack time of /s = 3 min is enough to reduce the total cost by 17.6% about baseline) and the variation of headways at cv = 0.42. Strategy S0 with /s = 6 min minimises the travel time of users at the expenses of increasing the operating cost so that this strategy is the more expensive considering total cost. Strategy S1 with no slacks can enhance the system performance about the uncontrolled scenario, but the cost savings achieved are far away from those of strategy S0. Finally, strategy S2 outperforms previous strategies. When the green extension length is G = 5 sec, this strategy can reduce both operating and user costs about baseline scenario. As a result, the total cost is diminished by 20%, and the service regularity can be graded as LoS = B ($c_v$ = 0.35). If we continuously increase the green extension length, the performance of this strategy is outstanding, with total cost savings ranging from 20% to 34% and cv < 0.39 (LoS B or C). Nevertheless, the hybrid strategy S2 with slacks (/s = 3 min) presents the lowest coefficient of headway variation at the expenses of introducing one extra vehicle, increasing operating costs about strategies without slack times.

Eventually, the results obtained when the green time at intersections is g = 22.5 sec are relatively similar to those presented when g = 45 sec. Strategy S2 outperforms the indicators of other available strategies. However, the total cost savings are not as high as the previous ones, ranging among 13–16% while the variation of headways is maintained between $c_v$ = 0.30–0.36. This strategy can reduce user cost, whereas preserving the number of vehicles needed concerning the baseline scenario. Vehicles can be speeded up avoiding potential delays at intersections. This fact causes, in some instances, even lesser operating cost than the baseline scenario.

### 4.3.2.1.3 The unstable motion created by traffic light settings, traffic flows and demand rates at stops (Problem 3)

If we consider the test instance representing the local bus route of highest demand in Barcelona (H6 route), the results generally follow the same pattern explained above. The simulation is carried out during the peak morning time (6.00–9.00 AM). In that case, there is no disturbance artificially-generated since real traffic light control, heterogeneous user arrival rates at stops and car traffic flow, tend to make the headway adherence unstable. In this case,

we implement hybrid strategies based on the provision of slack time at headers together with the dynamic implementation of strategies S1 or S2. Fig. 31 summarises the simulated metrics in that route for different slack times at last stops ($\varphi_s$ = 1, 3 and 6 min). The implementation of higher slack times generally improves both travel times and the headway adherence of the corridor, when only the coefficients of headway variation when strategy S0 is implemented are greater than $c_v$ = 0.75, which corresponds to the Level of Service F (taking into account the classification of TRB, 2013). The introduction of dynamic controlling strategies significantly outperforms the performance of the bus network. Strategy S1 reduces the total cost by 14–28% and $c_v$ by 27–58% regarding the static controlling strategy with low slacks (strategy S0 $\varphi_s$ = 1 min). The level of service in that situation regarding the headway adherence criterion is E ($\varphi_s$ = 1 min) and D (/s = 3 or 6 min). However, when traffic light priority is activated for buses (strategy S2), the results are outstanding and outperform those provided by the speed modification controlling strategy (strategy S1). Strategy S2 improves TPT, ZT and coefficient of headway variation by 40–41%, 38–39%, 72–80% respectively, regarding the strategy S0. The time adherence variable can be controlled with strategy S2 below the threshold cv < 0.3, which corresponds to the level of service A or B. The regularity effects of dynamic controlling strategies on the bus service can be observed in Fig. 31a-c. Bus trajectories in the route direction A-B (Zona Universitària-Fabra i Puig) are depicted when the slack time at the ending stop is /s = 1 min. Although the inclusion of higher slack times ($\varphi_s$ P6 min) would improve the results of strategy S1, the actual performance of the service with strategy S2 does not get better with those slack times. Therefore, full dynamic bus controlling strategy (strategy S2) does not need any unproductive slack time at holding points to guarantee good headway adherence and user travel times.
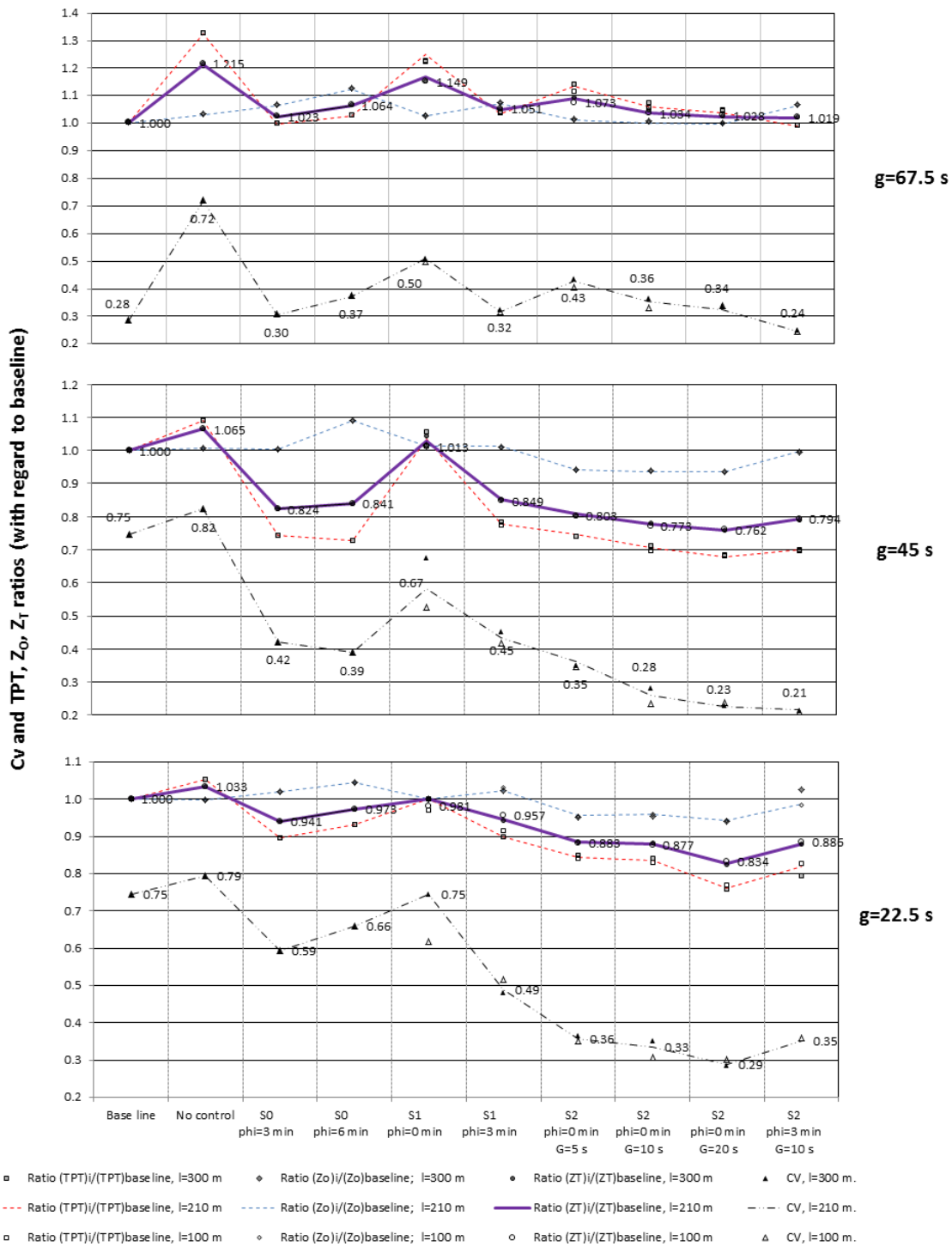
**Figure 30**. Sensitivity analysis of the performance of buses in problem 1.3, when g=22.5; 45 and 67.5 seg.
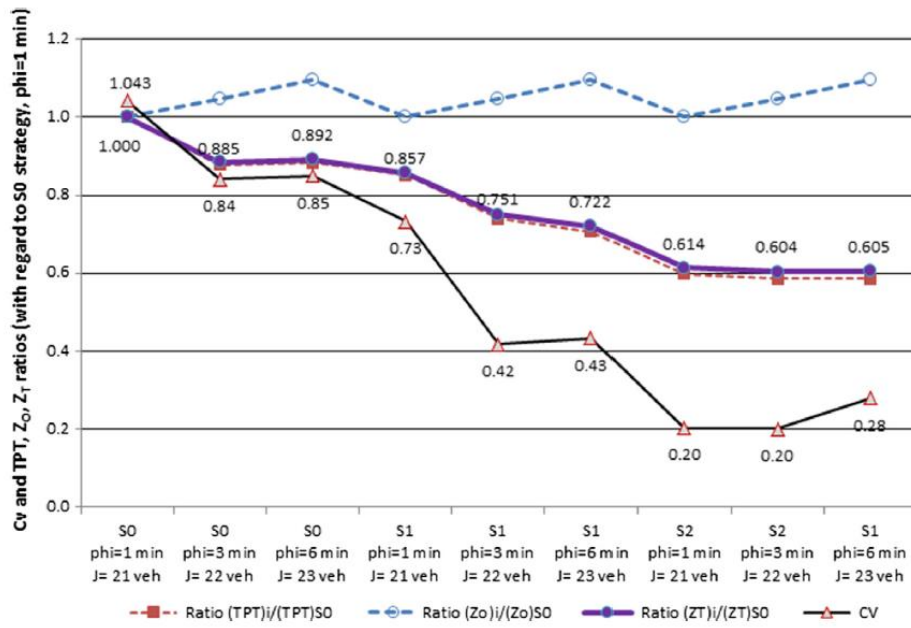
**Figure 31**. Total user travel time and headway adherence in bus route H6 considering different slack times at ending stops.
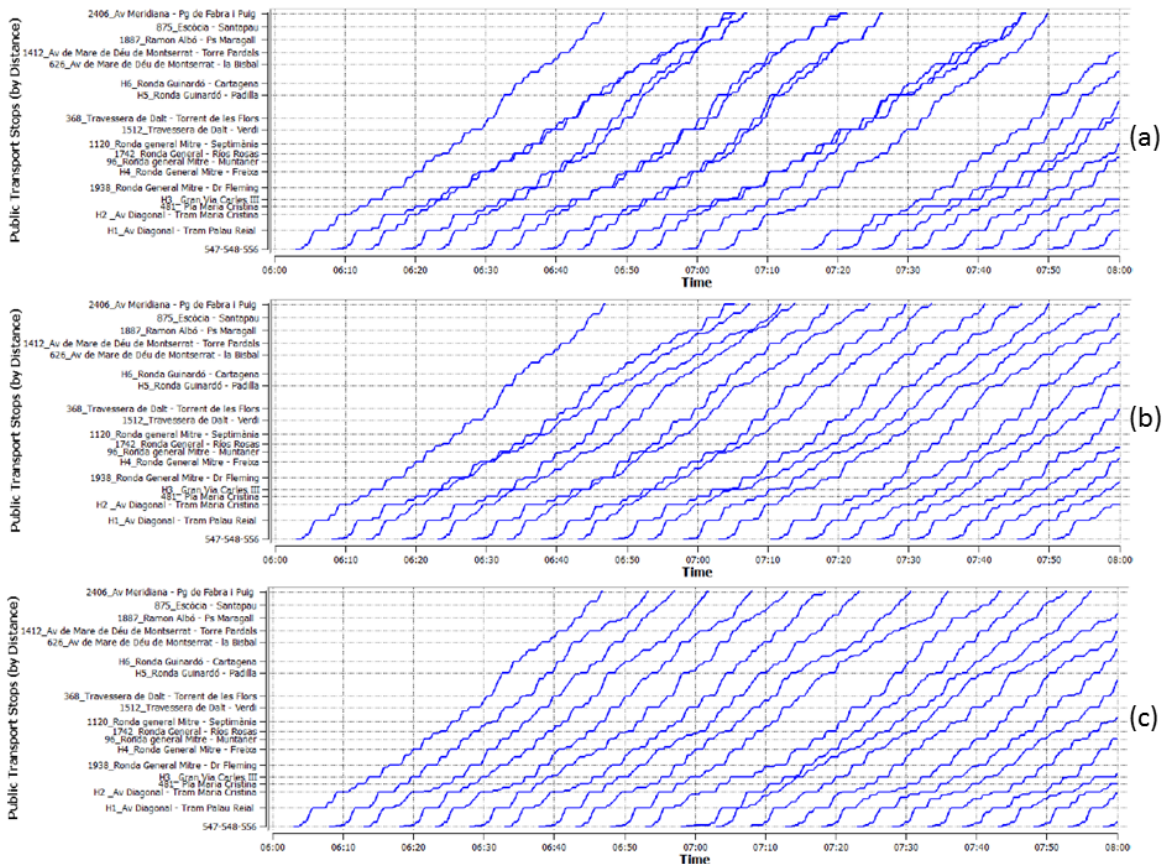


**Figure 32**. Simulation of bus trajectories in route H6 (direction Zona Universitària-Fabra i Puig) when $\varphi_s = 1$ min. (a) Strategy S0, (b) Strategy S1, (c) Strategy S2.

### 4.3.3 Final considerations and conclusions

These are the main considerations and conclusions that it may be drawn on this section:

— Main worldwide agencies use four metrics for calculating service regularity: EWT (Excess Wait Time), Standard Deviation, Wait Assessment, and Service Regularity

— Also, to measure headway adherence, the TCQSM considers the Coefficient of Variation of the actual headway, $C_v$, and issued a table that relates a wide range of this KPI to certain levels of service: from "service punctual like clockwork" to "many vehicles bunching"

— A visual methodology, which involves charts displaying all (scheduled and actual) vehicle headway throughout a full daily service span makes possible representing the gap between the scheduled and actual service, without using any formulation

— We analysed the efficiency of control strategies of bus bunching based on the user performance and operating costs incurred by the transit agency to run the service. An operational model was presented to reproduce how time disruptions propagate along the bus route when no controlling strategy is implemented.

— The model advances the contributions of Daganzo (2009) since it considers the vehicle capacity constraint in the formulations. Moreover, the modelling formulations could also estimate the deployment of existing controlling strategies to compensate disruptions: S0 introduced slack times at holding points (bus headers) and S1 modified the cruising speed of buses at each stop to maintain the targeted headway in a similar way presented in Daganzo (2009). Since strategy S1 actively reduced the speed of buses (i.e. it is impossible that buses run above the maximal cruising speed v), several buses would experience a higher round trip cycle time than the theoretical one. To overcome this problem, we proposed a new strategy (S2) that allowed only delayed buses (i.e. those with a higher time-headway with the vehicle ahead than the target value H) to be benefited by traffic light priority so that they could speed up.

— The results showed that the propagation of even a small disturbance in a specific bus produces irregular vehicle arrivals at stops, causing extra operating costs, user costs and coefficient of headway variation increment. Indeed, when the vehicle departures from terminals are not synchronised with traffic lights, the system does not need any exogenous to present an unstable performance. In these situations, the time headway adherence worsens as the percentage of green phase at intersections is reduced. The coefficients of headway variation may rise to $c_v \approx 0.75$ when the percentage of green time at intersections is $g/C_p \leq 0.45$. Therefore, transit managers should define a target time-headway compatible with the light cycle times in the bus corridor to reduce bus bunching.

— Vehicle capacity is an endogenous attribute of the system that contributes to mitigating the propagation of delays and the unstable motion of buses without exogenous controlling measures. When the delayed vehicle has enough capacity to accommodate the overall waiting passengers, the system tends to be more unstable. Any disturbance produces a dramatical increase in passenger travel times. However, the effects of operating costs are softened. On the other hand, if we consider vehicle capacity constraint, the total cost increases by almost 50% regarding the idealised performance with perfect regularity.

— Strategy S2 resulted in being the best control method in terms of total passenger travel time, operating costs and total costs. This fact justifies the need for speeding up delayed buses when adaptive cruising speed modification is performed. The effectiveness of this strategy does not depend on the number of intersections but on the traffic light settings: the green time (g) and the green extension (G). The total cost savings of this control strategy are essentially more relevant when vehicle departures are not synchronised with signal settings and for corridors with a low percentage of green time at intersections (i.e. the most unstable motion of buses considered). The coefficient of headway variation can be slightly higher to the minimal one obtained with strategy S0 with larger slacks unless headway variations range among the level of service A or B. Nevertheless, Strategy S2 only provided competitive results when the green extension time was significant ($G \geq 10$ sec). This fact would produce adverse effects on the traffic and passenger flow in the streets near to the intersections.

Therefore, when the bus route under analysis runs along a corridor with important traffic volumes in the crossing streets, we recommend hybrid control strategies. They consist of providing minimal slack times (less than 2-3 minutes) in the bus schedule as well as implementing dynamic strategy S2 with a green extension time of G=10 seconds, to recover larger and unpredictable disruptions. Hybrid strategies were the second-best control alternative, only outperformed by Strategy S2 with G=20 sec. They generally increase the total cost of the system by at most 4% in problems with vehicle capacity constraint, regarding Strategy S2 with no slacks. The control strategy S0 based on holding points is effective to maintain the bus performance at the same level of service as in the baseline case in ideal problems. However, it requires much slack time to control the system performance (6 minutes at terminals) for routes with high disruptions as well as high passenger flow. For medium-demand problems, lower slacks (3 minutes) seem to be sufficient to guarantee a similar total passenger travel time when no disturbance takes place. Therefore, it is a blind, not-adaptive strategy since bus managers cannot define in advance a minimal slack time to tackle the possible deviations that can appear. This strategy can keep total travel times stable at the expense of increasing operating cost. The effectiveness of the control strategy S1 is significantly dependent on the stabilisation parameters $f_f$ and $f_r$ that reduce the cruising speed proportional to the headway deviation. Although this strategy keeps the number of resources constant in comparison to strategy S0, it was unable to alleviate the effects of bunching on the total travel time of users.

— Consequently, in some capacitated problems, this strategy presents higher total costs than strategies with slack time. Strategy S1 only outperformed the results provided by Strategy S0 with low slack times when the vehicle capacity was supposed to be unlimited. This situation corresponds to the idealistic hypothesis considered in Daganzo (2009), where this cruising speed modification strategy was presented.

— It's assumed that: i) a delayed bus could not be overtaken by other buses and ii) the boarding time per passenger was constant and independent to the vehicle occupancy and the number of passengers waiting at stops. If assumption ii) is considered valid and if we allow the model to consider overtaking, the results will not differ from the presented in the chapter. However, if assumption ii) is substituted by variable unit

boarding times, considering the crowdedness of stops and vehicles, the overtaking of buses may produce better results in passenger travel and waiting times. Moreover, another important assumption that deserves mentioning is that the passenger arrival rate at each stop was deterministic and constant during a predetermined stationary period. Therefore, the source of instability analysed was any exogenous disruption that incremented the running time between two consecutive stops and the delays at signalled intersections. Here, the model can be further improved if stochastic passenger arrivals are considered, as presented in Bowman and Turnquist (1981) or Fonzone et al. (2015).

## 4.4   Transit corridors served by two routes

### 4.4.1   Case instances

Three idealised physical base problems, referred by BP1-BP3, were defined by two symmetrical bus routes in terms of route segment length. The central route segment was always set to be $l_2^x = l_2^y = 10$ km long in both directions; however, the length of the branched segments varied between 1.5-6 km.  These input parameters were summarised in Table 19. In each instance, we generated different versions of the same problem with constant stop distances $\bar{s} = 250$, 300 and 500 meters. In all versions of the base problems, the distance between intersections was supposed constant and equal to $\bar{x}_{p,p+1} = 125$ meters.

**Table 19**. Physical attributes of problem instances

|  | BP 1 | BP 2 | BP 3 | ABP1 | ABP2 | H10 |
|---|---|---|---|---|---|---|
| Length of central segment i=2 (km) | 10 | | | 10 | | 8.75 |
| Length of branched segment i=1 (km) | 1.5 | 3 | 6 | 1.5 | 1.5 | 1.45 |
| Length of branched segment i=3 (km) | 1.5 | 3 | 6 | 1.5 | 3 | 2.89 |
| Length of branched segment i=4 (km) | 1.5 | 3 | 6 | 6 | 6 | 0.65 |
| Length of branched segment i=5 (km) | 1.5 | 3 | 6 | 6 | 1.5 | 4.60 |
| Stop distances (km) | 0.25-0.5 | | | 0.25-0.5 | | 0.29-0.425 |
| Intersection distances (km) | 0.125 | | | 0.125 | | 0.09-0.176 |

A modification of the base problem instances was generated in a new problem set called "asymmetrical branch problem" (ABP). This set contained two cases where the length of each route segment $i \neq 2$ had been chosen randomly in the discrete domain {1.5; 3; 6} km. Hence, the roundtrip travel time of routes A and B would be different, and the vehicle synchronisation would be more challenging to implement.   Therefore, the solution comparison of problem sets BP and ABP would describe how asymmetrical routes would affect transit system regularity, user performance and operating cost.

The rest of kinematic and economic input parameters were shared in all problem instances BP and ABP: the maximal cruising speed was $v_{max}= 50$ km/h, acceleration rate $a=15000$ km/h$^2$, vehicle capacity $C= 120$ pax/veh, unit distance cost $c_d=5$ Euros/veh-km, unit temporal cost $c_t=60$ Euros/veh-h, unit boarding time $\tau_b = 4$ sec/pax, unit alighting time $\tau_a=2$ sec/pax and value of time $\mu_N=10$ Euros/pax-h.

The total passenger flow in the system was considered 4400 pax/h in all physical instances BP and ABP. However, the passenger flows between route segments ranged in a different domain, maintaining the total flow of 4,400 pax/h. Three demand parameters described these scenarios. $D_t$ was the percentage of demand trips that start or end in the central segment. This term $D_t$ took into account the demand terms that contribute to the propagation of instability in the central segment. The second term $T_r$ was the percentage of trips that must transfer from route A to B and vice versa (trips between segments 1-5, 1-4, 3-4, 3-5). Eventually, $S_A$ was the percentage of demand trips served by route A and, therefore, $(1-S_A)$ would be the demand captured by route B. These two metrics assessed the demand symmetry in the corridor. Scenario D1 represents the symmetric demand distribution for the base case, where there is a moderate rate of transfers $T_r =18\%$ and a moderate instability demand rate $D_t=54.5\%$. D2 generates a new demand scenario with symmetric flows between routes (each route carries 2200 pax/h) where the transfer rates between route A and B present extremal values ($T_r =27.2\%$). D3 also maintains the flow symmetry between routes but incrementing the passenger flow from/to the central route segment up to $D_t =73\%$. These flows contribute to increase the instability and lack of regularity in the central segment. It is reasonable to expect that any disturbance will propagate faster due to the higher dwell times along this segment. D4 is a more unstable demand scenario than D3, where the percentage of trips which origin or destination is located in the central segment has been increased to be $D_t =93\%$ regarding the total flow. In Scenario D5, the percentage of trips boarding and alighting in the central segment has been maintained to $D_t = 93\%$, but in this case route A is responsible for the 71% of the total flow.

**Table 20**. Demand scenarios, traffic signal scenarios and control strategies settings

| | Scenarios | | | | | | | Control strategies | | | |
|---|---|---|---|---|---|---|---|---|---|---|---|
| | Demand | | | | | Signals | | | | | |
| | D1 | D2 | D3 | D4 | D5 | NoS | Half | S0 | S1 | S2 | S3 |
| *Demand attributes* | | | | | | | | | | | |
| Percentage of pax flow transferring, $T_r$ *(%)* | 18.2 | 27.3 | 9.1 | 3.6 | 3.6 | | | | | | |
| Percentage of pax flow boarding and alighting at the central segment, $D_t$ (%) | 54.5 | 54.5 | 73 | 93 | 93 | | | | | | |
| Percentage of pax flow captured by route A, $S_A$ *(%)* | 50 | 50 | 50 | 50 | 71 | | | | | | |
| *Signals* | | | | | | | | | | | |
| Traffic signal cycle time, $C_p$ (s) | | | | | | 100 | 100 | | | | |
| Green phase time, $g$ (s) | | | | | | 100 | 50 | | | | |
| *Control strategies* | | | | | | | | | | | |
| Holding time, $\theta_{max}$ (s) | | | | | | | | 0 | 5 | 0 | 5 |
| Green extension time, $G$ (s) | | | | | | | | 0 | 0 | 20 | 20 |

For all demand scenarios, in each route segment $i$, the boarding and alighting rates to/from other route segments $j$ ($j \neq i$) are uniformly distributed along with the whole segment extension, i.e. $B_{ij}^z(k') = B_{ij}^z \frac{\sum_{h=1}^{k'} s_h^{iz}}{l_i^z}$; $A_{ij}^z(k') = A_{ij}^z \frac{\sum_{h=1}^{k'-1} s_h^{iz}}{l_i^z}$ . However, it is supposed that the boarding of passengers whose origin and destination fall in the same route segment are uniformly distributed on the first half of the segment, while the alighting of passengers happens in the last half of the route segment: $B_{ii}^z(k') = \frac{B_{ii}^z}{l_i^z} \sum_{h=1}^{k'} 2s_h^{iz}$ when $0 < k' < \frac{n_s^{ix}}{2}$, $B_{ii}^z(k') = B_{ii}^z$ when $k' \geq \frac{n_s^{ix}}{2}$, $A_{ii}^z(k') = 0$ when $0 < k' < \frac{n_s^{ix}}{2}$, $A_{ii}^z(k') = \frac{A_{ii}^z}{l_i^z} \sum_{h=1}^{k'-1} 2s_h^{iz}$.

Two scenarios of traffic light settings are presented. In the first one, called *NoS*, we have assumed that the cycle time is $C_p = 100$ seconds and the green time of all intersections is $g = 100$ seconds. It means that there will be no effect of traffic lights since all signals will always be in the green phase. The second traffic light scenario, referred to as *Half*, maintains the former traffic cycle time, but it is evenly distributed between the green and red phase in all intersections, i.e. $g = 50$ seconds. This scenario will contribute to increasing the instability of the system in the central route segment. In both scenarios, the traffic signal offsets of the green phase have been calculated to provide a green wave along the corridor at a constant cruising speed $v_{max}$.

Finally, the numerical analysis is completed considering the optimisation results in the H10 route of the Barcelona bus network. The current layout of this corridor does not show any branched segment and it is operated at $H = 6$ minutes. The occupancy at the edges of the route is significantly low at this headway. Therefore, potential modification of the current bus corridor H10 into two branched routes in the sides (H10-A and H10-B) is proposed to correct this malfunction. In Fig. 33, the layouts of the two the routes are depicted. Route H10-A would be 13.175 km long from Badal St. to Olimpic de Badalona Station (roundtrip distance 26.3km), while the route H10-B trip from Pl. de Sants St. to Sant Adrià St. is 14.00 km long. The branches of route H10-B run closer to the sea front in Fig. 33. The length of each branch as well as physical and economic parameters were enumerated in Table 20. In this physical problem, we considered a demand matrix, different from the Scenarios listed in Table 20, which has been obtained from the actual ridership in the central corridor of H10 and other

lines currently operating the branched segments (TMB, 2018). From the available data, the total demand estimation along the corridor was supposed to be 3410 pax/h. The corresponding values for the demand parameters mentioned above are $D_t$=79%; $T_r$=6% and $S_A$=51%. Moreover, the cycle time in the Barcelona neighbourhood where the corridor runs along is C=90 s and the green phase time ranges between $g$=36-60 seconds.
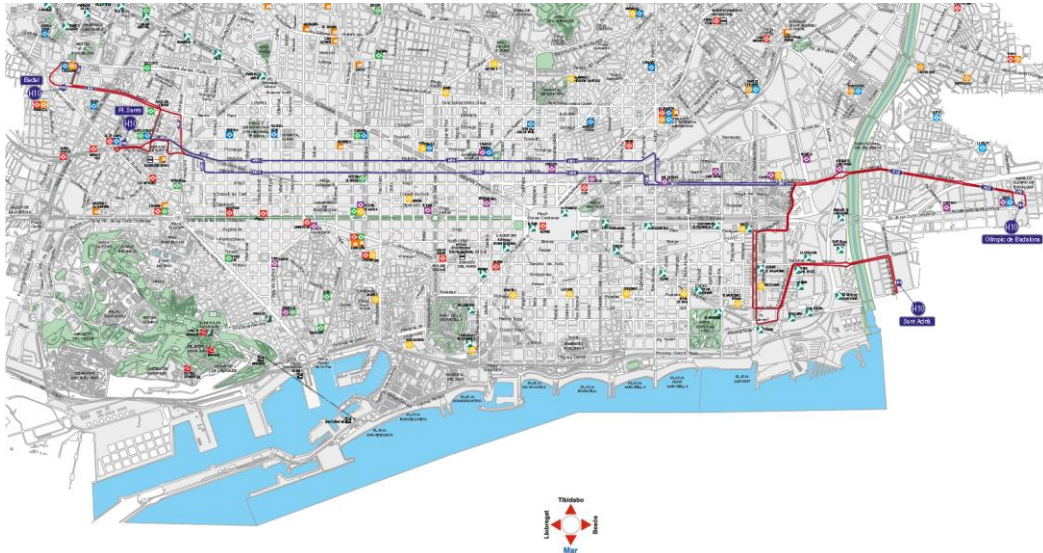


**Figure 33**. Barcelona's H10 bus corridor layout

## 4.4.2 Results

The analysis of the numerical results in different physical cases and scenarios was aimed at addressing the effect of the length and symmetry of route segments, the demand distribution, traffic lights and control strategies on the total cost and regularity of the system.

### 4.4.2.1 Effect of stop spacing and branch length

The number of vehicles, user, agency and total cost of the system that minimise the objective function P1 and P2 in problem instances B1-B3 are depicted in the bars of Fig. 34. Results are only provided for the base demand scenario D1, traffic signal scenario NoS and no control strategy (S0). The corresponding dotted line represents the coefficient of variation of headways in the central route segment shared by two lines, and continuous lines reflect the entrance times $t_{0,A} = t_0^{1x}$ and $t_{0,B} = t_0^{4x}$. The optimal headway obtained in the optimisation P1 and P2 in all problem instances is $H^*$= 300 seconds, although we obtained different entrance times. Generally, the solutions that minimise objective function P1 and P2 are the

same. They correspond to the situation where vehicles of route A and B are running evenly spaced at $H/2$ units of time in the common trunk ($t_{0,A}=0$s and $t_{0,B}=150$s), therefore the coefficient of variation of headways is $c_{vh}=0$. However, in specific instances, the minimisation of function P1 provides solutions where vehicles of route A and B do not maintain constant headways at the central route segment, causing the increment of the coefficient of variation of headways ($c_{vh}>0$). In these instances, the total cost of the system is minimised due to the synchronisation of inbound and outbound routes at transfer stops or the reduction of the number of vehicles in service. Hence, the user transfer time savings or operational cost savings are higher than the potential user waiting time increment along the central segment due to variable time headways. Two reasonable tendencies are identified in the results provided by the model: i) the longer the branched segments are, the higher both agency and user cost components are, and ii) the total cost is increased when the stop distance is diminished. The distance run by the whole fleet is the same in all problems, so that, the difference in the agency cost is due to the number of vehicles deployed.
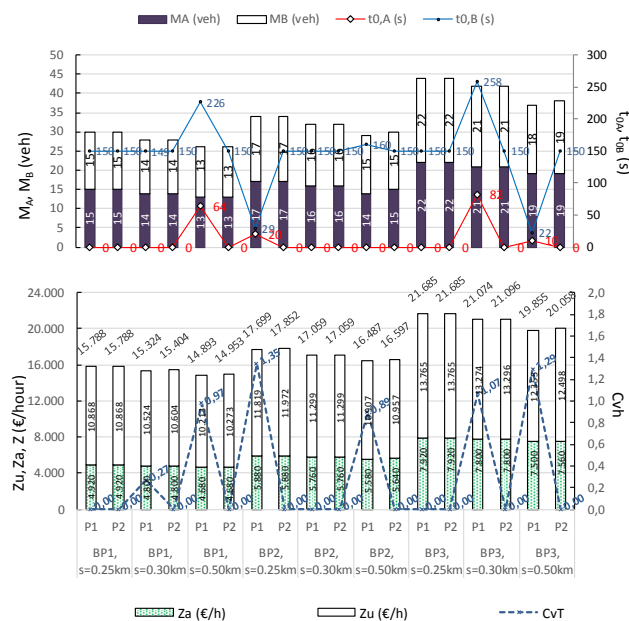


**Figure 34**. Performance and cost metrics in symmetric problem instances with different branched lengths and stop spacing

### 4.4.2.2 Effect of asymmetrical route's branch lengths

In Fig. 35, we summarise the bus cost and performance metrics in different instances where the branched segments of each route present different lengths (physical problems labelled by

ABP). In that case, the length of route A and B are different, generating asymmetric route layouts and therefore, roundtrip travel times. The combination of demand, traffic light scenario and control strategies is the same as in Section 4.4.2.1 (D1+NoS+Strategy S0). The optimal time headway is maintained to be $H^*=300s$. In this analysis, we considered an extra objective function to be minimised, labelled by (Min $c_{vx}$), that corresponds to the minimisation of the coefficient of variation of headways only in the direction of service $x$ (one-way). The mathematical formulation can be easily derived from Eq. (66). The general tendencies i) and ii) identified in section 4.4.2.1. are still maintained. However, the most important new effect is the lack of bus regularity in the central segment. Even for the objective function of optimisation P2, the different branch lengths make it impossible to guarantee null coefficients of variation of headways in the whole system ($c_{vh}$). In that case, we also plotted the coefficients of variation of headway just in the service direction $x$ ($c_{vx}$) and direction $y$ ($c_{vy}$) in the central route segment. Nevertheless, when the objective function is modified to minimise the variation of headways just in the direction of service $x$ (Min $c_{vx}$), we found that the system can guarantee $c_{vx}=0$. This is achieved by varying the previous values of entrance time $t_0^{1x}$ and $t_0^{4x}$, although the variation of headways in the opposite direction ($c_{vy}$) and in the whole system ($c_{vh}$) is worsened. It may be easily noted that the system operation in problems with asymmetric branches should be made independently for each service direction. If we inserted some slack at the ending stop of route segment $i=3$ and $i=5$ (Fig.17) in direction of service $x$, we would be able to control the entrance time of routes A and B in direction $y$; and therefore, alleviate time headway variations in the whole line. Doing it, the solution of the objective function P2 would be $c_{vh}=0$.
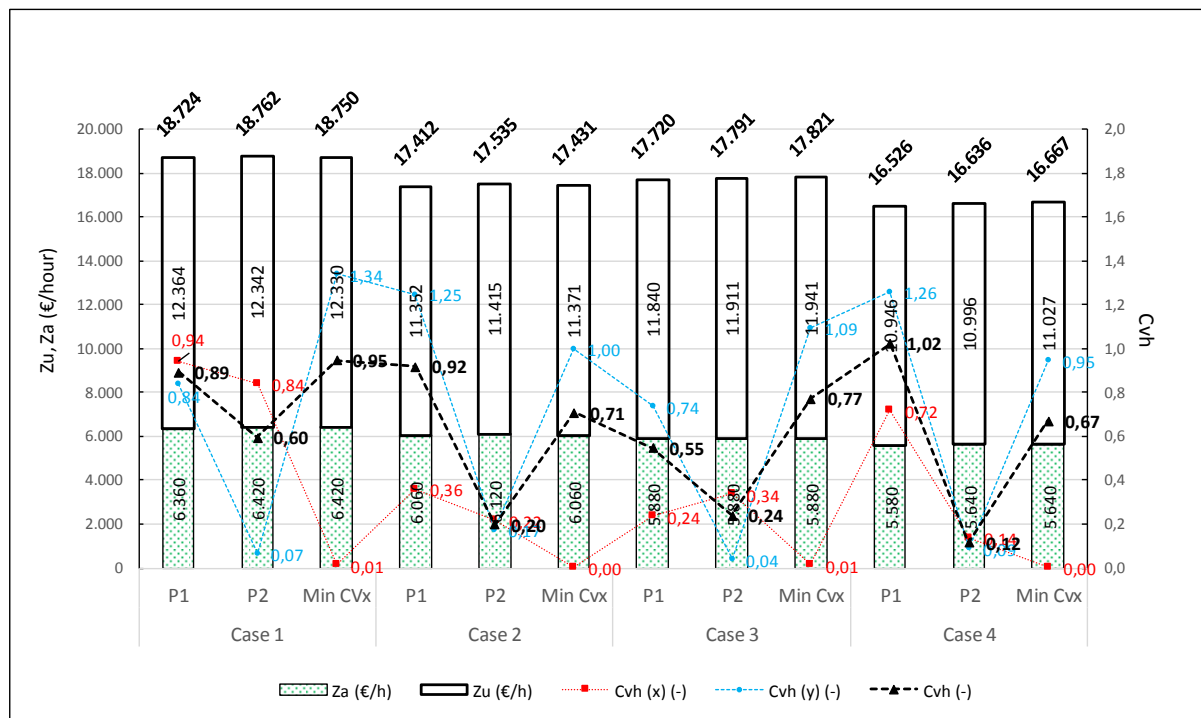
**Figure 35**. Performance and cost metrics in symmetric problem instances with different branched lengths and stop spacings

### 4.4.2.3    Effect of demand flow distribution

The optimisation results in the set of problems with different demand distribution are presented in Fig. 36. These instances are based on problem BP2 with a stop distance s=300 m. They share the same number of boarding passengers per hour (4.400 pax/h), but they differentiate each other depending on the passenger flow among route segments, i.e. the demand scenarios D1-D5. Since the current analysis was aimed at identifying the effects of demand distribution, the traffic signal scenario was considered to be NoS. Therefore, the effect of traffic lights settings is not still addressed.

The worst solution in terms of total cost (problem optimisation P1) is obtained in Scenario D2. The highest user cost is due to the high percentage of passengers transferring between lines ($T_r$=27%). On the contrary, if the percentage of passenger transhipments is reduced to $T_r$ =9%, $T_r$ =4%, corresponding to Scenarios D3 and D4 respectively, the user cost is also diminished, and the total cost of the system drops. However, in these instances, the demand fraction contributing to the central segment instability has increased ($D_t$=73% in D3 problem, $D_t$ =93% in D4 problem). The effect of this extra demand in the central corridor is that the coefficients of variation of headways are significantly worsened. Even when the objective

function P2 is considered, the system is unable to maintain a perfect regularity. Eventually, the instance D5 maintains the same $D_t$ and $T_r$ parameters as in instance D4; however, the demand captured by route A represents the 71% of the total amount (asymmetric demand matrix). In that case, both user and agency cost of the system is increased in D5 about D4 instance when considering objective function P1. The variation of headways is also worsened in asymmetric configurations when objective function P2 is taken into account. Therefore, asymmetric demand distribution penalises the optimisation aimed at minimising both total cost (P1) and time headway deviations (P2).
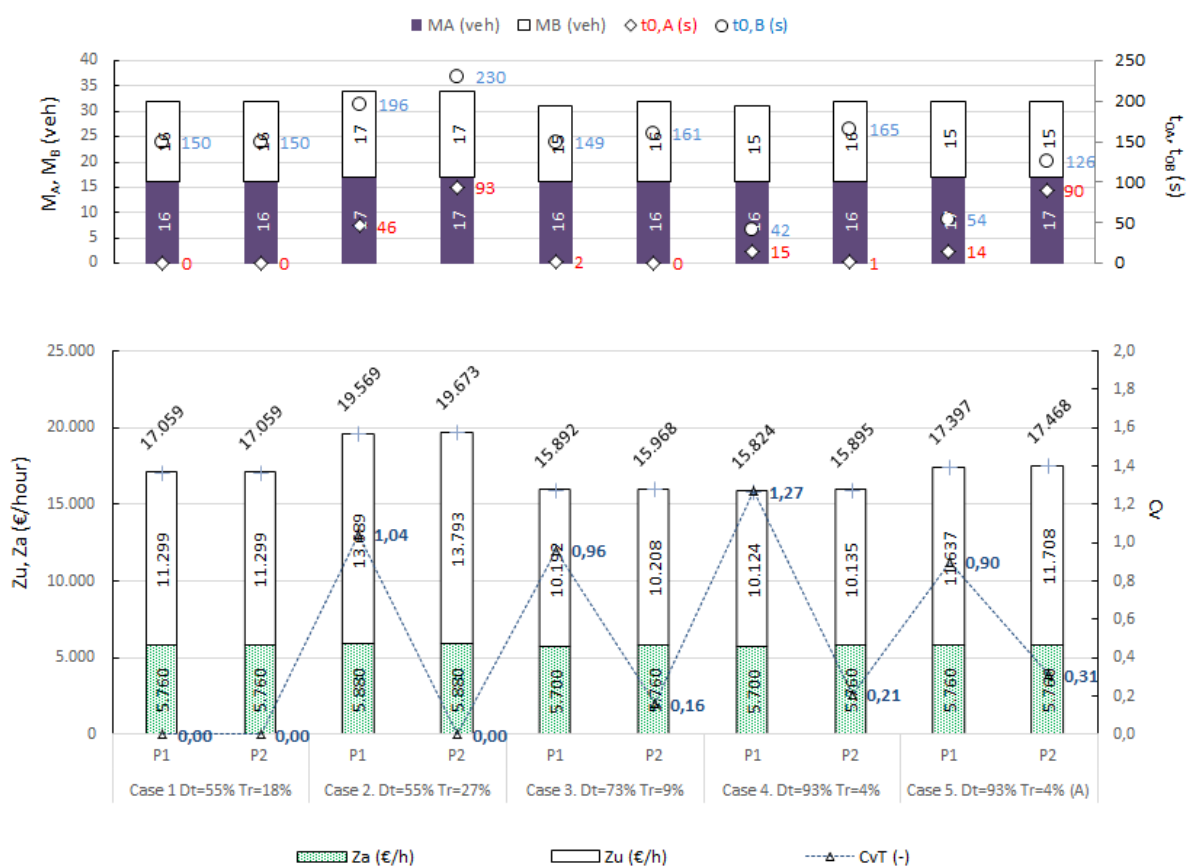


**Figure 36**. Performance and cost metrics in instances with different demand distribution

#### 4.4.2.4 Effect of traffic signals and control strategies

In this subsection, the effectiveness of the control strategies presented in Section 3.4.3 is addressed, considering their implementation in the physical problem BP2 with a stop distance s=300 m in all demand-based Scenarios. The novel situation is that traffic signals now cause bus delays since we consider Scenario called *Half*. Therefore, the green time of traffic lights

is $g$=50 seconds, i.e., the 50% of the total cycle time. The total cost of the system and the coefficient of variations of headways are compared among the following strategy settings:

— holding time strategy S1 when $\theta_{max}$=5s,

— green extension strategy S2 when $G$=20 s,

— hybrid strategy S3 considering slack times and green extension ($\theta_{max}$ =5s and $G$=20 s)

The natural motion of buses when overtaking is allowed (S0) is considered as the base case. We also include the strategy where overtaking is not permitted (S0-NO), and a line of buses may be formed at stops.

Fig. 37 summarises the results obtained by optimisation process P1 and P2. The best strategy in terms of total cost minimisation is S2, based on green extension activation at traffic lights. It can reduce the total cost of the system by -2 /-5% about Strategy S0. However, this strategy never achieves a minimally acceptable time headway adherence of buses in the central segment, since the coefficients of variations are $c_{vh}$>0.49. This strategy S2 outperforms the total cost savings for instances where the parameter $D_t$ is important, i.e. the demand terms contributing to the instability of the middle segment are significantly higher than the others. The strategy based on slacks (S1) generally improves the time headway adherence compared to strategy S2 and S0. However, this strategy always increases the roundtrip travel time of buses, penalising user in-vehicle travel times and operating costs. On average, it worsens the total cost of +3.6 /+4.9% about S0. However, the best strategy aimed at minimising the coefficient of variation of headways (P2 objective function) is strategy S3, maintaining $c_{vh}$<0.23 in all instances. This hybrid strategy was found to be the most efficient in terms of cost and headway variation in Estrada et al. (2016) when a single line was considered. However, the consideration of transfer times at stops in a corridor served by multiple lines requires an arrival time synchronisation rather than headway adherence. In these new spatial implementations, strategy S3 always increases the user cost component of the objective function P1. Finally, the strategy S0-NO (overtaking is not allowed) is never able to outperform the results when the natural motion of buses is not modified. This finding is consistent with the insights provided in Fonzone et al. (2015).
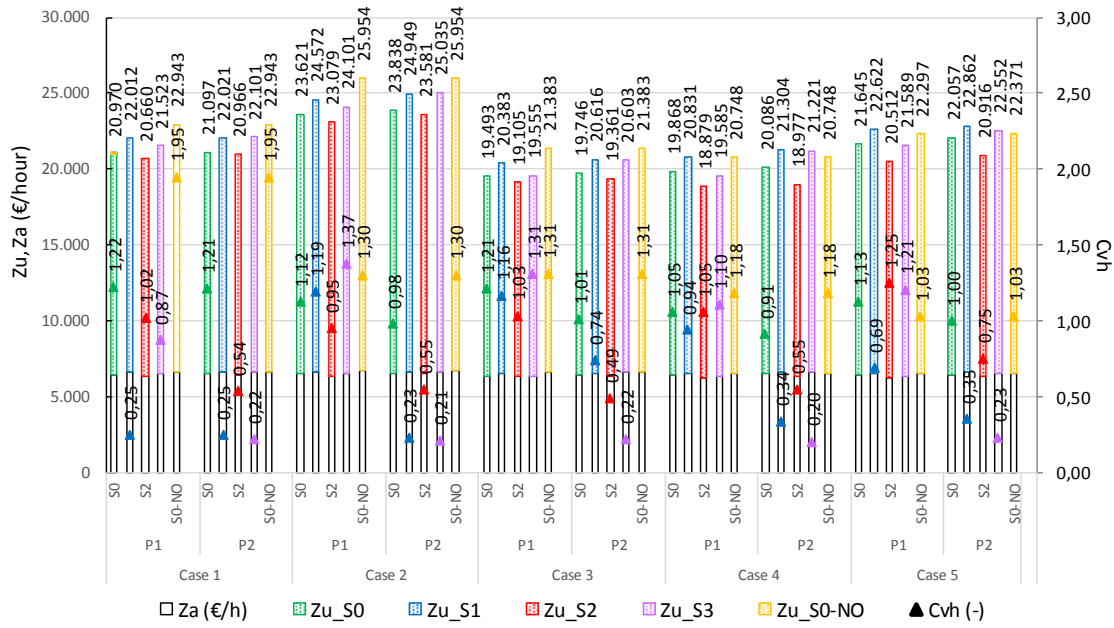
**Figure 37**. Performance and cost metrics by control strategies S0, S1, S2, S3 and S0-NO in instances with different demand distribution

### 4.4.2.5 Results in a real urban context

The optimisation of Barcelona's bus route H10 has been carried out for the demand scenario previously defined, considering the actual traffic light settings along the corridor. We compared the route performance under the same control strategies defined in Section 3.4.4, although we considered more combinations of parameters in Strategy S3 ($\theta_{max}$=5 sec, $g$=5sec in option a; $\theta_{max}$ =5 sec, $g$=5sec in option b; $\theta_{max}$ =5 sec, $g$=20sec in option c; and $\theta_{max}$ =10 sec, $g$=10sec in option d).

The results obtained are summarised in Fig. 38 and 39. The optimal headway provided by the optimisation model was $H^*$=450 seconds, shared in all control strategies scenarios. However, the entrance time at the edges of route segments $i$=1 and $i$=4 were different (Fig. 38). Due to the lowest transfer ratio ($T_r$) and total demand flow, the headway adherence was generally more stable ($c_{vh}$<0.3), even for Strategy S0. In the problem aimed at minimising the total cost (P1), the most efficient strategy resulted in being the one based on traffic signal extension (S2). However, this strategy presents a very poor service regularity, with a $c_{vh}$ metric three times higher than the strategy with no control (S0). The provision of the discrete green extension strategy and slightly delayed buses adds more instability to the system (poorer $c_{vh}$), but allows to minimise travel times. In Fig. 38, the entrance times of strategy S2 are

160

significantly different from other strategies, and they are set to minimise travel and transfer times. To fix this effect, hybrid strategy S3 (combining short slack times at holding points and the green extension measure) can provide similar results in terms of the total cost to the best strategy S2 while improving the variation of headways. The total cost of Strategy S3c is only 4Euros/h higher to the S0 counterpart. However, the coefficient of variation of headways has been diminished by 31%. When the objective function is changed, and the problem is aimed at minimising the headway variation (P2), the hybrid strategy S3d achieves an outstanding reduction ($c_{vh}$ =0.11). However, the system requires two additional buses in comparison to strategy S3c, due to the highest holding times ($\theta_{max}$ =10s). As it was suggested in Estrada et al. (2016), the most recommendable control strategy is the hybrid one, with small holding points distributed along the line and the possibility of the green extension of traffic lights.
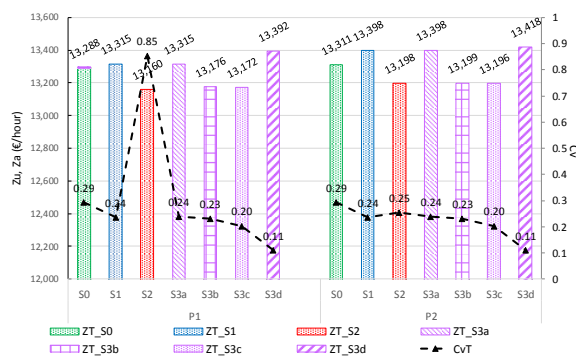


**Figure 38**. Total cost and coefficient of variation of headways corresponding to each control strategy
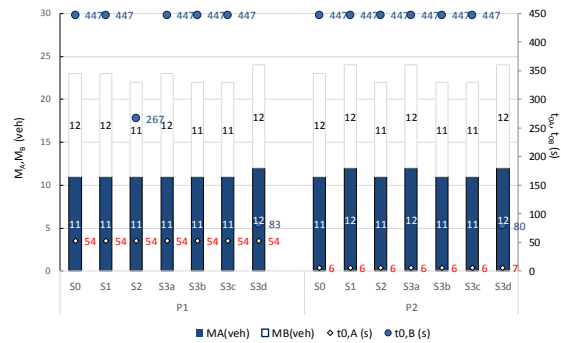


**Figure 39**. Fleet size and route entrance times corresponding to each control strategy

### 4.4.3 Final considerations and conclusions

— A transit corridor operated by two routes needs joint scheduling and dispatching of resources to guarantee a proper level of service

— An operational model such as the presented in this chapter is required to find out the optimal headway, vehicle entrance times in the corridor and control strategies that minimise the total cost of the system or the time-headway variation among routes

— The total cost should encompass the whole time of users spent in the system as well as the operating cost incurred by transit agencies. The latter depends on the control

strategies to tackle bus bunching since most of these measures improve time headway adherence at the expenses of reducing the commercial speed of buses

— A corridor with symmetric branches in terms of length and demand rates can be easily operated. Vehicles of complementary routes should depart from their initial stops every $H/2$ units of time. Doing this, they will run the middle segment evenly distributed. This synchronisation minimises the variation of headways along the corridor as well as the whole waiting and in-vehicle time of users. However, if we consider the transfer time spent by users travelling between the branched segments of the corridor, the solution may vary in terms of vehicle entrance time. In several instances, the consideration of user transfer times forces that two vehicles of different routes should run practically together to minimise the waiting times at transfer stops. In other instances, if the vehicles of one route start the operation in the central segment at headways lower than $H/2$ about the other line, the transit agency may reduce in one unit the fleet size of the former route. These facts may justify solutions of lower user and transit agency costs, although the system regularity is significantly worsened.

— Eventually, the values of the total system cost in problems aimed at minimising cost and coefficients of headway variation are practically the same. It has been demonstrated that, for the same ridership, the total cost of the system rises when the percentage of transfers among routes is increased. An increment of 1% in the transferring demand causes that the total cost is increased by 1.3%.

— In addition to that, the higher the passenger flow with origin or destination in the central segment is, the most unstable the operation in this central segment becomes. Indeed, we cannot ensure perfect regularity ($c_{vh}=0$) in systems where $D_t>0.7$.

— Asymmetric route layouts do not significantly increase the operational complexity of the system when the aggregated demand between route segments is the same. The relative offset between entrance times of route A and B should be defined considering the different travel time along with the initial branched sections. Therefore, they can start the operation of the central route segment maintaining a temporal distance $H/2$. As dwell times and travel time in this middle segment are the same for both routes, the

bus regularity is maintained, and coefficients of variation of headways are negligible. Nevertheless, this vehicle coordination can only be maintained in one direction of service. In the opposite direction, since vehicles have run branched route segments with different travel times, the operation in the central segment does not present an acceptable regularity. To fulfil high time headway adherence, holding points at the last stops of the direction of service in the two routes are required. At these stops, some slack should be inserted into the schedule. Two new entrance time variables should be optimised to guarantee perfect regularity in the opposite direction of the central segment as we did for the one-way. Nevertheless, when the demand rates between the branched and central section are unbalanced, route A and B present different dwell times in the central segment of the corridor. This fact causes that vehicles cannot maintain the headways in the whole roundtrip.

— The most important source of instability is traffic lights. When the relative green time of the traffic lights is switched from $g/C_p=1$ to $g/C_p=0.5$, the total cost incurred by users and transit agencies is increased by 20-26%, and the bus regularity in the central segment is really poor ($c_{vh}>=1.00$) considering the natural motion of buses when overtaking is allowed. If the overtaking operation is not allowed, the system is significantly worsened in terms of user travel times. Hence, control strategies are required to tackle the lack of regularity. Strategy S1 based on holding points, generally outperforms the regularity, maintaining $c_{vh}<0.3$. However, the increment of the level of service is achieved at the expenses of increasing travel times along the route. Therefore, the system is generally more expensive compared to the situation when buses are not controlled. Control strategy S2 based on green extension priority is typically the most efficient in terms of the total cost, although it hardly outperforms the regularity of the system. Indeed, hybrid strategies combining holding and green extension can maintain the total cost and headway regularity under acceptable thresholds. The previous statements were proposed from the numerical analysis point of view, in a set of test instances gathering a comprehensive combination of input parameters.

— In real implementations, it is expected that the fraction of demand rates captured in the central segment would be high, while the fraction of transfers would not be significant.

The example of Barcelona's bus route H10 follows these assumptions (central demand $D_t$=79% and transfer $T_r$=6%). The potentialities of hybrid strategies in this case instance are even better: the inclusion of a little slack $\theta_{max}$=5 sec and the deployment of green extension measure ($g$=20 s) diminish the total cost by 1% and improves the coefficient of variation of headways by 24%, in comparison to the strategy without control.

## 4.5 "Eixample Dret" transfer area

### 4.5.1.1 "Eixample Dret" transfer area

To illustrate the results obtained in section 2, the quality of the transfer area called "Eixample Dret" between routes H10 and V17 has been evaluated. This transfer area is located in the "Eixample" district, with a typical grid-shaped street network, chamfered corners, and full of services and businesses. It is surrounded by four twenty-meters wide streets (five metres for each sidewalk and ten meters for the road): Pau Claris, Llúria, Mallorca and Valencia streets, which define an octagonal-layout block with minor and major sides measuring 83.3 m and 21.2 m in length (Figure 3). Due to the street directions (anticlockwise), this transfer area differs slightly from the optimum design and, consequently, users must cross streets twice at each transfer. Table 21 shows transfer ridership and lengths in "Eixample Dret" transfer area.



**(A)**                                              **(B)**
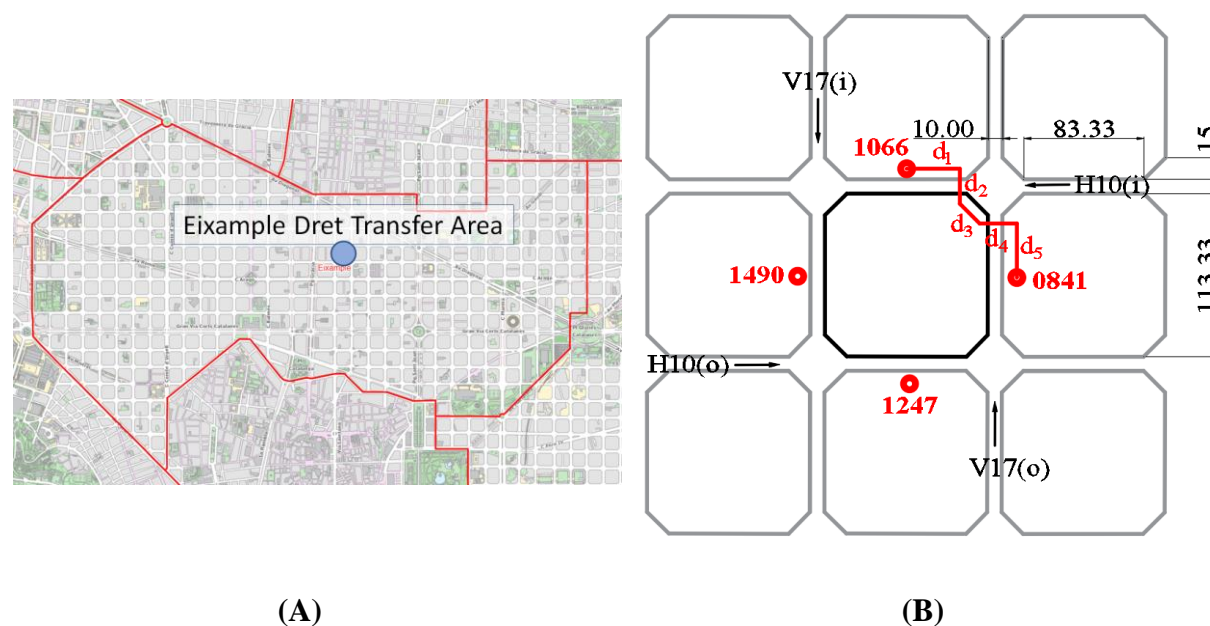
**Figure 40**. (A) Location of "Eixample Dret" Interchange Area within the "Eixample" district; (B) Scheme of the "Eixample Dret" transfer area. UTM coordinates (X=430,309.070; Y=4,583,146.010). Its orthogonal street-grid with octagonal blocks all around is a landmark of the urban planning of this part of the city.

**Table 21**. Physical characterisation of "Eixample Dret" transfer area and ridership share.

| Transfer | Stop I | Stop O | Distance (m) | Ridership (%) |
|---|---|---|---|---|
| H10(A) → V17(A) | 1247 | 0841 | 137 | 8.80% |
| H10(A) →V17(T) | 1247 | 1490 | 169 | 11.00% |
| H10(T) →V17(A) | 1066 | 0841 | 156 | 11.00% |
| H10(T) →V17(T) | 1066 | 1490 | 131 | 12.90% |
| V17(A) → H10(A) | 0841 | 1247 | 137 | 19.50% |
| V17(A) → H10(T) | 0841 | 1066 | 156 | 18.40% |
| V17(T) → H10(A) | 1490 | 1247 | 169 | 11.00% |
| V17(T) → H10(T) | 1490 | 1066 | 131 | 7.40% |

Note: (A) means the bus service in the direction between initial-ending stops 1-2, whereas (T) means the service in the opposite direction (2-1).

### 4.5.1.2 Boundary conditions

The walking time and its uncertainty are dependent on the pedestrian speed and traffic signals. Due to the impossibility of evaluating $(\mu_0, \sigma_0)$ for the entire range speeds, four reference values were considered: 0.85 m/s for adults over 65; 1.40 m/s for adults under 65 (average speed), 1.15 m/s (85th percentile) and 1.65 m/s (15th percentile) (Hoxie and Rubinstein, 1994; Browning et al., 2006; Mohler et al., 2007; Asher et al., 2012). In this area of the city, all signalled intersections present a traffic signal cycle of 90 seconds (42 second-green, 3 second-yellow and 45 second-red). Considering the previous assumptions, the traveling times on foot and their uncertainty have been evaluated by means of simulation for each reference speed $w$, obtaining the following outcomes: $(\mu_0, \sigma_0) = (2.74, 0.32)$ when $w$=0.85 m/s; $(\mu_0, \sigma_0) = (2.21, 0.37)$ when $w$=1.15 m/s; $(\mu_0, \sigma_0) = (1.95, 0.39)$ when $w$=1.40 m/s; and $(\mu_0, \sigma_0) = (1.77, 0.40)$ when $w$=1.65 m/s. Consequently, the joint estimation across the range of speed is $(\mu_0, \sigma_0) = (2.2, 0,6)$, being:

$$\mu_0 = 1/4[2.74 + 2.21 + 1.95 + 1.77] = 2.17 \cong 2.2 \text{ min}$$

$$\sigma_0 = (\sigma_{between}^2 + \sigma_{within}^2)^{1/2} = 0.57 \cong 0.6 \text{ min}$$

$$\sigma_{between}^2 = s^2(2.75, 2.21, 1.96, 1.76) = 0.1834$$

$$\sigma_{within}^2 = 1/4[0.32^2 + 0.37^2 + 0.39^2 + 0.40^2] = 0.1379$$

On the other hand, given the reference headway of the network, H = 8 min, the corresponding values for the experimental situation III are:

$$(\mu_2, \sigma_2) = (\mu_0 + H, (\sigma_0^2 + H^2/3)^{1/2}) = (2.2 + 8, (0.6^2 + 8^2/3)^{1/2}) = (10.2, 4.7)$$

### 4.5.1.3 Measurement of quality and results

In the context of the incomplete consensus of experts, the system of equations described in 2.6 provided us with the following solution: $a_{11} = -0.4217$; $a_{22} = -1.9402$; $a_{12} = -0.1477$. Consequently, the quality of the transfer will be evaluated based on the equation:

$$TQR(\mu_T, \sigma_T) = \max\{0, 100 - 0.42\mu_T^2 - 1.94\sigma_T^2 - 0.30\mu_T\sigma_T\} \qquad (77)$$

The results of the TQR's corresponding to the eight links, both scheduled and actual service provided; as well as the IQR's, of a sample corresponding to the 20 working days of October 2016, is shown in Table 22.

The results obtained may infer the penalty due to the loss of the quality components, such as layout design, synchronisation and regularity. The average loss due to the layout design can be evaluated as follows: $100 - TQR_0(2.2, 0.6) = 3.13\%$. The loss due to the lack of synchronisation of the routes will be: $TQR_0 - TQR(\text{scheduled}) = 96.87\% - 65.45\% = 31.42\%$. Finally, the loss due to the lack of regularity of the routes can be evaluated as: $TQR(\text{scheduled}) - TQR(\text{actual}) = 65.45\% - 41.43\% = 24.02\%$.

In this study, we gathered the operational data of a sample corresponding to the 20 working days of October 2016. We analysed the real arrival times of vehicles at the transfer area from GPS systems, the scheduled arrival time and the passenger demand flow in each transfer movement.

In Table 22, we present the TQR's index obtained in each transfer movement, both for scheduled and actual service and the global IQR's index when the sample data are replaced in equation (2.9).

The results obtained may infer the penalty due to the loss of the quality components, such as layout design, synchronisation and regularity. The average loss due to the layout design can be evaluated as follows: $100 - TQR_0(2.2, 0.6) = 3.13\%$. The loss due to the lack of synchronisation of the routes will be $TQR_0 - TQR(\text{scheduled}) = 96.87\% - 65.45\% = 31.42\%$. Finally, the loss due to the lack of regularity of the routes can be evaluated as $TQR(\text{scheduled}) - TQR(\text{actual}) = 65.45\% - 41.43\% = 24.02\%$.

**Table 22**. Scheduled and actual TQR and IQR of the sample at "Eixample Dret" Transfer Area

| Transfer | H10a-V17a | H10a-V17t | H10t-V17a | H10t-V17t | H17a-V10a | H17a-V10t | H17t-V10a | H17t-V10t | IQR |
|---|---|---|---|---|---|---|---|---|---|
| **Ridership** | 8.8% | 11.0% | 11.0% | 12.9% | 19.5% | 18.4% | 11.0% | 7.4% | |
| **Scheduled** | **63.47** | **65.05** | **63.10** | **68.40** | **67.91** | **68.66** | **54.99** | **67.79** | **65,45** |
| day 1 | 56.95 | 49.97 | 58.95 | 57.16 | 41.73 | 49.91 | 26.06 | 42.83 | 47.72 |
| day2 | 56.08 | 51.19 | 46.01 | 52.23 | 43.84 | 43.28 | 47.53 | 48.07 | 47.66 |
| day 3 | 53.94 | 42.36 | 57.48 | 51.90 | 50.32 | 39.56 | 28.13 | 45.12 | 45.95 |
| day 4 | 20.06 | 22.34 | 17.72 | 38.73 | 47.87 | 37.15 | 23.57 | 34.31 | 32.47 |
| day 5 | 40.10 | 31.19 | 44.53 | 24.02 | 35.19 | 29.66 | 29.77 | 34.54 | 33.11 |
| day 6 | 59.07 | 48.44 | 59.21 | 54.28 | 41.01 | 43.24 | 27.45 | 51.95 | 46.86 |
| day 7 | 46.01 | 49.76 | 49.81 | 47.92 | 44.98 | 47.11 | 47.96 | 48.44 | 47.48 |
| day 8 | 38.69 | 23.26 | 18.14 | 30.89 | 24.15 | 10.20 | 10.93 | 10.23 | 20.49 |
| day 9 | 46.56 | 39.34 | 43.30 | 40.78 | 53.46 | 50.25 | 45.73 | 51.77 | 46.98 |
| day 10 | 46.32 | 46.88 | 36.91 | 45.19 | 43.82 | 32.81 | 42.62 | 24.86 | 40.23 |
| day 11 | 32.30 | 33.21 | 36.75 | 39.52 | 51.28 | 45.53 | 38.74 | 40.86 | 41.30 |
| day 12 | 55.74 | 48.07 | 52.17 | 54.38 | 45.29 | 35.26 | 34.90 | 29.61 | 44.30 |
| day 13 | 34.29 | 28.00 | 25.27 | 34.28 | 44.65 | 45.36 | 35.56 | 29.22 | 36.43 |
| day 14 | 54.84 | 44.88 | 51.80 | 55.58 | 41.39 | 31.44 | 31.10 | 41.66 | 42.99 |
| day 15 | 56.35 | 54.19 | 45.59 | 61.55 | 22.44 | 33.72 | 23.71 | 37.07 | 39.81 |
| day 16 | 63.66 | 54.91 | 59.30 | 50.66 | 42.37 | 43.87 | 47.98 | 49.89 | 50.00 |
| day 17 | 44.81 | 28.34 | 53.24 | 24.70 | 46.08 | 41.20 | 30.53 | 46.93 | 39.50 |
| day 18 | 56.55 | 50.18 | 50.61 | 58.37 | 33.35 | 48.92 | 22.37 | 47.94 | 45.10 |
| day 19 | 57.20 | 37.21 | 40.29 | 41.73 | 36.90 | 43.11 | 32.70 | 34.76 | 40.24 |
| day 20 | 52.56 | 45.83 | 44.00 | 47.36 | 37.80 | 33.18 | 28.50 | 38.47 | 40.08 |
| **Actual (mean)** | **48.60** | **41.48** | **44.55** | **45.56** | **41.40** | **39.24** | **32.79** | **39.43** | **41.43** |

### 4.5.2 Discussion

The measuring system defined in this section, oriented to the management and service improvement, allows evaluating the transfer area quality (information and monitoring) and identifying inefficiencies (improvement). Regarding the global customer satisfaction KPI's (dell'Olio et al. 2011a, de Oña et al., 2015), the TQR relates to two dimensions of service, reliability and responsiveness. Loss of quality (100-TQR(actual)) can be broken down in root causes: $100\text{-}TQR_0$ is imputable to physical architecture constraints; $TQR_0\text{-}TQR$ (scheduled) is attributable to the lack of synchrony in time planning; and TQR (scheduled) -TQR(actual) is due to discrepancies between the actual service provided and the scheduled one. On the other hand, service provided without synchrony and with bunching effect service can be evaluated as $TQR_0\text{-}TQR_1$ and $TQR_1\text{-}TQR_2$. In these approaches, based on customer perception and in the incomplete consensus of experts, losses $100\text{-}TQR_0$, $TQR_0\text{-}TQR_1$ and $TQR_1\text{-}TQR_2$ are estimated objectively (based on functional satisfaction), while in the approach based on the consensus of experts, losses are estimated subjectively.

Within the city of Barcelona, the functional approach has allowed to demonstrate the suitability of the octagonal blocs as transfer areas, as well as other least demanding exchange areas in terms of walking times between stops (transfer areas at a junction, exchange areas in the middle of a block, near a roundabout, etc.). At the transfer area of "Eixample Dret", where routes H10 and V17 intersect, urban physical constraints have led to a loss of 3.13%. Besides, the loss due to lack of synchronisation in planning has been estimated at 96.87% - 65.45% = 31.42% and the loss due to the gap between the actual and scheduled service have been assessed at 65.45% -41.43% = 24.02%. Service improvement-oriented, the interest must be focused on time synchronisation and to reduce the daily variability between the actual and scheduled service. Loss due to lack of synchronisation in planning is very high and exceeds the maximum reference ($TQR_0$-$TQR_1$ = 96.87%-68.33% = 28.54%). The loss in execution is also significant (24.02% concerning its reference 65.45%), but the most important is its variability. For example, with an average of 44.55%, daily values vary between 17.72% and 59.30% (transfer H10t-V17a) and with an average of 32.79%, daily values range between 10.93% and 47.98% (transfer V17t-H10a).

On high-performance orthogonal networks, time synchronisation is quite relevant and challenging to achieve. Route headways are established according to the demand and, for that reason, it is frequent that headways are different from each other and not multiple. In these conditions ($H_1$, $H_2$ = 5, 6, 7, 8, 9, being $H_1 \neq H_2$) there is a randomness effect on the inbound and outbound route arrival and departure times. Also, the synchronisation of two routes at a transfer can affect the synchronisation at other transfer areas. To progress in this direction, the cost/quality binomial (offer/demand and expectations) is being reformed and tested with adjustments that improve the synchronisation throughout the whole network (Liu and Ceder, 2017, Liu et al., 2017, Paiva Fonseca et al., 2018). On the other hand, the daily variability between the actual and scheduled service executed has revealed that the agency can achieve a good enough headway adherence but has not been able to maintain it. Most certainly, new regulatory strategies should be applied to improve service regularity and headway adherence (Wu et al., 2016; Estrada et al., 2016).

The functional model presented allows the evaluation of the performance of the transfer areas in urban transport networks. The quadratic approach is generally applicable in other modes of transport, and the methodologies for calibrating the parameters of the model can be applied

directly, or they can be adapted with minimal adjustments. In particular, the approach based on customer perceptions can be applied without modification, both in the approach and in the resolution. The approach based on the consensus of experts requires choosing and characterizing three situations of interest in the scope of application (defining $(\mu_0, \sigma_0)$, $(\mu_1, \sigma_1)$ and $(\mu_2, \sigma_2)$, independently of the headway H), agreeing on the quality attributed to each of the new scenarios (TQR$_0$, TQR$_1$, TQR$_2$) and applying the resolution method described in (2.2.2). Finally, the approach based on the incomplete consensus of experts requires choosing a situation of interest in the scope of application $((\mu_2, \sigma_2))$, agreeing on the quality attributed in that scenario (TQR$_2$), maintaining the conditions of regularity described in (2.2.3) and applying the method of resolution explained in this thesis.

### 4.5.3   Final considerations and conclusions

These are the main considerations and conclusions that it may be drawn on this point:

— Transfer areas are important nodes where users can shift from one route to another on improved networks. The operating performance assessment is crucial to understand the transfer quality and how users are served, only in terms of total transfer disutility: walking time plus waiting time. The importance of transfers has been evident in many transport networks, as well as in surface transport (Nielsen et al., 2006; Guihaire et al., 2008).

— Three methods have been proposed to evaluate the service quality: the customer's satisfaction survey, the consensus of experts, and the incomplete consensus of experts, which has been developed as it can meet better real examples with different headways on each route and without route synchronisation.

— Setting out a quadratic approach, a mathematical expression to calculate the TQR, Transfer Quality Ratio, and the IQR, Transfer area Quality Ratio, both for scheduled and actual values, has been obtained. The second order (quadratic) functional approach was justified using Taylor's series approximation, and the parameter calibration was obtained in three complementary ways.

— Technical resolution is quite simple when considering the approximation based on consistent customer perceptions (4.1.2.2). In the end, a linear system of equations is set

out and its coefficients can be obtained using a single spreadsheet. On the contrary, the measuring dependency on changing perceptions over time can cause periodic changes in the referents, and as a result, discontinuities regarding data monitoring. Also, when customer perceptions are not consistent, calibration of coefficients requires solving an optimisation problem, which adds dimension to the issue. The approach based on the consensus of experts (4.1.2.2) is also an easy problem to solve (linear system of equations) when the conditions are consistent, and it turns to an optimisation problem when those consensus conditions are not consistent enough.

— On the other hand, based on the consensus achieved in situations of progressive loss of quality components, the estimation of the loss due to physical architecture, synchronisation and gap between actual and scheduled service is subjective. Finally, the approach based on the incomplete consensus of experts (4.1.2.3) provides stable referents over time and allows estimating objectively the loss of quality associated with each component.

— Nevertheless, technical justification is much more complex, and the resolution requires the use of appropriate software (nonlinear equation system). In this respect, libraries and functions that solve optimisation problems and systems of nonlinear equations have been referenced and an EXCEL spreadsheet was developed to obtain the solution when the approach 4.1.2.3 is taken.

— The measuring system defined in this thesis, oriented to the management and service improvement, allows evaluating the transfer area quality (information and monitoring) and identifying inefficiencies (improvement). Regarding the global customer satisfaction KPI's (dell'Olio et al. 2011a, de Oña et al., 2015), the TQR relates to two dimensions of service, reliability and responsiveness. Loss of quality (100-TQR(actual)) can be broken down in root causes: $100-TQR_0$ is imputable to physical architecture constraints; $TQR_0-TQR$ (scheduled) is attributable to the lack of synchrony in time planning; and TQR (scheduled)-TQR(actual) is due to discrepancies between the actual service provided and the scheduled one. On the other hand, service provided without synchrony and with bunching effect service can be evaluated as $TQR_0-TQR_1$ and $TQR_1-TQR_2$. In these approaches, based on customer perception and

in the incomplete consensus of experts, losses 100-$TQR_0$, $TQR_0$-$TQR_1$ and $TQR_1$-$TQR_2$ are estimated objectively (based on functional satisfaction), while in the approach based on the consensus of experts, losses are estimated subjectively.

— A real example from Barcelona Premium Bus Network has been calculated, taking a single transfer area with two routes intersecting at Eixample Dret, in the city centre. Assessing the scheduled and actual service, the loss in satisfaction of the three components are as follows: concerning infrastructure, by 3.31%; concerning desynchronisation between routes, by 31.42%; and concerning lack of regularity, by 24.02%. These outcomes underscore the importance of headway adherence (regularity) and the synchrony between the routes for the proposed model. Further developments may consist of applying this methodology to a more massive transfer area, with a more significant amount of bus routes or even with other transport modes like metro or tramway systems. Besides, a wide-range historical data value series can be collected to monitor the quality fluctuation, provided at the transfer area.

# Part V: CONCLUSIONS AND FUTURE RESEARCH

# Chapter VI

# Conclusions and future research

## 5.1 Main conclusions

The main conclusions of this study, broken down by topics, are cited below.

***Regarding Efficient Timetables:*** Schedule manufacturing is a crucial step to offer an excellent service to the users while fulfilling the operational requirements and securing costs at an acceptable level both for the operator and the system. Drawing up a bus route schedule is not simple and requires historical data, computer support, an appropriate methodology for obtaining timetables, as well as programmer's expertise for the completion. The schedule consists basically of two parts: vehicle scheduling, which represents the succession of scheduled trips throughout the day, and driving services, which are made up of workpieces that cover all those service hours defined in the vehicle scheduling and are always consistent with the conditions and regulations coming from the Union Agreement and the Operations Committees. The methodology for calculating optimal timetables is based on three elements: travel time, recovery time at route terminals, and time slots. HASTUS, developed by the Canadian company, Giro, has been the IT support since it allows the usage of historical data and makes processing all that information easy. The travelling time heterogeneity

(variability) along the route service span is the main problem we must face. The systematic deviations from the programmed times significantly affect the cost of the service. Within each time slot, the scheduled travel time agrees with the average actual travel times. The Recovery Time can be calculated by linking it to a statistical threshold of achievement. To ensure the departures at the terminals by 97.5%, within a time slot, Recovery Time can be calculated, assuming that the data follow a Normal distribution, such as the square root of the sum of variability of the travel times within the various hours of the time slot, and the variability of the travel times between the hours, multiplied by 1.96. Combining a maximum homogeneity with a maximum extension, the $\pm 1$ criterion fits very well and minimises the deviation within the time slots. Once these parameters are determined and the time slots are built, the appropriate supply can be sized from the headway, or set up this according to the available resources. This methodology has been applied to determining the timetables and the complete schedule of route H12, Gornal-Besos/Verneda, one of the Barcelona's New Bus Network premium routes. The support tool has been HASTUS.

***Regarding Headway Adherence:*** Worldwide agencies use four metrics for calculating service regularity: EWT (Excess Wait Time), Standard Deviation, Wait Assessment, and Service Regularity. Each of these methodologies has strengths and weaknesses: the EWT is the only method that fully incorporates the customer perspective as its output reflects the common experience of all passengers in the data sample. The Wait Assessment and service regularity indicators only reflect the experience of regular customers. The standard deviation method only reflects the experience of one standard deviation, approximately 68% of customers. The EWT is the only method that provides a normalisation for differences in scheduled headways and thanks to its customer focus as well, makes it suitable service regularity KPI for use in a benchmarking exercise, especially if the headways in each route are scheduled in regular intervals. Concerning Bus Bunching measurement, the TCQSM (TRB, 2009) proposes a service regularity appraising whilst setting a diverse level of service based on the coefficient of variation of the headway, that can also be related to the probability, P that a given transit vehicle's headway, $h_i$ will be off-headway by more than one-half the scheduled headway h. Although it is challenging to explain to the stakeholders, it is the best available measure for describing the bunching effect. Three strategies to keep headway adherence are proposed, based on slack times ($S_0$), on the cruising speed ($S_1$) and a combination of the cruising speed and signal priority ($S_2$). They were tested on the H6 route,

from Barcelona's New Bus Network. These strategies proposed to control the service regularity present a trade-off between headway adherence effectiveness and the cost of the resources deployed to achieve proper service regularity. Static control strategies based on slack times offer higher total cost (user and agency cost) to keep the bus motion stable. Since this strategy is neither scalable nor adaptive, we would need substantial slack times to maintain good headway adherence. In the test instance, the provision of slack time of $\phi_s = 6$ min was insufficient to mitigate the effects of irregular passenger arrivals at stops and variable traffic flow states. The coefficient of headway variation is $C_v > 0.8$; it means that the level of service can be graded as F concerning the classification of TCQSM. To tackle the bus bunching phenomena, it is crucial to perform dynamic control strategies based on a combination of the cruising speed modification and traffic light priority. This strategy outperforms the total cost of the system by 40% and allows maintaining the coefficient of headway variation below $C_v < 0.21$ (the maximal threshold to consider a level of service A).

***Regarding Corridors served by Two Routes:*** A transit corridor operated by two routes needs joint scheduling and dispatching of resources to guarantee a proper level of service. An operational model such as the presented in this thesis is required to find out the optimal headway, vehicle entrance times in the corridor and control strategies that minimise the total cost of the system or the time-headway variation among routes. The total cost should encompass the total time of users spent in the system as well as the operating cost incurred by transit agencies. The latter depends on the control strategies to tackle bus bunching since most of these measures improve time headway adherence at the expenses of reducing the commercial speed of buses. A corridor with symmetric branches in terms of length and demand rates can be easily operated. Vehicles of complementary routes should depart from their initial stops every $H/2$ units of time. Doing this, they will run the central segment evenly distributed. This synchronisation minimises the variation of headways along the corridor as well as the total waiting and in-vehicle time of users. However, if we consider the transfer time spent by users travelling between the branched segments of the corridor, the solution may vary in terms of vehicle entrance time. In several instances, the consideration of user transfer times forces that two vehicles of different routes should run practically together to minimise the waiting times at transfer stops. In other instances, if the vehicles of one route start the operation in the central segment at headways lower than $H/2$ about the other line, the transit agency may reduce in one unit the fleet size of the former route. These facts may

justify solutions of lower user and transit agency costs, although the system regularity is significantly worsened. Asymmetric route layouts do not significantly increase the operational complexity of the system when the aggregated demand between route segments is the same. The relative offset between entrance times of route A and B should be defined considering the different travel time along with the initial branched sections. Therefore, they can start the operation of the central route segment maintaining a temporal distance $H/2$. As dwell times and travel time in this middle segment are the same for both routes, the bus regularity is maintained, and coefficients of variation of headways are negligible. Nevertheless, this vehicle coordination can only be maintained in one direction of service. In the opposite direction, since vehicles have run branched route segments with different travel times, the operation in the central portion does not present an acceptable regularity. To fulfil high time headway adherence, holding points at the last stops of the direction of service in the two routes are required. At these stops, some slack should be inserted into the schedule. Two new entrance time variables should be optimised to guarantee perfect regularity in the opposite direction of the middle segment as we did for the one-way direction route.

Nevertheless, when the demand rates between the branched and central segment are unbalanced, route A and B present different dwell times in the central portion of the corridor. This fact causes that vehicles cannot maintain the headways in the whole roundtrip. In real implementations, it is expected that the fraction of demand rates captured in the central segment would be high, while the fraction of transfers would not be significant. The example of Barcelona's bus route H10 follows these assumptions (primary demand $D_t$=79% and transfer $T_r$=6%). The potentialities of hybrid strategies in this case instance are even better: the inclusion of a small slack $\theta_{max}$=5 sec and the deployment of green extension measure ($g$=20 s) diminish the total cost by 1% and improves the coefficient of variation of headways by 24%, in comparison to the strategy without control.

***Regarding Transfer Areas:*** Transfer areas are important nodes where users can shift from one route to another on improved networks. The operating performance assessment is crucial to understand the transfer quality and how users are served, only in terms of total transfer disutility: walking time plus waiting time. The importance of transfers has been evident in many transport networks, as well as in surface transport. Three methods have been proposed to evaluate the service quality: the customer's satisfaction survey, the consensus of experts,

and the incomplete consensus of experts, which has been developed as it can meet better real examples with different headways on each route and without route synchronisation. Setting out a quadratic approach, a mathematical expression to calculate the TQR, Transfer Quality Ratio, and the IQR, Transfer area Quality Ratio, both for scheduled and actual values, has been obtained. The second order (quadratic) functional approach was justified using Taylor's series approximation, and the parameter calibration was obtained in three complementary ways. Technical resolution is quite simple when considering the approximation based on consistent customer perceptions On the contrary, the measuring dependency on changing perceptions over time can cause periodic changes in the referents, and as a result, discontinuities regarding data monitoring. Also, when customer perceptions are not consistent, calibration of coefficients requires solving an optimisation problem, which adds dimension to the issue. The approach based on the consensus of experts is also an easy problem to solve (linear system of equations) when the conditions are consistent, and it turns to an optimisation problem when those consensus conditions are not consistent enough. On the other hand, based on the consensus achieved in situations of progressive loss of quality components, the estimation of the loss due to physical architecture, synchronisation and gap between actual and scheduled service are subjective. Finally, the approach based on the incomplete consensus of experts provides stable referents over time and allows estimating objectively the loss of quality associated with each component.

Nevertheless, technical justification is much more complex, and the resolution requires the use of appropriate software (nonlinear equation system). In this respect, libraries and functions that solve optimisation problems and systems of nonlinear equations have been referenced and an EXCEL spreadsheet was developed to obtain the solution when the approach 4.1.2.3 is taken. The measuring system defined in this thesis, oriented to the management and service improvement, allows evaluating the transfer area quality (information and monitoring) and identifying inefficiencies (improvement). Regarding the global customer satisfaction KPI's (dell'Olio et al. 2011a, de Oña et al., 2015), the TQR relates to two dimensions of service, reliability and responsiveness. Loss of quality (100-TQR(actual)) can be broken down in root causes: $100-TQR_0$ is imputable to physical architecture constraints; $TQR_0-TQR$ (scheduled) is attributable to the lack of synchrony in time planning; and TQR (scheduled)-TQR(actual) is due to discrepancies between the actual service provided and the scheduled one. On the other hand, service provided without

synchrony and with bunching effect service can be evaluated as $TQR_0$-$TQR_1$ and $TQR_1$-$TQR_2$. In these approaches, based on customer perception and in the incomplete consensus of experts, losses $100$-$TQR_0$, $TQR_0$-$TQR_1$ and $TQR_1$-$TQR_2$ are estimated objectively (based on functional satisfaction), while in the approach based on the consensus of experts, losses are estimated subjectively. A real example from Barcelona Premium Bus Network has been calculated, taking a simple transfer area with two routes intersecting at Eixample Dret, in the city centre. Assessing the scheduled and actual service, the loss in satisfaction of the three components are as follows: concerning infrastructure, by 3.31%; concerning desynchronisation between routes, by 31.42%; and concerning lack of regularity, by 24.02%. These outcomes underscore the importance of headway adherence (regularity) and the synchrony between the routes for the proposed model. Further developments may consist of applying this methodology to a more massive transfer area, with a larger amount of bus routes or even with other transport modes like metro or tramway systems. Besides, a wide-range historical data value series can be collected to monitor the quality fluctuation, provided at the transfer area.

***Regarding the Relationship Between the Topics:*** the four issues of the study are strongly interlinked, and a sequential continuity line can be established, starting with timetable manufacturing and putting them in operation. As Service Regularity is so important in the bus operation, we can measure it applying the explained methodology and also the Bus Bunching effect, using the Coefficient of variation of the headways, $C_{v,h}$. Three control strategies are proposed to secure headway adherence, which can be applicable to routes with conventional and complex layout (corridor sharing two bus routes, 2D-approach); Finally, we can assess the operating performance at the Transfer areas (again, 2D-approach) to complete this circle of bus operation improvement and provide a reliable service. Several elements recurrently appear on the topics: primary statistic: mean, standard deviation and variance; AVL data; normal distribution; time-headway; temporal sequences; scheduled and actual operation schemes; etc. All of these common denominators allow us to explain the links between the issues

## 5.2   Future research

The main lines for future research and development concerning every primary topic developed in this thesis are the following:

*Scheduled Timetables:*

We should get increased automation of the vehicle timetable definition process. The higher the automation, the better the schedule will become as we will avoid any subjectivity by the programmer (scheduler). Ideally, full automation will be the most challenging achievement we can reach. This automation should apply to any route profile, particularly to a corridor operated by two routes.

Another research line could be adjusting timetables to fully electric bus routes, considering the charging times that buses need at the opportunity charging stations and redefining recovery times, adding non-revenue times from the terminus to the opportunity charging stations and calculating how many resources should we add to the route carousel.

*Headway Adherence:*

As further research, we set a headway adherence analysis on a broader range of bus routes in several cities worldwide, with low regularity and frequent bunching, modelling or testing the goodness of the developed headway adherence strategies.

With the advancing technology, a new and innovative strategy could be developed by studying an online and permanent tracking system, in coordination with both the Municipal Traffic (traffic signals) and the Bus Control Centre (bus schedules). This way, the instability of the bus flow could be fixed continuously during the trip, and we get a perfect headway adherence.

More research concerning visual KPI's could be done to provide a direct view of the route/network operating performance.

*Corridors Served by Two Routes:*

Again, it could be of interest to apply the methodology to the operation of fully electric bus routes, fuelled by en route opportunity charging stations, with a shared central section layout.

Analysing the feasibility of extending this layout model to several instances in several urban areas to gain in efficiency and the territorial coverage could be another future research line to be developed.

*Transfer Areas:*

It could be of great interest to consider aggregating further data as traffic conditions, weather, etc. to report and explain irregularities in service provision.

Analysing the favourable effect of synchronising all bus routes intersecting each other at a transfer area could as well be of interest.

Analysing the favourable effect of applying strategies to get headway adherence to improve service regularity on every route intersecting each other at a transfer area. This means combining headway adherence strategies to increase service regularity and consequently, the quality ratios: TQR and IQT.

Increase the temporary size of the sample and study the KPI's evolution over time could help us to find out the level of stability of the operating provision at a specific transfer area. Any significant drop in quality could require some of the measures proposed and developed in this thesis.

We can contemplate as well calculate the operating quality at a vast transfer area, with more than two routes and even at multimodal transfer areas with other modes of transport, even railroad lines.

Part VI: REFERENCES

# References

## 6.1    References cited directly in the text:

Adamski, A., Turnau, A. (1998). Simulation support tool for real-time dispatching control in public transport. *Transportation Research Part A: Policy and Practice.* **32:2**, 73–87.

Amberg, B., Amberg, B., Kliewer, N. (2011). Increasing delay-tolerance of vehicle and crew schedules in public transport by sequential, partial-integrated and integrated approaches. *Proced.-Soc. Behav. Sci.*, **20**, 292-301.

Argote-Cabanero, J., Daganzo, C.F., Lynn, J.W. (2015). Dynamic control of complex transit systems. *Transportation Research Part B: Methodological.* **81:1**, 146–160.

Baaj, M.H., Mahmassani, H.S. (1990). TRUST: A LISP Program for the Analysis of Transit Route Configurations. *Transportation Research Record,* **1283**, 125–135.

Baaj, M.H., Mahmassami, H.S. (1995). Hybrid route generation heuristic algorithm for the design of transit networks. *Transportation Research Part C*, **3:1**, 31–50.

Badia, H., Estrada, M., Robusté, F. (2014). Competitive transit network design in cities with radial street patterns. *Transportation Research Part B: Methodological*, **59**, 161–181.

Badia, H., Estrada, M., Robusté, F. (2016). Bus network structure and mobility pattern: A monocentric analytical approach on a grid street layout. *Transportation Research Part B: Methodological*, **93**, 37–56.

Badia, H., Argote-Cabanero, J., Daganzo, C. F. (2017). How network structure can boost and shape the demand for bus transit, *Transportation Research Part A: Policy and Practice*, **103**, 83–94.

Barabino, B., Deiana, E., & Tilocca, P. (2012). Measuring service quality in urban bus transport: a modified Servqual approach. *International Journal of Quality and Service Sciences*, **4:3**, 238–252.

Barnett, A. (1974). On controlling randomness in transit operations. *Transportation Science,* **8:2**, 102–116.

Byrne, B.F., 1975. Public transportation line positions and headways for minimum user and system cost in a radial case. *Transportation Research,* **89:2-3**, 97–102.

Bartholdi III, J.J., Eisenstein, D.D. (2012). A self-coordinating bus route to resist bus bunching. *Transportation Research Part B: Methodological*. **46:4**, 481–491.

Bookbinder, J.H., Désilets, A. (1992). Transfer optimization in a transit network. *Transport Science*, **26:2**, 106–118.

Cascetta, E., & Carteni, A. (2014). A Quality-Based Approach to Public Transportation Planning: Theory and a Case Study. *International Journal of Sustainable Transportation*, **8:1**, 84–106.

Cascetta, E., Cartenì, A. (2014). The hedonic value of railways terminals: a quantitative analysis of the impact of stations quality on travellers' behaviour. *Transportation Research Part A Policy and Practice*, **61**, 41–52.

Ceder, A. Wilson, N.H.M. (1986). Bus Network Design. *Transportation Research Part B; Methodological,* **20: 4**, 331–344.

Ceder, A. (2001). Bus timetables with even passenger loads as opposed to even headways. *Transportation research record*, **1760**, 3–9.

Ceder, A., Golany, B., Tal, O. (2001). Creating bus timetables with maximal synchronization. *Transportation Research Part A: Policy and Practice*, **35:10**, 913–928.

Ceder, A. (2007). *Public Transit Planning and Operation: Theory Modeling and Practice.* Elsevier, Butterworth-Heinemann.

Chen, W., Yang, C., Feng, F., Chen, Z. (2012). An Improved Model for Headway-Based Bus Service Unreliability Prevention with Vehicle Load Capacity Constraint at Bus Stops. *Discrete Dynamics in Nature and Society,* **2012**, 1–13

Chen, J., Liu, Z., Zhu, S., Wang, W. (2015). The design of limited-stop bus service with capacity constraint and stochastic travel time. *Transportation Research Part E: Logistics and Transportation Review*, **83**, 1–15.

Cherry, T., Townsend, C. (2012). Assessment of potential improvements to metro-bus transfers in Bangkok, Thailand. *Transportation Research Record: Journal of the Transportation Research Board*, **2276**, 116–122.

Chowdhury, S., Ceder, A. (2013). Definition of Planned and Unplanned Transfer of Public transport Service and Users' Decision to Use Routes with Transfers. *Journal of Public Transportation*, **16:2**, 1–20.

Chowdhury, S., Ceder, A., & Sachdeva, R. (2014). The effects of planned and unplanned transfers on public transport users' perception of transfer routes. *Transportation Planning and Technology*, **37:2**, 154–168.

Chowdhury, S., Ceder, A. and Schwalger, B. (2015). The effects of travel time and cost savings on commuters' decision to travel on public transport routes involving transfers. *Journal of Transport Geography*, **43**, 151–159.

Chowdhury, S., Ceder, A. (2016). Users' willingness to ride an integrated public-transport service: A literature review. *Transport Policy*, **48**, 183–195.

Cortés, C.E., Sáez, D., Milla, F., Riquelme, M., Núñez, A. (2010). Hybrid predictive control for real-time optimization of public transport system' operations based on evolutionary multiobjective optimization. *Transportation Research Part C: Emerging Technologies,* **18:5**, 757–769.

Daganzo, C.F. (2009). A headway-based approach to eliminate bus bunching: systematic analysis and comparisons. *Transportation Research Part B: Methodological*, **43:10**, 913–921.

Daganzo, C. F. (2010). Structure of competitive transit networks. *Transportation Research Part B: Methodological*, Volume **44:4**, 434-446.

Daganzo, C.F., Pilachowski, J. (2011). Reducing bunching with bus-to-bus cooperation. *Transportation Research Part B: Methodological*. Volume **45:1**, 267–277.

De Oña, R. (2013). Analysis of service quality in public transportation using decision trees. (PhD. Thesis) Spain: Universidad Politecnica de Granada.

De Oña, J., de Oña, R., Eboli, L., Mazzulla, G. (2013). Perceived service quality in bus transit service: a structural equation approach. *Transport Policy*, **29**, 219–226.

De Oña, J., De Oña R. (2014). Quality of service in public transport based on customer satisfaction surveys: A review and assessment of methodological approaches. *Transportation Science*, **49:3,** 605–652.

De Oña, J., de Oña, R., Eboli, L., Mazzulla, G. (2016). Index numbers for monitoring transit service quality. *Transportation Research Part A: Policy and Practice*, **84:3**, 18–30.

Deb, K. and Chakroborty, P. (1998). Time scheduling of transit systems with transfer considerations using genetic algorithms. *Evolutionary Computation Journal,* **6:1**, 1–24.

Delgado, F., Muñoz, J.C., Giesen, R., Cipriano, A. (2009). Real-time control of buses in a transit corridor based on vehicle holding and boarding limits. *Transportation Research Record*, **2090**, 59–67.

Delgado, F., Muñoz, J.C., Giesen, R. (2012). How much can holding and/or limiting boarding improve transit performance? *Transportation Research Part B: Methodological*. **46:9**, 1202–1217.

dell'Olio, L., Ibeas, A., & Cecin, P. (2010). Modeling user perception of bus transit quality. *Transport Policy*, **17:6**, 388–397.

dell'Olio, L., Ibeas, A., & Cecin, P. (2011a). The quality of service desired by public transport users. *Transport Policy*, **18:1**, 217–227.

dell'Olio, L., Ibeas, A., Cecin, P., & dell'Olio, F. (2011b). Willingness to pay for improving service quality in a multimodal area. *Transportation Research Part C: Emerging Technologies*, **19:6**, 1060–1070.

Desaulniers, G., Hickman, M. (2007). Public transit. In: Barnhart, C., Laporte, G. (Eds.), Handbooks in operations research and management science. *Transportation*, **14**, 69–128.

Dessouky, M., Hall, R., Zhang, L., Singh, A. (2003). Real-time control of buses for schedule coordination at a terminal. *Transportation Research Part A: Policy and Practice*, **37:2**, 145–164.

Dziekan, K. (2008). Ease-of-use in public transportation—a user perspective on information and orientation aspects. Doctoral thesis in Traffic and Transport Planning, Infrastructure and Planning, Department of Transport and Economics, Royal Institute of Technology, Stockholm.

Eberlein, X.J., Wilson, N.H.M., Bernstein, D. (2001). The holding problem with real-time information available. *Transportation Science*. **35:1**, 1–18.

Eboli, L., Mazzulla, G. (2011). A methodology for evaluating transit service quality based on subjective and objective measures from the passenger's point of view. *Transport Policy*, **18:1**, 172-181.

Estrada, M., Roca-Riu, M., Badia, H., Robusté, F., Daganzo, C. F. (2011). Design and implementation of efficient transit networks: Procedure, case study and validity test. *Transportation Research Part A: Policy and Practice*, **45:9**, 935-950.

Estrada, M., Mension, J., Aymamí, J.M., Torres, L. (2016). Bus control strategies in corridors with signalized intersections. *Transportation Research Part C: Emerging Technologies*, **71**, 500–520.

Fonzone, A., Schmöcker, J.D., Liu, R. (2015). A model of bus bunching under reliability-based passenger arrival patterns. *Transportation Research Part C: Emerging Technologies*, **59**, 164–182.

Gong, X., Currie, G., Liu, Z. and Guo X. (2018). A disaggregate study of urban rail transit feeder transfer penalties including weather effects. *Transportation,* **45:5**, 1319–1349.

Guihaire, Valerie, Hao, Jin-Kao, (2008). Transit network design and scheduling: A global review. *Transportation Research Part A: Policy and Practice*, **42:10**, 1251–1273.

Guo, Z., Wilson, N. H. M. (2004). Assessment of the Transfer Penalty for Transit Trips Geographic Information System-based Disaggregate Modelling Approach. *Transportation Research Record, Journal of the Transportation Research Board*, **1872:1**, 10–18.

Guo, Z., Wilson, N. H. M. (2011). Assessing the Cost of Transfer Inconvenience in Public Transport Systems: A Case Study of the London Underground. *Transportation Research Part A: Policy and Practice*, **45:2**, 91–104.

Hadas, Y., Ceder, A. (2010). Optimal coordination of public-transit vehicles using operational tactics examined by simulation. *Transportation Research Part C: Emerging Technologies*, **18:6**, 879–895.

Hadas, Y., and P. Ranjitkar. (2012). Modeling Public-transport Connectivity with Spatial Quality of Transfer Measurements. *Journal of Transport Geography*, **22:C**, 137–147.

Hernández, D., Muñoz, J.C., Giesen, R., Delgado, F. (2015).  Analysis of real-time control strategies in a corridor with multiple bus services. *Transportation Research Part B, Methodological*, **78**, 83–105.

Hernandez, S., Monzon, A. (2016). Key factors for defining an efficient urban transport interchange: Users' perceptions. *Cities*, **50**, 158–167.

Hernandez, S., Monzon, A., de Oña, R. (2016). Urban transport interchanges: A methodology for evaluating perceived quality. *Transportation Research Part A: Policy and Practice*, **84:C**, 31-43.

Hill, S.A. (2003). Numerical analysis of a time – headway bus route model. *Physica A*, **328**, 261–273.

Holroyd, E.M. (1967). The optimum bus service: a theoretical model for a large uniform urban area. In L. C. Edie, R. Herman, and R. Rothery (Eds.), Vehicular Traffic Science, In Proceedings of the 3rd International Symposium on the Theory of Traffic Flow. *Elsevier*, New York.

Horowitz, A. J., & Zlosel, D. J. (1981). Transfer penalties: Another look at transit riders' reluctance to transfer. *Transportation*, **10:3**, 279-282.

Hu, J., Park, B.B., Lee, Y. (2015). Coordinated transit signal priority supporting transit progression under connected vehicle technology. *Transportation Research Part C: Emerging Technologies*, **55**, 393–408.

Huisman, D., Freling, R., Wagelmans, A.P.M., (2004). A robust solution approach to the dynamic vehicle scheduling problem. *Transportation Science*, **38:4**, 447–458.

Iseki, H. and Taylor, B. D. (2009). Not All Transfers Are Created Equal: Towards a Framework Relating Transfer Connectivity to Travel Behaviour. *Transport Reviews*, **29:6**, 777–800.

Iseki, H., Taylor, B. (2010). Style versus Service? An Analysis of User Perceptions of Transit Stops and Stations. *Journal of Public Transportation*, **13:3**, 23–48.

Knoppers, P., and Muller, T. (1995). Optimized Transfer Opportunities in Public Transport. *Transportation Science*, **29:1**, 101–105.

Kom, GA. and Kom, TM. (2000). Mathematical Handbook for Scientists and Engineers; definitions, theorems and formulas for reference and review. *Dover Publications, INC*, New York.

Kramkowski, S., Kliewer, N., Meier, C., (2009). Heuristic methods for increasing delay-tolerance of vehicle schedules in public bus transport. *In: Proceedings of the Metaheuristic International Conference VIII*. Hamburg, Germany.

Levinson, H., Zimmerman, S., Clinger, J., Rutherford, S., Smith, R.L., Cracknell, J., & Soberman, R. (2003). Bus Rapid Transit, Volume 1: Case Studies in Bus Rapid Transit. Transit Cooperative Research Program (TCRP) Report 90, *Transportation Research Board of the National Academies*.

Levinson, H.S., Zimmerman, S., Clinger, J., Gast, J., Rutherford; S. and Bruhn, E (2003). Bus Rapid Transit. Volume 2: Implementation Guidelines. Transit Cooperative Research Program (TCRP) Report 90, *Transportation Research Board of the National Academies*.

Liu, T., Ceder, A. (2017). Integrated Public Transport Timetable Synchronization and Vehicle Scheduling with Demand Assignment: A Bi-objective Bi-level Model Using Deficit Function Approach. *Transportation Research Procedia*, **23**, 341–361.

Liu, T., Ceder, A., Chowdhury, S. (2017). Integrated public transport timetable synchronization with vehicle scheduling. Transportmetrica A: *Transportation Science*, **13:10**, 932–954.

Liu, Z., Yan, Y., Qu, X., Zhang, Y. (2013). Bus stop-skipping scheme with random travel time. *Transportation Research Part C: Emerging Technologies*, **35**, 46–56.

Mishra, S., Welch, T.F., Jha, M. K. (2012). Performance indicators for public transit connectivity in multi-modal transportation networks, *Transportation Research Part A: Policy and Practice*, **46:7**, 1066–1085.

Muñoz, J.C., Cortés, C.E., Giesen, R., Sáez, D., Delgado, F., Valencia, F., Cipriano, A. (2013). Comparison of dynamic control strategies for transit operations. *Transportation Research Part C: Emerging Technologies*, **28**, 101–113.

Nathanail, E. (2008). Measuring the quality of service for passengers on the Hellenic railways. *Transportation Research Part A: Policy and Practice*, **42**, 48–66.

Naumann, M., Suhl, L., Kramkowski, S., (2011). A stochastic programming approach for robust vehicle scheduling in public bus transport. *Proced. – Social Behav. Sci.*, **20**, 826–835.

Navarrete, F. J., & de Dios Ortúzar, J. (2013). Subjective valuation of the transit transfer experience: The case of Santiago de Chile. *Transport Policy*, **25**, 138–147.

Nielsen, G., Nelson, J.D., Mulley, C., Tegner, G., Lind, G., Lange, T., (2005). Public transport: planning the networks. *HiTrans, Stavanger*, Norway.

Nielsen, G., Lange, T., As, C.C., Mulley, O.C., Nelson, J.D., (2006). Network planning and design for public transport success–and some pitfalls. *In European Transport Conference*. Strasbourg, France.

Newell, G.F., Potts, R.B. (1964). Maintaining a bus schedule. Proceedings of the 2nd *Australian Road Research Board*, **2**, 388–393.

Newell, G.F. (1979). Some issues relating to the optimal design of bus routes. *Transportation Science*, **13:1**, 20–35.

Nourbakhsh, S. M. and Ouyang, Y. (2012). A structured flexible transit system for low demand areas. *Transportation Research Part B: Methodological*, **46:1**, 204–216.

Ortúzar, J.D., Willumsen, L.G. (2011). Modelling Transport, 4th Ed. *John Wiley & Sons*, Chichester (United Kingdom).

Osuna, E.E., Newell, G.F. (1972). Control strategies for an idealized public transportation system. *Transportation Science*, **6**, 52–72.

Paiva Fonseca, J., Van der Hurk, E., Roberti, R., Larsen, A. (2018). A metaheuristic for transfer synchronization through integrated timetabling and vehicle scheduling. *Transportation Research Part B: Methodological*. **109**, 128–149.

Parasuraman, A., Zeithaml, V. A., Berry, L. L. (1988). Servqual. *Journal of Retailing*, **64:1**, 12–40.

Parasuraman, A., Berry, L. L., Zeithaml, V. A. (1991). Refinement and reassessment of the Servqual scale. *Journal of Retailing*, **67:4**, 420–450.

Rossetti, M.D., Turitto, T. (1998). Comparing static and dynamic threshold-based control strategies. Transportation Research Part A: Policy and Practice, **32:8,** 607–620.

Sáez, D., Cortés, C., Riquelme, M., Núñez, A., Milla, F., Tirachini, A. (2012). Hybrid predictive control strategy for a public transport system with uncertain demand. *Transportmetrica*, **8:1**, 61–86.

Salicrú, M., Fleurent, C., and Armengol, J. M. (2011). Timetable-based operation in urban transport: Run-time optimization and improvements in the operating process. *Transportation Research Part A: Policy and Practice*, **45:8**, 721–740.

Schakenbos, R., La Paix, L., Nijenstein, S., & Geurs, K. T. (2016). Valuation of a transfer in a multimodal public transport trip. *Transport Policy*, **46**, 72–81.

Schmöcker, J.D., Sun, W., Fonzone, A., Liu, R. (2016). Bus Bunching Along a Corridor Served by Two Lines. *Transportation Research Part B: Methodological*, **93:A**, 300–317.

Shen, Y., Xu, J., Li, J. (2016). A probabilistic model for vehicle scheduling based on stochastic trip times. *Transportation Research Part B: Methodological*, **85**, 19-31.

Sharaby, N., and Shiftan, Y. (2012). The impact of fare integration on travel behavior and transit ridership. *Transport Policy*, **21**, 63–70.

Spain, B. (2007). Analytical Conics. *Dover Publications Inc*. Mineola, New York. ISBN 10: 0486457737 / ISBN 13: 9780486457734.

Thompson, G.L. (1977). Planning considerations for alternative transit route structures. *Journal of the American Institute of Planners*, **43:2**, 158-168.

Transportation Research Board. (1999). A Handbook customer satisfaction and service quality. TCRP Report 47. *National Academy Press*, Washington, DC.

TRB (Ed.). (2013). Transit Capacity and Quality of Service Manual, third edition. Transit Cooperative Research Program, *Transportation Research Board of the National Academies*, Washington, DC.

Trompet, M., Liu, X. & Graham D. J. (2012). Development of a Key Performance Indicator to compare regularity of service between urban bus operator. *Transportation Research Record*, **2216**, 22-41.

Turnquist M.A. and Blume S.W. (1980). Evaluating potential effectiveness of headway control strategies for transit systems. *Transportation Research Record*, **746**, 25-29.

Turnquist, M.A. (1981). Strategies for improving reliability of bus transit service. *Transportation Research Record*, **818**, 25–29.

Wu, W.. Liu, R.. Jin, W. (2016). Designing robust schedule coordination scheme for transit networks with safety control margins. *Transportation Research Part B: Methodological*, **93**, 495–519.

Xuan, Y., Argote, J., Daganzo, C.F. (2011). Dynamic bus holding strategies for schedule reliability: optimal linear control and performance analysis. *Transportation Research Part B: Methodological*, **45:10**, 1831–1845.

Yoo, G.S. (2015). Transfer Penalty Estimation with Transit Trips from Smartcard Data in Seoul, Korea. *Journal of Civil Engineering*, **19:4**, 1108-1116.

Yu, B., Yang, Z. (2007). A dynamic holding strategy in public transit systems with real-time information. *Applied Intelligence*, **31:1**, 69–80.

Zhao, F. (2006). Large-scale transit network optimization by minimizing user cost and transfers. *Journal of Public Transportation*, **9:2**, 107-129.

## 6.2    Additional references:

AASHTO. (2014). Guide for Geometric Design of Transit Facilities on Highways and Streets. ISBN: 978-1-56051-522-7.

Aldaihania, M.M., Quadrifogliob, L., Dessoukyb, M.M., Hallb, R. (2004). Network design for a grid hybrid transit service. *Transportation Research Part A: Policy and Practice*, **38:7**, 511–530.

Anas, A., Arnott, R., Small, K.  (1998). Urban spatial structure. *Journal of Economic Literature,* **36:3**, 1426–1464.

Ceder, A., Butcher, M., and Wang, L. (2015). Optimization of bus stop placement for routes on uneven topography. *Transportation Research Part B: Methodological*, **74**, 40–61.

Cervero, R., (1998). The Transit Metropolis: A Global Inquiry. *Island Press*, Washington.

Chakroborty, P., Deb, K., Subrahmanyam. P.S. (1995). Optimal scheduling of urban transit systems using genetic algorithms. *Journal of Transportation Engineering*, **121:6**, 544–553.

Chakroborty, P., Deb, K. and Srinivas, B. (1998). Network-Wide Optimal Scheduling of Transit Systems Using Genetic Algorithms. *Computer-Aided Civil and Infrastructure Engineering*, **13**, 363–376.

Chen, X., Yu, L., Zhang, Y., Guo, J. (2009). Analyzing urban bus service reliability at the stop, route, and network levels, *Transportation Research Part A: Policy and Practice*, **43:8**, 722–734.

Clauss, T., Döppe, S. (2016). Why do urban travellers select multimodal travel options: A repertory grid analysis? *Transportation Research Part A: Policy and Practice*, **93:8**, 93–116.

COST, European Cooperation in Science and Technology. (2011). COST action TU603. Buses with High Level of Service. Fundamental Characteristics and Recommendations for Decision-making and Research. Results from 35 European Cities. *COST.*

Currie, G. (2005). The demand performance of bus rapid transit. *Journal of Public Transportation*, **8:1**, 41–55.

Eboli L, Mazzulla G. (2007). Service quality attributes affecting customer satisfaction for bus transit. *Journal of Public Transportation*, **10:3**, 21-34.

Eboli, L., Mazzulla, G. (2010).  How to Capture the Passengers' Point of View on a Transit Service through Rating and Choice Options. *Transport Reviews*, **30:4**, 435-450.

European Committee for Standardization. (2002). Transportation – Logistics and services – public passenger transport – service quality definition, targeting and measurement.

Fujii, S., Kitamura, R. (2003). What does a one-month free bus ticket do to habitual drivers? *Transportation*, **30:1**, 81–95.

Garver, M.S. (2003). Best practices in identifying customer-driven improvement opportunities. *Industrial Marketing Management*, **32:6**, 455–466.

Gschwender, A., Jara-Díaz, S., Bravo, C. (2016). Feeder-trunk or direct lines? Economies of density, transfer costs and transit structure in an urban context. *Transportation Research Part A: Policy and Practice*, **88:8**, 209–222.

Hall, R. (1985). Vehicle scheduling at a transportation terminal with random delay en route. *Transportation Science*, **19:3**, 308-320.

Hine, J., Scott, J. (2000). Seamless, accessible travel: users' views of the public transport journey and interchange. *Transport Policy*, **7:3**, 217-226.

Huse C, Evangelho F. (2007). Investigating business traveller heterogeneity: Low-cost vs full-service airline users? *Transportation Research Part E: Logistics and Transportation Review*, **43**, 259–268.

Ibarra-Rojas, O.J. Rios-Solis, Y.A. (2012). Synchronization of bus timetabling. *Transportation Research Part B: Methodological*, **46:5**, 599-614.

Ibarra-Rojas, O.J. Delgado, F., Giesen, R., Munoz, J.C. (2015). Planning, operation, and control of bus transport systems: a literature review. *Transportation Research Part B: Methodological*, **77**, 38–75.

Ibeas, A., dell'Olio, L., Alonso, B., Sainz, O. (2010). Optimizing Bus Stop Spacing in Urban Areas. *Transportation Research Part E: Logistics and Transportation Review*, **46:3**, 446-458.

Institute for Transportation and Development Policy. (2007) Bus Rapid Transit Guide 3rd Edition. *Institute for Transportation and Development Policy*. New York City.

Karlaftis M. G., Golias J, Papadimitriou E. (2001). Transit quality as an integrated traffic management strategy: Measuring perceived service. *Journal of Public Transportation*, **4:1**, 27–44.

Kim Y.K., Lee H.R. (2011). Customer satisfaction using low cost carriers. *Tourism Management*, **32:2**, 235–243.

Lee, A., Van Oort, N., Van Nes, R. (2014). Service reliability in a network context: Impacts of synchronizing schedules in long headway services. *Transportation Research Record: Journal of the Transportation Research Board*, **2417**, 18–26.

Levinson, H. S., Zimmerman, S., Clinger, J., Rutherford, S., Cracknell, J., and Soberman, R., (2002). Case Studies in Bus Rapid Transit-Draft Report (TCRP Project A-23). *Transportation Research Board of the National Academies*.

Mattsson, L-G., Jenelius, E. (2015). Vulnerability and resilience of transport systems - A discussion of recent research. *Transportation Research Part A: Policy and Practice*, Volume **81:3**, 16–34.

Minser J, Webb V. (2010). Quantifying the benefits: Application of customer loyalty modelling in public transportation context. *Transportation Research Record*, **2144**, 111–120.

Pternea, M., Kepaptsoglou, K., Karlaftis, M. G. (2015). Sustainable urban transit network design, *Transportation Research Part A: Policy and Practice*, **77**, 276–291.

Roca-Riu, M., Estrada, M., Trapote, C. (2012). The design of interurban bus networks in city centers, *Transportation Research Part A: Policy and Practice*, **46:8**, 1153–1165.

Rodrigue, J.P., Comtois, C., Slack, B., (2006). *The geography of transport systems.* Routledge, London.

Shafahi, Y., Khani, A. (2010). A practical model for transfer optimization in a transit network: model formulations and solutions. *Transportation Research Part A: Policy and Practice*, **44:6**, 377–389.

Sorussa, Jirapa. (2014). Optimizing the Synchronization of Multiple Bus Routes at Multiple Transfer Points Assuming Stochastic Bus Journey Times. *Theses and Dissertations*, Paper 765.

Theo A. Arentze, T. A., Molin, E.J.E. (2013). Travelers' preferences in multimodal networks: Design and results of a comprehensive series of choice experiments, *Transportation Research Part A: Policy and Practice*, **58**, 15–28.

TMB (2018). 2018 Basic data. Barcelona: Transports Metropolitans de Barcelona.

TMB. (2018). Operational data repository of bus service. ICT platform. Transports Metropolitans de Barcelona. Access only available for TMB operational board members, July 2018.

Tyrinopoulos Y, Antoniou C. (2008). Public transit user satisfaction: Variability and policy implications. *Transport Policy*, **15:4**, 260–272.

Van der Hoeven, F., Van Egmond, P., Van der Spek, S, Van Nes, A., Cré, I., Berends, H. & Hoogendoorn, C. (2014). New tools for design and operation of urban transport interchange

facilities, zones and development areas. *Proceedings of the 5th European Transport Research Conference in Paris, Innovative Mobility*, Part IX – Public Transport and soft modes. STS 35 – Integrated public transport services #18138.

Wang, Z., Chen, Y., Wang, H., Kang, H, Yu, Y. (2010). Optimization Methodology of Project Construction Scheduling for Intermodal Terminal Planning Problems. *Transportation Research Record*, **2144**, 189-196.

Weinstein A. (2000). Customer satisfaction among transit riders. How customer rank the relative importance of various service attributes. *Transportation Research Record*, **1735**, 123–132.

# APPENDIXES

# Appendix A

# The Bus with High-Level Service

## A.1   BHLS

### A.1.1   Background

The improved bus routes history begins with the concept of "busway", i.e., dedicated lanes only for public transport, which was first applied in Chicago in 1939. For regional transport, a lane of the "Henry Garnett Shirley Memorial" highway, between Washington DC. and Woodbridge (Virginia) was set aside for buses in 1971.

In the '70s, in Latin America arose the concept of BRT, Bus Rapid Transit, inspired by the extensive bus system deployed in Curitiba (Brazil), and also called "above ground metro", as it has ad hoc stations with special platforms and payment and validation outside. Later, in the '80s and '90s, other BRT systems appeared in Ottawa (Canada), Adelaide (Australia), Quito (Ecuador), etc. In the first decade of the 21st century, the Brisbane Busway system and the "Transmilenio" in Bogotá (Colombia) were implemented; the latter, a real high capacity system with the inclusion of passing lanes at the stations. Also, in this same decade, many other BRT services were developed in America, Asia, and in Central and South America as well.

According to the Bus Rapid Transit Planning Guide, Bus Rapid Transit, BRT, is "a high-quality bus-based transit system that delivers fast, comfortable, and cost-effective urban mobility through the provision of segregated right-of-way infrastructure, rapid and frequent operations, and excellence in marketing and customer service".

In Europe, there are many experiences of improved bus lines. Thus, several trunk bus networks were created in Sweden; in England and Ireland, several services in Quality Bus Corridors were developed; in France, under the name of High-level service buses (Bus à Haut Level-Service-BHNS, BHLS in English); in Germany, under the Metrobus concept; in the

Netherlands, Hoogwaardig Openbaar Vervoer - HOV; along with many other proposals aimed to enhance bus network schemes through a quality system-based approach.

The European COST action TU 603 BHLS took place from 2007 until 2011. According to its final report, BHLS is "a new wave of quality bus systems emerged in Europe, with many familiar elements: priority for buses in traffic, higher quality vehicles, improved comfort at stops, improved information to passengers, integrated ticketing, intelligent transport systems to improve operations, management and planning, etc. However, BHLS differs from the conventional approach in three main respects: the elements are combined holistically, to achieve a total product improvement rather than improve specific aspects. The BHLS is usually packaged as a concept, given a distinct identity, and marketed confidently to the target market. Finally, the BHLS usually serves urban and transport policy or strategic objectives and are not just technical or operational improvements".

Some specific European examples are Amsterdam, Eindhoven, Twente (Holanda); Dublin (Ireland); Essen, Hamburg, Öberhausen (Germany); Lorient, Metz, Nantes, Paris, Rouen, (Francia); Jonköping, Lund, Stockholm (Sweden); London, Cambridge, Leeds (United Kingdom). Particular interest has also the Barcelona's New Bus Network of Barcelona, which is detailed in the following section.

### A.1.2   Barcelona's New Bus Network

Since 2001, TMB, along with the Barcelona City Council, "BCN Ecologia", the Urban Ecology Agency, and the Centre for Innovation in Transport, Cenit, assigned to the UPC Barcelona Tech, have been carrying out research studies into four main areas: to better understand the functionality of the bus operation, to identify improvement opportunities, to implement several measures to make its bus network more efficient, and to find out about network layout models, different from the existent ones at that time.

During the biennium 2004-2006, TMB, together with "BCN Ecologia", was working on new layout design for Barcelona's Bus network: the orthogonal bus routes, a shape demand-based bus network system that would equally cover all parts of the municipality, ensuring regional uniformity all around. Its proposal of an instant implementation was its main drawback, and the project was put on hold for several years, and the Agency and the City Council, together

with the Centre for Innovation in Transport, carried on analysing the main factors that drive the commercial speed of the network instead, and this way, they gather and implement in 2006 a set of feasible improvement measures in various corridors of the city.

In 2009, a global study of the public transport network in Barcelona was started to develop a more efficient operating service while at the same time contributing to long-term improvements for the city's mobility. The collective goals were to help reduce circulatory congestion caused by the private automobile; to lead environmental improvements in the city; to increase social cohesion between the different boroughs; to create new customs and usages on public transport. Importantly, these objectives must have been fulfilled without increasing resources (i.e. adding new buses to the current operation).

The outcome of the project was a set of 11-premium routes (6 sea-mountain direction and 5 parallel to the coastline), named "RetBus", which followed a hub (grid) and spoke layout configuration, with an average distance between sea-mountain corridors of 1.300 m and stops each 650 m (430 m in the city centre). The route headway in the central grid area was 3 min and 6 min in the antennas. The commercial speed threshold that ensures the success of the model was 15 km/h.

In 2011-2012, the Agency in close collaboration with the City Council worked on the integration of the 2 models: the orthogonal bus network and the "RetBus", as they are in fact quite similar, and a hybrid model was defined, built with their common parts and, under diverse rational hypothesis, with the alignment of all those which were different, to finally get the most beneficial features for the citizens and users.

### A.1.2.1  The orthogonal network model (2004-2006)

This proposal is based on the orthogonal street layout of the central and most populated district in Barcelona: "l'Eixample" and consists of a network of 9 horizontal and 17 vertical routes, equally spaced out, in a grid structure, spreading out all around the municipality. Fig. 41 maps out the orthogonal route model and give us an idea of what it looked.

Main features of this model include the fact that it is isotropic (in other words, the same features all around). Is a shape-demand model, it defines one corridor next to the other without taking into account the demand, which is expected to be reorganised and to be

readapted to the new routes. Concerning the headway: 4-minute headway (15 buses per hour) on every corridor. The average distance between stops is 400 m. As bus priority measures, it proposes many additional bus lane sections, on every corridor. And finally, an instant implementation, from one day to the next, was set out.

This model would also define the new urban planning for the city as the groups of blocks between the orthogonal routes become the so-called superblocks, independent superstructures with different usages from the current ones and with calming traffic measures.

Main drawbacks of the model would be the following: isotropic model cannot run properly in a non-isotropic territory such as the city of Barcelona is. The 4-minute headway on every corridor can result, on one side, in lack of resources in the city centre; and, on the other, in oversupply in the outskirts. Operating buses at 4-minute headway is hugely complex, requires a lot of important tailored measures of priority for buses, and unavoidably the bunching effect arises far too often. Its immediate implementation is a big handicap because, apart from the difficulties to keep users correctly well informed, neither the City Council nor TMB can cope with such a large number of public works and operating internal procedures respectively that have to be completed simultaneously on time by a specific date.



**Figure 41.** Map of the orthogonal bus route layout. Source "BCN Ecologia"

### A.1.2.2 The "RetBus" model (2009)

TMB along with the Barcelona City Council and the CENIT defined in 2009 this model that was aimed at offering faster and more attractive bus services for long distance journeys, overcoming the mounting obstacles of conventional routes (overcrowding, both low commercial speed and regularity, unsuitable headways, etc.). It wishes to be a new way to design a public transport system with rational and sustainable management of resources.

The final bus network would increase its hierarchy and would be as the City had three networks in one: the high-performance network (the "RetBus"), the conventional network and the local routes.

For the "RetBus" graphic design, a simple methodology that allows different network topologies to be evaluated comprehensively was used. It is supposed that the target was serving a rectangular region and that its demand was uniformly distributed across the territory. From the opposite concepts of a grid and hub and spoke network, a hybrid model was defined, which can fit the vast majority of network topologies in existence.

Main features of this model include the fact that is a group of 11 high-level of service routes that follow a hybrid hub (grid) and spokes serve-demand model, with six in sea-mountain direction and five parallel to the coast-line routes. Five of them have complex layouts with antennas at the ends. Different headways are set: 3-minute headway in the grid zone and 6-minute headway in the antennas, with an average distance between sea-mountain corridors of 1.300 m and stops each 650 m (430 m, in the city centre). Diverse priority measures on each corridor: signal priority, new bus lane stretches, etc. The maximum capacity of this network was 60,000 pax/h. And gradual implementation was foreseen for its deployment.

Main drawbacks of the model would be the following: its high commercial speed threshold of 15 km/h to succeed was supposed to be too challenging for the city of Barcelona, and a large number of priority measures should have been deployed to reach the high threshold speed. Furthermore, the bus operation with antennas can cause operational troubles if they are not symmetric in demand and if departure times from the branches are not the right ones. Also, to ensure good regularity on the common corridors, several holding points should be set, and the

commercial speed of buses would drop; that is, we should sacrifice speed to run buses more regularly (See sections 3.3, 3.4, 4.3, and 4.4). Finally, the coexistence of premium routes running along with the normal services through the same axes can generate jamming among buses and could affect negatively to the operation.
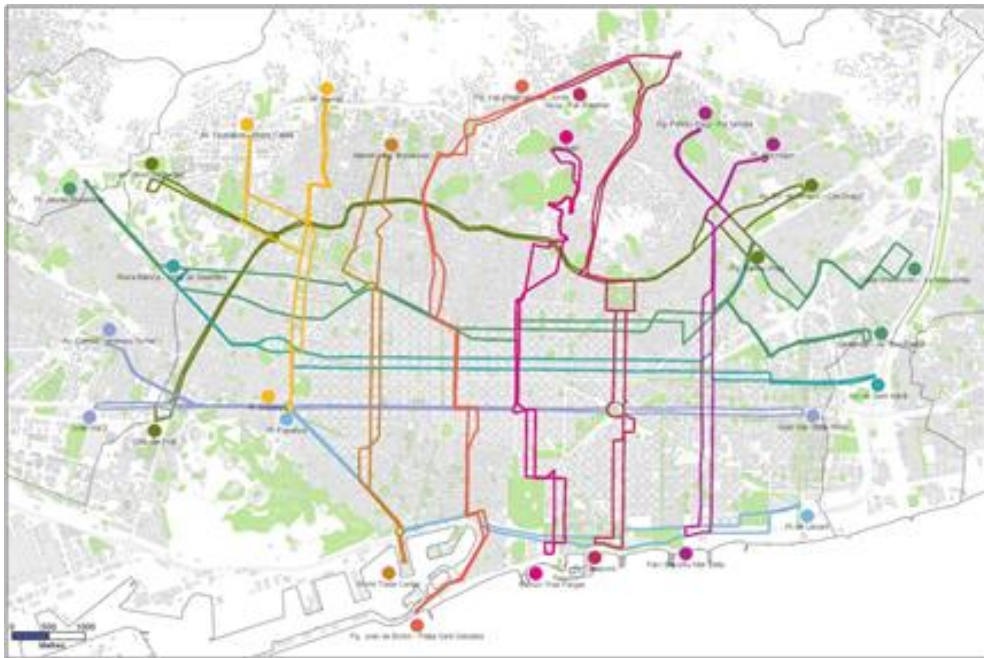


**Figure 42.** Map of the "RetBus" with its 11 original high-performance bus routes. Source: Cenit.

The schematically definition of the high-performance services is shown in Fig. 43:
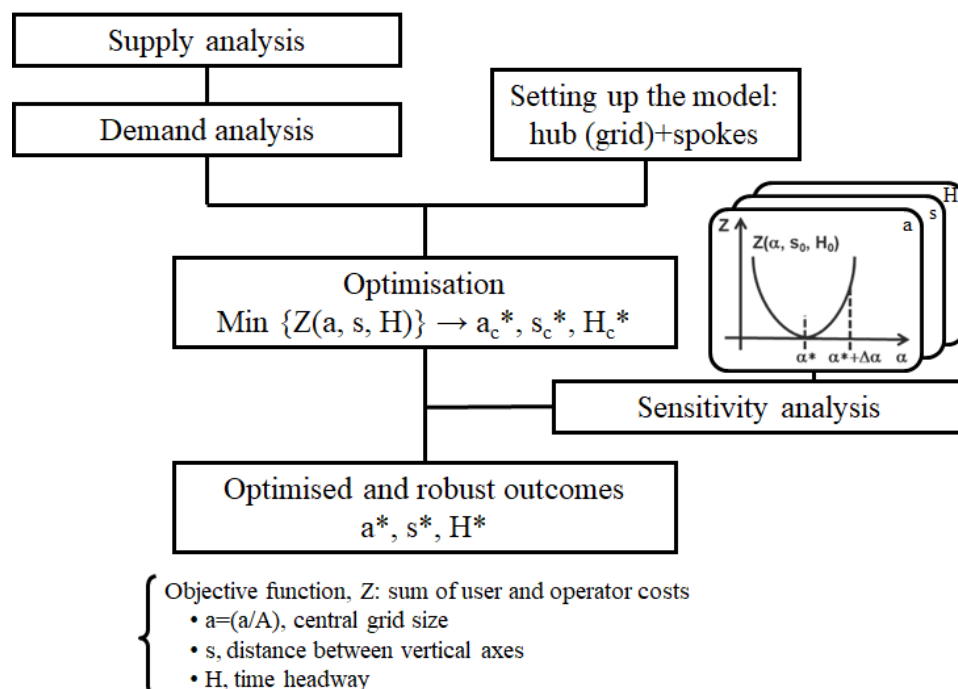
**Figure 43.** The workflow of the RetBus study.

The analysis of supply focused mainly on the railway modes, although it also contains data on the bus network. First, the outline of the current railway system and the new extensions planned in the short term were introduced. Afterwards the accessibility to the network considering the number of stops available in each zone and the bus stops influence zones was analysed.

To assess the connection among the different parts of the city by railway, some indicators to measure the speed in connecting two points according to the distance between them were defined. At a global network level, it was compared the ratio of vehicle-km and population of Barcelona with the same ratios from different cities with similar characteristics. Finally, the commercial speed of railway modes was analysed.

When considering the bus system, it was measured and mapped out the bus lane network and was analysed its capacity. The commercial speed was also analysed and characterised in thirty corridors.
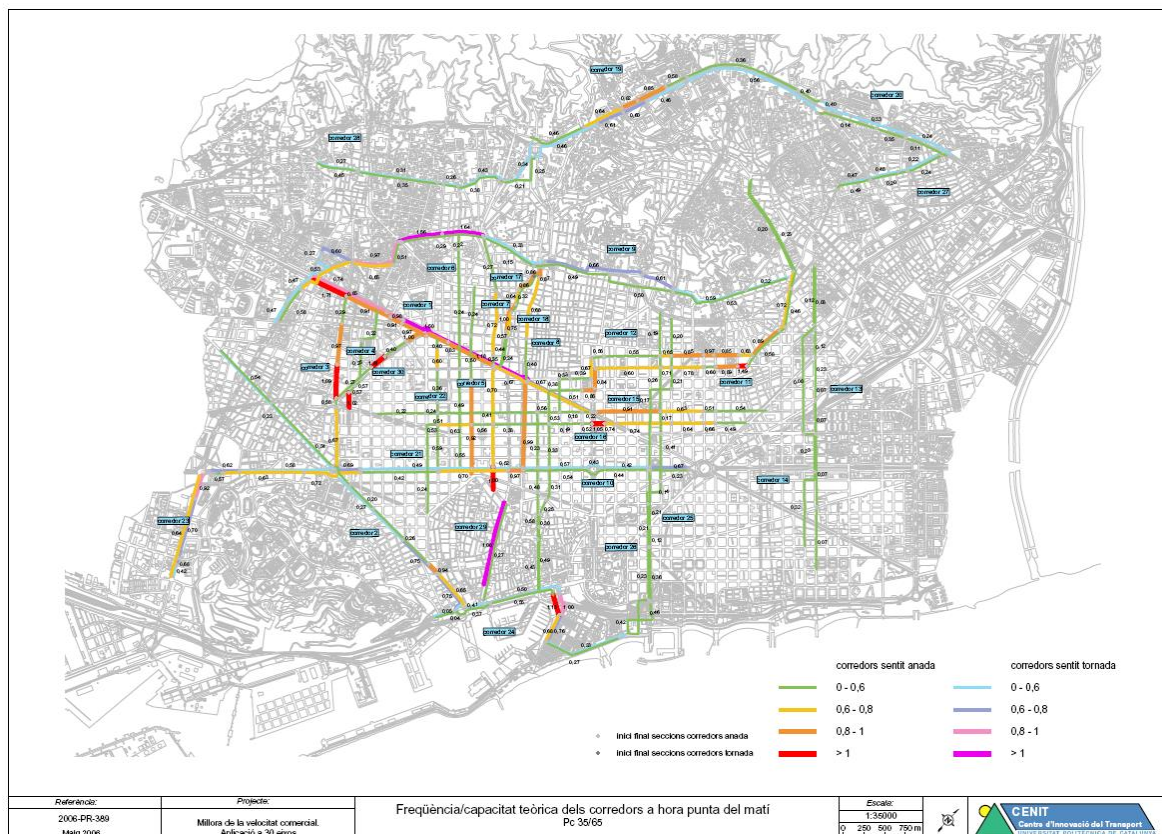


**Figure 44.** The capacity of existing bus lanes in 2009. Source: CENIT.

The analysis of demand was based on four types of graphs:

— Hotspots: To analyse the mobility experienced by different areas, it was marked each one with an activity value. This was calculated by adding -for each area- generated and attracted trips throughout the day among other transport zones. With a single value it could depict on a map which areas required more service.
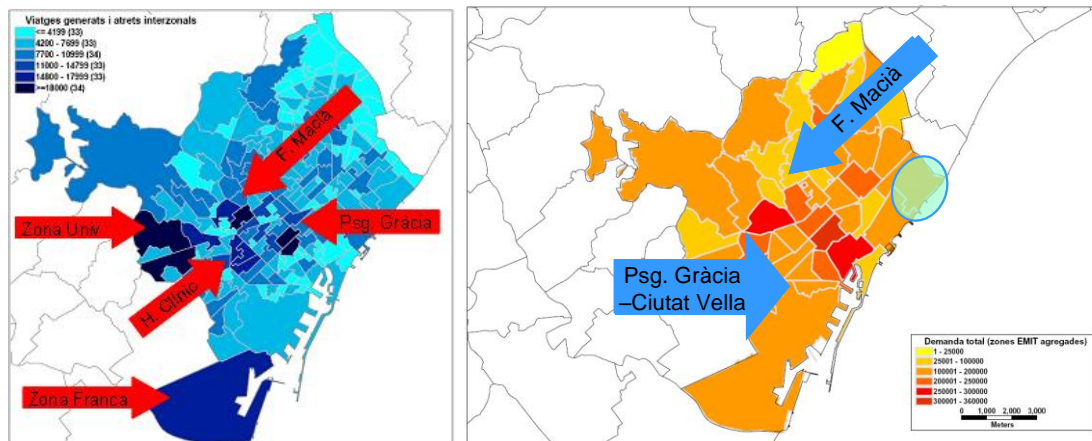


**Figure 45.** Hotspots, according to EMQ and EMIT. Source: CENIT, ATM and TMB

— Mobility destination: it was not only important to identify those areas that concentrate greater activity but at the same time to know where mobility is heading. For this reason, it was analysed the main direction of those areas with more trips, and the directions weighted by the demand of each zone.



$$direcció_i = \left( \frac{\sum_{j \neq i} D_{ij} *(x_j - x_i)}{DT_i}, \frac{\sum_{j \neq i} D_{ij} *(y_j - y_i)}{DT_i} \right)$$

$(x_i, y_i)$ posició del centroide zona $i$
$D_{ij}$ total de viatges (EMIT)
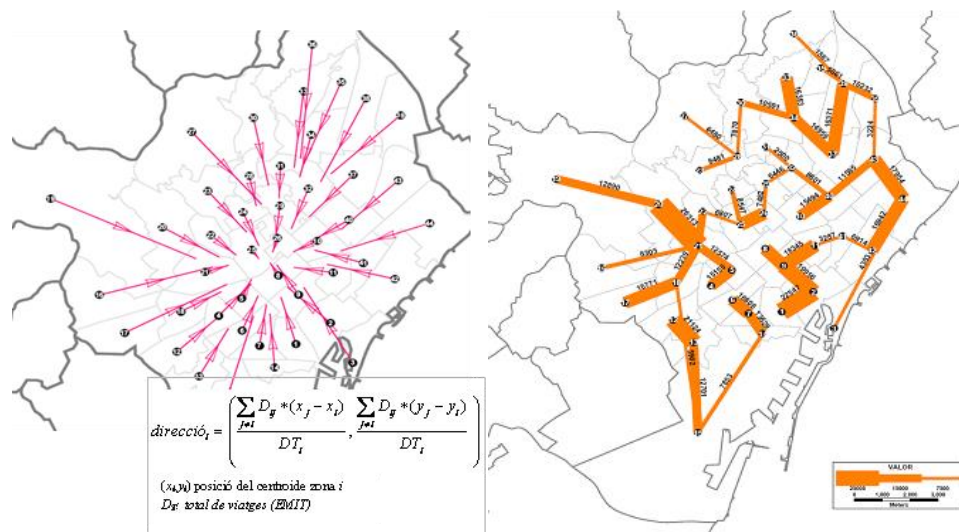
**Figure 46.** Mobility direction; left: weighted mobility, right: pairs of maximum mobility. Source: CENIT with data from ATM and TMB.

— Homogeneity of demand: the large discrepancies between different zones (residential, commercial, industrial, office, tourism, etc.) produced an unequal distributed demand between the pairs of zones. To detect the pairs with more traffic flows (illustrated below in dark blue), it was mapped relationships of areas with a higher number of passenger flow between them (it was an actual demand of 24.6%). At the same time, the graph on the left shows the evolution of the cumulative demand between two zones ordered by a number of trips. The difference with a homogeneous distribution of demand is clearly evident.
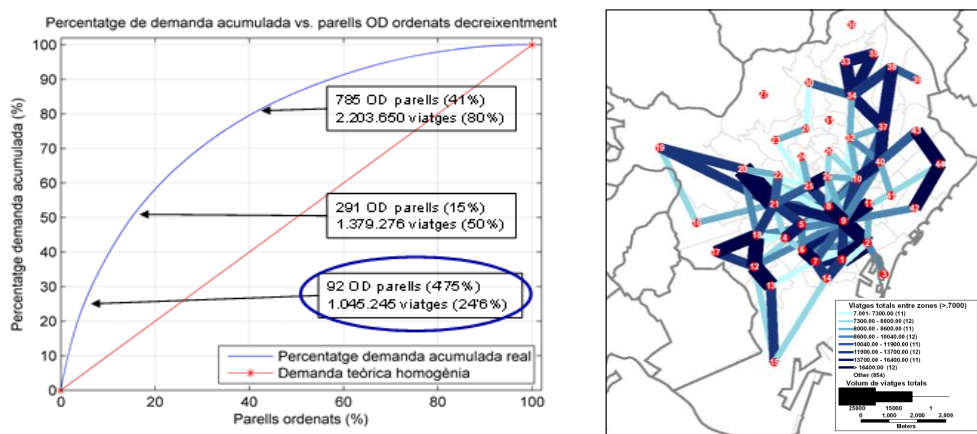


**Figure 47.** Homogeneity of demand. Left: percentage of cumulative demand for origin-destination pairs, decreasingly ordered; right: higher weighted relationships in terms of passengers.

— Occupancy ratio of bus routes: it could extract information about the demand for mobility, using also the occupancy of the existing routes. The more occupied routes in 2009 are listed and plotted graphically in Fig. 48.



| línia | inici - final | agregat (V/D) | % | % acumulat |
|---|---|---|---|---|
| 74 | Z.Univ – Fabra i Puig | 25245 | 3,551 | 3,551 |
| 7 | Diagonal mar – Z. Univ | 22539 | 3,170 | 6,721 |
| 33 | Z. Univ – Verneda | 21776 | 3,063 | 9,784 |
| 15 | H. St. Pau – Collblanc | 20671 | 2,907 | 12,691 |
| 32 | Est. Sant –Roquetes | 19967 | 2,808 | 15,499 |
| 34 | Sarrià – Virrei Amat | 19195 | 2,700 | 18,199 |
| 27 | Pl. Espanya – Roquetes | 18784 | 2,642 | 20,841 |
| 19 | Port Vell – Snt Genís | 17770 | 2,499 | 23,340 |
| 22 | Pl. Catalunya – Av Esplugues | 17121 | 2,408 | 25,748 |
| 73 | Maquinista – Pl. Kenney | 17001 | 2,391 | 28,140 |
| 17 | Barcelona – Vall d'Hebron | 16697 | 2,348 | 30,488 |
| 56 | Collblanc – Besós - Verneda | 16657 | 2,343 | 32,831 |
| 64 | Barceloneta – Pedralbes | 16045 | 2,257 | 35,087 |
| 43 | Les Corts – Sant Adrià | 15870 | 2,232 | 37,320 |
| 24 | Paral·lel – Carmel | 15461 | 2,175 | 39,494 |
| 41 | Pl. Francesc Macià – Diagonal Mar | 14995 | 2,109 | 41,603 |
| 47 | Pl. Catalunya – Canyelles | 14821 | 2,085 | 43,688 |
| 10 | Pg. Marítim – Montbau | 14696 | 2,067 | 45,755 |
| 72 | Pol. Pedrosa – Bonanova | 14416 | 2,028 | 47,783 |
| 59 | Pg. Marítim – R. M. Cristina | 13956 | 1,963 | 49,746 |
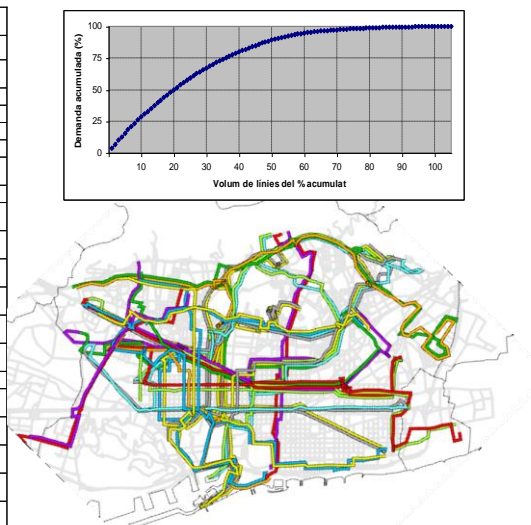
**Figure 48.** Occupancy of TMB bus routes (2009). Source: TMB

211

To analyse the costs and benefits of different networks in a compact way it was used a simple methodology which allowed different network topologies to have been evaluated comprehensively. It was used as a simplification of the real characteristics of the city, and it was possible to control the operation of various networks with only a short number of indicators.

It was supposed that we wanted to serve a rectangular region and that its demand was uniformly distributed across the territory. About network design, it was started from the opposite concepts of grid network and hub and spoke network. It was combined these concepts so that they could then represent the great majority of network topologies in existence.

The direct implementation of such networks could be very complicated by different factors: the structure and direction of streets, the undulations of the land, the differences between the theoretical rectangles, the lack or excess of demand at certain points, etc. However, this methodology allowed defining a basic structure of the optimal network for a certain city that afterwards must have been adapted to its reality, suffering as few changes as possible and not having been moved away excessively from the costs and benefits of the theoretical network.



Grid          Hub and spokes
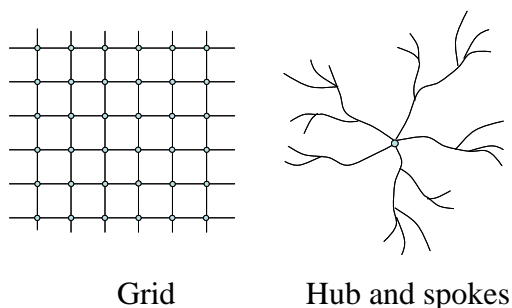
**Figure 49.** Two different network configurations.

Based on the above, Dr Carlos Daganzo, director at that time of UC-Berkeley Center for Future Urban Transport (CoEFUT), had defined a high-performance network for Barcelona having proposed a hybrid model. This hybrid consisted of a central rectangular lattice, antennas in the outskirts, and several possible configurations in the central area.

A grid network can be uniquely defined by two variables: s, the spacing of stops, and H, the headway. What characterises the performance of a network is, on the one hand, the operating

cost, which depends on the network length, and the other hand, the level of service in terms of travelling time provided to the users.

The relationship $\alpha = \dfrac{a}{A} = \dfrac{b}{B}$ indicates the size of the grid area regarding the entire scope of activity.
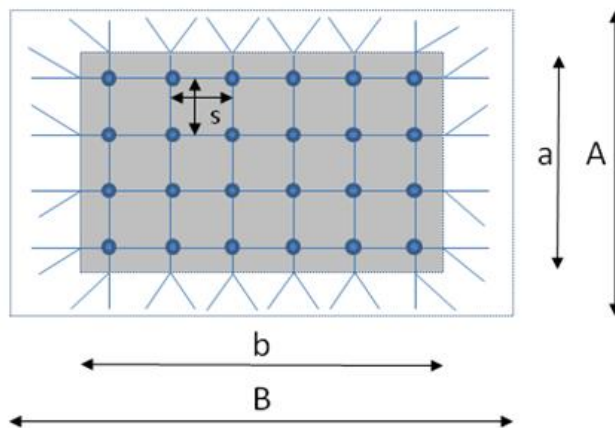
**Figure 50.** The basic configuration of the hybrid network and variables.

Modifications on the hybrid network model:
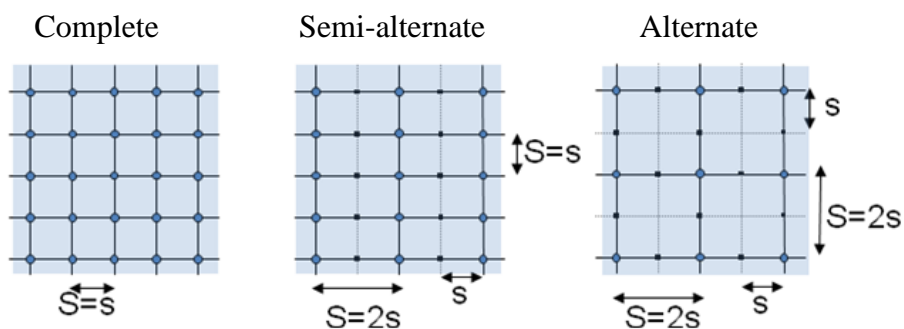
**Figure 51.** Hybrid model and possible configurations of the central zone. Source: CENIT

The problem to be solved consisted of minimizing the social cost function, Z = Z (Cost of the agency ($\alpha$, s, H) + Cost of the users ($\alpha$, s, H)), to calculate the optimised variables: $\alpha^*$, s* H*, with the following restrictions: the number of corridors and the headway, between a maximum value (by network capacity) and a minimum value (by operating issues).

$$min\left\{Z = [\pi_V V + \pi_M M + \pi_L L] + \left[A + W + T + \left(\frac{\delta}{v_w}\right)e_T\right] : s \geq 0, H \geq 0, 0 \leq \alpha \leq 1, 0 \leq C\right\}$$

$\underbrace{\qquad\qquad\qquad\qquad}_{\text{Cost of the Agency}}$ $\underbrace{\qquad\qquad\qquad\qquad}_{\text{Cost of the Users}}$

**Table 23**. Meaning of different terms of function Z

| | | |
|---|---|---|
| ***Terms for the agency as a function of α, s, H:*** | | |
| ***V*** | [veh-km/h] | Distance covered by vehicles per hour |
| ***M*** | [veh-h/h] | Number of buses and drivers |
| ***L*** | [km] | Length of the bus lane (both directions) |
| ***O*** | [pax/veh] | Size of buses |
| ***Terms for the user as a function of α, s, H:*** | | |
| ***A*** | [h] | Average approaching walking time |
| ***W*** | [h] | Average waiting time |
| ***T*** | [h] | Average travelling time on board the bus |
| $e_T$ | [-] | The average number of transfers |
| $v_c$ | [km/h] | Commercial speed of buses |
| ***Other parameters:*** | | |
| ***v*** | [km/h] | Travelling speed of vehicles |
| $v_w$ | [km/h] | Walking speed |
| ***C*** | [pax] | Vehicle occupancy |
| ***d*** | [km] | Time penalty for a long transfer |
| ***Weighs:*** | | |
| In euros: $\$_V$(€/veh-km), $\$_M$ (€/veh-h) and $\$_L$ (€/km-h), known unit costs, as function as: V, M and L | | |
| In hours (social cost): $\pi_V=\$_V/(\lambda\mu)$, $\pi_M=\$_M/(\lambda\mu)$ and $\pi_L=\$_L/(\lambda\mu)$, weights in € become hours of passenger transported dividing them by a factor $(\lambda\mu)$, where μ is the time of the user [$/person], and λ is the hourly demand [pax/h] | | |

Finally, a sensitivity analysis to test the robustness of the variables was performed:



$$s/s^* = 1\pm5\% \rightarrow Z=1{,}01\cdot Z^*$$
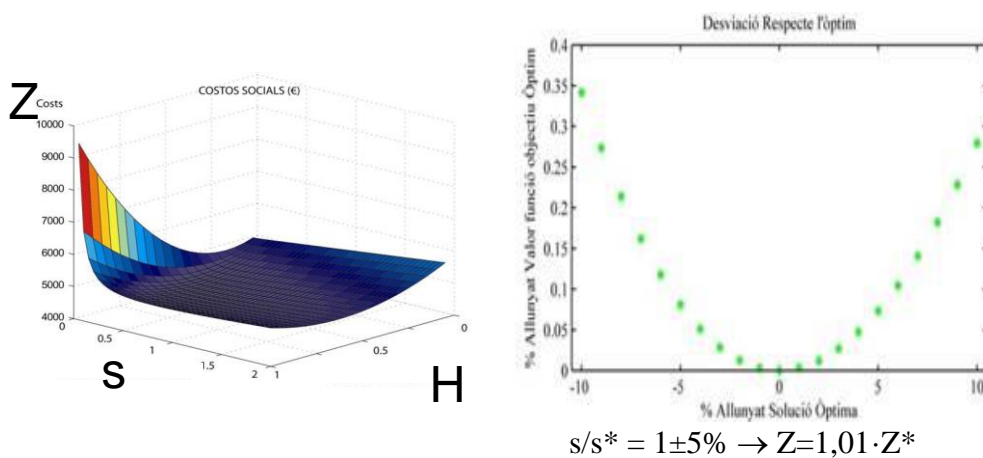
**Figure 52.** Representation of Z as a function as s and H, and sensitivity of Z = Z (s). Source: CENIT

### A.1.2.3 The integrated Bus model for Barcelona

In 2012, together with the City Council, TMB completed the integration of the two explained models and defined, without adding more resources to the system, a new product to offer to the citizens: a bus network with high level of service routes, based on two main issues: a user-friendly layout and a better supply (5-8 minute time headway) with wider daily service span (from 7:00 am to 9:00 pm on working days). This section explains the criteria and supporting hypothesis in which the integration of the two models (A: the orthogonal network, and B: the "RetBus") was based.

Both models aim to enhance the efficiency of the former bus network without increasing the currently available resources and take advantage of the benefits of the existing Integrated Fare System in the Metropolitan Region of Barcelona, as well as a set of priority measures for the bus, deployed all together in various corridors.

In both models, the average travel time decreases, which benefits both passenger and citizen, as well as the operator. And both models consist of horizontal and vertical axes, crossing one to each other perpendicularly.

The reticulated area of Model B has dimensions quite similar to the global city of Barcelona, the relationship between the reticulated rectangle and a rectangle of 10 x 5 km$^2$, which could be assimilated to the built-up area of the city of Barcelona, is 0.8.

The model A also keeps (totally or in part) diagonal lines and some intercity, specifically as follows: 7, 46, 51, 57, 62, 63, 65, 78, 94, 95, 96, 97, 155, 157 and 165, as well as twenty-two routes of the Bus of the Neighbourhood service. So, it can state that it also has a definite hierarchy of services as model B does.

The average distance between stops in model B is 433 m in the city centre and 650 m in the outskirts, very similar to the average distance between stops proposed in model A, which is 400 m (the equivalent of 3 blocks in the Eixample district). Furthermore, studies conducted by TMB have shown that the optimal distance between stops for Barcelona is about 420 m.

In both models, the rate of the bus to bus transfers increases significantly from the former network, so every stop at the interchange areas should be placed in a way that minimises the distance between them, penalising as less as possible all connections.

The ratio: number of horizontal routes from model B/number of horizontal route from model A = 5/9 ≈ 0.5; and the ratio: number of vertical routes from model B/number of vertical routes from model A = 71/16 ≈ 0.5. That is, in both cases, for each H and V route from model B, there are almost two from Model A. This means that from one out every two routes, or they are coincident or very similar.

The extension of the model across the Metropolitan Region would be possible in both cases by the implementation of large interchanges at the four corners of Barcelona, which would become real gates for entering and leave the city.

### A.1.2.4  BCN's New Bus Network final model

The following scheme summarises Barcelona's Bus Network change:
— Premium routes (28)
  — Orthogonal (H, V) and Diagonal (D) grid routes
  — Wide range network
  — Under development since 2012
— Conventional routes (43)
  — Radial network
  — Medium range network
  — Under restructuring since 2012
— Local and feeder routes (27)
  — Local Bus of Neighbourhood and Feeder routes
  — Short range network
  — Small changes throughout the project

It is as if the city has three networks in one: the premium routes, the conventional routes and the local routes.

The premium routes are the new horizontal, vertical and diagonal, which have been implemented since 2012. The conventional routes are those that remain with or without changes after the following deployment phases; there are urban routes, those with their itineraries within the city; and interurban routes, those with their courses throughout Barcelona and other surrounding towns. Finally, the local routes are those that serve steep and difficult-to-access boroughs as the "Local Bus of the Neighbourhood" do and the feeder routes, those that remain unchanging or those that come from the conventional routes after having experienced cuts or other changes.

### A.1.2.4.1  Premium route main features

Main features of the model include: maximum connectivity (from one end to the other of the city, without antennas), with an overall of 28 high level of service routes: 8 horizontal, 17 vertical and 3 diagonal, defining a serve demand-oriented route system, with high and very high frequency routes (5-8 min headway, depending on the route) from 7:00 am to 9:00 pm. Furthermore, it sets only one route per corridor, an average distance between stops is 400 m, and 90% of journeys can be made with 0-1 transfers. Concerning its implementation, it is gradual, at a rate of 4-5 routes every year, which also encompasses the restructuring of the conventional routes.

### A.1.2.4.2  Premium route nomenclature

The routes are named and represented this way: horizontal routes, with an "H" plus an even number, and blue colour; vertical routes, with a V plus an odd number, and green colour; diagonal routes: with a "D" plus digits 20, 30 and 40, and purple colour.
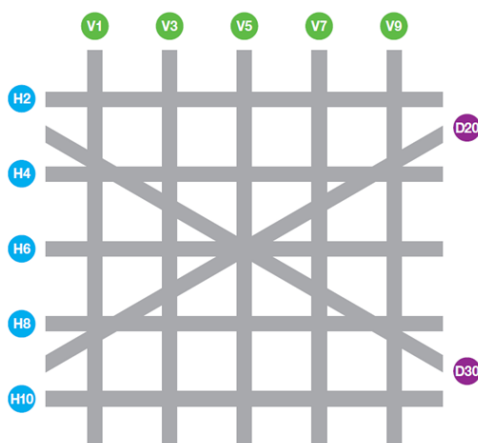


**Figure 53.** Schematic way to name and represent the new routes. Source: TMB.

### A.1.2.4.3 Transfer areas

The transfer areas become fundamental in a model that follows an orthogonal grid. There are two options to travel from one point to another (from the origin to the destination), as shown in Fig. 54.
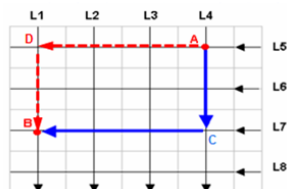


**Figure 54.** The two possible itineraries from point A (origin) to point B (destination) on a grid way structure. Source: proprietary development.

In both cases a switch of path/route is essential and should be done at the intersections of the horizontal and vertical routes, where bus stops should be placed as closely as possible to each other to make transfers as comfortable as conceivable.

Taking advantage of the original octagonal shape junction at the Eixample crossroads, ideal transfer areas were proposed, as shown in Fig. 55; but, due to several problems, especially right turnings of private vehicle and closeness of bus stops when axes are only one block apart from each other, they were eventually rejected.
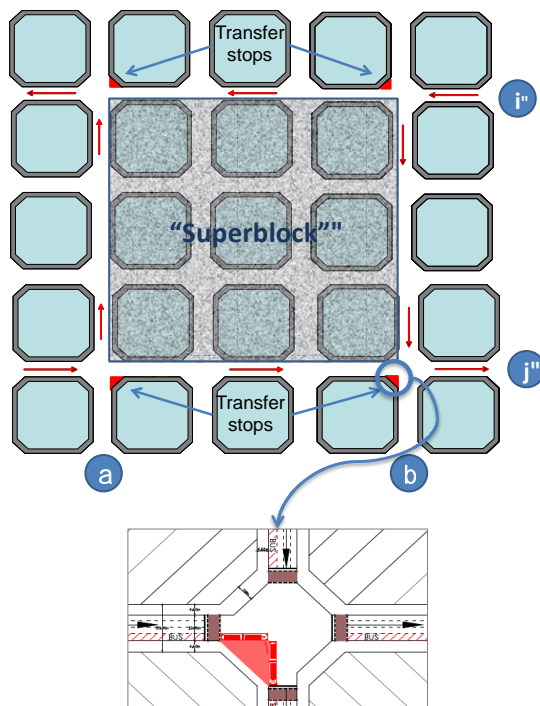


**Figure 55.** Ideal configuration: routes (α, β, i and j) 3 blocks apart from each other. Then the transfer stops are separated 400 m, and the connections would be able to do at the same point: at the appropriate chamfered street corner. Source: "BCN Ecologia" and proprietary development.

218

For all general transfer areas, tailored studies have been made at each location after designing specific signposting expressly created to direct passengers from the arrival bus stop to the transfer ones.

The procedure of guidance consists of the use of three informative elements: shelters, billboards, and spots on the ground at the pedestrian crossings. When passengers get to the arrival stop, they have at their disposal all the information displayed on the shelter or pole that indicate where the various transfer stops are. Then our passengers proceed in the appropriate direction, and when it looks like they could lose their way, a billboard keeps them in the right way. They can find more information about the transfer stops on the pavement beside the crosswalk.

**Implementation phases:**



**Figure 56.** Premium route final layout map, after implementing Phase 5.2.b. Source: TMB

These are the routes implemented on every phase and subphase:

— Phase 1, routes H6, H12, V7, V21, and D20
— Phase 2, routes H8, H10, H16, V3, and V17
— Phase 3, routes H14, V15, and V27
— Phase 4, routes H4, V11, and V13
— Phase 5:
    — Subphase 5.1, routes V5, V29, V31 and D40
    — Subphase 5.2.a, routes V9, V33 and D50
    — Subphase 5.2.b, routes H2, V1, V23, V25 and V33

The changes in the premium network were the following:

— Phase 3, routes H16 (change of itinerary)
— Subphase 5.1, route H16 (new change of course)
— Subphase 5.2.b, routes H6, H8, H10, V13, V15 and V17

The project was completed in November 2018.

### A.1.2.4.4 Operational improvements

As main operational improvements implemented, we can consider the deployment of the double bus stop scheme, the extension of the signal priority at the crossings, both dynamic and green wave based, the particular turnings only for buses, and regulation of axes with diverse routes.

On the high-performance corridors, it is essential that the conventional routes do not stop or block the advance of buses routes. Therefore, when the aggregate frequency of conventional routes is quite significant at any bus stop, which is located on a high-performance corridor, there should be a noticeable increase in the use of the stop and therefore avoiding any possible bus queue upstream. A useful measure to achieve this is to set up a double stop, with two platforms in a row, allowing for simultaneous access and alight to/from the buses.

The extension of the traffic light priority, green wave based, allows the advance of the bus over the private vehicle, which if course, experiences a decrease in their commercial speed. A successful example is that one set up on General Mitre Av., a signal priority green wave based of almost 2.5 km long.

The implementation of dynamic traffic light priority at certain intersections, currently at 20 of them and on two bus terminals (with a countdown clock at the signal showing drivers the suitable time to departure), brings to the bus an additional phase, which avoids stopping at the traffic light.

In total, traffic light adjustments at 65 crossings were set to facilitate the circulation of buses.

The regulation of the public transport corridors, as opposed to the management of each route separately, so that buses from different routes can run well regulated, fulfilling their headway.

### A.1.2.4.5  Infrastructure improvements

As main improvements in infrastructure, the following elements have considered: changing of street directions, the creation of exclusive bus lanes and creation and enhancement of new other sections of bus lane (47.6 km in seven years); and the deployment of new bus stops as well as the removal of several existing ones. In total during the whole process of deploying Barcelona's New Bus Network, a total of 809 improvement actions have been carried out at the stops: shelter renovation, accessibility improvement, new path for vision impaired people, pavement improvement, tree pit adjustment, etc.

New sections of special bus lane like the double bus lane (kerb + offset) on Gran Via Corts Catalanes Av, Besòs direction, from Spain Sq. to Balmes St.; the dedicated bus lane also on Gran Via Corts Catalanes, Llobregat direction, from Marina St. to Spain Sq.; and the circular curb bus lane at Spain Sq.

Also, new other sections of the conventional bus lane, with a maximum width, in some cases together with amendments on the existing sections and with turn right limitations, were set.

Improved stops have been set up too: enhanced poles and new shelters with better design and services: ticket machines, real-time information on arrivals of vehicles and incidents, and with the possibility of looking up customer information in real time about different transport modes anywhere in the city. Also, a special signposting had been designed and installed at the transfer stops.

### A.1.2.4.6  Evolution in ridership

Fig. 57 displays the growth in patronage from the beginning of the implementation until the present day. In the beginning, with only 5 routes, the percentage of the premium route patronage with respect the total Bus network was only 8%. Nowadays, once completed the project, this percentage raised up to 60%.

Fig. 58 ranks the 28 premium routes according to passenger boarding on weekdays in December 2018. Horizontal routes are the busiest ones. Outstandingly, H6, H4, and H8 surpass 30,000 pax/day. Concerning vertical routes, we can highlight V13, V15, and V3 are close to 20.000 pax/day. D40 and D20 surpass 20,000 pax/day.
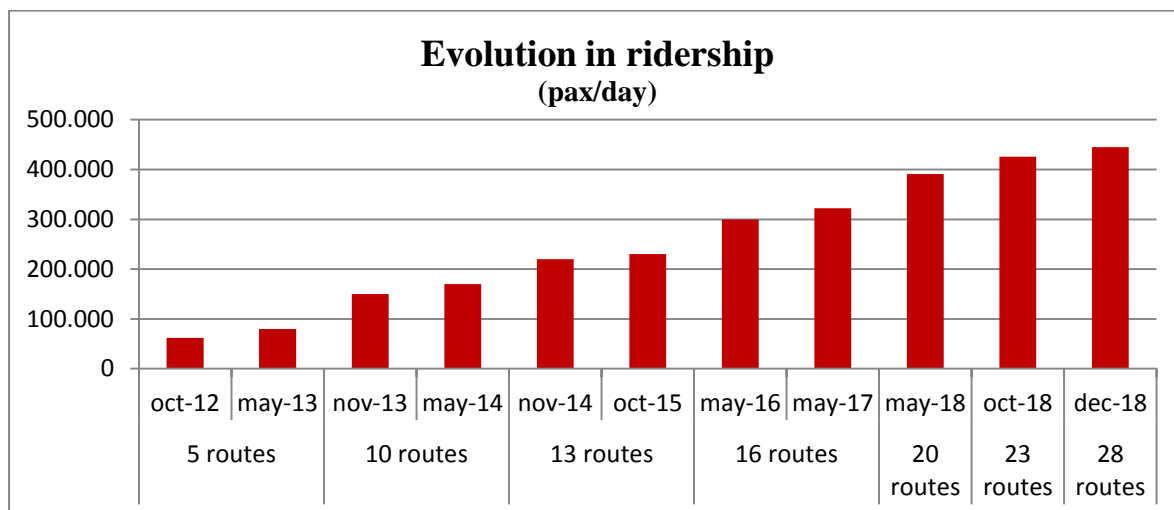


**Figure 57.** Evolution in ridership from 2012 (with five routes) until 2018 (with 28 routes). Source: TMB

## Passenger boardings on a working day
### (pax/day)
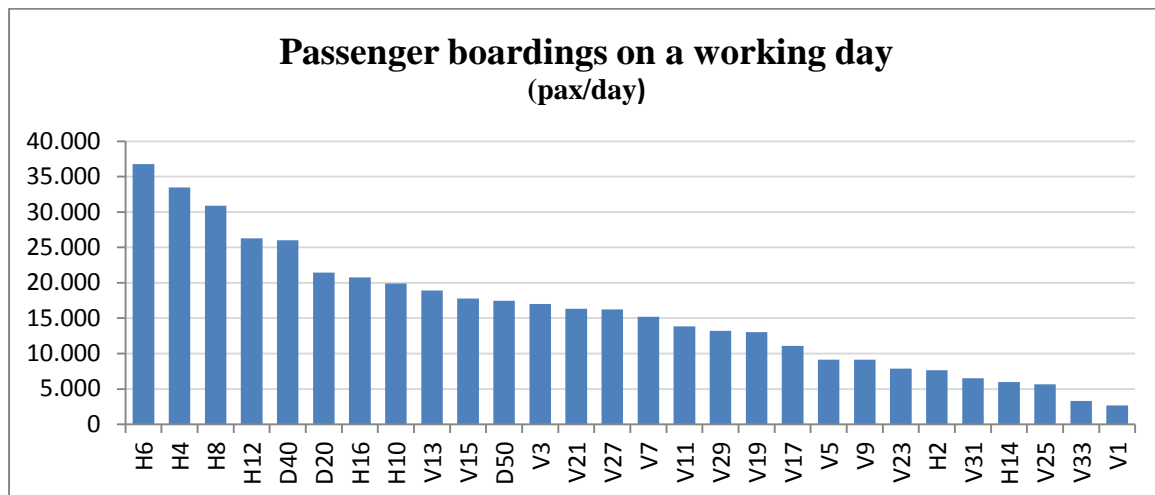


**Figure 58.** Average passenger boardings on weekdays in December 2018. Source: TMB

# Appendix B

# Scheduled timetables

## B.1   Scheduled timetables

### B.1.1   Working with HASTUS (1)

#### B.1.1.1   Loading data

Load HASTUS IT application, then from the main menu, select "Red", and "Analizar los tiempos de recorrido por vinculo" as shown in Fig. 59.
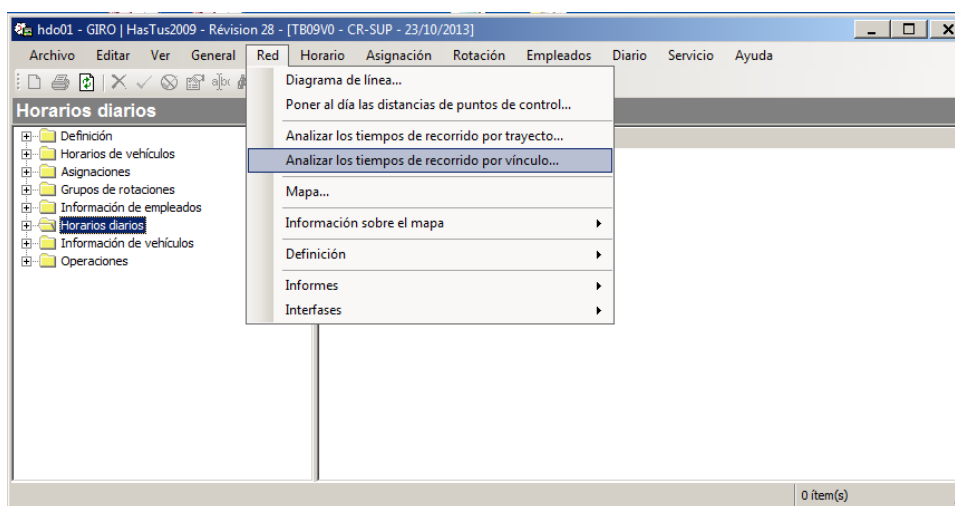


**Figure 59**. HASTUS 2009, Spanish version, screenshot 1.

Select from "Archivo" the option "Versiones activas"
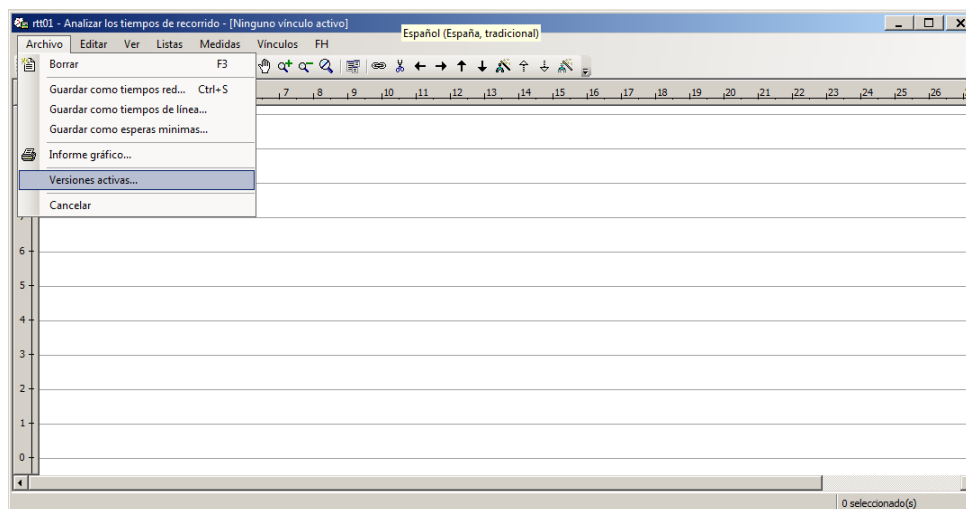
**Figure 60**. HASTUS 2009, Spanish version, screenshot 2.

Select the version of the route that we want to analyse and accept.
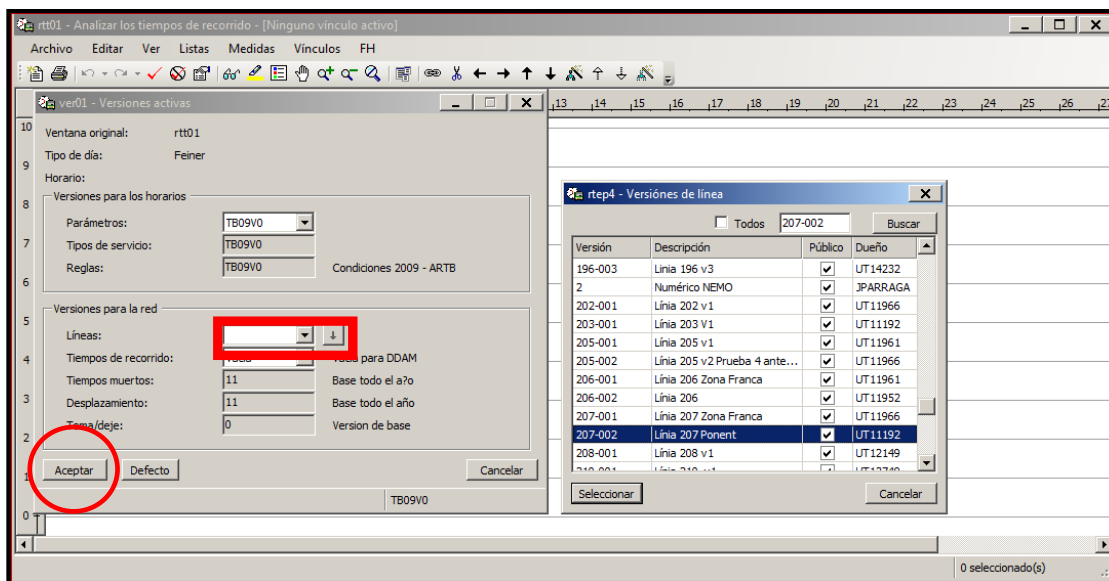


**Figure 61**. HASTUS 2009, Spanish version, screenshot 3.

Linkages, Select "Optimizar los tiempos de recorrido por línea".
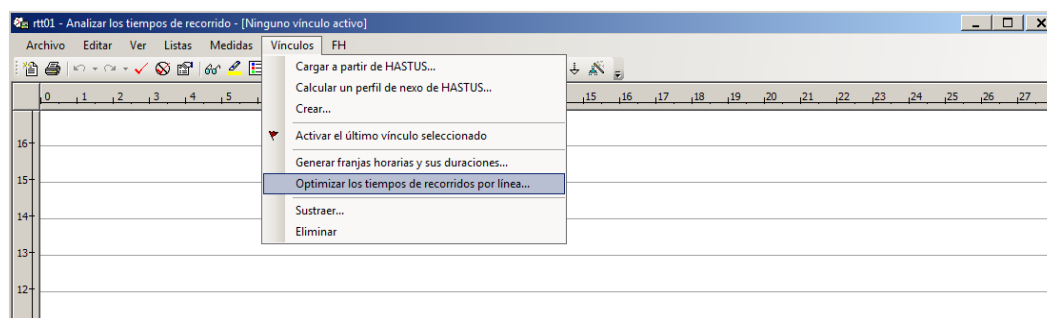


**Figure 62**. HASTUS 2009, Spanish version, screenshot 4.

In a headway-basis operation system (regularity), select the option "Sólo cargar las medidas". In a timetable-basis operation system (punctuality), the option is not necessary.

Click "Optimizar". The data is loaded graphically into the system. HASTUS display a point cloud.
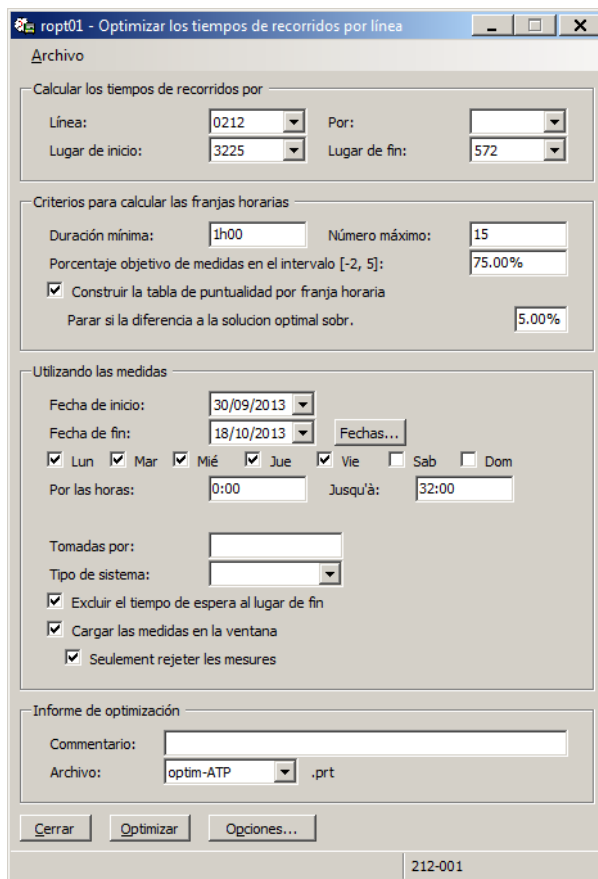
**Figure 63**. HASTUS 2009, Spanish version, screenshot 5.
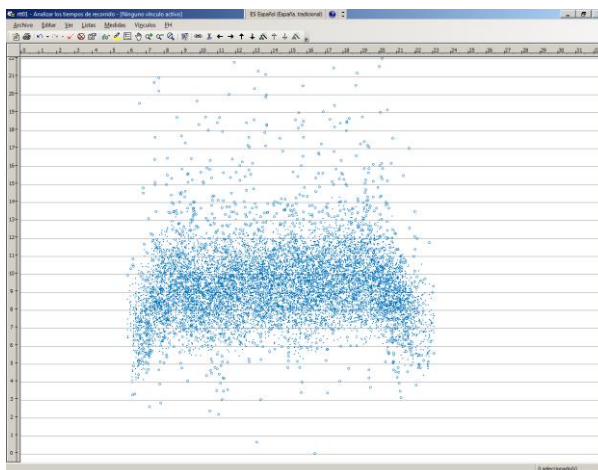


**Figure 64**. HASTUS 2009, Spanish version, screenshot 6.

### B.1.1.2 Inserting links

From the main menu "Vinculos", select "Crear".
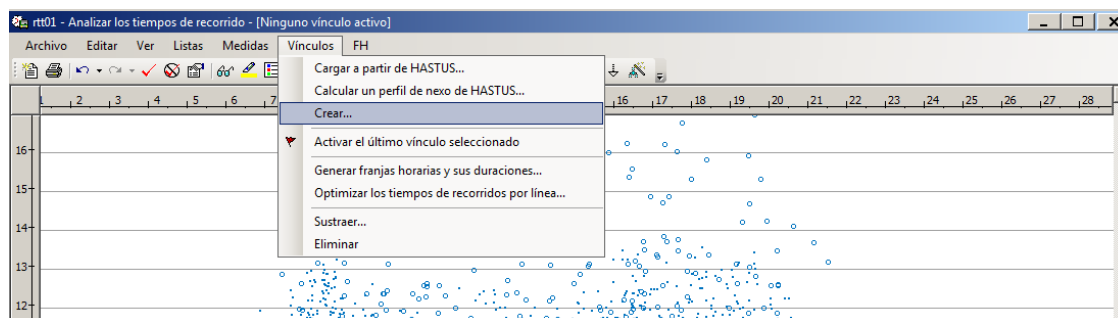
**Figure 65**. HASTUS 2009, Spanish version, screenshot 7.
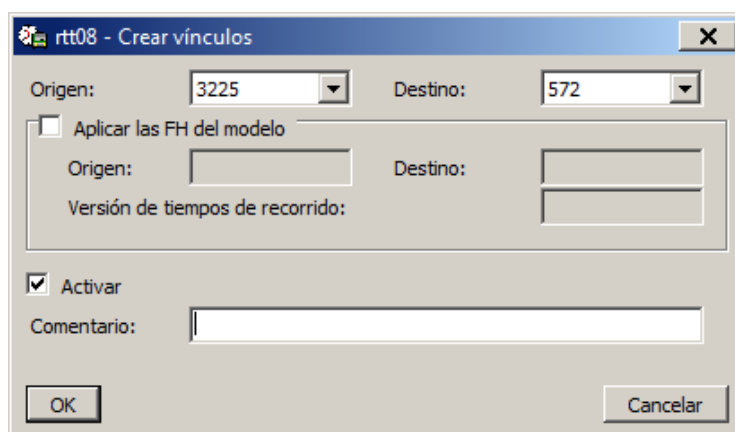


**Figure 66**. HASTUS 2009, Spanish version, screenshot 8.

Repeat the link creating process ["Vinculos"/"Crear"] until completing all the partial travel sections and the whole trip.
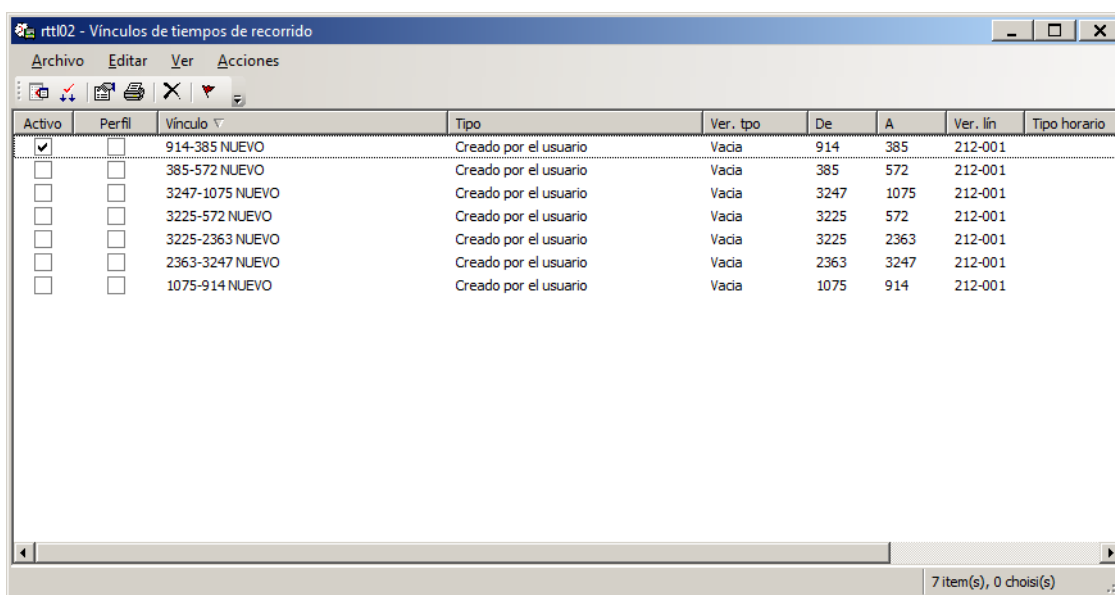


**Figure 67**. HASTUS 2009, Spanish version, screenshot 9. The final result for route H12 (outbound).

228

### B.1.1.3  Obtaining average travel times

From the main menu "Vínculos", select "Generar franjas horarias y sus duraciones…"
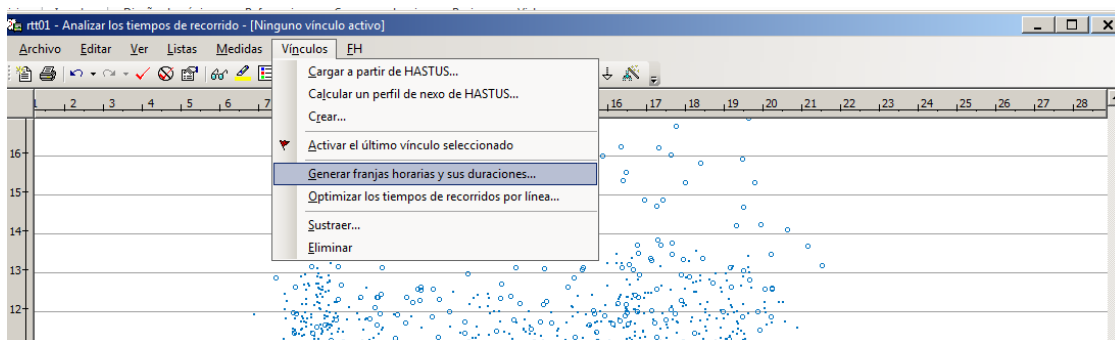


**Figure 68**. HASTUS 2009, Spanish version, screenshot 10.

Time slots and average travelling times are generated for the active link that we have at that moment. By default, the active link is the last generated link.

The information by hours is achieved by selecting:

— Increase: 1:00 h

— Standard deviation: 1.00

Even so, it is possible that HASTUS generates time slots greater than 1 hour. In that case, the disaggregation will be forced in the graphic presentation mode.
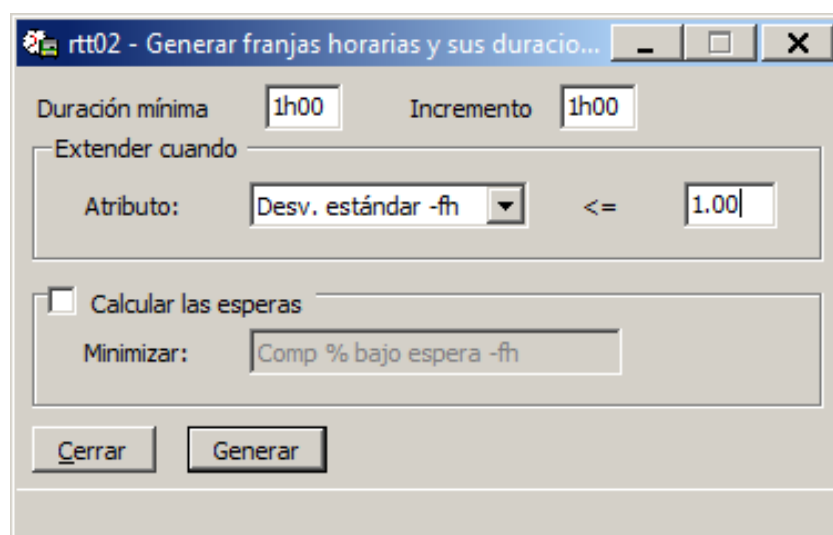


**Figure 69**. HASTUS 2009, Spanish version, screenshot 11.

Outcome: the point cloud and the link created with the time slots proposed by the system.
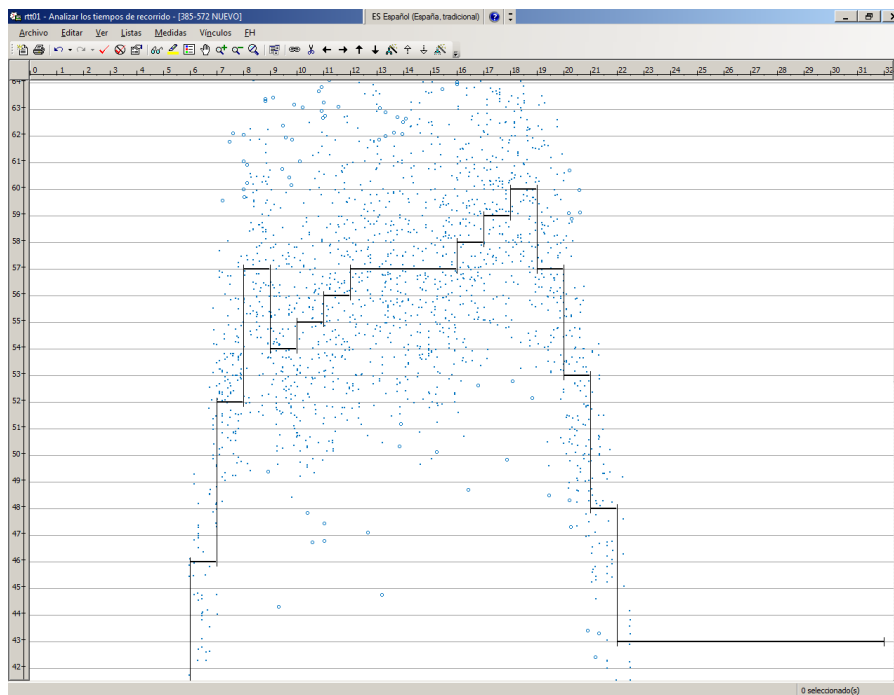


**Figure 70**. HASTUS 2009, Spanish version, screenshot 12.

Without changing the average travel times, define 1:00 h time slots
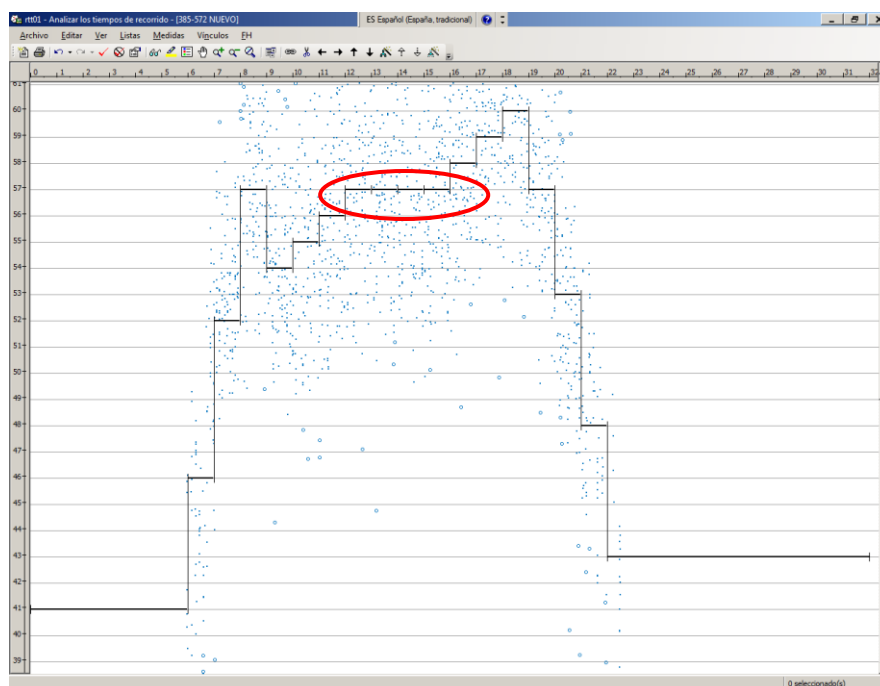


**Figure 71**. HASTUS 2009, Spanish version, screenshot 13.

From the main menu "Editar", select "Seleccionar" all time slots
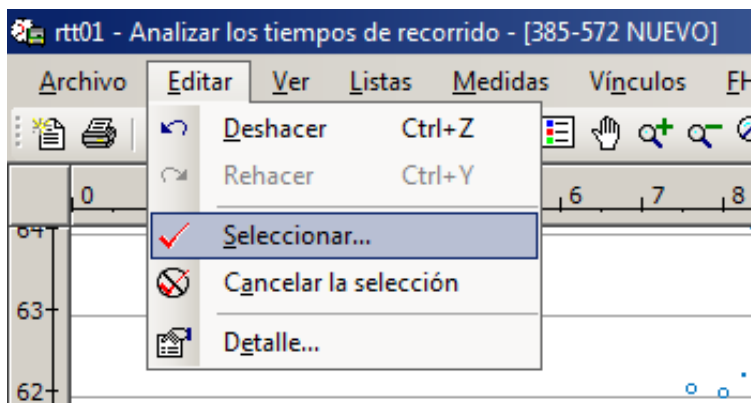


**Figure 72**. HASTUS 2009, Spanish version, screenshot 14.

Select "Incluir los objetos"
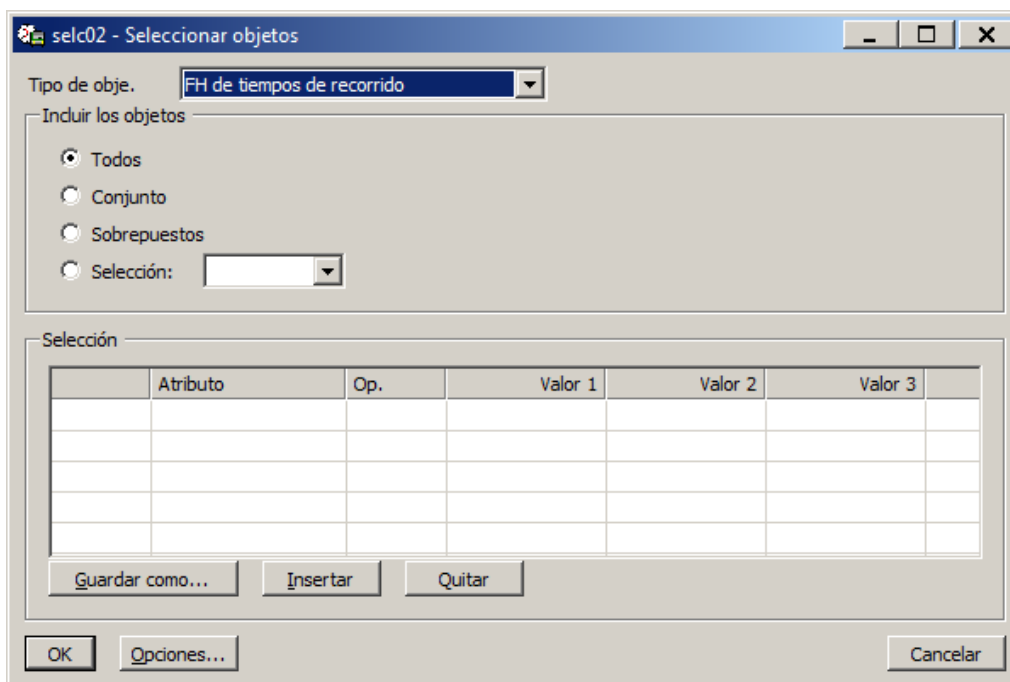


**Figure 73**. HASTUS 2009, Spanish version, screenshot 15.

### B.1.1.4  Synchorinising times

The synchronisation option aims to get the average travel times and the standard deviation in 1:00 hour time slots for partial trips and the whole journey.

From the main menu, FH, select "Sincronizar"
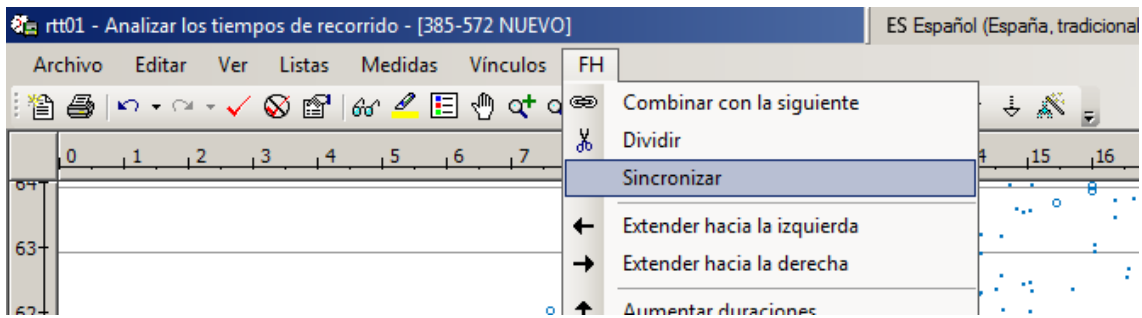


**Figure 74**. HASTUS 2009, Spanish version, screenshot 16.

And then, "Recalcular las duraciones"
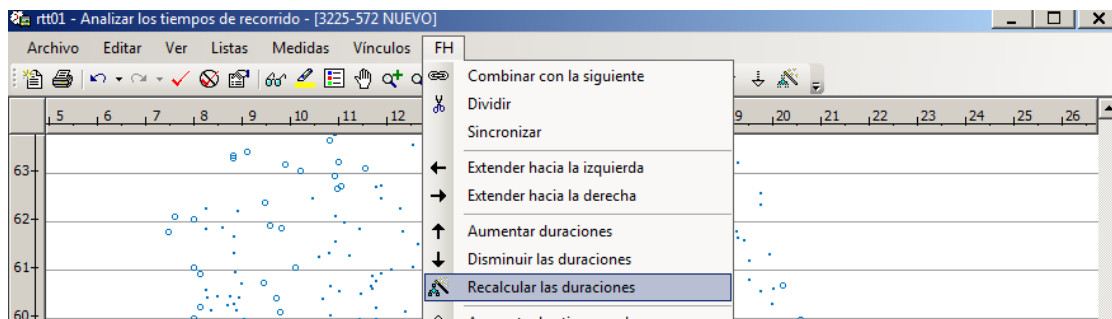


**Figure 75**. HASTUS 2009, Spanish version, screenshot 17.

From the main menu, select "Listas" and "Franjas horarias" to visualise the numerical outcomes as lists.
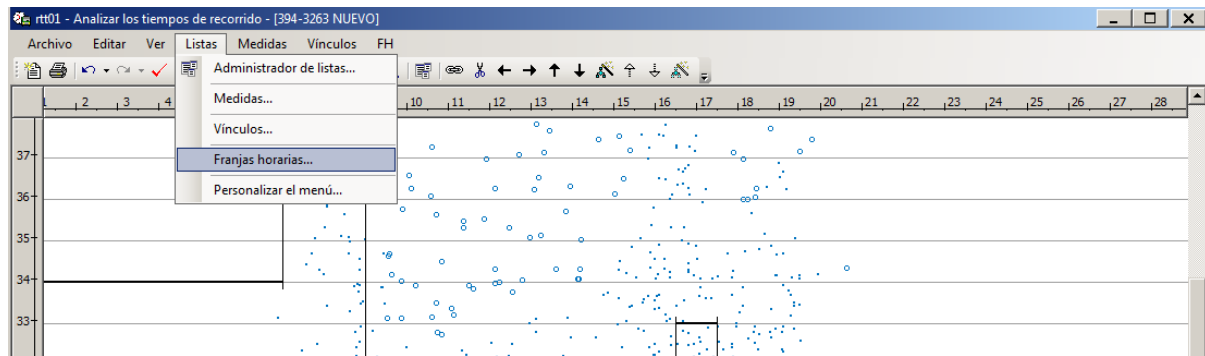


**Figure 76**. HASTUS 2009, Spanish version, screenshot 18.

The output is a list:



**Figure 77**. HASTUS 2009, Spanish version, screenshot 19.


### B.1.1.5  Exporting to a worksheet

From the main menu "Archivo", select "Exportar las listas a Excel"



**Figure 78**. HASTUS 2009, Spanish version, screenshot 20.

In an Excel worksheet, we can arrange all the information corresponding to the average travel times between consecutive checkpoints (within a time slot of 1 h), the average travel time between the origin and the destination stops (time spectrum) and the standard deviation in travel time between the origin and the destination stops (within a time slot of 1h).

**Table 24**. Route H12 – Outbound, Timetable.

| Hour | | Links | | | | | | | Spectrum | |
|------|------|-----------|-----------|-----------|----------|---------|---------|------|----------|-----|
| Inicio | Fin | 3225-2363 | 2363-3247 | 3247-1075 | 1075-914 | 914-385 | 385-572 | SUMA | 3225-572 | s |
| 6:00 | 6:59 | 7 | 8 | 5 | 7 | 8 | 8 | 43 | 46 | 4,0 |
| 7:00 | 7:59 | 9 | 10 | 7 | 8 | 9 | 9 | 52 | 52 | 2,6 |
| 8:00 | 8:59 | 10 | 11 | 7 | 9 | 9 | 10 | 56 | 57 | 2,9 |
| 9:00 | 9:59 | 9 | 11 | 7 | 9 | 9 | 9 | 54 | 54 | 2,6 |
| 10:00 | 10:59 | 10 | 10 | 7 | 9 | 9 | 9 | 54 | 55 | 3,2 |
| 11:00 | 11:59 | 10 | 10 | 7 | 9 | 9 | 10 | 55 | 56 | 3,2 |
| 12:00 | 12:59 | 10 | 10 | 7 | 10 | 9 | 10 | 56 | 57 | 3,3 |
| 13:00 | 13:59 | 10 | 10 | 8 | 10 | 9 | 10 | 57 | 57 | 2,9 |
| 14:00 | 14:59 | 10 | 10 | 8 | 10 | 9 | 10 | 57 | 57 | 3,4 |
| 15:00 | 15:59 | 11 | 10 | 7 | 9 | 9 | 10 | 56 | 57 | 2,9 |
| 16:00 | 16:59 | 10 | 11 | 8 | 9 | 9 | 10 | 57 | 58 | 3,1 |
| 17:00 | 17:59 | 11 | 10 | 8 | 9 | 9 | 11 | 58 | 59 | 2,7 |
| 18:00 | 18:59 | 11 | 10 | 8 | 10 | 9 | 11 | 59 | 60 | 3,3 |
| 19:00 | 19:59 | 11 | 10 | 8 | 10 | 9 | 11 | 59 | 57 | 3,0 |
| 20:00 | 20:59 | 10 | 9 | 8 | 9 | 9 | 10 | 55 | 53 | 3,0 |
| 21:00 | 21:59 | 9 | 9 | 7 | 8 | 8 | 8 | 49 | 48 | 3,1 |
| 22:00 | 22:59 | 9 | 7 | 6 | 7 | 7 | 8 | 44 | 43 | 2,8 |

**Remark 1.** HASTUS provides information about the travel times of each link about the start time of the trip at the origin checkpoint. For example, for link 3225-2363, the value 7 min, presented at the 1-hour time slot 6:00-6:59, should be read as the average travel time between the nodes 3225 and 2363 in all those journeys that have been started (at the node 3225) at the 6:00-6:59 hour. Similarly, 46 min is the average travel time between the nodes 3225 and 572 of those journeys that have been started (at the node 3225) at the 1-hour time slot 6:00-6:59.

This way of presenting the information explains that the sum of times corresponding to the links of one hour does not meet with the total travel time within the hour (spectrum). Thus, for example, the route that leaves at 6:47 dedicates the following time in its route: $7 + 8 + 7 + 8 + 9 + 9 = 48$ minutes (neither 46 nor 52).

**Table 25**. Route H12 – Outbound, spectrum.

| Start | End | 3225-2363 | 2363-3247 | 3247-1075 | 1075-914 | 914-385 | 385-572 | 3225-572 | s |
|---|---|---|---|---|---|---|---|---|---|
| 6:00 | 6:59 | 7 | 8 | 5 | 7 | 8 | 8 | 46 | 4,0 |
| 7:00 | 7:59 | 9 | 10 | 7 | 8 | 9 | 9 | 52 | 2,6 |

Internally, HASTUS builds the schedules following the scheme shown in Table 24. The time defined in each journey is the sum of the times of their links, and these are obtained at each link entrance time.

**Remark 2.** The partial times of the links are used internally by HASTUS to build route schedules. The roundup to one minute can generate problems by excess and by default when they are mostly made in the same direction (it would be preferable to work with decimal and round up at the end of the calculation). The spectrum times are not used to build the journey schedules; they are used to build homogeneous time slots. The standard deviation of the spectrum times is used to determine the recovery time (RT).

**Table 26**. Route H12 – Inbound, Timetable.

| Hour | | Links | | | | | | | | Spectrum | |
|---|---|---|---|---|---|---|---|---|---|---|---|
| Inicio | Fin | 572-383 | 383-247 | 247-1081 | 1081-707 | 707-3236 | 3236-3023 | 3023-3225 | SUMA | 572-3225 | s |
| 6:00 | 6:59 | 6 | 6 | 9 | 3 | 7 | 6 | 6 | **43** | 45 | 3,5 |
| 7:00 | 7:59 | 9 | 7 | 9 | 3 | 7 | 9 | 7 | **51** | 56 | 5,0 |
| 8:00 | 8:59 | 10 | 9 | 10 | 3 | 8 | 11 | 8 | **59** | 58 | 3,1 |
| 9:00 | 9:59 | 8 | 8 | 10 | 3 | 8 | 10 | 7 | **54** | 54 | 2,9 |
| 10:00 | 10:59 | 7 | 7 | 11 | 3 | 8 | 9 | 7 | **52** | 54 | 2,7 |
| 11:00 | 11:59 | 7 | 7 | 10 | 3 | 8 | 9 | 7 | **51** | 53 | 3,0 |
| 12:00 | 12:59 | 7 | 7 | 10 | 3 | 9 | 9 | 7 | **52** | 53 | 2,8 |
| 13:00 | 13:59 | 7 | 7 | 10 | 3 | 9 | 10 | 7 | **53** | 53 | 2,5 |
| 14:00 | 14:59 | 7 | 7 | 10 | 3 | 8 | 9 | 8 | **52** | 52 | 2,8 |
| 15:00 | 15:59 | 7 | 7 | 10 | 3 | 8 | 9 | 8 | **52** | 53 | 3,0 |
| 16:00 | 16:59 | 7 | 7 | 10 | 3 | 9 | 9 | 8 | **53** | 54 | 2,7 |
| 17:00 | 17:59 | 7 | 7 | 11 | 3 | 9 | 10 | 8 | **55** | 55 | 2,8 |
| 18:00 | 18:59 | 8 | 7 | 11 | 3 | 9 | 9 | 8 | **55** | 55 | 2,7 |
| 19:00 | 19:59 | 7 | 7 | 10 | 4 | 9 | 9 | 8 | **54** | 53 | 3,0 |
| 20:00 | 20:59 | 7 | 6 | 9 | 3 | 9 | 8 | 7 | **49** | 49 | 2,4 |
| 21:00 | 21:59 | 6 | 6 | 9 | 3 | 7 | 8 | 7 | **46** | 45 | 2,6 |
| 22:00 | 22:59 | 6 | 6 | 8 | 3 | 7 | 7 | 6 | **43** | 43 | 3,2 |

## B.1.2 Working with HASTUS (2)

### B.1.2.1 Average time and standard deviations within time slots

Once created the links and generated the time slots with time amplitude, HASTUS allows for subdividing the slots and getting a more adjusted estimation of the average transit times and the standard deviation per time slot.

Initial graphic:
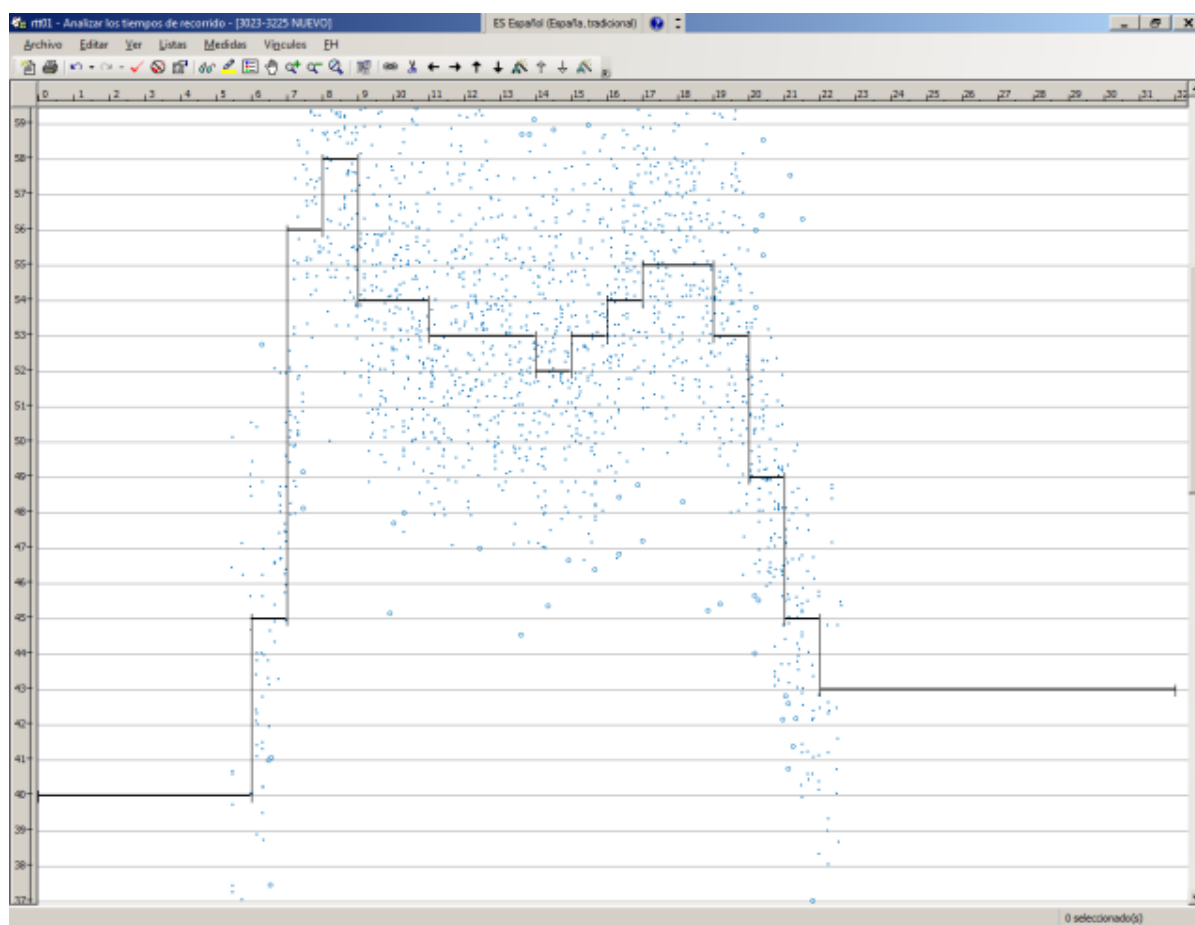


**Figure 79**. HASTUS 2009, Spanish version, screenshot 21.

Step 1. Subdivision of the 1-hour time slot. In the graphical presentation, make manual adjustments to the full path link to subdivide the 7:00-7:59 band into two 30' time slot, and recalculate the durations.
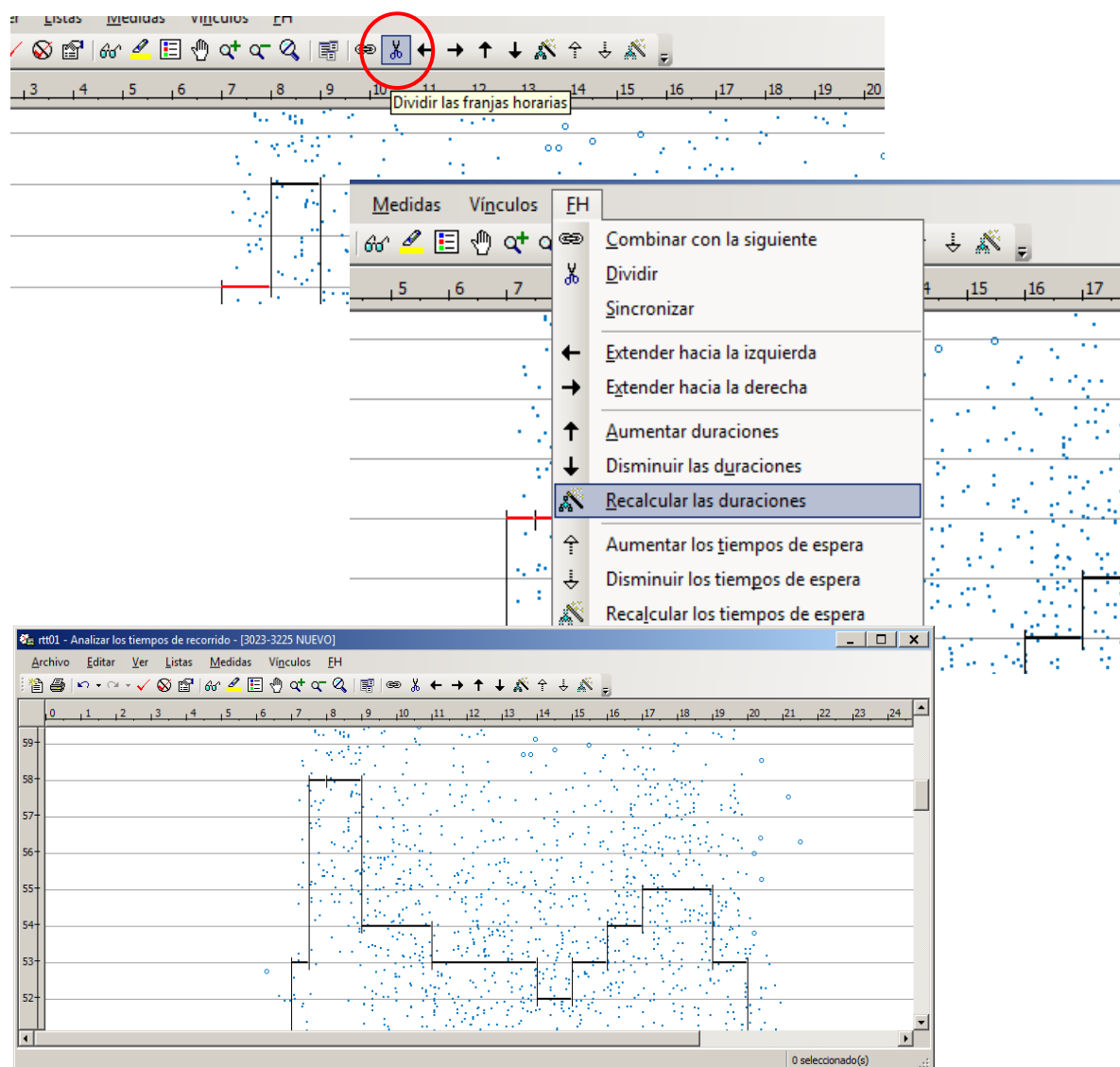
**Figure 80**. HASTUS 2009, Spanish version, screenshot 22.

Once recalculated the duration of the trips, select all the time slots in the menu ("Editar/Seleccionar/FH de tiempos de recorrido") and synchronise the time slots through the menu option ("FH/Sincronizar"). Result: list with the average transit times and standard deviation on the sub time slots and on the whole route in the 30-minute sub time slots corresponding to 7:00-7:59.

**Figure 81**. HaTtus 2009, Spanish version, screenshot 23.

Step 2. Calculation of typical journey deviations in time slot that groups several hours. On the screen that shows the average time of passage per complete journey (in 1-hour time slots initially proposed by HASTUS or on the screen with subdivisions), make the cuts and the necessary adjustments to reproduce the predefined groupings
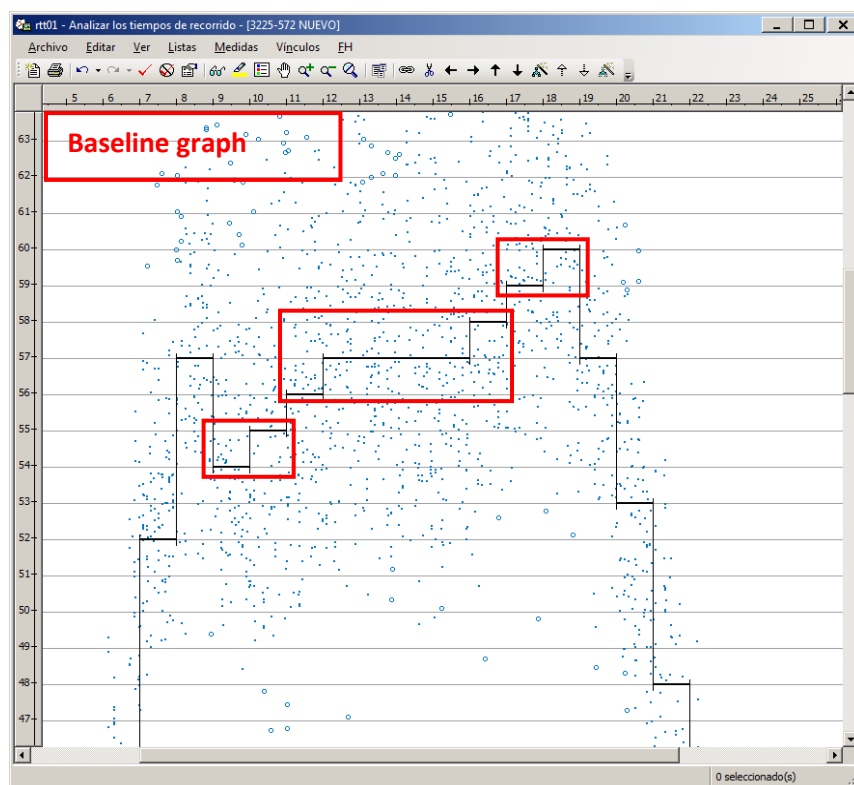


**Figure 82**. HASTUS 2009, Spanish version, screenshot 24.
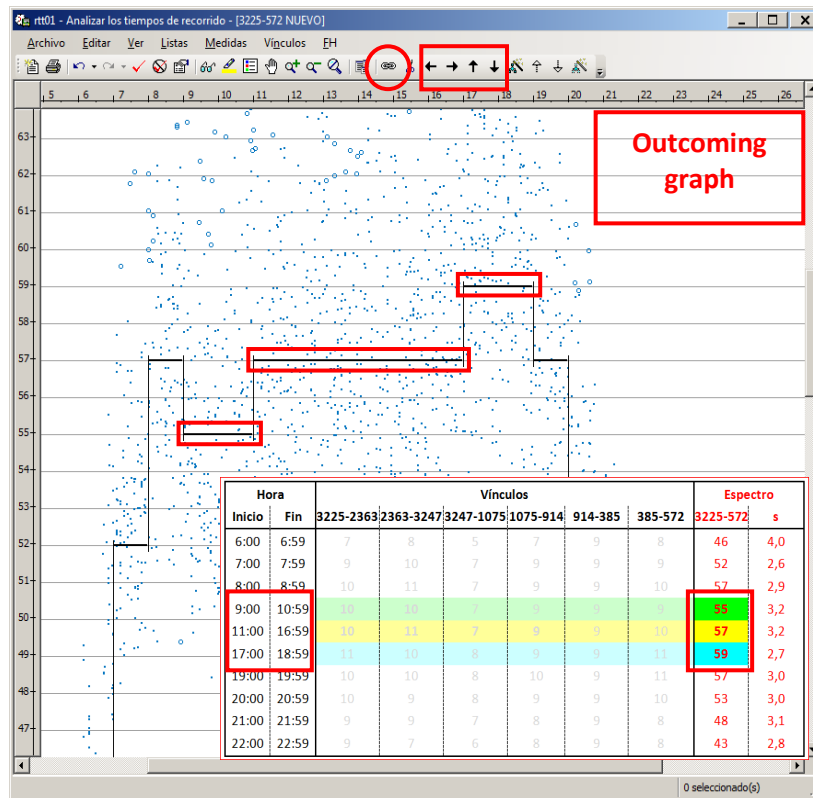
**Figure 83**. HASTUS 2009, Spanish version, screenshot 25.

The standard deviations "s" needed to calculate the RT's are obtained by recalculating the durations ("FH/Recalcular las duraciones")
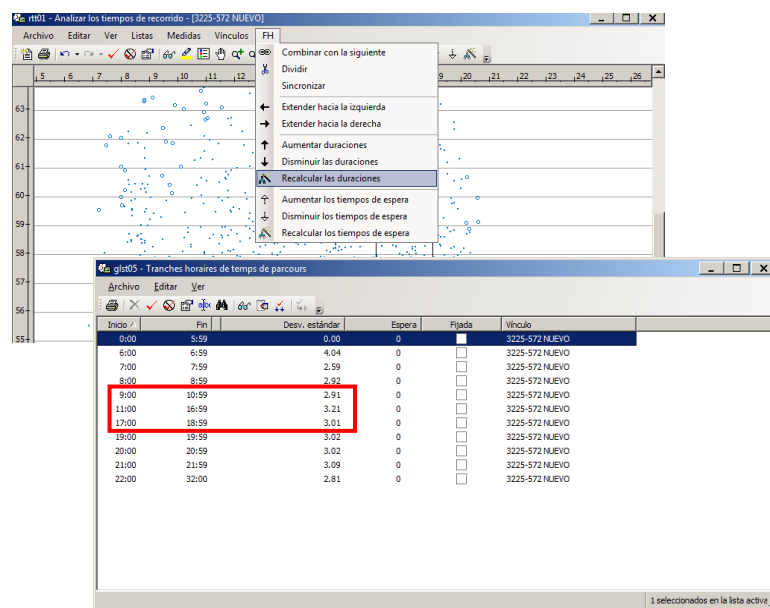


**Figure 84**. HASTUS 2009, Spanish version, screenshot 26.

The RT of the slots is evaluated in $RT = 1.96 \cdot \sigma_{TS}$.

**Remark 3.** It is possible that during the process of recalculation of durations, HASTUS alters the transit times per trips we have entered manually. This modification is not critical: the transit time per trip has been used only to build slots (and although slightly modified by the effect of rounding, a single time is maintained for the strip); HASTUS uses only the partial times of the links to build the timetables of the journeys (not the total journey time); and this change does not alter the calculation of the standard deviation s.

### B.1.3 Excel worksheet

**Table 27**. Template to draw up timetables with E1min time slots

| inicio | final | maxinodo 1 | maxinodo 2 | maxinodo 3 | maxinodo 4 | maxinodo 5 | maxinodo 6 | maxinodo 7 | maxinodo 8 | maxinodo 9 | maxinodo 10 | s |
|--------|-------|-----------|-----------|-----------|-----------|-----------|-----------|-----------|-----------|-----------|------------|---|
| | | | | | | | | | | | | |
| Promedio tiempos de paso | | #¡DIV/0! | #¡DIV/0! | #¡DIV/0! | #¡DIV/0! | #¡DIV/0! | #¡DIV/0! | #¡DIV/0! | #¡DIV/0! | #¡DIV/0! | #¡DIV/0! | #¡DIV/0! |
| 0:00 | 0:00 | | | | | | | | | | | TRI |

**Drawing up timetables for time slots. Criterium ±1 minute**

| Start | End | node1 | node 2 | node 3 | node 4 | node 5 | node 6 | node 7 | node 8 | node 9 | node 10 | trip | s | RT |
|-------|-----|-------|--------|--------|--------|--------|--------|--------|--------|--------|---------|------|---|-----|
| 11:00 | 11:59 | 7 | 7 | 10 | 3 | 8 | 9 | 7 | | | | 53 | 3 | |
| 12:00 | 12:59 | 7 | 7 | 10 | 3 | 9 | 9 | 7 | | | | 53 | 2,8 | |
| 13:00 | 13:59 | 7 | 7 | 10 | 3 | 9 | 10 | 7 | | | | 53 | 2,5 | |
| 14:00 | 14:59 | 7 | 7 | 10 | 3 | 8 | 9 | 7 | | | | 52 | 2,8 | |
| 15:00 | 15:59 | 7 | 7 | 10 | 3 | 8 | 9 | 7 | | | | 53 | 3 | |
| 16:00 | 16:59 | | | | | | | | | | | | | |
| Average transit times | | 7,00 | 7,00 | 10,00 | 3,00 | 8,40 | 9,20 | 7,00 | #DIV/0! | #DIV/0! | #DIV/0! | 52,80 | 2,82 | |
| Round up transit times | | 7,00 | 7,00 | 10,00 | 3,00 | 8,00 | 10,00 | 7,00 | #DIV/0! | #DIV/0! | #DIV/0! | 53,00 | 2,82 | 5,97 |

<div align="right">

# Appendix C

# Headway adherence

</div>

## C.1 Headway Adherence

### C.1.1 Mathematical prove of the expression for calculating the average user waiting time at a bus stop

The aim will be to prove Eq. (9/C.1):

$$\overline{w} = \frac{1}{2} \cdot \overline{h} \cdot (1 + C_{v,h}^2) \qquad\qquad \text{(C.1)}$$

We consider a certain bus route and its users arriving at a bus stop with a constant ratio λ (it can be proved that with a variable ratio, finally, we get the same conclusion). In such a way that during a period T, the total users are: N = λ·T. In this period, a certain number of buses arrive at the stop with diverse headways $h_k$. It is supposed that the users waiting at the stop can instantaneously get on the buses. Fig. 85 shows the system of user queues at the stop. In as much as users are arriving at the stop, they wait for the bus to be served. This way, a certain user i arrives at a certain given time and waits to be served an equivalent time at the horizontal section shown in Fig. 85. The blue curve represents the accumulated number of users that have arrived at the stop, and the red curve represents the number of users who have to get on the bus and have been transported.
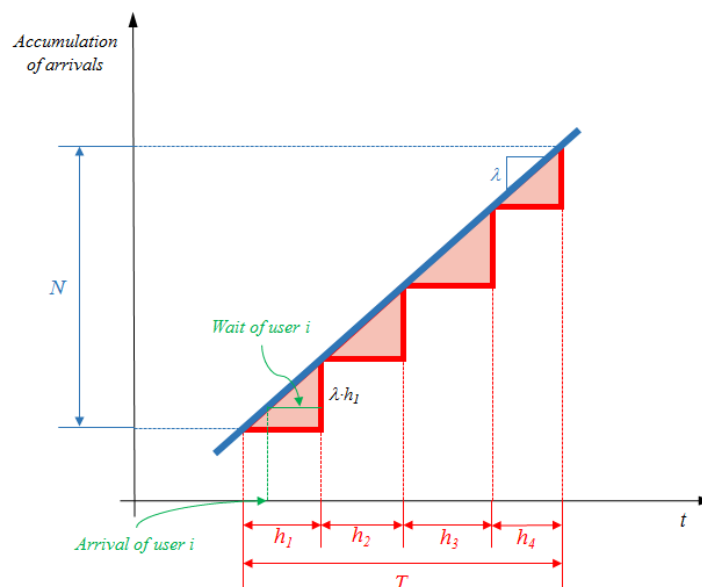


**Figure 85**. Accumulate number of user arrivals (in blue) and served (in red) at a bus stop

The generic function of the amount of served users is, therefore, as follows:

$$N(T) = \sum_{k=1}^{K} \lambda \cdot h_k = \lambda \cdot T \tag{C.2}$$

Thus, the total waiting for the users who must be served by a bus is the shaded triangular area:

**Table 28**. Calculation of the total wait time

| Headway | Avg. wait time | Num. of affected users | Total wait time |
|---|---|---|---|
| $h_1$ | $h_1/2$ | $\lambda \cdot h_1$ | $h_1/2 \cdot \lambda \cdot h_1$ |
| $h_2$ | $h_2/2$ | $\lambda \cdot h_2$ | $h_2/2 \cdot \lambda \cdot h_2$ |
| … | … | … | … |
| $h_k$ | $h_k/2$ | $\lambda \cdot h_k$ | $h_k/2 \cdot \lambda \cdot h_k$ |
| | | | $\sum_{k=1}^{K} \frac{1}{2} \cdot \lambda \cdot h_k^2$ |

As proved above, evaluated in a period T, the total wait time can be calculated as:

$$W(T) = \sum_{k=1}^{K} \frac{1}{2} \cdot \lambda \cdot h_k^2 \tag{C.3}$$

The average waiting for $\bar{w}$ of the user is given by the quotient:

$$\bar{w} = \frac{W(T)}{N(T)} = \frac{\frac{1}{2} \sum_k h_k^2}{\sum_k h_k} \tag{C.4}$$

Dividing numerator and denominator by $k$, the above expression results in:

$$\bar{w} = \frac{\frac{1}{2} \overline{h^2}}{\bar{h}} \tag{C.5}$$

As the average of the squares is equivalent to the sum of the variance of a sample and the mean square:

$$s_h^2 = \frac{(h_1 - \bar{h})^2 + \cdots + (h_k - \bar{h})^2}{k} = \frac{h_1^2 - 2h_1\bar{h} + \bar{h}^2 + \cdots + h_k^2 - 2h_k\bar{h} + \bar{h}^2}{k} =$$

$$= \frac{h_1^2 + \cdots + h_k^2}{k} - \frac{2h_1\bar{h} + \cdots + 2h_k\bar{h}}{k} + \frac{k \cdot \bar{h}^2}{k} = \overline{h^2} - 2\bar{h} \cdot \bar{h} + \bar{h}^2 = \overline{h^2} - \bar{h}^2 \Rightarrow$$

$$s_h^2 = \overline{h^2} - \bar{h}^2 \Rightarrow \overline{h^2} = \bar{h}^2 + s_h^2 \tag{C.6}$$

the equation (C.4) can be rewritten this way:

$$\overline{w} = \frac{\frac{1}{2}(\bar{h}^2 + s_h^2)}{\bar{h}} = \frac{1}{2}\left(\bar{h} + \frac{s_h^2}{\bar{h}}\right) = \frac{1}{2}\bar{h} \cdot (1 + C_{v,h}^2) \tag{C.7}$$

As we have intended to prove.

## C.1.2 The relationship between P and C$_{v,h}$

The relationship between the probability, P that a given transit vehicle's headway, $h_i$ will be off-headway by more than one-half the scheduled headway h, and the coefficient of variation of headway, C$_{vh}$ thresholds, i.e.: $P[|h_i - h| > 0.5 \cdot h] \leftrightarrow C_{v,h}$ can be demonstrated this way:

$$P[|h_i - h| > 0.5 \cdot h] = P\left[\frac{|h_i - h|}{h} > 0.5\right] = P\left[\left|\frac{h_i}{h} - 1\right| > 0.5\right]$$

$$= 1 - P\left[\left|\frac{h_i}{h} - 1\right| \le 0.5\right] = 1 - P\left[-0.5 \le \frac{h_i}{h} - 1 \le 0.5\right]$$

$$= 1 - P\left[0.5 \le \frac{h_i}{h} \le 1.5\right] = 1 - P[0.5 \cdot h \le h_i \le 1.5 \cdot h] \tag{C.8}$$

$$h_i \sim N(\mu_h, \sigma_h)$$

$$\begin{cases} \hat{\mu}_h = \bar{h}_\iota \\ \hat{\sigma}_h = s(h_i) \end{cases}$$

$$\frac{h_i - \bar{h}_\iota}{s(h_i)} \sim N(0,1)$$

$$P\left[-a \le \frac{h_i - \bar{h}_i}{s(h_i)} \le a\right] = P[-a \cdot s(h_i) \le h_i - \bar{h}_i \le a \cdot s(h_i)]$$

$$= P[\bar{h}_i - a \cdot s(h_i) \le h_i \le \bar{h}_i + a \cdot s(h_i)] \tag{C.9}$$

$$\begin{cases} P[0.5 \cdot \bar{h}_\iota \le h_i \le 1.5 \cdot \bar{h}_\iota] = 1 - \alpha \\ P[\bar{h}_i - a_{1-\alpha} \cdot s(h_i) \le h_i \le \bar{h}_i + a_{1-\alpha} \cdot s(h_i)] = 1 - \alpha \end{cases}$$

$$0.5 \cdot \bar{h}_\iota = \bar{h}_\iota - a_{1-\alpha} \cdot s(h_i) \Leftrightarrow 0.5 \cdot \bar{h}_\iota = a_{1-\alpha} \cdot s(h_i) \Leftrightarrow \frac{0.5}{a_{1-\alpha}} = \frac{s(h_i)}{\bar{h}_\iota} = C_{v,h}$$

$$\frac{0.5}{C_{v.h}} = a_{1-\alpha} \qquad\qquad (C.10)$$

Normal Distribution, $N(0,1)$



| P | 1-α/2 | Z ≡ a₁₋α | Cᵥₕ |
|---|---|---|---|
| ≤ 2% | 0,990 | 2,33 | 0,21 |
| ≤ 10% | 0,950 | 1,65 | 0,30 |
| ≤ 20% | 0,900 | 1,28 | 0,39 |
| ≤ 33% | 0,835 | 0,97 | 0,52 |
| ≤ 50% | 0,750 | 0,67 | 0,74 |
| > 50% | - | - | ≥ 0,75 |
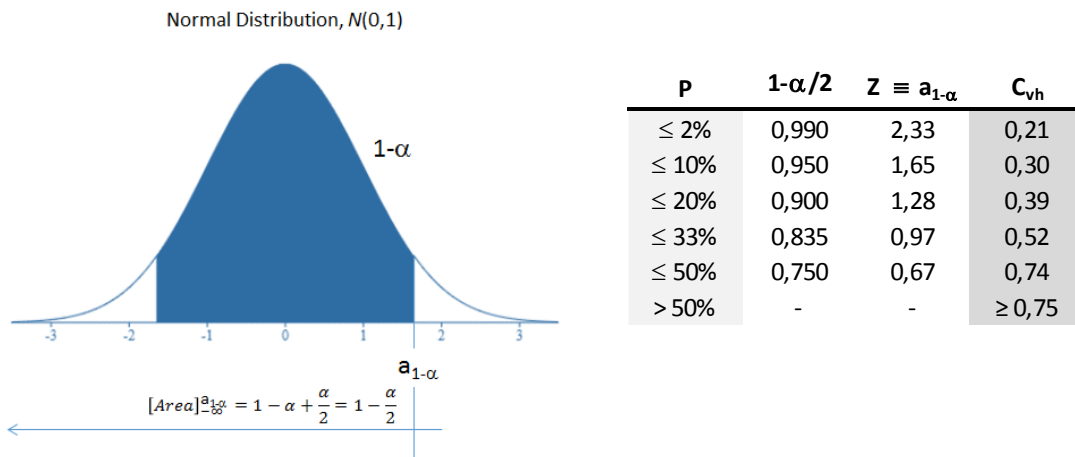
**Figure 86**. Normal Distribution and tail and $C_{v,h}$ associated values

Although it is difficult to explain to the stakeholders, it is the best available measure for describing the bunching effect.

## C.1.3 Traffic light settings of Problem 3

**Table 29**. Traffic light setting corresponding to Problem 3

| Intersection name | Signal phase | Green time ($g$, in seconds) | Cycle (Cp, in seconds) | Green time percentage ($g/C_p$) |
|---|---|---|---|---|
| Direction: Zona Universitaria to Fabra i Puig | | | | |
| Gonzalez Tables - Diagonal | 1 | 29 | 150 | 19% |
| Diagonal - Gregorio Marañon | 1 | 78 | 150 | 52% |
| Pius XII oest | 1 | 34 | 120 | 28% |
| Puis XII est | 1 | 34 | 120 | 28% |
| Diagonal / Maria Cristina | 1 | 34 | 120 | 28% |
| Mitre -Dr Roux | 5 | 60 | 108 | 56% |
| Mitre - Fleming | 5 | 50 | 108 | 46% |
| Mitre - Augusta | 5 | 50 | 108 | 46% |
| Mitre - Ganduxer - Freixa | 5 | 55 | 108 | 51% |
| Mitre - Mandri | 5 | 39 | 108 | 36% |
| Mitre -Muntaner | 5 | 35 | 108 | 32% |
| Mitre - Balmes | 5 | 41 | 108 | 38% |
| Mitre - Vallirana - Padua | 5 | 63 | 108 | 58% |
| Trav. Dalt - Torrent de l'Olla | 5 | 84 | 120 | 70% |
| Trav. Dalt - Verdi | 5 | 84 | 120 | 70% |
| Trav. Dalt - Massens - St. josep muntanya | 5 | 75 | 120 | 63% |
| Trav. Dalt - Escorial | 5 | 66 | 120 | 55% |
| Rda. Guinardó - Pi i Maragall - Pl. Alfons el Savi | 5 | 44 | 91 | 48% |
| Rda Guinardó - Tunels Rovira - Lepant | 5 | 25 | 91 | 27% |
| Rda. Guinardó - Padill - Túnels | 5 | 16 | 108 | 15% |
| Rda. Guinardó - Cartagena | 5 | 15 | 91 | 16% |
| Maragall - Ramon Albó | 5 | 10 | 91 | 11% |
| Felip II - Ramon Albó | 5 | 41 | 91 | 45% |
| Arnau d'Oms - Escòcia | 5 | 45 | 91 | 49% |
| Meridiana - Escocia - Dublin | 6 | 36 | 110 | 33% |

| Intersection name | Signal phase | Green time ($g$, in seconds) | Cycle (Cp, in seconds) | Green time percentage ($g/C_p$) |
|---|---|---|---|---|
| Direction: Fabra i Puig to Zona Universitaria | | | | |
| Meridiana - Fabra i Puig | 4 | 3 | 100 | 3% |
| Fabra i Puig - Arnau d'Oms | 5 | 37 | 91 | 41% |
| Fabra i Puig - Pi i Molist | 5 | 17 | 91 | 19% |
| Av. Borbó - Costa i Cuxart | 7 | 34 | 90 | 38% |
| Av. Borbó - Pg. Maragall - Av. Mare de Déu Montse | 6 | 28 | 91 | 31% |

| | | | | |
|---|---|---|---|---|
| Rda. Guinardó - Cartagena | 5 | 15 | 91 | 16% |
| Rda. Guinardó - Padill - Túnels | 5 | 16 | 108 | 15% |
| Rda Guinardó - Tunels Rovira - Lepant | 5 | 25 | 91 | 27% |
| Rda. Guinardó - Pi i Maragall - Pl. Alfons el Savi | 5 | 44 | 91 | 48% |
| Trav. Dalt - Escorial | 5 | 66 | 120 | 55% |
| Trav. Dalt - Massens - St. josep muntanya | 5 | 75 | 120 | 63% |
| Trav. Dalt - Verdi | 5 | 84 | 120 | 70% |
| Trav. Dalt - Torrent de l'Olla | 5 | 84 | 120 | 70% |
| Mitre - Vallirana - Padua | 5 | 63 | 108 | 58% |
| Mitre - Balmes | 5 | 41 | 108 | 38% |
| Mitre -Muntaner | 5 | 35 | 108 | 32% |
| Mitre - Mandri | 5 | 39 | 108 | 36% |
| Mitre - Ganduxer - Freixa | 5 | 55 | 108 | 51% |
| Mitre - Augusta | 5 | 50 | 108 | 46% |
| Mitre - Fleming | 5 | 50 | 108 | 46% |
| Mitre -Dr Roux | 5 | 60 | 108 | 56% |
| Pl. Prat de la Riba | 5 | 14 | 108 | 13% |
| Pg. Manuel Girona - Capita Arenas | 7 | 37 | 85 | 44% |
| Diagonal / Maria Cristina | 1 | 26 | 120 | 22% |
| Puis XII est | 1 | 34 | 120 | 28% |
| Pius XII oest | 1 | 34 | 120 | 28% |
| Diagonal - Gregorio Marañon | 1 | 78 | 150 | 52% |

# Appendix D

# Transit corridors served by two routes

## D.1    Transit corridors served by two routes

## D.1.1   Vehicle capacity constraint

The vehicle capacity constraint to be fulfilled in each route segment $i$ in the direction of service $x$ or $y$ is defined in Table 30.

**Table 30**. Summary of vehicle capacity constraint formulation for all route segments and available directions

| Route Segment | Formulation |
|---|---|
| i=1 direction x | $$H \cdot \max_{k^*}\left\{\sum_{j=1}^{5} B_{1j}^{x}(k^*) - A_{11}^{x}(k^*)\right\} \le C$$ |
| i=1 direction y | $$H \cdot \max_{k^*}\left\{B_{31}^{y} + B_{51}^{y} + B_{21}^{y} + B_{41}^{x} + B_{11}^{y}(k^*) - \sum_{j=1}^{5} A_{j1}^{y}(k^*)\right\} \le C$$ |
| i=2 direction x Route A | $$H \cdot \max_{k^*}\left\{B_{12}^{x} + B_{13}^{x} + B_{15}^{x} + B_{23}^{x}(k^*) + \frac{B_{22}^{x}(k^*)}{2} - \frac{A_{22}^{x}(k^*)}{2} - A_{12}^{x}(k^*)\right\} \le C$$ |
| i=2 direction y Route A | $$H \cdot \max_{k^*}\left\{B_{31}^{y} + B_{32}^{y} + B_{34}^{y} + B_{21}^{y}(k^*) + \frac{B_{22}^{y}(k^*)}{2} - \frac{A_{22}^{y}(k^*)}{2} - A_{32}^{y}(k^*)\right\} \le C$$ |
| i=2 direction x Route B | $$H \cdot \max_{k^*}\left\{B_{42}^{x} + B_{43}^{x} + B_{45}^{x} + B_{25}^{x}(k^*) + \frac{B_{22}^{x}(k^*)}{2} - \frac{A_{22}^{x}(k^*)}{2} - A_{42}^{x}(k^*)\right\} \le C$$ |
| i=2 direction y Route B | $$H \cdot \max_{k^*}\left\{B_{51}^{y} + B_{54}^{y} + B_{52}^{y} + B_{24}^{y}(k^*) + \frac{B_{22}^{y}(k^*)}{2} - \frac{A_{22}^{y}(k^*)}{2} - A_{52}^{y}(k^*)\right\} \le C$$ |
| i=3 direction x | $$H \cdot \max_{k^*}\left\{B_{13}^{x} + B_{23}^{x} + B_{43}^{x} + B_{53}^{y} + B_{33}^{x}(k^*) - \sum_{i=1}^{5} A_{i3}^{x}(k^*)\right\} \le C$$ |
| i=3 direction y | $$H \cdot \max_{k^*}\left\{\sum_{i=1}^{5} B_{3i}^{y}(k^*) - A_{33}^{y}(y^*)\right\} \le C$$ |

| i=4 direction x | $$H \cdot \max_{k^*} \left\{ \sum_{i=1}^{5} B_{4i}^x (k^*) - A_{44}^x(k^*) \right\} \leq C$$ |
|---|---|
| i=4 direction y | $$H \cdot \max_{k^*} \left\{ B_{54}^y + B_{34}^y + B_{24}^y + B_{14}^x + B_{44}^y(k^*) - \sum_{i=1}^{5} A_{i4}^y (k^*) \right\} \leq C$$ |
| i=5 direction x | $$H \cdot \max_{x^*} \left\{ B_{15}^x + B_{25}^x + B_{35}^y + B_{45}^x + B_{55}^x(k^*) - \sum_{i=1}^{5} A_{i5}^x (k^*) \right\} \leq C$$ |
| i=5 direction y | $$H \cdot \max_{k^*} \left\{ \sum_{i=1}^{5} B_{5i}^y (k^*) - A_{55}^y(k^*) \right\} \leq C$$ |

In route segment $i=1$ in direction $x$, the vehicle starts the motion at stop $k=1$ with 0 passengers on board. In the following stops, people travelling to this and other route segments may board. The only potential alighting movements are the ones generated by trips whose origin and destination are located along the length of segment $i=1$. In direction $y$, the vehicle occupancy at stop $k=1$ considers all the passengers that have boarded in previous segments, i.e. $H(B_{31}^y + B_{51}^y + B_{21}^y + B_{41}^x)$ to travel to route segment $i=1$. For $k>1$, the vehicle occupancy includes the positive contribution of cumulative boarding passengers along segment $i=1$ in direction $y$ as well as the negative contribution of cumulative alighting passengers travelling from all route segments.

The estimation of vehicle occupancies of route segments $i=3, 4, 5$ can be similarly obtained following the explanations for route segment $i=1$. However, the estimation of vehicle occupancy in route segment $i=2$ for bus route A and B needs further explanation. The contributions in the vehicle occupancy of passengers that have boarded in previous branching sections are affected by the time headway $H$. The operating time headway in branched segments is always $H$. However, all terms $A_{22}^x(k), A_{22}^y(k), B_{22}^x(k)$ and $B_{22}^y(k)$ are divided by 2 since people may choose between service A and B and therefore, the time headway of service in the trunk line is $H/2$.

### D.1.2 Route segment entrance time compatibility

The entrance times at segment $i=1$ and $i=4$ in direction x are considered to be decision variables. Once they are defined, the entrance time of the rest segments should be calculated sequentially in the order that vehicle runs along each route A and B. These entrance times need to verify the temporal compatibility with regard to the previous segment visited in the route A or B. Therefore, they are evaluated as the summation of the entrance time and the total travel time in the previous route segment. The resulting compatibility formulae are summarised in Equation (D.1).

$$t_{0,A}^{2x} = t_0^{1x} + \Delta T^{1x}(t_0^{1x})$$
$$t_{0,B}^{2x} = t_{IN0}^{4x} + \Delta T^{4x}(t_0^{4x})$$
$$t_0^{3x} = t_{0,A}^{2x} + \Delta T_A^{2x}(t_{0,A}^{2x})$$
$$t_0^{5x} = t_{0,B}^{2x} + \Delta T_B^{2x}(t_{0,B}^{2x})$$
$$t_0^{3y} = t_0^{3x} + \Delta T^{3x}(t_0^{3x})$$
$$t_0^{5y} = t_0^{5x} + \Delta T^{5x}(t_0^{5x})$$
$$t_{0,A}^{2y} = t_0^{3y} + \Delta T^{3y}(t_0^{3y})$$
$$t_{0,B}^{2y} = t_0^{5y} + \Delta T^{5y}(t_0^{5y})$$
$$t_0^{1y} = t_{0,A}^{2y} + \Delta T_A^{2y}(t_{0,B}^{2y})$$
$$t_0^{4y} = t_{0,B}^{2y} + \Delta T_B^{2y}(t_{0,B}^{2y})$$

(D1)

### D.1.3 Travel times between stop k and the first intersection

The estimation of travel time $tt_0^{iz}(k)$ between stop $k$ and the first intersection $\boldsymbol{p_1^{iz}}$ located downstream in route segment $i$ (direction z) would consider two different situations, represented by vehicle 1 and 2 in the following explanation. In Fig. 87 we plot the speed profile of vehicles 1 and 2 departing from stop $k$ at instantaneous speed $v_i=0$ to the first intersection, achieving the maximal cruising speed $v_i=v_{max}$. In Fig. 88 we plot the corresponding vehicle trajectories of these vehicles in a space-time diagram. We assume that vehicle 1 requires an acceleration time $\tau_1 = v_{max,1}/a$ lower than the corresponding to vehicle 2, $\tau_2 = v_{max,2}/a$ due to a different value of $v_{max}$. The required distances to achieve the maximal cruising speed for these vehicles are $x_{\tau,1} = \frac{1}{2}a\tau_1^2$ and $x_{\tau,2} = \frac{1}{2}a\tau_2^2$. Considering

the available distance $\Delta z$ between stop $k$ and first intersection, vehicle 1 achieves the maximal cruising speed before it arrives to intersection $\boldsymbol{p_1^{iz}}$ ($\Delta z \geq x_{\tau,1}$), while vehicle 2 is still accelerating when it arrives to $\boldsymbol{p_1^{iz}}$ ($\Delta z < x_{\tau,2}$). Therefore, the total travel time of vehicle 1 to overcome the distance $\Delta z$ in the segment of analysis is $tt(1) = \frac{(\Delta z - x_{\tau,1})}{v_{max}} + \tau_1$. However, the travel time of vehicle 2, referred by $tt(2)$, is the time needed to overcome the distance $\Delta z$ with a constant acceleration rate, i.e. $\Delta z = \frac{1}{2} a \cdot (tt(2))^2$. With some algebra, the travel time between stop $k$ and the first stop in the route segment $i$ direction $z$, given the maximal cruising speed $v_{max}$ and acceleration $a$, is computed by Equation (D2).

$$tt_0^{iz}(k) = \begin{cases} \dfrac{\Delta z}{v_{max}} + \dfrac{\tau}{2} & if \ \Delta z > \dfrac{1}{2} a \tau^2 \\ \sqrt{2 \cdot \Delta z / a} & otherwise \end{cases} \tag{D2}$$
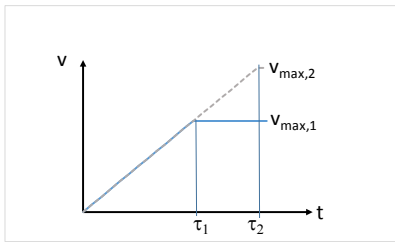


**Figure 87**.Speed profile in the speed-time diagram of vehicles between the stop and the next intersection
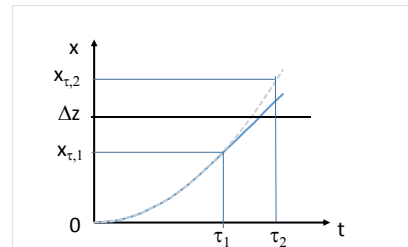


**Figure 88**. Vehicle trajectories in space-time diagram of vehicles between the stop and the next intersection
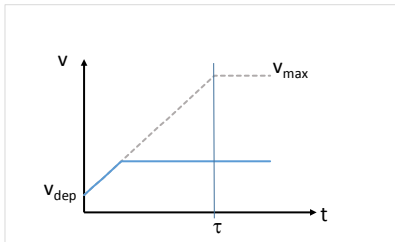


**Figure 89**.Speed profile in the speed-time diagram between consecutive intersections
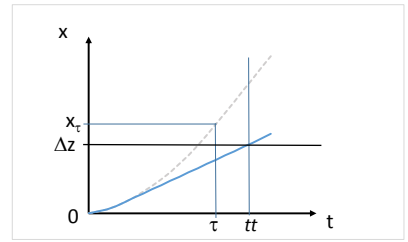


**Figure 90**. Vehicle trajectories in space-time diagram between successive intersections

### D.1.4 Travel times between intersections $\boldsymbol{p_j^{iz}, p_{j+1}^{iz}}$

We suppose that the instantaneous speed at which the vehicle crosses the intersection $\boldsymbol{p_j^{iz}}$ ($j=1,.., m_k^{iz} - 1$) is $v_{dep} = v_{dep}(j)$, where $v_{dep}(j)$, may range between (0, $v_{max}$). The lower bound means that the vehicle had to stop due to the red phase signal. The distance between intersections $\boldsymbol{p_j^{iz}}$ and $\boldsymbol{p_{j+1}^{iz}}$ is labeled by $\Delta z = x\left(p_{j+1}^{iz}\right) - x(p_j^{iz})$. The corresponding speed profile and vehicle trajectory is depicted in Figs. 89 and 90 respectively. The acceleration

time needed to achieve the maximal cruising speed would be $\tau_3 = (v_{max} - v_{dep})/a$. The distance run during the acceleration phase is $x_\tau = v_{dep}\tau_3 + \frac{1}{2}a\tau_3^2$. We consider two different situations. If $x_\tau < \Delta z$, the travel time between intersections is computed by $tt = \frac{(\Delta z - x_\tau)}{v_{max}} + \tau_3$. However, if the intersections spacing distance is too small to achieve the maximal cruising speed ($x_\tau > \Delta z$), the travel time $tt$ should be calculated through equation $\Delta z = v_{dep}tt + \frac{1}{2}a(tt)^2$. With some algebra, the travel time to overcome the distance $\Delta z$ between two intersections in route segment $i$ direction $z$ is calculated by Equation (D3).

$$tt_j^{iz}(k) = \begin{cases} \dfrac{\Delta z}{v_{max}} + \dfrac{(v_{max} - v_{dep}(j))^2}{2av_{max}} & if \quad \dfrac{v_{dep}(v_{max} - v_{dep})}{a} + \dfrac{1}{2}a\left\{\dfrac{(v_{max} - v_{dep})}{a}\right\}^2 < \Delta z \\ \dfrac{-v_{dep}(j) + \sqrt{2 \cdot \Delta z \cdot a + v_{dep}(j)^2}}{a} & otherwise \end{cases} \tag{D3}$$

The estimation of the departure speed from the intersection $\boldsymbol{p}_{j+1}^{iz}$ in case the traffic light is in green will be defined by Equation (D4)

$$v_{des}(j+1) = \begin{cases} v_{max} & if \quad \dfrac{v_{dep}(v_{max} - v_{dep})}{a} + \dfrac{1}{2}a\left\{\dfrac{(v_{max} - v_{dep})}{a}\right\}^2 < \Delta z \\ \sqrt{2 \cdot \Delta z \cdot a + v_{dep}^2} & otherwise \end{cases} \tag{D4}$$

### D.1.5 Travel time between the last intersection $\boldsymbol{p}_{m_k^{iz}}^{iz}$ and stop k+1

The analysis may consider 5 potential situations, depending on the feasible bus speed profiles along the distance $\Delta z = \sum_{m=1}^{k} s_m^{iz} - \boldsymbol{x}(\boldsymbol{p}_{m_k^{iz}}^{iz})$ between the last intersection and the next stop $k+1$. These situations are depicted in Figs. 91 and 92 in a speed-time and space-time diagram respectively.
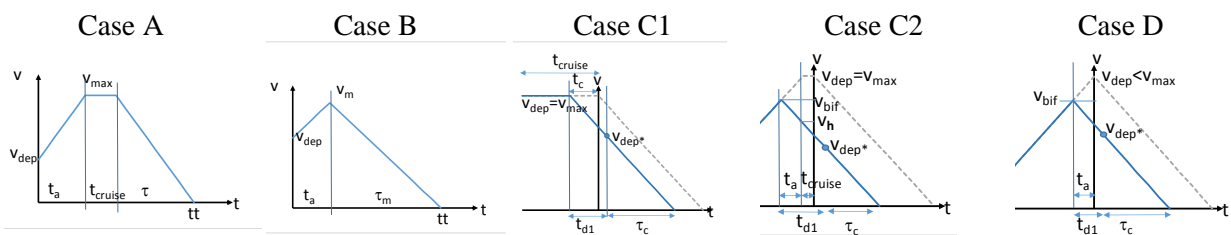


**Figure 91**.Speed profile in the speed-time diagram between last intersection and the next stop
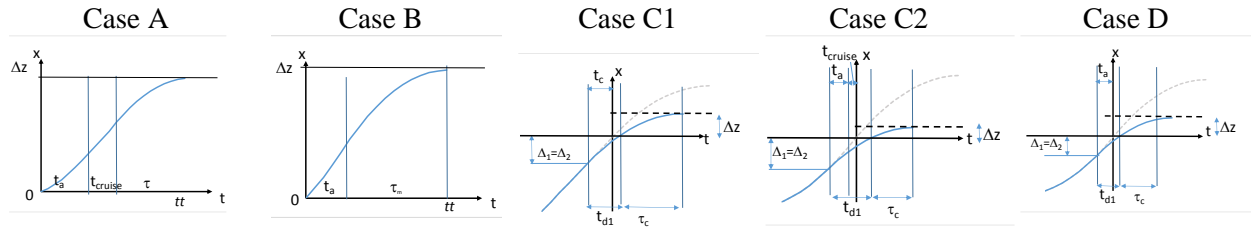
**Figure 92**. Vehicle trajectory in the space-time diagram between last intersection and the next stop

**Case A.** It is supposed that the distance $\Delta z$ is large enough to accelerate, achieve the maximal cruising speed and reduce constantly the speed up to stop the vehicle. We suppose that vehicle departs from intersection $j=m_k^{iz}$ at speed $v_{dep}(m_k^{iz})$. The acceleration time needed to achieve the maximal cruising speed is $t_a = (v_{max} - v_{dep}(m_k^{iz}))/a$ while the braking time before arriving to stop $k+1$ is $\tau = v_{max}/a$. The distance travelled during this time $(t_a + \tau)$ can be demonstrated to be $x_\tau = \frac{(v_{max})^2}{a} + \frac{\left(v_{des}(m_k^{iz})\right)^2}{2a}$. Therefore, if $x_\tau < \Delta z$, the travel time between intersection $j=m_k^{iz}$ and stop $k+1$ can be calculated by $tt = t_a + \frac{(\Delta z - x_\tau)}{v_{max}} + \tau$. With some algebra, the travel time to overcome the distance $\Delta z$ between intersection $p_{m_k^{iz}}^{iz}$ and next stop $k+1$ in route segment $i$ direction $z$ is calculated by Equation (D5). The following cases (b-d) are analyzed when $x_\tau > \Delta z$.

$$tt_j^{iz}(k) = \frac{.\Delta z}{v_{max}} + \frac{v_{max} - v_{dep}(m_k^{iz})\left(1 - \frac{v_{dep}(j)}{2v_{max}}\right)}{a} \qquad if \quad \frac{(v_{max})^2}{a} + \frac{\left(v_{des}(m_k^{iz})\right)^2}{2a} < \Delta z \qquad (D5)$$

**Case B.** This situation happens when the vehicle departs from intersection $j=m_k^{iz}$ at speed $v_{dep}(m_k^{iz}) < v_{max}$. Due to the distance limitation, the vehicle only accelerates until the instantaneous speed $v_m$ ($v_m > v_{dep}$) is achieved, consuming a time $t_a = \frac{v_m - v_{dep}(m_k^{iz})}{a}$. After that, a uniformly deaccelerating motion phase is undergone until the vehicle stops at the location of stop $k+1$, spending $\tau_m = \frac{v_m}{a}$. The distance run during this time $(t_a + \tau_m)$ should be equal to the distance $\Delta z$ between the last intersection and next stop $k+1$. Therefore, the following equation states: $\Delta z = t_a \cdot v_{dep}(m_k^{iz}) + \frac{1}{2}at_a^2 + \frac{1}{2}a\tau_m^2$. This situation can only happen if $\Delta z > \frac{1}{2}a\left(\frac{v_{dep}(m_k^{iz})}{a}\right)^2$, i.e. the required distance to change speed from $v = v_{dep}(m_k^{iz})$ to $v = 0$ is lower than the available distance between the intersection and the stop.

With some algebra, the maximal speed peak is $v_m = \sqrt{a\Delta z + \frac{\left(v_{dep}(m_k^{iz})\right)^2}{2}}$ and the corresponding travel time to overcome the distance $\Delta z$ between intersection $p_{m_k^{iz}}^{iz}$ and route $k+1$ in route segment $i$ direction $z$ is calculated by Equation (D6).

$$t_{m_k^{iz}}^{iz}(k) = \frac{2\sqrt{a\Delta z + \frac{\left(v_{dep}(m_k^{iz})\right)^2}{2}} - v_{dep}(m_k^{iz})}{a} \quad if \quad \frac{(v_{max})^2}{a} + \frac{\left(v_{des}(m_k^{iz})\right)^2}{2a} > \Delta z > \frac{1}{2}a\left(\frac{v_{dep}(m_k^{iz})}{a}\right)^2 \quad (D6)$$

**Case C.** This case represents the situation when $v_{dep}\left(m_k^{iz}\right) = v_{max}$ and $\Delta z < \frac{1}{2}a\left(\frac{v_{dep}(m_k^{iz})}{a}\right)^2$. It is impossible to stop the vehicle in the available distance $\Delta z$ between the last intersection and the next stop $k+1$. It means that this vehicle must have started braking in the segment between intersections $j=m_k^{iz} - 1$, $j+1=m_k^{iz}$ to arrive at stop $k+1$ at instantaneous speed $v_i=0$ with a constant deceleration rate. The required instantaneous speed at intersection $j = m_k^{iz}$ will be modified to be $v_{dep*} = \sqrt{2a\Delta z}$, imposing the vehicle must be stopped in a distance $\Delta z$, consuming $\tau_c = \frac{v_{dep*}}{a}$ units of time. In that case, we have to consider two potential cases. Let $t_{cruise}$ be the amount of time the vehicle is running at the maximal cruising speed $v_{max}$ before arriving at intersection $m_k^{iz}$.

> **Case C1.** This situation happens when $t_{cruise} > \frac{v_{max}-v_{dep*}}{a}$, i.e., the vehicle would achieve the maximal cruising speed in the segment between intersections $j=m_k^{iz} - 1$, $j+1=m_k^{iz}$ in the modified speed pattern. The speed profile of the theoretical bus trajectory must be modified $t_c$ units of time before arriving at the intersection. In this time period, the modelled trajectory of the vehicle has overcome a distance $\Delta 1 = v_{max}t_c$ to arrive at the last intersection. In order to guarantee the compatibility, this distance must be equal to the one run by the modified trajectory, $\Delta 2 = v_{max}(t_{d1}) - \frac{1}{2}at_{d1}^2$, where $t_{d1} = (v_{max} - v_{dep*})/a$. Letting $\Delta 1 = \Delta 2$, we can obtain $t_c = \frac{(v_{max}-v_{des*})}{a} - \frac{(v_{max}-v_{des*})^2}{2av_{max}}$. Therefore, the travel time can be computed as $tt = t_{d1} + \tau_c - t_c$. Finally, the corresponding travel time to overcome the distance $\Delta z$ between intersection $p_{m_k^{iz}}^{iz}$ and stop $k+1$ in route segment $i$ direction $z$ is calculated by Equation (D7).

$$tt^{iz}_{m^{iz}_k}(k) = \frac{\sqrt{2a\Delta z}}{a} - \frac{(v_{max} - \sqrt{2a\Delta z})^2}{2av_{max}} \tag{D7}$$

**Case C2.** Oppositely to case C1, this situation happens when $t_{cruise} < \frac{v_{max}-v_{dep*}}{a}$, i.e., the vehicle could not achieve the maximal cruising speed in the segment between intersections $j=m^{iz}_k - 1$, $j+1=m^{iz}_k$ in the modified speed pattern. Let us assume from Fig. 35 that the maximal speed achieved is $v_{bif}$ to be able to hold at stop $k+1$. Therefore, the speed profile of the bus must be modified $(t_{cruise} + t_a)$ units of time before arriving at the intersection, where $t_a = (v_{max} - v_{bif})/a$. In this time period, the modelled trajectory of the vehicle has overcome a distance $\Delta 1 = v_{bif}t_a + \frac{1}{2}at_a^2 + t_{cruise}v_{max}$ to arrive at the last intersection $p^{iz}_{m^{iz}_k}$. In order to guarantee the compatibility, this distance must be equal to the one run by the modified trajectory, $\Delta 2 = v_{bif}(t_{d1}) - \frac{1}{2}at_{d1}^2$, where $t_{d1} = (v_{bif} - v_{dep*})/a$. Letting $\Delta 1 = \Delta 2$, we can obtain $v_{bif} = \sqrt{\frac{v_{max}^2 + v_{dep*}^2 + 2v_{max}at_{cruise}}{2}}$. Therefore, the travel time can be computed as $tt = t_{d1} + \tau_c - (t_{cruise} + t_a)$. Finally, the corresponding travel time to overcome the distance $\Delta z$ between intersection $p^{iz}_{m^{iz}_k}$ and stop $k+1$ in route segment $i$ direction $z$ is calculated in Equation (D8).

$$tt^{iz}_{m^{iz}_k}(k) = \frac{2\sqrt{\frac{v_{max}^2 + v_{dep}^2 + 2v_{max}at_{cruise}}{2}} - v_{max}}{a} - t_{cruise} \tag{D8}$$

**Case D.** Finally, this case represents the situation when $v_{dep}(m^{iz}_k) < v_{max}$ and $\Delta z < \frac{1}{2}a\left(\frac{v_{dep}(m^{iz}_k)}{a}\right)^2$. As it is justified in Case C, the vehicle must have started braking in the segment between intersections $j=m^{iz}_k - 1$, $j+1=m^{iz}_k$ to arrive at stop $k+1$ at instantaneous speed $v_i=0$ with a constant deceleration rate. The required speed at intersection $j = m^{iz}_k$ will be modified to be $v_{dep*} = \sqrt{2a\Delta z}$, consuming $\tau_c = \frac{v_{dep*}}{a}$ units of time. It forces that the vehicle should have started braking $t_a = (v_{dep} - v_{bif})/a$ units of time before the arrival of the theoretical vehicle at the intersection, when the instantaneous speed was $v_{bif}$. During this time $t_a$, the theoretical vehicle has overcome a total distance $\Delta 1 = v_{bif}t_a + \frac{1}{2}at_a^2$. Distance

$\Delta 2 = v_{bif} t_{d1} - \frac{1}{2} a t_{d1}^2$ should be run by the vehicle with the modified trajectory during the time $t_{d1} = (v_{bif} - v_{dep*})/a$. As the condition $\Delta 2 = \Delta 1$ must be verified to ensure compatibility, we obtain with some algebra $v_{bif} = \sqrt{\frac{v_{dep}^2 + v_{dep*}^2}{2}}$. The travel time can be computed as $tt = t_{d1} + \tau_c - t_a$. Hence, the corresponding travel time to overcome the distance $\Delta z$ between intersection $p_{m_k^{iz}}^{iz}$ and stop $k+1$ in route segment $i$ direction $z$ is estimated in Equation (D9).

$$tt_{m_k^{iz}}^{iz}(k) = \frac{\left( \sqrt{2(v_{dep}^2 + 2a\Delta z)} - v_{dep} \right)}{a} \tag{D9}$$

# Appendix E

# Transfer areas

## E.1   Transfer areas

### E.1.1   Semi-axes and rotating angle

For a prefixed quality, the values $\mu_T, \sigma_T$ that meet equation:

$$TQR(\mu_T, \sigma_T) = 100 + a_{11}\mu_T^{\,2} + a_{22}\sigma_T^{\,2} + 2a_{12}\mu_T\sigma_T$$

define an ellipse centred at the point (0.0), with semi-axles a and b, and rotation angle θ (Remark 3). In this context, it is of interest to relate a, b and θ with the parameters $a_{11}, a_{22}$ and $a_{12}$.

The change of coordinates due to the angle rotation θ (Kom and Kom, 2000),

$$\begin{pmatrix} \mu_T \\ \sigma_T \end{pmatrix} = \begin{pmatrix} \cos\theta & -\sin\theta \\ \sin\theta & \cos\theta \end{pmatrix} \cdot \begin{pmatrix} x \\ y \end{pmatrix}$$

allows obtaining the reduced equation of the oblique ellipse. In particular, the following equals,

$$100 - TQR + a_{11}\mu_T^{\,2} + a_{22}\sigma_T^{\,2} + 2a_{12}\mu_T\sigma_T$$

$$= 100 + (x.y) \cdot \begin{pmatrix} \cos\theta & \sin\theta \\ -\sin\theta & \cos\varphi \end{pmatrix} \cdot \begin{pmatrix} a_{11} & a_{12} \\ a_{12} & a_{22} \end{pmatrix} \cdot \begin{pmatrix} \cos\theta & -\sin\theta \\ \sin\theta & \cos\theta \end{pmatrix} \cdot \begin{pmatrix} x \\ y \end{pmatrix}$$

$$= 100 - TQR + Ax^2 + By^2 + Cxy$$

relate the coefficients of the rotated ellipse with the parameters that define the straight ellipse of the reduced equation, $x^2/a^2 + y^2/b^2 = 1$ (when C = 0), being

$$A = a_{11}\cos^2\theta + a_{12}\sin 2\theta + a_{22}\sin^2\theta$$
$$B = a_{11}\sin^2\theta - a_{12}\sin 2\theta + a_{22}\cos^2\theta$$
$$C = 1/2(a_{22} - a_{11})\sin 2\theta + a_{11}\cos 2\theta$$

Consequently,

$$a = \left(\frac{TQR - 100}{A}\right)^{1/2} = \left(\frac{TQR - 100}{0.5(A + B) + 0.5(A - B)}\right)^{1/2}$$

$$= \left(\frac{2(TQR - 100)}{a_{11} + a_{22} + sig(a_{11} - a_{22})[(a_{11} - a_{22})^2 + 4a_{12}^2]^{1/2}}\right)^{1/2} \tag{E.1}$$

$$b = \left(\frac{TQR - 100}{B}\right)^{1/2} = \left(\frac{TQR - 100}{0.5(A + B) - 0.5(A - B)}\right)^{1/2} \tag{E.2}$$

$$= \left( \frac{2(TQR - 100)}{a_{11} + a_{22} - \text{sig}(a_{11} - a_{22})[(a_{11} - a_{22})^2 + 4a_{12}^2]^{1/2}} \right)^{1/2}$$

$$\theta = \frac{1}{2} \tan^{-1} \left( \frac{2a_{12}}{a_{11} - a_{22}} \right), \quad \text{when } C = 0 \tag{E.3}$$

### E.1.2 Domain quadratic boundary

We should calculate the maximum angle $\theta_{max}$ at which point the boundary of ellipse becomes a straight line. Then, we will set $\theta = \theta_{max}/2$. Two methods are considered:

a.- Method based on the mean error

b.- Method based on the curvature

#### E.1.2.1 Method based on the mean error

This method consists of 3 stages:

1.- Determining the mean as a function of the parameter $\alpha$, $\alpha \in (0,1)$, proportional to the length of the major semi-axle of the ellipse a; and $\beta \in [0, 0.2]$, that leads the vertical movement of the segment $\overline{BA}$.

2.- Determining $\alpha$, so that the mean error is $\leq 5\%b$, where b is the minor semi-axel of the ellipse.

3.- Determining the maximum value of angle $\theta_{max}$ and $\theta_1$.

*Mean error as a function of $\alpha$ and $\beta$*

Ellipse $\frac{x^2}{a^2} + \frac{y^2}{b^2} = 1 \Leftrightarrow y = b \cdot \left( 1 - \frac{x^2}{a^2} \right)^{1/2} = b \cdot (1 - \alpha^2)^{1/2}, \; for \; x = \alpha \cdot a$
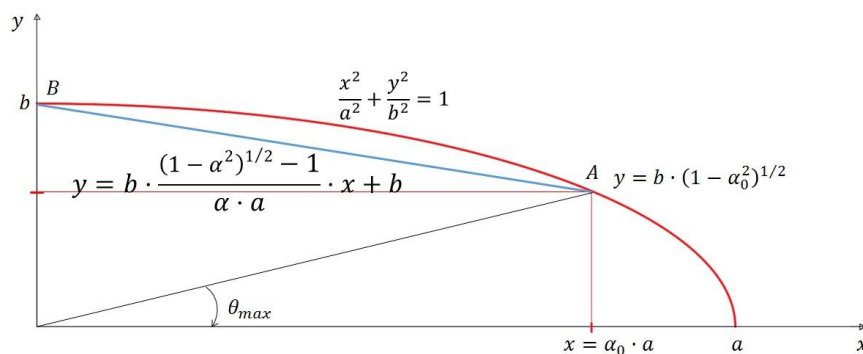


**Figure 93.** Representation of ¼ ellipse and chord $\overline{AB}$ and angle $\theta_{max}$.

The equation of the chord passing through: $(0, b) \; and \; \left( \alpha a, (1 - \alpha^2)^{1/2} \right) \implies$

$$y = b \frac{(1 - \alpha^2)^{1/2} - 1}{\alpha a} x + b$$

If we want to move the chord AB vertically upwards using parameter $\beta \in [0, 0.2]$, the equation of the chord will be:

$$y = b \frac{(1 - \alpha^2)^{1/2} - 1}{\alpha \cdot a} x + b + \beta b \implies y = b \left[ \frac{(1 - \alpha^2)^{1/2} - 1}{\alpha \cdot a} x + (1 + \beta) \right]$$

Consequently, for each $\alpha$ and $\beta$, the mean error will be:

$$EM_{\alpha.\beta} = \frac{\int_{x=0}^{x=\alpha a} abs \left[ b \cdot \left( 1 - \frac{x^2}{a^2} \right)^{1/2} - b \left( \frac{(1 - \alpha^2)^{1/2} - 1}{\alpha a} x + (1 + \beta) \right) \right] dx}{\alpha \cdot a}$$

And the mean error, $EM_\alpha = \min_\beta \{ EM_{\alpha,\beta} \}$

*Determining $\alpha$ so that the mean error $\leq 0.05b$*

$$EM_{\alpha.\beta} = \frac{b \cdot \int_{x=0}^{x=\alpha a} abs \left[ \left( 1 - \left( \frac{x}{a} \right)^2 \right)^{1/2} - \left( \frac{(1 - \alpha^2)^{1/2} - 1}{\alpha} \left( \frac{x}{a} \right) + (1 + \beta) \right) \right] dx}{\alpha \cdot a}$$

Replacing the variable under analysis: $\frac{x}{a} = t \Rightarrow x = a \cdot t \Rightarrow dx = a \cdot dt$

$$EM_{\alpha.\beta} = \frac{a \cdot b \cdot \int_{t=0}^{t=\alpha} abs \left[ (1 - t^2)^{1/2} - \left( \frac{(1 - \alpha^2)^{1/2} - 1}{\alpha} t + (1 + \beta) \right) \right] dt}{\alpha \cdot a}$$

If $EM_{\alpha,\beta} \leq 0.05 \cdot b$, then:

$$I = \frac{1}{\alpha} \cdot \int_0^\alpha abs \left[ (1 - t^2)^{1/2} - \left( \frac{(1 - \alpha^2)^{1/2} - 1}{\alpha} t + (1 + \beta) \right) \right] dt \leq 0.05$$

Independent term of a and b, semi-axles of the ellipse.

At this point, with a small routine with MatLab IT application, we vary $\alpha$ and $\beta$, and we determine for each value of the minimum value of the integral according to the different values of $\beta$. Finally, we take as the value of $\alpha$, that one that makes that the integral value is just under 0:05.

Varying $\alpha$ and $\beta$ with length increments, $\Delta = 0.01$, with in the ranges: $\alpha \in [0.6, 0.95] \wedge \beta \in [0, 0.2]$. We can get the following values of the integral, I from Table 30:
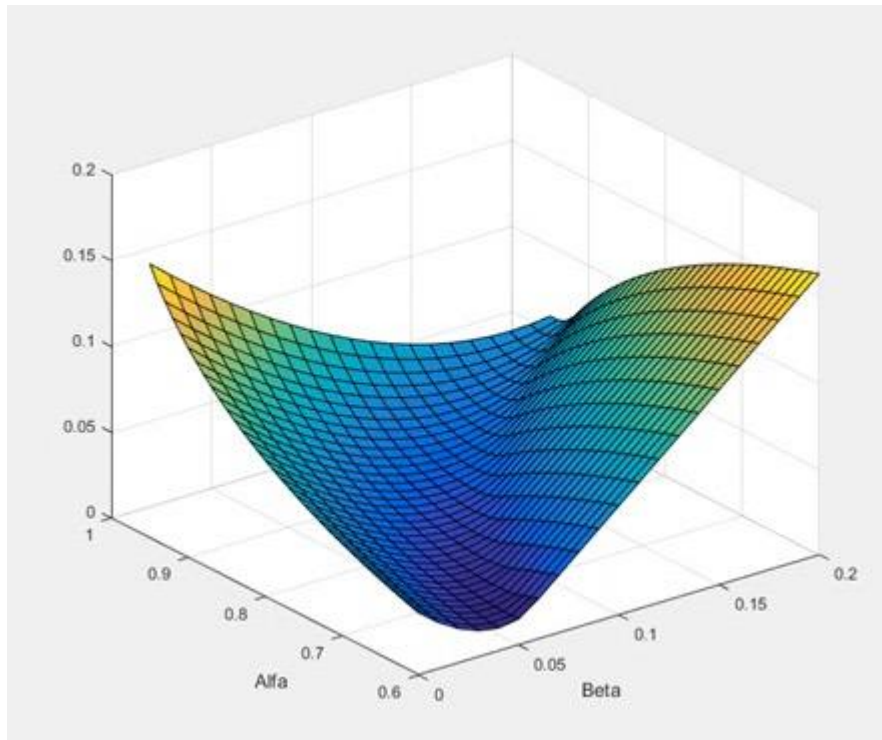
**Figure 94.** Graphic representation of I($\alpha$, $\beta$)

**Table 31**. Numeric representation of I($\alpha$, $\beta$) and minimum values of rows and columns.

| Alfa, $\alpha$ \ Beta, $\beta$ | 0,00 | 0,01 | 0,02 | 0,03 | 0,04 | 0,05 | 0,06 | 0,07 | 0,08 | 0,09 | 0,10 | 0,11 | 0,12 | 0,13 | 0,14 | 0,15 | 0,16 | 0,17 | 0,18 | 0,19 | 0,20 | Min |
|---|---|---|---|---|---|---|---|---|---|---|---|---|---|---|---|---|---|---|---|---|---|---|
| 0,60 | 0,0363 | 0,0272 | 0,0201 | 0,0154 | 0,0134 | 0,0153 | 0,0237 | 0,0337 | 0,0437 | 0,0537 | 0,0637 | 0,0737 | 0,0837 | 0,0937 | 0,1037 | 0,1137 | 0,1237 | 0,1337 | 0,1437 | 0,1537 | 0,1637 | 0,0134 |
| 0,61 | 0,0378 | 0,0286 | 0,0215 | 0,0165 | 0,0141 | 0,0151 | 0,0222 | 0,0322 | 0,0422 | 0,0522 | 0,0622 | 0,0722 | 0,0822 | 0,0922 | 0,1022 | 0,1122 | 0,1222 | 0,1322 | 0,1422 | 0,1522 | 0,1622 | 0,0141 |
| 0,62 | 0,0393 | 0,0302 | 0,0229 | 0,0176 | 0,0149 | 0,0152 | 0,0207 | 0,0307 | 0,0407 | 0,0507 | 0,0607 | 0,0707 | 0,0807 | 0,0907 | 0,1007 | 0,1107 | 0,1207 | 0,1307 | 0,1407 | 0,1507 | 0,1607 | 0,0149 |
| 0,63 | 0,0409 | 0,0317 | 0,0243 | 0,0189 | 0,0157 | 0,0154 | 0,0193 | 0,0291 | 0,0391 | 0,0491 | 0,0591 | 0,0691 | 0,0791 | 0,0891 | 0,0991 | 0,1091 | 0,1191 | 0,1291 | 0,1391 | 0,1491 | 0,1591 | 0,0154 |
| 0,64 | 0,0426 | 0,0334 | 0,0258 | 0,0202 | 0,0167 | 0,0158 | 0,0185 | 0,0274 | 0,0374 | 0,0474 | 0,0574 | 0,0674 | 0,0774 | 0,0874 | 0,0974 | 0,1074 | 0,1174 | 0,1274 | 0,1374 | 0,1474 | 0,1574 | 0,0158 |
| 0,65 | 0,0443 | 0,0350 | 0,0274 | 0,0216 | 0,0178 | 0,0164 | 0,0182 | 0,0257 | 0,0357 | 0,0457 | 0,0557 | 0,0657 | 0,0757 | 0,0857 | 0,0957 | 0,1057 | 0,1157 | 0,1257 | 0,1357 | 0,1457 | 0,1557 | 0,0164 |
| 0,66 | 0,0461 | 0,0368 | 0,0291 | 0,0230 | 0,0189 | 0,0171 | 0,0181 | 0,0239 | 0,0339 | 0,0439 | 0,0539 | 0,0639 | 0,0739 | 0,0839 | 0,0939 | 0,1039 | 0,1139 | 0,1239 | 0,1339 | 0,1439 | 0,1539 | 0,0171 |
| 0,67 | 0,0479 | 0,0386 | 0,0308 | 0,0246 | 0,0202 | 0,0179 | 0,0182 | 0,0223 | 0,0321 | 0,0421 | 0,0521 | 0,0621 | 0,0721 | 0,0821 | 0,0921 | 0,1021 | 0,1121 | 0,1221 | 0,1321 | 0,1421 | 0,1521 | 0,0179 |
| 0,68 | 0,0498 | 0,0405 | 0,0326 | 0,0262 | 0,0215 | 0,0189 | 0,0186 | 0,0215 | 0,0302 | 0,0402 | 0,0502 | 0,0602 | 0,0702 | 0,0802 | 0,0902 | 0,1002 | 0,1102 | 0,1202 | 0,1302 | 0,1402 | 0,1502 | 0,0186 |
| 0,69 | 0,0518 | 0,0424 | 0,0344 | 0,0279 | 0,0230 | 0,0200 | 0,0191 | 0,0211 | 0,0282 | 0,0382 | 0,0482 | 0,0582 | 0,0682 | 0,0782 | 0,0882 | 0,0982 | 0,1082 | 0,1182 | 0,1282 | 0,1382 | 0,1482 | 0,0191 |
| 0,70 | 0,0539 | 0,0445 | 0,0364 | 0,0297 | 0,0246 | 0,0212 | 0,0199 | 0,0211 | 0,0261 | 0,0361 | 0,0461 | 0,0561 | 0,0661 | 0,0761 | 0,0861 | 0,0961 | 0,1061 | 0,1161 | 0,1261 | 0,1361 | 0,1461 | 0,0199 |
| 0,71 | 0,0560 | 0,0466 | 0,0384 | 0,0316 | 0,0262 | 0,0225 | 0,0207 | 0,0212 | 0,0249 | 0,0340 | 0,0440 | 0,0540 | 0,0640 | 0,0740 | 0,0840 | 0,0940 | 0,1040 | 0,1140 | 0,1240 | 0,1340 | 0,1440 | 0,0207 |
| 0,72 | 0,0582 | 0,0488 | 0,0405 | 0,0335 | 0,0280 | 0,0240 | 0,0218 | 0,0216 | 0,0243 | 0,0318 | 0,0418 | 0,0518 | 0,0618 | 0,0718 | 0,0818 | 0,0918 | 0,1018 | 0,1118 | 0,1218 | 0,1318 | 0,1418 | 0,0216 |
| 0,73 | 0,0605 | 0,0510 | 0,0427 | 0,0356 | 0,0299 | 0,0256 | 0,0230 | 0,0223 | 0,0240 | 0,0295 | 0,0395 | 0,0495 | 0,0595 | 0,0695 | 0,0795 | 0,0895 | 0,0995 | 0,1095 | 0,1195 | 0,1295 | 0,1395 | 0,0223 |
| 0,74 | 0,0629 | 0,0534 | 0,0450 | 0,0378 | 0,0319 | 0,0273 | 0,0243 | 0,0231 | 0,0241 | 0,0281 | 0,0371 | 0,0471 | 0,0571 | 0,0671 | 0,0771 | 0,0871 | 0,0971 | 0,1071 | 0,1171 | 0,1271 | 0,1371 | 0,0231 |
| 0,75 | 0,0654 | 0,0559 | 0,0474 | 0,0401 | 0,0340 | 0,0292 | 0,0258 | 0,0241 | 0,0244 | 0,0273 | 0,0346 | 0,0446 | 0,0546 | 0,0646 | 0,0746 | 0,0846 | 0,0946 | 0,1046 | 0,1146 | 0,1246 | 0,1346 | 0,0241 |
| 0,76 | 0,0680 | 0,0585 | 0,0499 | 0,0425 | 0,0362 | 0,0311 | 0,0275 | 0,0254 | 0,0251 | 0,0270 | 0,0322 | 0,0420 | 0,0520 | 0,0620 | 0,0720 | 0,0820 | 0,0920 | 0,1020 | 0,1120 | 0,1220 | 0,1320 | 0,0251 |
| 0,77 | 0,0707 | 0,0611 | 0,0526 | 0,0450 | 0,0385 | 0,0333 | 0,0293 | 0,0268 | 0,0259 | 0,0270 | 0,0308 | 0,0393 | 0,0493 | 0,0593 | 0,0693 | 0,0793 | 0,0893 | 0,0993 | 0,1093 | 0,1193 | 0,1293 | 0,0259 |
| 0,78 | 0,0735 | 0,0639 | 0,0553 | 0,0476 | 0,0410 | 0,0355 | 0,0313 | 0,0284 | 0,0270 | 0,0274 | 0,0301 | 0,0365 | 0,0465 | 0,0565 | 0,0665 | 0,0765 | 0,0865 | 0,0965 | 0,1065 | 0,1165 | 0,1265 | 0,0270 |
| 0,79 | 0,0765 | 0,0669 | 0,0582 | 0,0504 | 0,0437 | 0,0380 | 0,0334 | 0,0302 | 0,0283 | 0,0281 | 0,0299 | 0,0344 | 0,0435 | 0,0535 | 0,0635 | 0,0735 | 0,0835 | 0,0935 | 0,1035 | 0,1135 | 0,1235 | 0,0281 |
| 0,80 | 0,0796 | 0,0700 | 0,0612 | 0,0534 | 0,0464 | 0,0406 | 0,0357 | 0,0321 | 0,0299 | 0,0291 | 0,0301 | 0,0333 | 0,0404 | 0,0504 | 0,0604 | 0,0704 | 0,0804 | 0,0904 | 0,1004 | 0,1104 | 0,1204 | 0,0291 |
| 0,81 | 0,0828 | 0,0732 | 0,0644 | 0,0564 | 0,0494 | 0,0433 | 0,0383 | 0,0343 | 0,0317 | 0,0303 | 0,0306 | 0,0329 | 0,0378 | 0,0472 | 0,0572 | 0,0672 | 0,0772 | 0,0872 | 0,0972 | 0,1072 | 0,1172 | 0,0303 |
| 0,82 | 0,0862 | 0,0766 | 0,0677 | 0,0597 | 0,0525 | 0,0463 | 0,0410 | 0,0367 | 0,0337 | 0,0319 | 0,0315 | 0,0329 | 0,0364 | 0,0438 | 0,0538 | 0,0638 | 0,0738 | 0,0838 | 0,0938 | 0,1038 | 0,1138 | 0,0315 |
| 0,83 | 0,0898 | 0,0802 | 0,0713 | 0,0632 | 0,0558 | 0,0494 | 0,0439 | 0,0394 | 0,0359 | 0,0337 | 0,0327 | 0,0334 | 0,0358 | 0,0408 | 0,0502 | 0,0602 | 0,0702 | 0,0802 | 0,0902 | 0,1002 | 0,1102 | 0,0327 |
| 0,84 | 0,0936 | 0,0840 | 0,0750 | 0,0668 | 0,0594 | 0,0528 | 0,0470 | 0,0422 | 0,0385 | 0,0358 | 0,0343 | 0,0342 | 0,0358 | 0,0393 | 0,0464 | 0,0564 | 0,0664 | 0,0764 | 0,0864 | 0,0964 | 0,1064 | 0,0342 |
| 0,85 | 0,0976 | 0,0880 | 0,0790 | 0,0707 | 0,0631 | 0,0564 | 0,0504 | 0,0454 | 0,0413 | 0,0382 | 0,0362 | 0,0355 | 0,0362 | 0,0387 | 0,0435 | 0,0524 | 0,0624 | 0,0724 | 0,0824 | 0,0924 | 0,1024 | 0,0355 |
| 0,86 | 0,1019 | 0,0922 | 0,0832 | 0,0748 | 0,0671 | 0,0602 | 0,0541 | 0,0488 | 0,0443 | 0,0409 | 0,0385 | 0,0372 | 0,0372 | 0,0387 | 0,0421 | 0,0482 | 0,0581 | 0,0681 | 0,0781 | 0,0881 | 0,0981 | 0,0372 |
| 0,87 | 0,1064 | 0,0967 | 0,0876 | 0,0792 | 0,0714 | 0,0643 | 0,0580 | 0,0525 | 0,0478 | 0,0439 | 0,0411 | 0,0393 | 0,0386 | 0,0393 | 0,0415 | 0,0458 | 0,0536 | 0,0636 | 0,0736 | 0,0836 | 0,0936 | 0,0386 |
| 0,88 | 0,1113 | 0,1016 | 0,0924 | 0,0839 | 0,0760 | 0,0688 | 0,0623 | 0,0565 | 0,0515 | 0,0473 | 0,0441 | 0,0417 | 0,0405 | 0,0404 | 0,0417 | 0,0446 | 0,0497 | 0,0587 | 0,0687 | 0,0787 | 0,0887 | 0,0404 |
| 0,89 | 0,1165 | 0,1068 | 0,0976 | 0,0890 | 0,0810 | 0,0736 | 0,0669 | 0,0609 | 0,0557 | 0,0512 | 0,0475 | 0,0447 | 0,0429 | 0,0421 | 0,0426 | 0,0444 | 0,0482 | 0,0538 | 0,0635 | 0,0735 | 0,0835 | 0,0421 |
| 0,90 | 0,1221 | 0,1124 | 0,1031 | 0,0945 | 0,0864 | 0,0789 | 0,0720 | 0,0658 | 0,0602 | 0,0554 | 0,0514 | 0,0481 | 0,0458 | 0,0444 | 0,0441 | 0,0450 | 0,0473 | 0,0513 | 0,0579 | 0,0679 | 0,0779 | 0,0441 |
| 0,91 | 0,1282 | 0,1184 | 0,1092 | 0,1004 | 0,0922 | 0,0846 | 0,0776 | 0,0711 | 0,0653 | 0,0602 | 0,0558 | 0,0521 | 0,0493 | 0,0473 | 0,0463 | 0,0464 | 0,0476 | 0,0502 | 0,0546 | 0,0618 | 0,0718 | 0,0463 |
| 0,92 | 0,1348 | 0,1251 | 0,1158 | 0,1070 | 0,0987 | 0,0909 | 0,0837 | 0,0770 | 0,0710 | 0,0656 | 0,0608 | 0,0568 | 0,0534 | 0,0509 | 0,0493 | 0,0485 | 0,0488 | 0,0503 | 0,0531 | 0,0577 | 0,0652 | 0,0485 |
| 0,93 | 0,1422 | 0,1324 | 0,1230 | 0,1142 | 0,1058 | 0,0979 | 0,0905 | 0,0836 | 0,0774 | 0,0716 | 0,0666 | 0,0621 | 0,0583 | 0,0553 | 0,0530 | 0,0516 | 0,0510 | 0,0515 | 0,0531 | 0,0560 | 0,0606 | 0,0510 |
| 0,94 | 0,1503 | 0,1405 | 0,1312 | 0,1222 | 0,1137 | 0,1057 | 0,0982 | 0,0911 | 0,0846 | 0,0786 | 0,0732 | 0,0683 | 0,0641 | 0,0606 | 0,0577 | 0,0556 | 0,0543 | 0,0538 | 0,0544 | 0,0560 | 0,0588 | 0,0538 |
| 0,95 | 0,1596 | 0,1498 | 0,1404 | 0,1314 | 0,1228 | 0,1146 | 0,1069 | 0,0997 | 0,0929 | 0,0866 | 0,0809 | 0,0757 | 0,0710 | 0,0670 | 0,0636 | 0,0608 | 0,0588 | 0,0575 | 0,0570 | 0,0575 | 0,0589 | 0,0570 |

We take as value of I, I = 0.0485 ≤ 0.0500 (the closest), that corresponds to $\alpha$ = 0.92

*Determination of the maximum value of angle $\theta_{max}$ and $\theta_1$*

According to Fig. 93:

$$\tan \theta_{max} = \frac{b(1 - \alpha_0^2)^{1/2}}{\alpha_0 a} = \frac{(1 - \alpha_0^2)^{1/2}}{\alpha_0} \cdot \frac{b}{a}$$

$$\theta_{max} = \tan^{-1}\left(\frac{(1 - \alpha_0^2)^{1/2}}{\alpha_0} \cdot \frac{b}{a}\right) = \tan^{-1}\left(0.426 \cdot \frac{b}{a}\right)$$

We take half the angle $\theta_{max}$. Therefore, finally, $\theta_1 = \theta_{max}/2$

$$\theta_1 = \frac{1}{2}\tan^{-1}\left(0.426 \cdot \frac{b}{a}\right) \tag{E.4}$$

**Table 32**. Set of angles $\theta_{max}$ and $\theta_1 = \theta_{max}/2$ values for several a and b (semi-axles of an ellipse)

| a/b | $\theta_{max}$ | $\theta_1$ |
|---|---|---|
| (min/min) | (DEG) | (DEG) |
| 5.0 | 4.9 | 2.5 |
| 4.5 | 5.4 | 2.7 |
| 4.0 | 6.1 | 3.1 |
| 3.5 | 6.9 | 3.5 |
| 3.0 | 8.1 | 4.1 |
| 2.5 | 9.7 | 4.9 |
| 2.0 | 12.0 | 6.0 |
| 1.5 | 15.9 | 8.0 |
| 1.0 | 23.1 | 11.6 |

### E.1.2.2  The method based on the application of the curvature formula

We determine the rotation angle $\theta$, studying the curvature function of an ellipse and its derivatives. We assume a straight ellipse, centred at the origin of coordinates and semi-axles a and b, so that: $a > b > 0$. In Cartesian coordinates, its expression is:

$$\frac{\mu_T^2}{a^2} + \frac{\sigma_T^2}{b^2} = 1$$

In parametric coordinates, we have:

$$\begin{cases} \mu_T = a \cdot \cos t \\ \sigma_T = b \cdot \sin t \end{cases}$$

The expression of the curvature function $\kappa(t)$ of an ellipse is:

$$\kappa(t) = \frac{\dot{x}(t)\ddot{y}(t) - \ddot{x}(t)\dot{y}(t)}{\left(\dot{x}^2(t) + \dot{y}^2(t)\right)^{3/2}} = \frac{ab}{(a^2 sin^2 t + b^2 cos^2 t)^{3/2}}$$

This function has, within the interval: $0 \le t \le \pi/2$, a maximum value at $t = 0$, which equals to: $a/b^2$; and a minimum value at $t = \pi/2$, which equals to: $b/a^2$.

Studying the function $\kappa(t)$ and its successive derivatives: $\kappa'(t)$ and $\kappa''(t)$, we can determine the angle $t_1$ that marks the boundary, beyond which, the ellipse arch remaining is quite equal to a straight line. The maximum rotation angle $\theta_{max}$ will be obtained from $t_1$. Figs. 95 and 96 illustrate all the above.



**Figure 95**. Geometric relations between a, a', and b with t and $\theta$

$$\begin{cases} b \cdot sint = a' \cdot sin\theta \\ a \cdot cost = a' \cdot cos\theta \end{cases}$$

$$\sin t = \frac{a' \cdot \sin \theta}{b} \rightarrow \theta = \sin^{-1}\left(\frac{b}{a'}\sin t\right) \rightarrow \theta = \sin^{-1}\left(\frac{b \sin t}{(a^2 \cos^2 t + b^2 \sin^2 t)^{1/2}}\right) \qquad (E.5)$$

Determining $t_1$:

**Figure 96** Plot of functions: $\kappa(t)$, $\kappa'(t)$ and $\kappa''(t)$ and their singular points. Determination of $t_1$ using the WolframAlfa IT application

So, this way, we calculate the angle $\theta(t_0)$. To get the design angle, obtained from this second method, we consider two possibilities: $\theta_2 = \theta(t_1)$ or $\theta'_2 = 2\,\theta(t_0)$. Table 33 shows the values of $\theta_2$ and $\theta'_2$, taking several values of the quotient a/b (semi-axles of the ellipse):

**Table 33**. Values of angles $\theta(t_0)$, $\theta_2(t_1)$, and $\theta'_2=2\theta(t_0)$ for several values of a/b.

| a/b (min/min) | $\theta(t_0)$ (DEG) | $\theta_2 = \theta(t_1)$ (DEG) | $\theta'_2 = 2\theta(t_0)$ (DEG) |
|---|---|---|---|
| 6.0 | 0.8 | 1.4 | 1.6 |
| 5.5 | 1.0 | 1.7 | 2.0 |
| 5.0 | 1.2 | 2.0 | 2.3 |
| 4.5 | 1.4 | 2.5 | 2.9 |
| 4.0 | 1.8 | 3.2 | 3.7 |
| 3.5 | 3.0 | 4.3 | 6.0 |
| 3.0 | 3.3 | 5.9 | 6.6 |
| 2.5 | 4.9 | 8.8 | 9.7 |
| 2.0 | 7.9 | 14.6 | 15.7 |
| 1.5 | 15.3 | 30.2 | 30.5 |
| 1.0 | 45.0 | - | 90.0 |

### E.1.2.3  Comparison between the two methods

Table 34 and Fig. 97 show a numeric and graphics comparison between the two methods. Results are quite similar from values of the quotient a/b greater than 3.5.

**Table 34**. Comparison between $\theta_1$ and $\theta_2$ values

| a/b (min/min) | $\theta_1 = \theta_{max}/2$ (DEG) | $\theta_2 = \theta(t_1)$ (DEG) | $\theta'_2 = 2\theta(t_0)$ (DEG) |
|---|---|---|---|
| 6.0 | *2.0* | 1.4 | 1.6 |
| 5.5 | *2.1* | 1.7 | 2.0 |
| 5.0 | *2.5* | 2.0 | 2.3 |
| 4.5 | *2.7* | 2.5 | 2.9 |
| 4.0 | *3.1* | 3.2 | 3.7 |
| 3.5 | *3.5* | 4.3 | 6.0 |
| 3.0 | *4.1* | 5.9 | 6.6 |
| 2.5 | *4.9* | 8.8 | 9.7 |
| 2.0 | *6.0* | 14.6 | 15.7 |
| 1.5 | *8.0* | 30.2 | 30.5 |
| 1.0 | *11.6* | - | 90.0 |
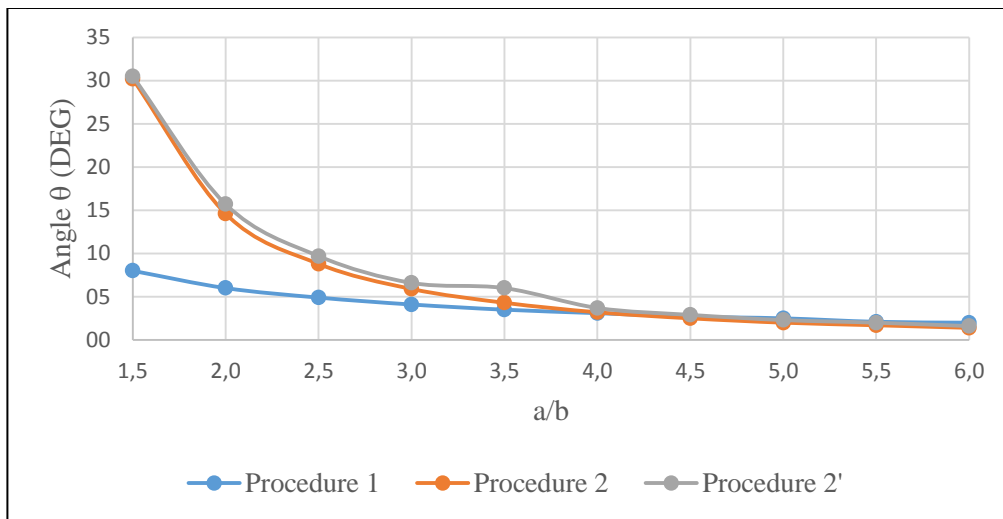
**Figure 97**. Graph comparison between the two methods

### E.1.3 Proportionality of the semi-axes (regularity condition 1)

The condition of proportionality between the semi-axes of the ellipse that determine the quality points and the maximum acceptable values of $\mu$ and $\sigma$ ($\mu > \sigma$) provides the following equality:

$$\frac{b}{a} = \frac{\sigma_2}{\mu_2} \tag{E.6}$$

which is a regularity condition that can be justified by (1) the almost linearity between $\mu_T$ and $\sigma_T$, and (2) because the direction defined by the points (0,0) and (a, b) provides the mean quadratic gradient between 'b' and 'a' $(((a^2 + b^2)/2)^{1/2})$.

### E.1.3.1 Justification (simplified model)

The loss of satisfaction /quality has been related to the physical characteristics of the transfer, the synchrony between the contribution and reception routes, and the headway adherence on the affected routes. Without synchrony or with lack of headway adherence on the affected routes (loss of quality), the arrival of the users to the reception route occurs at random times within headways between consecutive buses. Specifically, with probabilities $p_1$, $p_2$, ..., $p_n$, the waiting times in a time slot can be associated to uniform distributions $U_1(0, H_1)$, $U_2(0, H_2)$, ..., $U_n(0, H_n)$, where $H_1$, $H_2$,..., $H_n$ are the actual headways between consecutive buses and $p_j = \sum_{i=1}^{n} H_i$ (j = 1, ..., n).

With this simplified model, the expected waiting time value on the reception route ($\mu_i = H_i/2$) and its standard deviation ($\sigma_i = H_i/\sqrt{12}$) are linearly related in each experimental situation, $\sigma_i = 0.57 \cdot \mu_i$, and when adding the walking time between the contribution and reception routes, we have that $\mu_T = \mu_0 + \mu_i$ ($\mu_0$ average walking time) and

$$\sigma_T = (\sigma_0^2 + \sigma_i^2)^{1/2} = (\sigma_0^2 + 0.32(\mu_T - \mu_0)^2)^{1/2} \tag{E.7}$$

($\sigma_0$ standard deviation of walking time). For prefixed physical characteristics of the transfer area ($\mu_0, \sigma_0$), the relationship (E.7) presents a very high linear adjustment in reasonable situations (Table 36) although $\sigma_T/\mu_T$ is not constant in general. The linear adjustment has been shown in a prospective nature simulation with the following characteristics:

*Response*

— Coefficient of correlation $R_0^2$, in the linear adjustment $\sigma_T = a \cdot \mu_T$ ('a' is a constant to be estimated)

— Coefficient of correlation $R_L^2$, in the linear adjustment $\sigma_T = a \cdot \mu_T + b$ ('a' and 'b' are constants to be estimated)

*Experimental conditions*

— $\mu_0$ covers the range {1; 1.5; 2; 2.5; 3; 3.5}

— $\sigma_0$ covers the range {0.4; 0.6; 0.8; 1}

— $\mu_T = \mu_0 + \mu_i$ covers the range {1; 1.1; 1.2; ... ; 7.9; 8}

**Table 35**. Linear adjustment of the relationship $\sigma_T = (\sigma_0^2 + 0.32(\mu_T - \mu_0)^2)^{1/2}$

| $\sigma_0$ | $\mu_0$ | $R_0^2$ | $R_L^2$ | $\sigma_0$ | $\mu_0$ | $R_0^2$ | $R_L^2$ |
|---|---|---|---|---|---|---|---|
| 0.4 | 1.0 | 0.98 | 0.9999 | 0.8 | 1.0 | 0.99 | 0.9989 |
| 0.4 | 1.5 | 0.96 | 0.9999 | 0.8 | 1.5 | 0.98 | 0.9989 |
| 0.4 | 2.0 | 0.92 | 0.9999 | 0.8 | 2.0 | 0.96 | 0.9989 |
| 0.4 | 2.5 | 0.90 | 0.9999 | 0.8 | 2.5 | 0.93 | 0.9989 |
| 0.4 | 3.0 | 0.87 | 0.9999 | 0.8 | 3.0 | 0.90 | 0.9989 |
| 0.4 | 3.5 | 0.84 | 0.9999 | 0.8 | 3.5 | 0.88 | 0.9989 |
| 0.6 | 1.0 | 0.98 | 0.9995 | 1.0 | 1.0 | 0.99 | 0.9979 |
| 0.6 | 1.5 | 0.97 | 0.9995 | 1.0 | 1.5 | 0.99 | 0.9979 |
| 0.6 | 2.0 | 0.94 | 0.9995 | 1.0 | 2.0 | 0.97 | 0.9979 |
| 0.6 | 2.5 | 0.91 | 0.9995 | 1.0 | 2.5 | 0.95 | 0.9979 |
| 0.6 | 3.0 | 0.88 | 0.9995 | 1.0 | 3.0 | 0.93 | 0.9979 |
| 0.6 | 3.5 | 0.85 | 0.9995 | 1.0 | 3.5 | 0.90 | 0.9979 |

Thus, the simplified model has shown that the loss of quality for lack of synchrony or headway adherence unfulfillment occurs fundamentally in one direction of the space defined by the variables $\mu_T$ and $\sigma_T$ ($R_L^2 > 0.99$) and, although in each transfer area $\sigma_T/\mu_T$ is not constant in general, the correlation $R_0^2$ is very strong. On the other hand, the concentric ellipses that define the $TQR(\mu_T, \sigma_T)$ values (previously set $a_{11}$, $a_{22}$ and $a_{12}$),

$$TQR(\mu_T, \sigma_T) = 100 + a_{11}{\mu_T}^2 + a_{22}{\sigma_T}^2 + 2a_{12}\mu_T\sigma_T$$

allow degrading quality levels in a range that varies between 'b' (minimum: in direction $(0, \sigma_T)$) and 'a' (maximum: in direction $(\mu_T, 0)$). The condition $\sigma_2/\mu_2 = b/a$ is justified by the almost linearity between $\mu_T$ and $\sigma_T$, and because the direction defined by the points $(0,0)$ and $(a, b)$ provides the mean quadratic gradient between 'b' and 'a' $(((a^2 + b^2)/2)^{1/2})$.



Eixample Dret. Transfer H10a → V17a
$\mu_T - \sigma_T$

Eixample Dret. Transfer H10a → V17t
$\mu_T - \sigma_T$

Eixample Dret. Transfer H10t → V17a
$\mu_T - \sigma_T$

Eixample Dret. Transfer H10t → V17t
$\mu_T - \sigma_T$
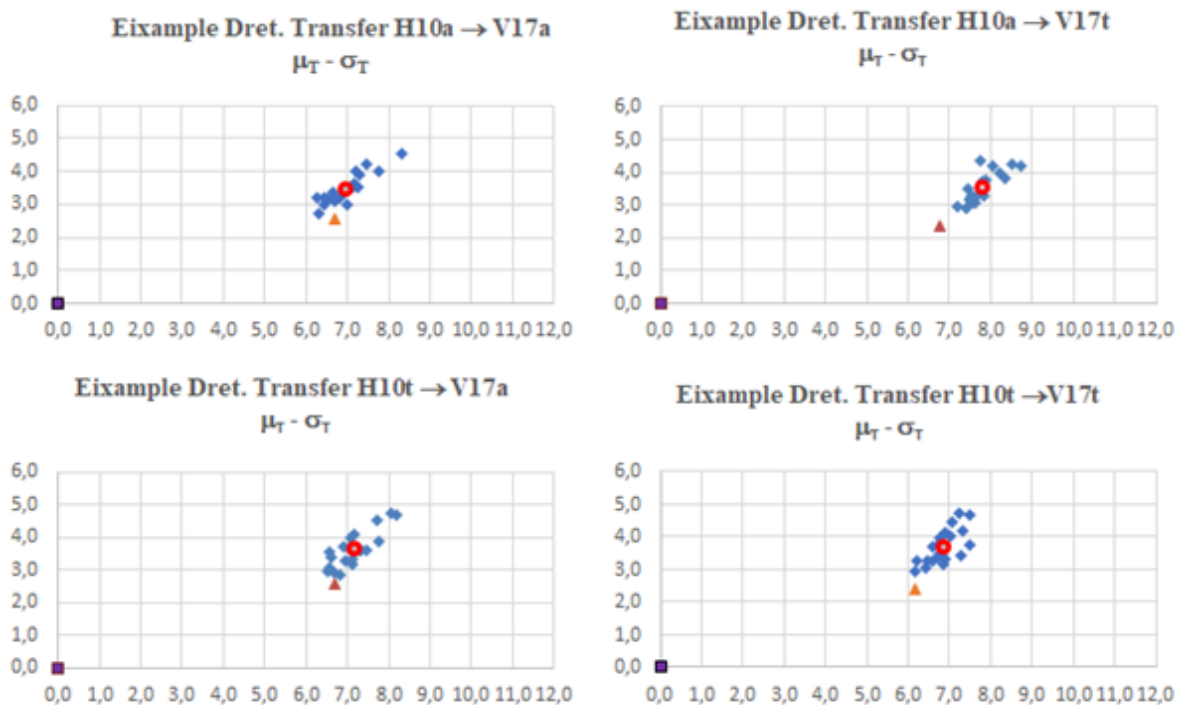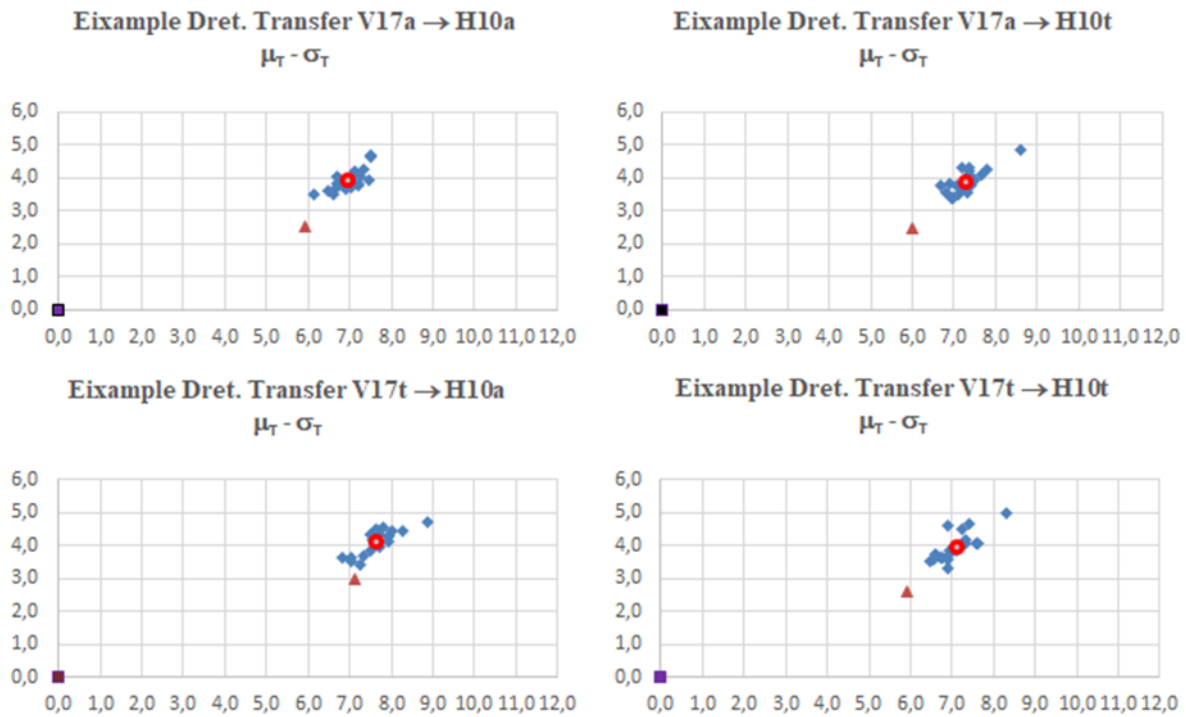
**Figure 98**. Daily actual achievements, an average of actual achievements, and scheduled values at the Eixample Dret Transfer Area. (◆$(\mu.\sigma)_a$ actual achievements, ⬤$(\bar{\mu},\bar{\sigma})$ average actual achievements, ▲$(\mu.\sigma)_s$ scheduled values).

Replacing 'a' and 'b' by their expressions, according to Eq. (E.1) and Eq. (E.2), and considering that TQR=0, after some algebra, we get:

$$\frac{\sigma_2}{\mu_2} = \frac{b}{a} = \left(\frac{a_{11} + a_{22} + [(a_{11} - a_{22})^2 + 4a_{12}{}^2]^{1/2}}{a_{11} + a_{22} - [(a_{11} - a_{22})^2 + 4a_{12}{}^2]^{1/2}}\right)^{1/2}$$

$$= \left(\frac{\left(a_{11} + a_{22} + [(a_{11} - a_{22})^2 + 4a_{12}{}^2]^{1/2}\right)\left(a_{11} + a_{22} + [(a_{11} - a_{22})^2 + 4a_{12}{}^2]^{1/2}\right)}{\left(a_{11} + a_{22} - [(a_{11} - a_{22})^2 + 4a_{12}{}^2]^{1/2}\right)\left(a_{11} + a_{22} + [(a_{11} - a_{22})^2 + 4a_{12}{}^2]^{1/2}\right)}\right)^{1/2}$$

$$= -\frac{\left(a_{11} + a_{22} + [(a_{11} - a_{22})^2 + 4a_{12}{}^2]^{1/2}\right)}{2(a_{11}a_{22} - a_{12}{}^2)^{1/2}}$$

Consequently, the parameters $a_{11}, a_{22}$ and $a_{12}$ should meet the following regularity condition:

$$\frac{a_{11} + a_{22} + [(a_{11} - a_{22})^2 + 4a_{12}{}^2]^{1/2}}{2(a_{11}a_{22} - a_{12}{}^2)^{1/2}} + \frac{\sigma_2}{\mu_2} = 0 \qquad\qquad\text{(E.8)}$$

### E.1.4  Rotating angle (regularity condition 2)

To ensure that the maximum of $TQR(\mu_T, \sigma_T)$ is achieved in $(\mu_T, \sigma_T) = (0,0)$ and that $TQR(\mu_T, \sigma_T)$ is decreasing in the arguments $(\mu_T, \sigma_T)$), the coefficients of the quadratic model

(71) must be negative ($a_{11}<0$, $a_{22}<0$ and $a_{12}<0$, remark 3). On the other hand, the linear approximation is insufficient to characterize satisfaction (remark 2). Consequently, the angle of rotation ($\theta$) corresponding to the elliptical sections that defines the quadratic model (level curves) must satisfy: i) $\theta<0$, since $a_{12}\neq0$ (Appendix E1); and ii) $\theta>\theta$max and $\theta_{max} = -\tan^{-1}\left(0.426\frac{b}{a}\right)$, Appendix E2), since the difference between the chord (ellipse) and the best linear fit (straight line) must be significant ($>0.05\cdot$b).

In this context, the rotation angle $\theta_{max}/2$ minimises the mean square error in the allowable range [$\theta_{max}$, 0]. In particular, T=$\theta_{max}/2$ is the solution to the optimisation problem,

$$min_T \, E(\theta - T)^2$$

Subject to $\theta{\approx}U[\theta_{max},0]$

$$E(\theta - T)^2 = E(\theta^2) - 2TE(\theta) + T^2 = \frac{\theta_{max}^2}{12} + \left(\frac{\theta_{max}}{2} - T\right)^2$$

Thus, to get the 3$^{rd}$ equation of the non-linear system (75), we consider the following expressions, previously determined, linking the rotating angle with coefficients $a_{11}$, $a_{22}$, and $a_{12}$:

$$\text{from Eq. (E.3): } \tan 2\theta = \frac{2a_{12}}{a_{11}-a_{22}};$$

$$\text{from Eq. (E.4): } \tan 2\theta = -0.426\frac{b}{a};$$

We also consider the condition of proportionality,

$$\text{from Eq. (E.6): } \frac{b}{a} = \frac{\sigma_2}{\mu_2}$$

Consequently, the parameters $a_{11}, a_{22}$ and $a_{12}$ should meet the following regularity condition:

$$a_{11}(0.426\,\sigma_2) - a_{22}(0.426\,\sigma_2) + a_{11}(2\mu_2) = 0 \qquad\qquad \text{(E.9)}$$

### E.1.5  Explicit solution of the non-linear system of equations

The system of equations (75),

$$\left.\begin{array}{c} a_{11}{\mu_2}^2 + a_{22}{\sigma_2}^2 + 2a_{12}\mu_2\sigma_2 + (100 - TQR_2) = 0 \\ \dfrac{a_{11} + a_{22} + [(a_{11} - a_{22})^2 + 4{a_{12}}^2]^{1/2}}{2(a_{11}a_{22} - {a_{12}}^2)^{1/2}} + \dfrac{\sigma_2}{\mu_2} = 0 \\ a_{11}(0.426\sigma_2) - a_{22}(0.426\sigma_2) + a_{12}(2\mu_2) = 0 \end{array}\right\} \qquad \text{(E.10)}$$

conditioned on: $a_{11} < 0, a_{22} < 0, a_{12} < 0, a_{11}a_{22} - a_{12}^2 > 0$ and $a_{11} > a_{22}$ ($\mu_{max} > \sigma_{max}$)
admits an explicit solution. First and third equations enable to express $a_{11}$ and $a_{22}$ as linear
functions of $a_{12}$: $a_{11} = -\alpha - (\beta + \gamma)a_{12}$ and $a_{22} = -\alpha - \beta a_{12}$, and replacing into the
second equation, the system is reduced to,

$$\frac{-2\alpha - (2\beta + \gamma)a_{12} + [(\gamma^2 + 4)a_{12}^2]^{1/2}}{2(\alpha^2 + (2\alpha\beta + \alpha\gamma)a_{12} + (\beta(\beta + \gamma) - 1)a_{12}^2)^{1/2}} + \frac{\sigma_2}{\mu_2} = 0$$

being,

$$\alpha = \frac{100 - TQR_2}{\mu_2^2 + \sigma_2^2}, \quad \beta = \frac{2}{\mu_2^2 + \sigma_2^2}\left(\mu_2\sigma_2 - \frac{\mu_2^3}{0.426\sigma_2}\right), \quad \gamma = \frac{2\mu_2}{0.426\sigma_2}$$

Considering that $a_{12} < 0$ and after some algebra, the system of equations (E.10) can be
turned into a second-degree equation, with an immediate solution:

$$c_1 a_{12}^2 + c_2 a_{12} + c_3 = 0$$

where:

$$c_1 = 4(\beta(\beta + \gamma) - 1)\sigma_2^2 - \left(2\beta + \gamma + (\gamma^2 + 4)^{1/2}\right)^2\mu_2^2$$
$$c_2 = 4(2\alpha\beta + \alpha\gamma)\sigma_2^2 - 4\alpha\left(2\beta + \gamma + (\gamma^2 + 4)^{1/2}\right)\mu_2^2$$
$$c_3 = 4\alpha^2(\sigma_2^2 - \mu_2^2)$$

Mathematical proof:

From equation 3:

$$a_{11}(0.426\sigma_2) - a_{22}(0.426\sigma_2) + a_{12}(2\mu_2) = 0$$
$$a_{11}(0.426\sigma_2) = a_{22}(0.426\sigma_2) - a_{12}(2\mu_2)$$
$$a_{11} = a_{22} - \frac{2\mu_2}{0.426\sigma_2}a_{12} \qquad \text{(E.11)}$$

From the 1$^{st}$ equation;

$$a_{11}{\mu_2}^2 + a_{22}{\sigma_2}^2 + 2a_{12}\mu_2\sigma_2 + (100 - TQR_2) = 0$$
$$\left(a_{22} - \frac{2\mu_2}{0.426\sigma_2}a_{12}\right){\mu_2}^2 + a_{22}{\sigma_2}^2 + 2a_{12}\mu_2\sigma_2 + (100 - TQR_2) = 0$$

$$a_{22}\mu_2{}^2 - \frac{2\mu_2^3}{0.426\sigma_2}a_{12} + a_{22}\sigma_2{}^2 + 2a_{12}\mu_2\sigma_2 + (100 - TQR_2) = 0$$

$$a_{22}(\mu_2{}^2 + \sigma_2{}^2) + 2a_{12}\left(\mu_2\sigma_2 - \frac{\mu_2^3}{0.426\sigma_2}\right) + (100 - TQR_2) = 0$$

$$a_{22} = -\frac{2a_{12}}{\mu_2{}^2 + \sigma_2{}^2}\left(\mu_2\sigma_2 - \frac{\mu_2^3}{0.426\sigma_2}\right) - \frac{100 - TQR_2}{\mu_2{}^2 + \sigma_2{}^2} \qquad (E.12)$$

From the 2$^{nd}$ equation:

$$\frac{a_{11} + a_{22} + [(a_{11} - a_{22})^2 + 4a_{12}{}^2]^{1/2}}{2(a_{11}a_{22} - a_{12}{}^2)^{1/2}} + \frac{\sigma_2}{\mu_2} = 0$$

Numerator,

$$[(a_{11} - a_{22})^2 + 4a_{12}{}^2]^{1/2} = \left[\left(-\frac{2\mu_2}{0.426\sigma_2}a_{12}\right)^2 + 4a_{12}^2\right]^{1/2} = 2\left[\left(\left(\frac{\mu_2}{0.426\sigma_2}\right)^2 + 1\right)a_{12}^2\right]^{1/2}$$

$$a_{11} + a_{22} = 2\left(a_{22} - \frac{\mu_2}{0.426\sigma_2}a_{12}\right) = 2\left(-\frac{2a_{12}}{\mu_2{}^2 + \sigma_2{}^2}\left(\mu_2\sigma_2 - \frac{\mu_2^3}{0.426\sigma_2}\right) - \frac{100 - TQR_2}{\mu_2{}^2 + \sigma_2{}^2} - \frac{\mu_2}{0.426\sigma_2}a_{12}\right)$$

$$= -2\underbrace{\frac{100 - TQR_2}{\mu_2{}^2 + \sigma_2{}^2}}_{\alpha} - \underbrace{\left(\frac{4}{\mu_2{}^2 + \sigma_2{}^2}\left(\mu_2\sigma_2 - \frac{\mu_2^3}{0.426\sigma_2}\right) + \frac{2\mu_2}{0.426\sigma_2}\right)}_{2\beta}\underbrace{a_{12}}_{\gamma}$$

This way, Eq. (An.1) and Eq. (An. 2) would thereby read thus:

$$a_{22} = -\alpha - \beta a_{12}$$

$$a_{11} = a_{22} - \gamma a_{12}$$

$$a_{11} = -\alpha - \beta a_{12} - \gamma a_{12} = -\alpha - (\beta + \gamma)a_{12}$$

Denominator,

$$2(a_{11}a_{22} - a_{12}{}^2)^{1/2} = 2\left((-\alpha - (\beta + \gamma)a_{12})(-\alpha - \beta a_{12}) - a_{12}{}^2\right)^{1/2}$$

$$= 2(\alpha^2 + \alpha(2\beta + \gamma)a_{12} + (\beta(\beta + \gamma) - 1)a_{12}^2)^{1/2} = 2(\alpha^2 + \beta^* a_{12} + \gamma^* a_{12}^2)^{1/2}$$

This way, Eq. 2 can be written thus:

$$\frac{-2\alpha - (2\beta + \gamma)a_{12} + (\gamma^2 + 4)^{1/2}a_{12}}{2(\alpha^2 + \beta^* a_{12} + \gamma^* a_{12}^2)^{1/2}} + \frac{\sigma_2}{\mu_2} = 0$$

$$4(\alpha^2 + \beta^* a_{12} + \gamma^* a_{12}^2)\sigma_2^2 = \left(-2\alpha - (2\beta + \gamma)a_{12} + (\gamma^2 + 4)^{1/2} a_{12}\right)^2 \mu_2^2$$

$$4(\alpha^2 + \beta^* a_{12} + \gamma^* a_{12}^2)\sigma_2^2$$
$$- \left(4\alpha^2 + \left(4\alpha(2\beta + \gamma) - 4\alpha(\gamma^2 + 4)^{1/2}\right)a_{12}\right.$$
$$+ \left.\left((2\beta + \gamma)^2 + (\gamma^2 + 4) - 2(2\beta + \gamma)(\gamma^2 + 4)^{1/2}\right)a_{12}^2\right)\mu_2^2 = 0$$

This will result in a quadratic equation on $a_{12}$

c, term on $\alpha_{12}^0$
$$c = 4\alpha^2(\sigma_2^2 - \mu_2^2)$$
b, term on $\alpha_{12}^1$
$$b = 4\sigma_2^2\beta^* - 4\mu_2^2\left(\alpha(2\beta + \gamma) - \alpha(\gamma^2 + 4)^{1/2}\right)$$
a, term on $\alpha_{12}^2$
$$a = 4\sigma_2^2\gamma^* - \mu_2^2\left((2\beta + \gamma)^2 + (\gamma^2 + 4) - 2(2\beta + \gamma)(\gamma^2 + 4)^{1/2}\right)$$

$$c_1 = 4(\beta(\beta + \gamma) - 1)\sigma_2^2 - \left(2\beta + \gamma + (\gamma^2 + 4)^{1/2}\right)^2 \mu_2^2$$
$$c_2 = 4(2\alpha\beta + \alpha\gamma)\sigma_2^2 - 4\alpha\left(2\beta + \gamma + (\gamma^2 + 4)^{1/2}\right)\mu_2^2$$
$$c_3 = 4\alpha^2(\sigma_2^2 - \mu_2^2)$$

The system of equations (75, E.10), conditioned on: $a_{11} < 0, a_{22} < 0, a_{12} < 0, a_{11}a_{22} - a_{12}^2 > 0$ and $a_{11} > a_{22}$ ($\mu_{max} > \sigma_{max}$) admits an explicit solution. To facilitate the resolution of this second-degree equation, an Excel worksheet has been designed. The user has only to launch the Excel application and enter or modify the following parameters: ($\mu_0$, $\sigma_0$) (the traveling time on foot and its uncertainty), H (the headway) and TQR$_2$ (the level of quality of ($\mu_2$, $\sigma_2$), a point inside the elliptic domain (TQR$_2\neq$0) or on the boundary (TQR$_2$=0)). The spreadsheet calculates the coefficients a$_{11}$, a$_{22}$ and a$_{12}$ of the ellipse directly (tab 2, "Calculations"), and the solution is displayed in the first tab, "Entry Data" (Figure 99).

Excel spreadsheet:

**Data entry**

| | |
|---|---|
| $\mu_o=$ | 2,2 |
| $\sigma_o=$ | 0,6 |
| H= | 8 |
| $TQR_2=$ | 0 |

**Solution**

| $a_{11}$ | $a_{22}$ | $a_{12}$ |
|---|---|---|
| ---- | | ---- |
| -0,4217 | -1,9402 | -0,1477 |

**INSTRUCCTIONS FOR USE**

1) This EXCEL application consists of two spreadsheets. Spreadsheet #1: data entry and solution of the non-linear system of equations. Spreadsheet #2: calculations.

2) Spreadsheet #1, data entry in green cells: μo and σo are the mean and the standard deviation of the walking time between the outbound and inbound route stops; H is the route headway; and $TQR_2$, the level of service quality with most buses bunched.

3) Spreadsheet #1, solution of the non-linear system of equations that met the regularity conditions: $a_{11}$, $a_{22}$ and $a_{12}$.

4) Spreadsheet #2, calculations: intermediate and final calculations

Remark. Brown cells contain formulas: please, do not manipulate them.

Tab 1

| | |
|---|---|
| $\mu_o=$ | 2,20 |
| $\sigma_o=$ | 0,60 |
| H= | 8,00 |
| $TQR_2=$ | 0,00 |
| $\mu_2=$ | 10,20 |
| $\sigma_2=$ | 4,66 |

$$a_{11}\mu_2{}^2 + a_{22}\sigma_2{}^2 + 2a_{12}\mu_2\sigma_2 + (100 - TQR_2) = 0$$
$$\frac{a_{11} + a_{22} + [(a_{11} - a_{22})^2 + 4a_{12}{}^2]^{1/2}}{2(a_{11}a_{22} - a_{12}{}^2)^{1/2}} + \frac{\sigma_2}{\mu_2} = 0$$
$$a_{11}(0.426\sigma_2) - a_{22}(0.426\sigma_2) + a_{12}(2\mu_2) = 0$$

**Intermediate parameters**

| | |
|---|---|
| $\alpha=$ | 0,7953 |
| $\beta=$ | -7,7519 |
| $\gamma=$ | 10,2815 |

$$\alpha = \frac{100 - TQR_2}{\mu_2^2 + \sigma_2^2}, \quad \beta = \frac{2}{\mu_2^2 + \sigma_2^2}\left(\mu_2\sigma_2 - \frac{\mu_2^3}{0.426\sigma_2}\right), \quad \gamma = \frac{2\mu_2}{0.426\sigma_2}$$

**Second degree equation coefficients**

| | | Part 1 | Part 2 |
|---|---|---|---|
| $c_1=$ | -4658,0468 | -1788,3370 | 2869,7099 |
| $c_2=$ | -2098,7275 | -360,4115 | 1738,3160 |
| $c_3=$ | -208,3556 | -208,3556 | |

$$c_1 = 4(\beta(\beta + \gamma) - 1)\sigma_2^2 - (2\beta + \gamma + (\gamma^2 + 4)^{1/2})^2 \mu_2^2$$
$$c_2 = 4(2\alpha\beta + \alpha\gamma)\sigma_2^2 - 4\alpha(2\beta + \gamma + (\gamma^2 + 4)^{1/2})\mu_2^2$$
$$c_3 = 4\alpha^2(\sigma_2^2 - \mu_2^2)$$

| Parameters | | | regularity conditions | | | | Validation |
|---|---|---|---|---|---|---|---|
| $a_{11}$ | $a_{22}$ | $a_{12}$ | $a_{11}<0$ | $a_{22}<0$ | $a_{12}<0$ | $a_{11}\cdot a_{22}-a^2_{12}>0$ | solution |
| -0,0292 | -3,1432 | -0,3029 | 1 | 1 | 1 | 0 | NOT Ok |
| -0,4217 | -1,9402 | -0,1477 | 1 | 1 | 1 | 1 | Ok |

Tab 2

**Figure 99**. The aspect of the EXCEL spreadsheet with Tabs 1 and 2.

### E.1.6   A software implementation of numerical developments

Two routines have been created with MatLab to solve/calculate:

a. The 3x3 nonlinear system of equations

b. The integral, I for calculating the parameter α

### E.1.6.1   Coefficients a₁₁, a₂₂ and a₁₂

The non-linear system of equations:

$$\left.\begin{array}{l} a_{11}\mu_2{}^2 + a_{22}\sigma_2{}^2 + 2a_{12}\mu_2\sigma_2 + (100 - TQR_2) = 0 \\ \dfrac{a_{11} + a_{22} + [(a_{11} - a_{22})^2 + 4a_{12}{}^2]^{1/2}}{2(a_{11}a_{22} - a_{12}{}^2)^{1/2}} + \dfrac{\sigma_2}{\mu_2} = 0 \\ a_{11}(0.426\sigma_2) - a_{22}(0.426\sigma_2) + a_{12}(2\mu_2) = 0 \end{array}\right\}$$

has been solved using the following routine that reads from an Excel file (Fig. 90) the variables, and the initial condition. It calculates a solution and writes it down into the same Excel file.
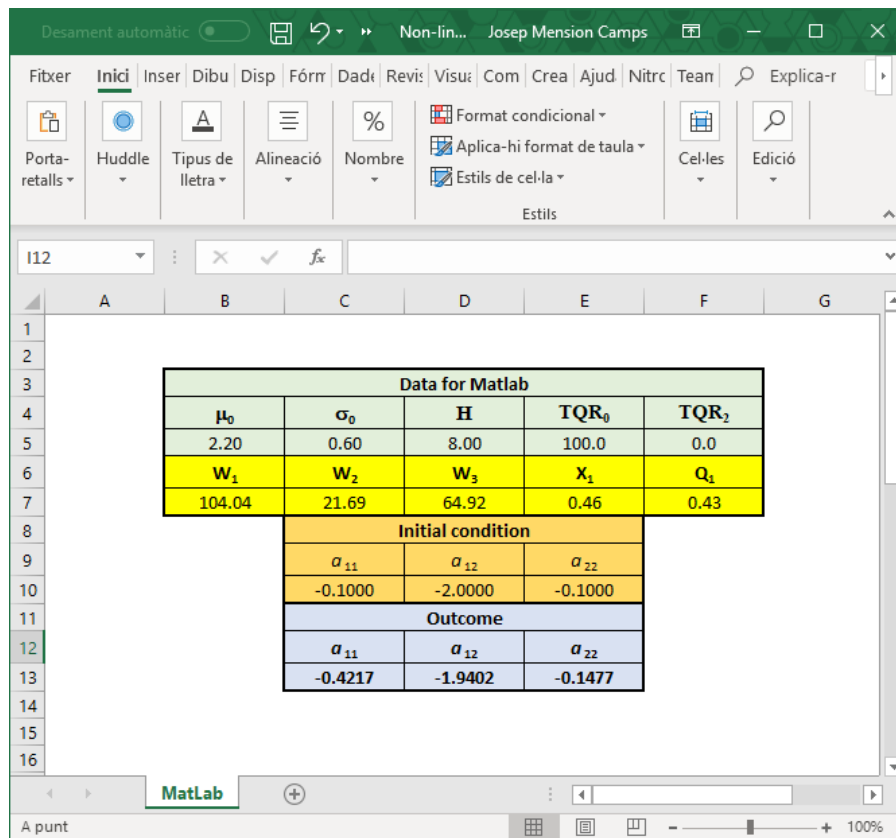


**Figure 100**. Excel form from which the routine read the variables and bump into it the outcome

Code:

```
%INITIALIZE
% clc
% clear all
function Equation_3
%Open File to process
FilterSpec='*.xlsx';
[NomArxiu,PathName,FilterIndex] = uigetfile(FilterSpec);
%Create Acontrl Excel
haxc = actxserver('Excel.Application');
%Make Excel Visible
haxc.Visible=1;
%Pointer to Excel books
hwkbk = haxc.Workbooks;
%Open Book. Pointer to it
hLlibre=hwkbk.Open([PathName,NomArxiu]);
%Verify whether it's already opened
JaObert=hLlibre.ReadOnly;
%Make a warn and wait
while JaObert
    %hLlibre.Save;
    hLlibre.Close;
    he=errordlg('File open for Another Application, Close it to
Continue','Error Excel Opened','modal');
    Quit(haxc);
    uiwait(he)
    hLlibre=hwkbk.Open([PathName,NomArxiu]);
    JaObert=hLlibre.ReadOnly;
end
%Pointer to the sreadsheets of the open book
hfulls=hLlibre.Sheets;
%First Spreadsheet is the only one to be active. Others spreadsheets
are ignored
hF1 = hfulls.Item(1);
```

```
Nom=hF1.get('Name');

fprintf(['Processant Full ',Nom,'\n']);

%Pointer to range structure

%Read general characteristics

Rang1=hF1.get('Range','E5');

TQR0=Rang1.Value;

Rang1=hF1.get('Range','F5');

TQR2=Rang1.Value;


Rang1=hF1.get('Range','B7');

W1=Rang1.Value;

Rang1=hF1.get('Range','C7');

W2=Rang1.Value;

Rang1=hF1.get('Range','D7');

W3=Rang1.Value;

Rang1=hF1.get('Range','E7');

X1=Rang1.Value;

Rang1=hF1.get('Range','F7');

Q1=Rang1.Value;


%X has now the initial condition and later on the solution

Rang1=hF1.get('Range','C10');

X(1)=Rang1.Value;

Rang1=hF1.get('Range','D10');

X(2)=Rang1.Value;

Rang1=hF1.get('Range','E10');

X(3)=Rang1.Value;


fprintf('Suggeriment inicial:   %8.6f %8.6f %8.6f\n',X);


function F = root3d(x)

F(1)= W1*x(1)+W2*x(2)+W3*x(3)+TQR0-TQR2;

F(2)=  X1+(x(1)+x(2)+sqrt((x(1)-x(2))^2+4*x(3)^2))/(2*sqrt(x(1)*x(2)-
x(3)^2));

F(3)= Q1*X1*x(1)-Q1*X1*x(2)+2*x(3);
```

281

```
end


fun=@root3d;


x0=X;
X=fsolve(fun,x0);
fprintf('Valor final:   %8.6f %8.6f %8.6f\n',X);


%Write to Excel all calculated data


Rang1=get(hF1,'Range','C13:E13');
set(Rang1,'Value',X);
%Close books
hLlibre.Save
hLlibre.Close
%Close axc
Quit(haxc)
end
```

### E.1.6.2  Integral I for calculating the parameter α

$$I = \frac{1}{\alpha} \cdot \int_0^\alpha abs\left[(1-t^2)^{1/2} - \left(\frac{(1-\alpha^2)^{1/2}-1}{\alpha}t + (1+\beta)\right)\right] dt$$

$$\alpha \in [0.6, 0.95] \;\wedge\; \beta \in [0, 0.2]$$

To evaluate I(α, β) numerically, and calculate minimum values per rows, we created the following routine:

```
%Give back the function values for each combination of parameters A
& B
%A = 0.6:0.01:0.95
%B = 0:0.01:0.2
%Return:
%Integral, row, column, minimum value, absolute mínimum value
```

282

```
function [Minim,Integral,MinimperFila,Alfa,Beta]=Integral_a_b
clc
clear all
Integral=zeros(36,21);
MinimperFila=zeros(36,1);
IndexColumna=zeros(36,1);
    for J=1:36
        A(J)=0.6+0.01*(J-1);
        for K=1:21
            B(K)=0.01*(K-1);
            %anonymous fuction
            Ft=@(t)        abs(sqrt(1-t.*t)-1-B(K)-(sqrt(1-A(J)*A(J))-
            1)/A(J)*t)/A(J);
            %Calculate integral
            Integral(J,K)=quad(Ft,0,A(J));
        end
        %Minimum values for each row (A)
        [MinimperFila(J),IndexColumna(J)] = min(Integral(J,:));
    end
%Give back the corresponding values and the minimum
[Minim,IndexFila]=min(MinimperFila);
Alfa=A(IndexFila);
Beta=B(IndexColumna(IndexFila));
surf(B,A,Integral)
xlabel('Beta');
ylabel('Alfa');
disp(A)
disp(B)
disp(Integral)
    for J=1:36
        disp(J); disp(IndexColumna(J)); disp(MinimperFila(J))
    end
end
```

283

### E.1.6.3 Distinctive walking transfer time between two stops of an octagonal transfer area – type 1

Fig. 101 shows the four types of octagonal transfer areas of the Eixample district in Barcelona.
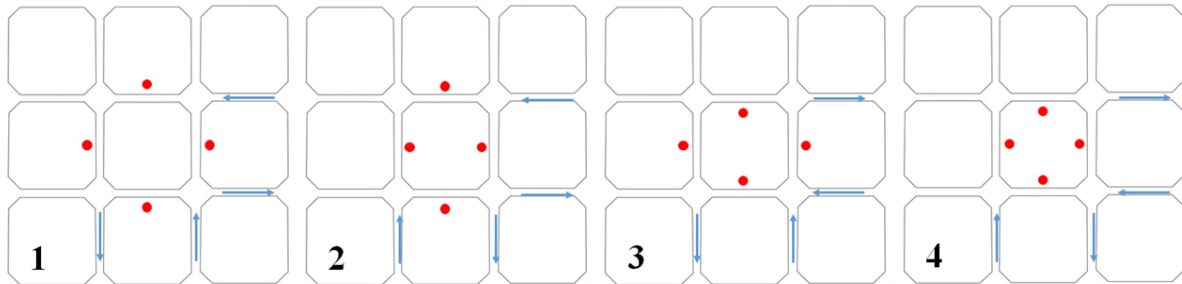


**Figure 101**. Possible location of stops at an octagonal block in Barcelona, depending on the street directions

The purpose of this section is to set the common values $(\mu_0, \sigma_0)$ of an octagonal transfer area, type 1. $\mu_0$ is the average walking transfer time of reference between two any bus stops and $\sigma_0$ is its associated standard deviation. Fig. 102 shows the generic path from stop A to stop B.
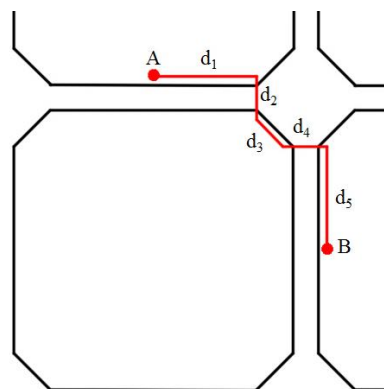


**Figure 102**. Partial distances from stop A to B

First, we measure the distances $d_1$, $d_2$, $d_3$, $d_4$, and $d_5$ and we consider three walking speeds: 1.65 m/s, 1.40 m/s, 1.10 m/s and 0.85 m/s, constant in each section $d_i$.

For each theoretical walking speed, we calculate the time needed to travel the distances $d_1$, $d_2$, $d_3$, $d_4$, and $d_5$, considering the effect of signals as well.

For each walking speed, we determine the average walking time and its standard deviation. All these figures are shown in the tables below.

Signal phase: 90s, split up this way: 42s green, 3s amber (pedestrians can't cross), and 45 red (pedestrians can't pass).

**Table 36**. Outcomes corresponding to v=1.65 m/s

| | | |
|---|---|---|
| Minimum time | 1.25 | min |
| Maximum time | 2.48 | min |
| Average time | 1.76 | min |
| Standard deviation | 0.40 | min |

**Table 37**. Calculating walking time with v=1.65 m/s

Total time = $d_1$+Cycle+$d_2$+$d_3$+Waiting time+$d_4$+$d_5$

| Speed: | 1.65 m/s | | | | | | |
|---|---|---|---|---|---|---|---|
| | $d_1$ | | $d_2+d_3$ | | | $d_4+d_5$ | |
| | 41.65 Walk. Time | | 31.21 Walk. Time | | | 51.65 Walk. Time | |
| L/speed | 25.24 | | 18.92 | | | 31.30 | |
| Round up | 25.00 | Cycle | 19.00 | Cycle | Waiting time | 31.00 | Total |
| Iteration | T1 | T.L. 1 | T2 | T.L. 2 | T.L. 2 | T3 | Time |
| 0 | 25 | 0 | 19 | 45 | 26 | 31 | 101 |
| 1 | 25 | 0 | 19 | 44 | 25 | 31 | 100 |
| 2 | 25 | 0 | 19 | 43 | 24 | 31 | 99 |
| 3 | 25 | 0 | 19 | 42 | 23 | 31 | 98 |
| 4 | 25 | 0 | 19 | 41 | 22 | 31 | 97 |
| 5 | 25 | 0 | 19 | 40 | 21 | 31 | 96 |
| 6 | 25 | 0 | 19 | 39 | 20 | 31 | 95 |
| 7 | 25 | 0 | 19 | 38 | 19 | 31 | 94 |
| 8 | 25 | 0 | 19 | 37 | 18 | 31 | 93 |
| 9 | 25 | 0 | 19 | 36 | 17 | 31 | 92 |
| 10 | 25 | 0 | 19 | 35 | 16 | 31 | 91 |
| 11 | 25 | 0 | 19 | 34 | 15 | 31 | 90 |
| 12 | 25 | 0 | 19 | 33 | 14 | 31 | 89 |
| 13 | 25 | 0 | 19 | 32 | 13 | 31 | 88 |
| 14 | 25 | 0 | 19 | 31 | 12 | 31 | 87 |
| 15 | 25 | 0 | 19 | 30 | 11 | 31 | 86 |
| 16 | 25 | 0 | 19 | 29 | 10 | 31 | 85 |
| 17 | 25 | 0 | 19 | 28 | 9 | 31 | 84 |
| 18 | 25 | 0 | 19 | 27 | 8 | 31 | 83 |

| | | | | | | | |
|----|----|----|----|----|----|----|-----|
| 19 | 25 | 0  | 19 | 26 | 7  | 31 | 82  |
| 20 | 25 | 0  | 19 | 25 | 6  | 31 | 81  |
| 21 | 25 | 0  | 19 | 24 | 5  | 31 | 80  |
| 22 | 25 | 0  | 19 | 23 | 4  | 31 | 79  |
| 23 | 25 | 0  | 19 | 22 | 3  | 31 | 78  |
| 24 | 25 | 0  | 19 | 21 | 2  | 31 | 77  |
| 25 | 25 | 0  | 19 | 20 | 1  | 31 | 76  |
| 26 | 25 | 0  | 19 | 19 | 0  | 31 | 75  |
| 27 | 25 | 0  | 19 | 18 | 0  | 31 | 75  |
| 28 | 25 | 0  | 19 | 17 | 0  | 31 | 75  |
| 29 | 25 | 0  | 19 | 16 | 0  | 31 | 75  |
| 30 | 25 | 0  | 19 | 15 | 0  | 31 | 75  |
| 31 | 25 | 0  | 19 | 14 | 0  | 31 | 75  |
| 32 | 25 | 0  | 19 | 13 | 0  | 31 | 75  |
| 33 | 25 | 0  | 19 | 12 | 0  | 31 | 75  |
| 34 | 25 | 0  | 19 | 11 | 0  | 31 | 75  |
| 35 | 25 | 0  | 19 | 10 | 0  | 31 | 75  |
| 36 | 25 | 0  | 19 | 9  | 0  | 31 | 75  |
| 37 | 25 | 0  | 19 | 8  | 0  | 31 | 75  |
| 38 | 25 | 0  | 19 | 7  | 0  | 31 | 75  |
| 39 | 25 | 0  | 19 | 6  | 0  | 31 | 75  |
| 40 | 25 | 0  | 19 | 5  | 0  | 31 | 75  |
| 41 | 25 | 0  | 19 | 4  | 0  | 31 | 75  |
| 42 | 25 | 48 | 19 | 3  | 26 | 31 | 149 |
| 43 | 25 | 47 | 19 | 2  | 26 | 31 | 148 |
| 44 | 25 | 46 | 19 | 1  | 26 | 31 | 147 |
| 45 | 25 | 45 | 19 | 0  | 26 | 31 | 146 |
| 46 | 25 | 44 | 19 | 0  | 26 | 31 | 145 |
| 47 | 25 | 43 | 19 | 0  | 26 | 31 | 144 |
| 48 | 25 | 42 | 19 | 0  | 26 | 31 | 143 |
| 49 | 25 | 41 | 19 | 0  | 26 | 31 | 142 |
| 50 | 25 | 40 | 19 | 0  | 26 | 31 | 141 |
| 51 | 25 | 39 | 19 | 0  | 26 | 31 | 140 |
| 52 | 25 | 38 | 19 | 0  | 26 | 31 | 139 |
| 53 | 25 | 37 | 19 | 0  | 26 | 31 | 138 |
| 54 | 25 | 36 | 19 | 0  | 26 | 31 | 137 |
| 55 | 25 | 35 | 19 | 0  | 26 | 31 | 136 |
| 56 | 25 | 34 | 19 | 0  | 26 | 31 | 135 |
| 57 | 25 | 33 | 19 | 0  | 26 | 31 | 134 |
| 58 | 25 | 32 | 19 | 0  | 26 | 31 | 133 |
| 59 | 25 | 31 | 19 | 0  | 26 | 31 | 132 |
| 60 | 25 | 30 | 19 | 0  | 26 | 31 | 131 |
| 61 | 25 | 29 | 19 | 0  | 26 | 31 | 130 |
| 62 | 25 | 28 | 19 | 0  | 26 | 31 | 129 |
| 63 | 25 | 27 | 19 | 0  | 26 | 31 | 128 |
| 64 | 25 | 26 | 19 | 0  | 26 | 31 | 127 |
| 65 | 25 | 25 | 19 | 0  | 26 | 31 | 126 |
| 66 | 25 | 24 | 19 | 0  | 26 | 31 | 125 |
| 67 | 25 | 23 | 19 | 0  | 26 | 31 | 124 |
| 68 | 25 | 22 | 19 | 0  | 26 | 31 | 123 |
| 69 | 25 | 21 | 19 | 0  | 26 | 31 | 122 |

| | | | | | | |
|---|---|---|---|---|---|---|
| 70 | 25 | 20 | 19 | 0 | 26 | 31 | 121 |
| 71 | 25 | 19 | 19 | 0 | 26 | 31 | 120 |
| 72 | 25 | 18 | 19 | 0 | 26 | 31 | 119 |
| 73 | 25 | 17 | 19 | 0 | 26 | 31 | 118 |
| 74 | 25 | 16 | 19 | 0 | 26 | 31 | 117 |
| 75 | 25 | 15 | 19 | 0 | 26 | 31 | 116 |
| 76 | 25 | 14 | 19 | 0 | 26 | 31 | 115 |
| 77 | 25 | 13 | 19 | 0 | 26 | 31 | 114 |
| 78 | 25 | 12 | 19 | 0 | 26 | 31 | 113 |
| 79 | 25 | 11 | 19 | 0 | 26 | 31 | 112 |
| 80 | 25 | 10 | 19 | 0 | 26 | 31 | 111 |
| 81 | 25 | 9 | 19 | 0 | 26 | 31 | 110 |
| 82 | 25 | 8 | 19 | 0 | 26 | 31 | 109 |
| 83 | 25 | 7 | 19 | 0 | 26 | 31 | 108 |
| 84 | 25 | 6 | 19 | 0 | 26 | 31 | 107 |
| 85 | 25 | 5 | 19 | 0 | 26 | 31 | 106 |
| 86 | 25 | 4 | 19 | 0 | 26 | 31 | 105 |
| 87 | 25 | 3 | 19 | 48 | 26 | 31 | 104 |
| 88 | 25 | 2 | 19 | 47 | 26 | 31 | 103 |
| 89 | 25 | 1 | 19 | 46 | 26 | 31 | 102 |

**Table 38**. Outcomes corresponding to v=1.40 m/s

| | | |
|---|---|---|
| Minimum time | 1.48 | min |
| Maximum time | 2.67 | min |
| Average time | 1.96 | min |
| Standard deviation | 0.39 | min |

**Table 39**. Calculating walking time with v=1.40 m/s

$$\text{Total time} = d_1 + \text{Cycle} + d_2 + d_3 + \text{Waiting time} + d_4 + d_5$$

| Speed: | 1.4 m/s | | | | | | |
|---|---|---|---|---|---|---|---|
| | $d_1$ | | $d_2+d_3$ | | | $d_4+d_5$ | |
| | 41.65 Walk. Time | | 31.21 Walk. Time | | | 51.65 Walk. Time | |
| L/speed | 29.75 | | 22.29 | | | 36.89 | |
| Round up | 30.00 | Cycle | 22.00 | Cycle | Waiting time | 37.00 | Total |
| Iteration | T1 | T.L. 1 | T2 | T.L. 2 | T.L. 2 | T3 | Time |
| 0 | 30 | 0 | 22 | 45 | 23 | 37 | 112 |
| 1 | 30 | 0 | 22 | 44 | 22 | 37 | 111 |
| 2 | 30 | 0 | 22 | 43 | 21 | 37 | 110 |

| | | | | | | | |
|---|---|---|---|---|---|---|---|
| 3 | 30 | 0 | 22 | 42 | 20 | 37 | 109 |
| 4 | 30 | 0 | 22 | 41 | 19 | 37 | 108 |
| 5 | 30 | 0 | 22 | 40 | 18 | 37 | 107 |
| 6 | 30 | 0 | 22 | 39 | 17 | 37 | 106 |
| 7 | 30 | 0 | 22 | 38 | 16 | 37 | 105 |
| 8 | 30 | 0 | 22 | 37 | 15 | 37 | 104 |
| 9 | 30 | 0 | 22 | 36 | 14 | 37 | 103 |
| 10 | 30 | 0 | 22 | 35 | 13 | 37 | 102 |
| 11 | 30 | 0 | 22 | 34 | 12 | 37 | 101 |
| 12 | 30 | 0 | 22 | 33 | 11 | 37 | 100 |
| 13 | 30 | 0 | 22 | 32 | 10 | 37 | 99 |
| 14 | 30 | 0 | 22 | 31 | 9 | 37 | 98 |
| 15 | 30 | 0 | 22 | 30 | 8 | 37 | 97 |
| 16 | 30 | 0 | 22 | 29 | 7 | 37 | 96 |
| 17 | 30 | 0 | 22 | 28 | 6 | 37 | 95 |
| 18 | 30 | 0 | 22 | 27 | 5 | 37 | 94 |
| 19 | 30 | 0 | 22 | 26 | 4 | 37 | 93 |
| 20 | 30 | 0 | 22 | 25 | 3 | 37 | 92 |
| 21 | 30 | 0 | 22 | 24 | 2 | 37 | 91 |
| 22 | 30 | 0 | 22 | 23 | 1 | 37 | 90 |
| 23 | 30 | 0 | 22 | 22 | 0 | 37 | 89 |
| 24 | 30 | 0 | 22 | 21 | 0 | 37 | 89 |
| 25 | 30 | 0 | 22 | 20 | 0 | 37 | 89 |
| 26 | 30 | 0 | 22 | 19 | 0 | 37 | 89 |
| 27 | 30 | 0 | 22 | 18 | 0 | 37 | 89 |
| 28 | 30 | 0 | 22 | 17 | 0 | 37 | 89 |
| 29 | 30 | 0 | 22 | 16 | 0 | 37 | 89 |
| 30 | 30 | 0 | 22 | 15 | 0 | 37 | 89 |
| 31 | 30 | 0 | 22 | 14 | 0 | 37 | 89 |
| 32 | 30 | 0 | 22 | 13 | 0 | 37 | 89 |
| 33 | 30 | 0 | 22 | 12 | 0 | 37 | 89 |
| 34 | 30 | 0 | 22 | 11 | 0 | 37 | 89 |
| 35 | 30 | 0 | 22 | 10 | 0 | 37 | 89 |
| 36 | 30 | 0 | 22 | 9 | 0 | 37 | 89 |
| 37 | 30 | 0 | 22 | 8 | 0 | 37 | 89 |
| 38 | 30 | 0 | 22 | 7 | 0 | 37 | 89 |
| 39 | 30 | 0 | 22 | 6 | 0 | 37 | 89 |
| 40 | 30 | 0 | 22 | 5 | 0 | 37 | 89 |
| 41 | 30 | 0 | 22 | 4 | 0 | 37 | 89 |
| 42 | 30 | 48 | 22 | 3 | 23 | 37 | 160 |
| 43 | 30 | 47 | 22 | 2 | 23 | 37 | 159 |
| 44 | 30 | 46 | 22 | 1 | 23 | 37 | 158 |
| 45 | 30 | 45 | 22 | 0 | 23 | 37 | 157 |
| 46 | 30 | 44 | 22 | 0 | 23 | 37 | 156 |
| 47 | 30 | 43 | 22 | 0 | 23 | 37 | 155 |
| 48 | 30 | 42 | 22 | 0 | 23 | 37 | 154 |
| 49 | 30 | 41 | 22 | 0 | 23 | 37 | 153 |
| 50 | 30 | 40 | 22 | 0 | 23 | 37 | 152 |
| 51 | 30 | 39 | 22 | 0 | 23 | 37 | 151 |

| 52 | 30 | 38 | 22 | 0  | 23 | 37 | 150 |
| 53 | 30 | 37 | 22 | 0  | 23 | 37 | 149 |
| 54 | 30 | 36 | 22 | 0  | 23 | 37 | 148 |
| 55 | 30 | 35 | 22 | 0  | 23 | 37 | 147 |
| 56 | 30 | 34 | 22 | 0  | 23 | 37 | 146 |
| 57 | 30 | 33 | 22 | 0  | 23 | 37 | 145 |
| 58 | 30 | 32 | 22 | 0  | 23 | 37 | 144 |
| 59 | 30 | 31 | 22 | 0  | 23 | 37 | 143 |
| 60 | 30 | 30 | 22 | 0  | 23 | 37 | 142 |
| 61 | 30 | 29 | 22 | 0  | 23 | 37 | 141 |
| 62 | 30 | 28 | 22 | 0  | 23 | 37 | 140 |
| 63 | 30 | 27 | 22 | 0  | 23 | 37 | 139 |
| 64 | 30 | 26 | 22 | 0  | 23 | 37 | 138 |
| 65 | 30 | 25 | 22 | 0  | 23 | 37 | 137 |
| 66 | 30 | 24 | 22 | 0  | 23 | 37 | 136 |
| 67 | 30 | 23 | 22 | 0  | 23 | 37 | 135 |
| 68 | 30 | 22 | 22 | 0  | 23 | 37 | 134 |
| 69 | 30 | 21 | 22 | 0  | 23 | 37 | 133 |
| 70 | 30 | 20 | 22 | 0  | 23 | 37 | 132 |
| 71 | 30 | 19 | 22 | 0  | 23 | 37 | 131 |
| 72 | 30 | 18 | 22 | 0  | 23 | 37 | 130 |
| 73 | 30 | 17 | 22 | 0  | 23 | 37 | 129 |
| 74 | 30 | 16 | 22 | 0  | 23 | 37 | 128 |
| 75 | 30 | 15 | 22 | 0  | 23 | 37 | 127 |
| 76 | 30 | 14 | 22 | 0  | 23 | 37 | 126 |
| 77 | 30 | 13 | 22 | 0  | 23 | 37 | 125 |
| 78 | 30 | 12 | 22 | 0  | 23 | 37 | 124 |
| 79 | 30 | 11 | 22 | 0  | 23 | 37 | 123 |
| 80 | 30 | 10 | 22 | 0  | 23 | 37 | 122 |
| 81 | 30 | 9  | 22 | 0  | 23 | 37 | 121 |
| 82 | 30 | 8  | 22 | 0  | 23 | 37 | 120 |
| 83 | 30 | 7  | 22 | 0  | 23 | 37 | 119 |
| 84 | 30 | 6  | 22 | 0  | 23 | 37 | 118 |
| 85 | 30 | 5  | 22 | 0  | 23 | 37 | 117 |
| 86 | 30 | 4  | 22 | 0  | 23 | 37 | 116 |
| 87 | 30 | 3  | 22 | 48 | 23 | 37 | 115 |
| 88 | 30 | 2  | 22 | 47 | 23 | 37 | 114 |
| 89 | 30 | 1  | 22 | 46 | 23 | 37 | 113 |

**Table 40**. Input data and outcomes corresponding to v=1.15 m/s

| | | |
|---|---|---|
| Minimum time | 1.80 | min |
| Maximum time | 2.90 | min |
| Average time | 2.21 | min |
| Standard deviation | 0.37 | min |

**Table 41**.Calculating walking time with v=1.15 m/s

$$\text{Total time} = d_1 + \text{Cycle} + d_2 + d_3 + \text{Waiting time} + d_4 + d_5$$

| Speed: | 1.15 m/s | | | | | | |
|---|---|---|---|---|---|---|---|
| | $d_1$ | | $d_2+d_3$ | | | $d_4+d_5$ | |
| | 41.65 Walk. Time | | 31.21 Walk. Time | | | 51.65 Walk. Time | |
| L/speed | 36.22 | | 27.14 | | | 44.91 | |
| Round up | 36.00 | Cycle | 27.00 | Cycle | Waiting time | 45.00 | Total |
| Iteration | T1 | T.L. 1 | T2 | T.L. 2 | T.L. 2 | T3 | Time |
| 0 | 36 | 0 | 27 | 45 | 18 | 45 | 126 |
| 1 | 36 | 0 | 27 | 44 | 17 | 45 | 125 |
| 2 | 36 | 0 | 27 | 43 | 16 | 45 | 124 |
| 3 | 36 | 0 | 27 | 42 | 15 | 45 | 123 |
| 4 | 36 | 0 | 27 | 41 | 14 | 45 | 122 |
| 5 | 36 | 0 | 27 | 40 | 13 | 45 | 121 |
| 6 | 36 | 0 | 27 | 39 | 12 | 45 | 120 |
| 7 | 36 | 0 | 27 | 38 | 11 | 45 | 119 |
| 8 | 36 | 0 | 27 | 37 | 10 | 45 | 118 |
| 9 | 36 | 0 | 27 | 36 | 9 | 45 | 117 |
| 10 | 36 | 0 | 27 | 35 | 8 | 45 | 116 |
| 11 | 36 | 0 | 27 | 34 | 7 | 45 | 115 |
| 12 | 36 | 0 | 27 | 33 | 6 | 45 | 114 |
| 13 | 36 | 0 | 27 | 32 | 5 | 45 | 113 |
| 14 | 36 | 0 | 27 | 31 | 4 | 45 | 112 |
| 15 | 36 | 0 | 27 | 30 | 3 | 45 | 111 |
| 16 | 36 | 0 | 27 | 29 | 2 | 45 | 110 |
| 17 | 36 | 0 | 27 | 28 | 1 | 45 | 109 |
| 18 | 36 | 0 | 27 | 27 | 0 | 45 | 108 |
| 19 | 36 | 0 | 27 | 26 | 0 | 45 | 108 |
| 20 | 36 | 0 | 27 | 25 | 0 | 45 | 108 |
| 21 | 36 | 0 | 27 | 24 | 0 | 45 | 108 |
| 22 | 36 | 0 | 27 | 23 | 0 | 45 | 108 |
| 23 | 36 | 0 | 27 | 22 | 0 | 45 | 108 |
| 24 | 36 | 0 | 27 | 21 | 0 | 45 | 108 |
| 25 | 36 | 0 | 27 | 20 | 0 | 45 | 108 |
| 26 | 36 | 0 | 27 | 19 | 0 | 45 | 108 |

| | | | | | | | |
|---|---|---|---|---|---|---|---|
| 27 | 36 | 0 | 27 | 18 | 0 | 45 | 108 |
| 28 | 36 | 0 | 27 | 17 | 0 | 45 | 108 |
| 29 | 36 | 0 | 27 | 16 | 0 | 45 | 108 |
| 30 | 36 | 0 | 27 | 15 | 0 | 45 | 108 |
| 31 | 36 | 0 | 27 | 14 | 0 | 45 | 108 |
| 32 | 36 | 0 | 27 | 13 | 0 | 45 | 108 |
| 33 | 36 | 0 | 27 | 12 | 0 | 45 | 108 |
| 34 | 36 | 0 | 27 | 11 | 0 | 45 | 108 |
| 35 | 36 | 0 | 27 | 10 | 0 | 45 | 108 |
| 36 | 36 | 0 | 27 | 9 | 0 | 45 | 108 |
| 37 | 36 | 0 | 27 | 8 | 0 | 45 | 108 |
| 38 | 36 | 0 | 27 | 7 | 0 | 45 | 108 |
| 39 | 36 | 0 | 27 | 6 | 0 | 45 | 108 |
| 40 | 36 | 0 | 27 | 5 | 0 | 45 | 108 |
| 41 | 36 | 0 | 27 | 4 | 0 | 45 | 108 |
| 42 | 36 | 48 | 27 | 3 | 18 | 45 | 174 |
| 43 | 36 | 47 | 27 | 2 | 18 | 45 | 173 |
| 44 | 36 | 46 | 27 | 1 | 18 | 45 | 172 |
| 45 | 36 | 45 | 27 | 0 | 18 | 45 | 171 |
| 46 | 36 | 44 | 27 | 0 | 18 | 45 | 170 |
| 47 | 36 | 43 | 27 | 0 | 18 | 45 | 169 |
| 48 | 36 | 42 | 27 | 0 | 18 | 45 | 168 |
| 49 | 36 | 41 | 27 | 0 | 18 | 45 | 167 |
| 50 | 36 | 40 | 27 | 0 | 18 | 45 | 166 |
| 51 | 36 | 39 | 27 | 0 | 18 | 45 | 165 |
| 52 | 36 | 38 | 27 | 0 | 18 | 45 | 164 |
| 53 | 36 | 37 | 27 | 0 | 18 | 45 | 163 |
| 54 | 36 | 36 | 27 | 0 | 18 | 45 | 162 |
| 55 | 36 | 35 | 27 | 0 | 18 | 45 | 161 |
| 56 | 36 | 34 | 27 | 0 | 18 | 45 | 160 |
| 57 | 36 | 33 | 27 | 0 | 18 | 45 | 159 |
| 58 | 36 | 32 | 27 | 0 | 18 | 45 | 158 |
| 59 | 36 | 31 | 27 | 0 | 18 | 45 | 157 |
| 60 | 36 | 30 | 27 | 0 | 18 | 45 | 156 |
| 61 | 36 | 29 | 27 | 0 | 18 | 45 | 155 |
| 62 | 36 | 28 | 27 | 0 | 18 | 45 | 154 |
| 63 | 36 | 27 | 27 | 0 | 18 | 45 | 153 |
| 64 | 36 | 26 | 27 | 0 | 18 | 45 | 152 |
| 65 | 36 | 25 | 27 | 0 | 18 | 45 | 151 |
| 66 | 36 | 24 | 27 | 0 | 18 | 45 | 150 |
| 67 | 36 | 23 | 27 | 0 | 18 | 45 | 149 |
| 68 | 36 | 22 | 27 | 0 | 18 | 45 | 148 |
| 69 | 36 | 21 | 27 | 0 | 18 | 45 | 147 |
| 70 | 36 | 20 | 27 | 0 | 18 | 45 | 146 |
| 71 | 36 | 19 | 27 | 0 | 18 | 45 | 145 |
| 72 | 36 | 18 | 27 | 0 | 18 | 45 | 144 |
| 73 | 36 | 17 | 27 | 0 | 18 | 45 | 143 |
| 74 | 36 | 16 | 27 | 0 | 18 | 45 | 142 |
| 75 | 36 | 15 | 27 | 0 | 18 | 45 | 141 |
| 76 | 36 | 14 | 27 | 0 | 18 | 45 | 140 |
| 77 | 36 | 13 | 27 | 0 | 18 | 45 | 139 |

| 78 | 36 | 12 | 27 | 0 | 18 | 45 | 138 |
| 79 | 36 | 11 | 27 | 0 | 18 | 45 | 137 |
| 80 | 36 | 10 | 27 | 0 | 18 | 45 | 136 |
| 81 | 36 | 9 | 27 | 0 | 18 | 45 | 135 |
| 82 | 36 | 8 | 27 | 0 | 18 | 45 | 134 |
| 83 | 36 | 7 | 27 | 0 | 18 | 45 | 133 |
| 84 | 36 | 6 | 27 | 0 | 18 | 45 | 132 |
| 85 | 36 | 5 | 27 | 0 | 18 | 45 | 131 |
| 86 | 36 | 4 | 27 | 0 | 18 | 45 | 130 |
| 87 | 36 | 3 | 27 | 48 | 18 | 45 | 129 |
| 88 | 36 | 2 | 27 | 47 | 18 | 45 | 128 |
| 89 | 36 | 1 | 27 | 46 | 18 | 45 | 127 |

**Table 42**. Input data and outcomes corresponding to v=0.85 m/s

| Minimum time | 2.45 | min |
|---|---|---|
| Maximum time | 3.38 | min |
| Average time | 2.75 | min |
| Standard deviation | 0.32 | min |

**Table 43**. Calculating walking time with v=0.85 m/s

$$\text{Total time} = d_1 + \text{Cycle} + d_2 + d_3 + \text{Waiting time} + d_4 + d_5$$

| Speed: | 0.85 m/s | | | | | | |
|---|---|---|---|---|---|---|---|
| | $d_1$ | | $d_2+d_3$ | | | $d_4+d_5$ | |
| | 41.65 Walk. Time | | 31.21 Walk. Time | | | 51.65 Walk. Time | |
| L/speed | 49.00 | | 36.72 | | | 60.76 | |
| Round up | 49.00 | Cycle | 37.00 | Cycle | Waiting time | 61.00 | Total |
| Iteration | T1 | T.L. 1 | T2 | T.L. 2 | T.L. 2 | T3 | Time |
| 0 | 49 | 0 | 37 | 45 | 8 | 61 | 155 |
| 1 | 49 | 0 | 37 | 44 | 7 | 61 | 154 |
| 2 | 49 | 0 | 37 | 43 | 6 | 61 | 153 |
| 3 | 49 | 0 | 37 | 42 | 5 | 61 | 152 |
| 4 | 49 | 0 | 37 | 41 | 4 | 61 | 151 |
| 5 | 49 | 0 | 37 | 40 | 3 | 61 | 150 |
| 6 | 49 | 0 | 37 | 39 | 2 | 61 | 149 |
| 7 | 49 | 0 | 37 | 38 | 1 | 61 | 148 |
| 8 | 49 | 0 | 37 | 37 | 0 | 61 | 147 |
| 9 | 49 | 0 | 37 | 36 | 0 | 61 | 147 |

| | | | | | | | |
|---|---|---|---|---|---|---|---|
| 10 | 49 | 0 | 37 | 35 | 0 | 61 | 147 |
| 11 | 49 | 0 | 37 | 34 | 0 | 61 | 147 |
| 12 | 49 | 0 | 37 | 33 | 0 | 61 | 147 |
| 13 | 49 | 0 | 37 | 32 | 0 | 61 | 147 |
| 14 | 49 | 0 | 37 | 31 | 0 | 61 | 147 |
| 15 | 49 | 0 | 37 | 30 | 0 | 61 | 147 |
| 16 | 49 | 0 | 37 | 29 | 0 | 61 | 147 |
| 17 | 49 | 0 | 37 | 28 | 0 | 61 | 147 |
| 18 | 49 | 0 | 37 | 27 | 0 | 61 | 147 |
| 19 | 49 | 0 | 37 | 26 | 0 | 61 | 147 |
| 20 | 49 | 0 | 37 | 25 | 0 | 61 | 147 |
| 21 | 49 | 0 | 37 | 24 | 0 | 61 | 147 |
| 22 | 49 | 0 | 37 | 23 | 0 | 61 | 147 |
| 23 | 49 | 0 | 37 | 22 | 0 | 61 | 147 |
| 24 | 49 | 0 | 37 | 21 | 0 | 61 | 147 |
| 25 | 49 | 0 | 37 | 20 | 0 | 61 | 147 |
| 26 | 49 | 0 | 37 | 19 | 0 | 61 | 147 |
| 27 | 49 | 0 | 37 | 18 | 0 | 61 | 147 |
| 28 | 49 | 0 | 37 | 17 | 0 | 61 | 147 |
| 29 | 49 | 0 | 37 | 16 | 0 | 61 | 147 |
| 30 | 49 | 0 | 37 | 15 | 0 | 61 | 147 |
| 31 | 49 | 0 | 37 | 14 | 0 | 61 | 147 |
| 32 | 49 | 0 | 37 | 13 | 0 | 61 | 147 |
| 33 | 49 | 0 | 37 | 12 | 0 | 61 | 147 |
| 34 | 49 | 0 | 37 | 11 | 0 | 61 | 147 |
| 35 | 49 | 0 | 37 | 10 | 0 | 61 | 147 |
| 36 | 49 | 0 | 37 | 9 | 0 | 61 | 147 |
| 37 | 49 | 0 | 37 | 8 | 0 | 61 | 147 |
| 38 | 49 | 0 | 37 | 7 | 0 | 61 | 147 |
| 39 | 49 | 0 | 37 | 6 | 0 | 61 | 147 |
| 40 | 49 | 0 | 37 | 5 | 0 | 61 | 147 |
| 41 | 49 | 0 | 37 | 4 | 0 | 61 | 147 |
| 42 | 49 | 48 | 37 | 3 | 8 | 61 | 203 |
| 43 | 49 | 47 | 37 | 2 | 8 | 61 | 202 |
| 44 | 49 | 46 | 37 | 1 | 8 | 61 | 201 |
| 45 | 49 | 45 | 37 | 0 | 8 | 61 | 200 |
| 46 | 49 | 44 | 37 | 0 | 8 | 61 | 199 |
| 47 | 49 | 43 | 37 | 0 | 8 | 61 | 198 |
| 48 | 49 | 42 | 37 | 0 | 8 | 61 | 197 |
| 49 | 49 | 41 | 37 | 0 | 8 | 61 | 196 |
| 50 | 49 | 40 | 37 | 0 | 8 | 61 | 195 |
| 51 | 49 | 39 | 37 | 0 | 8 | 61 | 194 |
| 52 | 49 | 38 | 37 | 0 | 8 | 61 | 193 |
| 53 | 49 | 37 | 37 | 0 | 8 | 61 | 192 |
| 54 | 49 | 36 | 37 | 0 | 8 | 61 | 191 |
| 55 | 49 | 35 | 37 | 0 | 8 | 61 | 190 |
| 56 | 49 | 34 | 37 | 0 | 8 | 61 | 189 |
| 57 | 49 | 33 | 37 | 0 | 8 | 61 | 188 |
| 58 | 49 | 32 | 37 | 0 | 8 | 61 | 187 |
| 59 | 49 | 31 | 37 | 0 | 8 | 61 | 186 |
| 60 | 49 | 30 | 37 | 0 | 8 | 61 | 185 |

| 61 | 49 | 29 | 37 | 0 | 8 | 61 | 184 |
| 62 | 49 | 28 | 37 | 0 | 8 | 61 | 183 |
| 63 | 49 | 27 | 37 | 0 | 8 | 61 | 182 |
| 64 | 49 | 26 | 37 | 0 | 8 | 61 | 181 |
| 65 | 49 | 25 | 37 | 0 | 8 | 61 | 180 |
| 66 | 49 | 24 | 37 | 0 | 8 | 61 | 179 |
| 67 | 49 | 23 | 37 | 0 | 8 | 61 | 178 |
| 68 | 49 | 22 | 37 | 0 | 8 | 61 | 177 |
| 69 | 49 | 21 | 37 | 0 | 8 | 61 | 176 |
| 70 | 49 | 20 | 37 | 0 | 8 | 61 | 175 |
| 71 | 49 | 19 | 37 | 0 | 8 | 61 | 174 |
| 72 | 49 | 18 | 37 | 0 | 8 | 61 | 173 |
| 73 | 49 | 17 | 37 | 0 | 8 | 61 | 172 |
| 74 | 49 | 16 | 37 | 0 | 8 | 61 | 171 |
| 75 | 49 | 15 | 37 | 0 | 8 | 61 | 170 |
| 76 | 49 | 14 | 37 | 0 | 8 | 61 | 169 |
| 77 | 49 | 13 | 37 | 0 | 8 | 61 | 168 |
| 78 | 49 | 12 | 37 | 0 | 8 | 61 | 167 |
| 79 | 49 | 11 | 37 | 0 | 8 | 61 | 166 |
| 80 | 49 | 10 | 37 | 0 | 8 | 61 | 165 |
| 81 | 49 | 9 | 37 | 0 | 8 | 61 | 164 |
| 82 | 49 | 8 | 37 | 0 | 8 | 61 | 163 |
| 83 | 49 | 7 | 37 | 0 | 8 | 61 | 162 |
| 84 | 49 | 6 | 37 | 0 | 8 | 61 | 161 |
| 85 | 49 | 5 | 37 | 0 | 8 | 61 | 160 |
| 86 | 49 | 4 | 37 | 0 | 8 | 61 | 159 |
| 87 | 49 | 3 | 37 | 48 | 8 | 61 | 158 |
| 88 | 49 | 2 | 37 | 47 | 8 | 61 | 157 |
| 89 | 49 | 1 | 37 | 46 | 8 | 61 | 156 |

**Table 44**.Summary

| SUMMARY TABLE | | | |
|---|---|---|---|
| **Speed** | **Average** | **Std. deviation** | **Variance** |
| **0.85** | 2.75 | 0.32 | 0.10 |
| **1.15** | 2.21 | 0.37 | 0.14 |
| **1.40** | 1.96 | 0.39 | 0.15 |
| **1.65** | 1.76 | 0.40 | 0.16 |

Var. between: $s^2$(2.75, 2.21, 1.96, 1.76):      0.18

Var. within: $(0.32^2+0.37^2+0.39^2+0.40^2)/4$:      0.14

Variance: $((\text{Var. Between})^2+ (\text{Var. Within})^2)^{1/2}$:      0.23

**Average:**      **2.17**
**Total Std. deviat.:**      **0.57**